Cristiana Di Russo

Analysis and Numerical Approximations of Hydrodynamical Models of Biological Movements

COORDINATORE DEL DOTTORATO

Prof. Renato Spigler

DIRETTORI DI TESI

Prof. Roberto Natalini
IAC-CNR

Dott.ssa Magali Ribot
Université Nice Sophia Antipolis

Esame Finale Anno 2010

Ringraziamenti

Il primo grazie va al mio direttore di tesi Roberto Natalini, per avermi guidato su un tema di ricerca estremamente interessante e mostrato vari aspetti della matematica applicata.

Lo ringrazio per la disponibilità e la pazienza con cui mi ha seguito nella preparazione di questa tesi, e per l'entusiasmo con cui mi ha coinvolto in tanti e diversi progetti, in particolare quelli di divulgazione. Desidero ringraziarlo per le lunghe chiacchierate e per i tanti consigli che mi ha dato nel corso di questi anni.

Ringrazio Magali Ribot per essere stata condirettrice della mia tesi. Grazie per essere stata sempre presente nonostante la distanza, per l'aiuto nell'implementazione e nella correzione dei codici numerici, per l'incoraggiamento nei momenti di sconforto e per...i Mikado!

Desidero inoltre ringraziare l'Istituto per le Applicazioni del Calcolo "M. Picone" del CNR per avermi ospitato, nelle sue diverse sedi, in tutti questi anni.

Un grande grazie va ad Alice Sepe, non solo per la sua collaborazione, ma per aver condiviso "gioie e dolori" del dottorato. La ringrazio per le osservazioni ed i consigli durante la stesura della tesi, e soprattutto per le trasferte e le tante "imprese" compiute insieme!

Ringrazio inoltre Fabrizio Clarelli per la sua collaborazione e...per gli innumerevoli caffé.

I would also like to thank Jean-Baptiste Lagaert, Guillemette Chapuisat and Marie Aimée Dronne for their collaboration on the project Stroke during Cemracs '09.

I wish to thank Prof. R. Spigler, Prof. P. D'Ancona, Prof. E. Grenier and Prof. P. Marcati for accepting to be members in my thesis committee.

Desidero ringraziare anche altre due mie compagne di viaggio: Laura per il sostegno morale e pratico ed i consigli "diplomatici", ed Astridh per le trasferte sempre divertenti e le tante risate.

Inoltre ringrazio i dottorandi di Roma Tre, ed in particolare le mie compagne di ufficio Alice, Elisa e Silvia, per aver reso le giornate in Dipartimento più allegre e spensierate.

Ed infine un immenso grazie ai miei genitori e a mia sorella Simona, per avermi sempre capito, incoraggiato e sostenuto.

Contents

Introduction

The aim of this thesis is to investigate some hydrodynamical models arising in biology, from both the analytical and the numerical point of view.

Nowadays, mathematical analysis of biological phenomena has become an important tool to explore complex processes, and to detect mechanisms that might not be evident to the experimenters. In the present work we are interested in the movement of populations of cells, which can be influenced by changes in the environment.

The reaction to an external stimulus is generally called taxis; typically the word taxis is preceded by a prefix, that is determined by the type of stimulus that organisms in a given system respond to. Several types of taxis are well know, like the aerotaxis, the response of an organism to variation in oxygen concentration, or the phototaxis, the response to variation in light intensity and direction. In this thesis we focus on chemotaxis, i.e. the influence of chemical substances present in the environment on the movement of mobile species.

For example, a large number of insects and animals rely on an acute sense of smell for transmitting information between members of their species. Since pheromone release is an important mean for communication, predation and attraction mating partners, it influences the direction of the population movements [114, 115].

Chemotaxis can lead to strictly oriented or partially oriented and partially tumbling movements. The movement towards a higher/lower concentration of the chemical substance is termed positive/negative chemotaxis. The substances that lead to positive chemotaxis are chemoattractants and those leading to negative chemotaxis are repellents.

As shown in [114, 115], chemotaxis is decisive in biological processes. For example, the formation of cells aggregations (amoebae, bacteria, etc) occurs during the response of the species populations to the change of the chemical concentrations in the environment. In multicellular organisms, chemotaxis of cell populations plays a crucial role throughout the life cycle: during embryonic development it plays a role in organizing cell positioning, for example during gastrulation [52] and patterning of the nervous system [132]; in the adult life, it directs immune cell migration to sites of inflammation [178], [47] and fibroblasts into wounded regions to initiate healing. These same mechanisms are used during cancer growth, allowing tumor cells to invade the surrounding environment [41] or stimulating new blood vessel growth [101]. Thus communication by chemical signals determines how cells arrange and organize themselves.

The movement of bacteria under the effect of a chemical substance has been a widely studied topic in Mathematics in the last decades, and numerous models have been proposed. Moreover it is possible to describe this biological phenomenon at different scales. For example, by considering the population density as a whole, it is possible to obtain macroscopic models of partial differential equations. One of the most celebrated model of this class is the one proposed by Patlak in 1953

[133] and subsequently by Keller and Segel in 1970 [89].

It is given by a coupled reaction-advection-diffusion system for the space and time evolution of the density $u = u(x, t)$ of cells, and the chemical concentration $\phi = \phi(x, t)$ at time t and position $x \in \mathbb{R}^n$,

$$
\begin{cases}
\partial_t u & = & \nabla \cdot (-D_1 \nabla \phi + D_2 \nabla u), \\
\\
\partial_t \phi & = & \nabla \cdot (D_\phi \nabla \phi) + u f(\phi) - \phi k_\phi,
\end{cases}
\tag{1}
$$

where $\nabla \cdot$ denotes the divergence respect to the spatial variable. In the Patlak-Keller-Segel (PKS) system, the evolution of density of bacteria is described by a parabolic equation, and the density of chemoattractant is generally driven by a parabolic or an elliptic equation. The behavior of this system is now quite well-known: in the one-dimensional case, the solution is always global in time. In several space dimensions, if initial data are small enough in some norms, the solution will be global in time and rapidly decaying in time; while on the opposite, it will explode in finite time at least for some large initial data.

The simplicity, the analytical tractability, and the capacity to replicate some of the key behaviors of chemotactic populations are the main reasons of the success of this model of chemotaxis. In particular, the ability to display auto-aggregation, has led to its prominence as a mechanism for self-organization of biological systems.

Moreover, there exists a lot of variations of system (1) to describe biological processes in which chemotaxis is involved. They differ in the functional forms of the three main mechanisms involved in the chemotactical movement. They are: the sensing of the chemoattractant, which has an effect on the oriented movement of the species, the production of the chemoattractant by a mobile species or an external source, and the degradation of the chemoattractant by a mobile species or an external effect.

For instance in Chapter 3, we propose a model of PKS type to describe the inflammatory process which occurs during ischemic stroke [47], where the chemotactic sensitivity has a saturation term. Since the biological process involves different type of cells and chemical substances, and some of them are able to move, while others do not have any mobility, we adopt both ordinary and partial differential equations.

However, the approach of PKS model is not always sufficiently precise to describe the biological phenomena [59]. As a matter of fact, the diffusion leads to fast dissipation or explosive behaviors and prevents us to observe intermediate organized structures, like aggregation. Moreover it is not able to reproduce the "run and tumble" behavior.

The main reason is that this approach describe processes on a long time scale, while for short time range one gets better a description from models with finite characteristic speed.

The "run and tumble" (the movement along straight lines, the sudden stop and the change of direction) is described quite well by a stochastic process, called velocity-jump process [76, 155]. It can be studied by a kinetic transport equation introduced in [123], which reads

$$
\partial_t f + v \cdot \nabla_x f = \mathcal{T}(S, f),
\tag{2}
$$

where $f(t, x, v)$ denotes the density of cells, depending on time t, position x and velocity $v \in sS^{n-1}$ with $s > 0$. It is interesting to note that parabolic chemotaxis equations, such as the PKS model (1) can be obtained as the diffusion limit of the transport equation (2), after the rescaling $t \to \epsilon^2 t$, $x \to \epsilon x$. This shows that the PKS system (1) corresponds to a long time asymptotic of the transport model.

At an intermediate scale between diffusion and kinetic models we can find hyperbolic models. This class of models can be derived as a fluid limit of the transport equation (2), but with a different scaling, namely the hydrodynamic scaling $t \to \epsilon t$, $x \to \epsilon x$ [31], which gives hydrodynamical systems. Starting from a transport equation for the chemosensitive movements, in [74] Hillen shows a kinetic derivation of hyperbolic models by the moment closure method, thus obtaining the Cattaneo model for chemosensitive movement. Using the first two moments he obtains the model:

$$\begin{cases} \partial_t u + \nabla \cdot v = 0, \\\\ \partial_t v + \gamma^2 \nabla u = -v + h(\phi, \nabla\phi)g(u), \\\\ \partial_t \phi = \Delta\phi + au - b\phi. \end{cases} \tag{3}$$

It is a hyperbolic-parabolic system where $x \in \mathbb{R}^n$, $t \geq 0$, u is the population density, v are the fluxes, ϕ is the concentration of chemical species, and the source terms g, h are smooth functions.

Hyperbolic models can also be obtained by phenomenological derivations and continuum mechanics, as done by Gamba et al. to describe the vasculogenesis process. In [66, 150] they proposed the model:

$$\begin{cases} \partial_t \rho + \nabla \cdot (\rho u) = 0, \\\\ \partial_t (\rho u) + \nabla \cdot (\rho u \otimes u) + \nabla P(\rho) = -\alpha\rho u + \mu\rho\nabla\phi, \\\\ \partial_t \phi = D\Delta\phi + a\rho - \frac{\phi}{\tau}, \end{cases} \tag{4}$$

where ρ is the density of endothelial cells, u their velocity and ϕ is the concentration of the chemoattractant.

In this hydrodynamical framework, in Chapter 6 we propose a model for the growth of phototrophic biofilms. Starting from the ideas of the mixture theory [138, 14, 137], we write some balance equations which contain the main assumptions coming from biophysical considerations (mass and momentum conservation, influence of nutrients and light, ...). In the biofilm we consider four phases: Bacteria, Dead Cyanobacteria, Extracellular matrix of polymeric substances and Liquid, a common velocity for the solid phases, and a velocity for the liquid. Then the model reads

$$\begin{cases} \partial_t B + \nabla \cdot (B\mathbf{v_S}) = \Gamma_B, \\\\ \partial_t D + \nabla \cdot (D\mathbf{v_S}) = \Gamma_D, \\\\ \partial_t E + \nabla \cdot (E\mathbf{v_S}) = \Gamma_E, \\\\ \partial_t L + \nabla \cdot (L\mathbf{v_L}) = \Gamma_L, \\\\ \partial_t((1-L)\mathbf{v_S}) + \nabla \cdot ((1-L)\mathbf{v_S} \otimes \mathbf{v_S}) + (1-L)\nabla P = \nabla\Sigma + (M - \Gamma_L)\mathbf{v_L} - M\mathbf{v_S}, \\\\ \partial_t(L\mathbf{v_L}) + \nabla \cdot (L\mathbf{v_L} \otimes \mathbf{v_L}) + L\nabla P = -(M - \Gamma_L)\mathbf{v_L} + M\mathbf{v_S}, \\\\ \nabla \cdot ((1-L)\mathbf{v_S} + L\mathbf{v_L}) = 0, \end{cases} \tag{5}$$

where P is the hydrostatic pressure. We will give more details on the biological phenomenon and the model formulation in what follows.

Let us focus our attention now on models (3), (4), and (5), from an analytical point of view.

We can observe that system (3) is a semilinear hyperbolic-parabolic system, where the damped wave equation is coupled to a parabolic one.

On the other hand, system (4) is a quasilinear hyperbolic-parabolic system, where the last equation does not change with respect to the previous system, while the hyperbolic part is essentially given by the isentropic Euler equations. Biofilm system (5) seems to be of intermediate kind between an incompressible system, since the average velocity, unlike the phase velocities, is divergence free, and a compressible system, on behalf on the presence of the pressure term that we find in the compressible gas equations.

These three systems are strictly related and they could be seen almost as encapsulated. As a matter of fact, the differential part of Cattaneo Hillen model can be also seen as the linearization of the Gamba-Preziosi model (4) and the biofilm one (5), like a sort of "building block" for the others.

Moreover, system (4) can be useful for a rigorous study of the biofilm model since the hyperbolic part is essentially the same. Then the investigation of toy-models like (3) is an important tool for a deeper understanding of the solutions dynamics to more complete ones, from an analytical, a numerical, and also modeling perspective.

In this thesis we investigate two different aspects of the mathematical description of cells movements. The first part is devoted to the analytical and numerical study of hyperbolic models of chemotaxis (3), (4).

The second one is devoted to the modeling and the numerical approximation of two biological processes: inflammation during ischemic stroke and the growth of phototrophic biofilms.

Part I: Analysis and Numerical Approximations

First we investigate the analytical behavior of some hyperbolic-parabolic systems.

The results we obtain, i.e. the global existence in time of smooth solution to the Cauchy problem for small initial data and their asymptotic behavior, are a first step towards the study of the behavior of solutions in general, including also more realistic situations.

It could be extremely interesting to individuate a threshold for pattern formation or blow up, as in the parabolic case. We showed numerically that with "large" initial data blow up may occur, but we did not find a precise threshold nor proved it analytically.

Analysis

We start our analytical study by considering the semilinear hyperbolic-parabolic system (3). The coupling of this type of equations has been widely studied by Kawashima and Shizuta [86, 87, 153]. Under the smallness assumption on the initial data and the dissipation condition on the linearized system, they were able to prove global (in time) existence and asymptotic stability of smooth solutions to the initial value problem for a general class of symmetric hyperbolic-parabolic systems.

System (3) does not enter in this framework. As a matter of fact, due to the presence of the source term au, the dissipative condition fails.

In order to obtain our global existence result, we follow a different approach, i.e. the one proposed by Guarguaglini et al. [70] for the one-dimensional case. The basic idea is to consider the hyperbolic and parabolic equation "separately", and to take advantage of their respective properties. Let us explain this approach with more details.

Thanks to the Green function of the heat equation Γ^p, and the Duhamel's formula, we know that, the solution to the parabolic equation is:

$$\phi(x,t) = (e^{-bt}\Gamma^p(t) * \phi_0)(x) + \int_0^t e^{-b(t-s)}\Gamma^p(t-s) * (au(s))\,ds.$$

On the other hand for the damped wave equation,

$$\begin{cases} \partial_t u + \nabla \cdot v = 0, \\[2mm] \partial_t v + \gamma^2 \nabla u = -v, \end{cases} \tag{6}$$

we have, by the theory of dissipative systems [154], that the presence of the dissipative term $-v$ enforces a faster decay of the solution. This implies that we can write the solution of the hyperbolic part of system (3), as

$$w(x,t) = (\Gamma^h(t) * w_0)(x) + \int_0^t \Gamma^h(t-s) * H(\phi, \nabla\phi, w)(s)\,ds,$$

where $w = (u,v)$, $H(\phi, \nabla\phi, w) = [0, h(\phi, \nabla\phi)g(u)]^t$.

Our strategy has been to use the decomposition of the Green function of dissipative hyperbolic systems done by Bianchini at al. [17] and its precise decay rates.

Indeed in [17] the authors proposed a detailed description of the multidimensional Green function for a class of partially dissipative systems. They analyzed the behavior of the Green function for the linearized problem, decomposing it into two main terms. The first term is the diffusive one, and consists of heat kernels, while the slower term consists of the hyperbolic part. Moreover they gave a more precise description of the behavior of the diffusive part, which is decomposed into four blocks, which decay with different decay rates. They showed that solutions have canonical projections on two different components: the conservative part and the dissipative part. The first one, which formally corresponds to the conservative part of the equations, decays in time like the heat kernel, since it corresponds to the diffusive part of the Green function. On the other side, the dissipative part is strongly influenced by the dissipation and decays at a rate $t^{-\frac{1}{2}}$ faster than the conservative one.

By these refined estimates we were able to prove global existence of smooth solutions for small initial data, and to determine at the same time their asymptotic behavior.

Moreover, unlike in [70], we are able to prove the global existence of solution not only of the perturbations of the zero state, but also of small constant states. To obtain this result, we proceed along the lines of the zero state case. In order to get the decay of solutions, we need to adapt our technique to treat the linear term which does not present enough polynomial decay.

Besides, we are able to show decay rates of the L^∞ norm of solution of order $O(t^{-\frac{n}{2}})$, faster than the one obtained in [70] which was $O(t^{-\frac{n}{4}})$.

The parabolic and hyperbolic models of chemotaxis are expected to have the same behavior for long time. We investigate this aspect analytically and prove that solutions to the PKS model have the same decay rates as solutions to (3). Moreover we show that the difference between the solution of PKS model and the hyperbolic one decays with a rate of $O(t^{-\frac{n}{2}})$ in L^2, so $t^{-\frac{n}{4}}$ faster than the decay of solutions themselves.

The following step in our study is the investigation of the behavior of the quasilinear hyperbolic-parabolic system (4).

We analyze the one-dimensional case only. Unfortunately, it is not possible to adopt the same technique of the semilinear case. In order to understand why, let us write the solutions to (4) as

$$U(t) = \Gamma^h(t) * U_0 + \int_0^t \partial_x \Gamma^h(t-s) * \left[\bar{f}'(\overline{U})U(s) - \bar{f}(U(s)) \right] + \int_0^t \Gamma^h(t-s) * h(U + \overline{U}, \partial_x \phi) ds$$

where $U = (\rho, \rho u)$, $h(U + \overline{U}, \partial_x \phi) = [0, (\rho + \bar{\rho})\partial_x \phi)]^t$ and Γ^h is the Green function of the linearized hyperbolic system.

The main problem is the presence of the term $\partial_x \Gamma^h(t-s) * \left[\bar{f}'(\overline{U})U(s) - \bar{f}(U(s)) \right]$, because due to this term, it is not possible to achieve a global existence result. As a matter of fact starting from $U \in H^s(\mathbb{R})$, we get $U \in H^{s+1}(\mathbb{R})$ and we cannot close the estimates.

Then to obtain a global existence result we use a different approach. As done before we look at the hyperbolic part of (4) without the source term $\mu \rho \partial_x \phi$, i.e. we consider isentropic Euler equations with damping. This system enters in a particular framework proposed by Hanouzet and Natalini. In [73], they determined sufficient conditions which guarantee the global existence in time of smooth solutions; these are the entropy dissipation condition and the Shizuta-Kawashima condition (SK). The first one is a condition for systems which are endowed with a strictly convex entropy. Even if the strict convexity guarantees that the entropy estimates are equivalent to the L^2 estimate, and the dissipation the invariance in the same norm, this condition is too weak to prevent the formation of singularities. Indeed there exist systems that satisfy this condition and do not admit the global existence of smooth solutions. The condition (SK) is a generalization of the Kawashima condition for hyperbolic-parabolic problem. In terms of stability it guarantees the necessary coupling between conserved and non conserved quantities in order to have dissipation effects, in both the state variables. Following the work by Hanouzet and Natalini in [73], our approach is based on energy estimates for the parabolic and hyperbolic equations. As a matter of fact, thanks to the estimates for the parabolic equation, we are able to treat also the source term $\mu(\bar{\rho} + \rho)\partial_x \phi$.

Once that the global existence for smooth solutions has been obtained, both for perturbation of zero state and perturbation of small constant states, we are able to determine the asymptotic behavior for large times of solutions, by using the decay rates of the Green functions as done in the previous case.

Numerical Approximations

We proved theorems of global existence of smooth solutions for these systems, and our results hold only for small regular initial data, so we are motivated to use numerical simulations as a tool to investigate the evolution of solutions also for large data.

One goal would be to know whether the hyperbolic system (3) has the same behavior as the parabolic system (1), that is to say global existence for small initial data in some norms, and blow up of solutions for some large initial data. It has also to be noticed that the previous analytical results about global existence of solutions were obtained on the whole space, whereas numerical simulations are performed on a bounded domain.

Hyperbolic equations have been the subject of intensive research in the last decades because they can be applied to a lot of different fields, e.g. gas dynamic, optics, geophysics, biology. Regarding conservation laws, it is well known that, for example for quasilinear system, solutions naturally develop discontinuities (shock waves). Then the construction of stable and consistent numerical schemes is not an easy task, since the presence of these discontinuities generates oscillations in the schemes. Moreover it is often difficult to find an effective numerical approximation to hyperbolic

equations with a source term due to problems like stiffness of the source term, instability of the solutions, incorrect approximation of stationary solutions, and loss of mass conservation.

We use an adaptation of the relaxation method proposed by Aregba-Driollet and Natalini [13]. The main advantages of the relaxation approximation are the simple formulation, even for general multidimensional systems of conservation laws, and the easy numerical implementation.

Moreover this framework presents some special properties: the scalar and the system cases are treated in the same way at the numerical level; all the approximating problems are in diagonal form, which is very convenient for numerical and theoretical purposes; we could easily change the number and the geometry of the velocities involved in our construction to improve the accuracy of the method. Even if these algorithms are not optimal, they illustrate how to construct an efficient and simple approximation even for very complicated systems.

For this reason we applied this method to different systems, starting from wave equation, up to the biofilm model (5).

Part II: Modeling and Numerical Approximations

In the second part of the thesis, we are interested in biological problems with the aim to create models able to reproduce the main mechanisms involved. Then we focus on the modeling and the numerical simulations of the processes. We derive these models starting from phenomenological observations "making everything as simple as possible, but not simpler".

We propose different models of partial differential equation to describe respectively the inflammation during ischemic stroke and the growth of phototrophic biofilms.

Inflammation during ischemic stroke

Strokes consist in the rapidly developing loss of brain functions due to a disturbance in the cerebral blood flow. During a stroke, the affected area of the brain is unable to function, leading to troubles in moving, walking, seeing, speaking or understanding. It is a medical emergency and can cause permanent neurological damage, complications, and death.

We focus our study on one of the pathophysiological mechanisms involved in ischemic stroke, the inflammatory process [45, 83]. In a general setting, inflammation is a complex biological response of vascular tissues to harmful stimuli such as pathogens, damaged cells or irritants.

During ischemic stroke, inflammation is triggered to eliminate the dead cells but can also lead to the death of some other cells. Then inflammation influences the survival of neurons and glial cells both in a positive and a negative way.

We are interested in understanding which influence dominates, depending on the situation. Our final aim is to understand if and how it is possible to control the positive and negative aspects of this biological process, and this could be helpful for the development of new therapeutic strategies in ischemic stroke.

We have considered as a starting point in our study the cell model proposed recently by T. Lekelov-Boissard et al. [33]. This ODEs model took into account the two phases of inflammation: activation of microglia and infiltration of blood leukocytes, but did not consider the space dimension. Then we introduce it in the model, more precisely we introduce the diffusion and the chemotaxis of proteins and leukocytes.

The model includes many parameters and one of the main problems is to determine the values of these parameters. We fix these values with different methods. Some parameters are determined

by fitting the results of the model to real data coming from experiments, other parameters thanks to biological knowledge and the remaining parameters so that the system is not disturbed. We have found a set of parameter values that allows to obtain realistic simulations of the biological phenomenon.

Growth of phototrophic biofilms

A biofilm is a complex gel-like aggregation of microorganisms like bacteria, cyanobacteria, algae, protozoa and fungi, embedded in an extracellular matrix of polymeric substances (EPS). EPS develops resistance to antibiotics, to our immune system, to disinfectants or cleaning fluids.

Even if a biofilm contains water, it is mainly a solid phase. Biofilms can develop on surfaces which are in permanent contact with water, i.e. solid/liquid interfaces, but the growth of microorganisms also occurs in different types of interfaces such as air/solid, liquid/liquid or air/liquid.

Biofilms are found everywhere: in industrial process, on medical devices, but also on the surface of monuments. In this thesis, we are interested on the formation and evolution of biofilms on fountains walls, i.e.: on stone substrates and under a water layer. These biofilms cause much damage, such as unaesthetic biological patinas, decoesion and loss of substrate material from the surface of monuments or degradation of the internal structure.

Our first goal is to introduce a model which keeps the physical finite speed of propagation of the fronts. Then we propose the hydrodynamical model (5), where the inertial terms in the momentum equations in turn guarantees the hyperbolicity of the system and the finite speed of propagation. Actually, in most of the models coming from the mixture theory approach, as for instance [137, 58], these terms are neglected, in order to simplify the analysis and the numerical approximation. In fact, diffusive terms stabilize the fluid and prevent possible breakdowns or other instabilities. On the other hand, this simplification introduces a non-physical infinite speed of propagation in the problem, and makes it difficult to study effectively the evolution of interfaces between the solid (biofilm) and the liquid (water) phases. We prefer to keep the inertial terms and to solve the full hyperbolic problem using some robust and Riemann Solver-free scheme like the relaxation schemes [13].

However, there are two important differences with respect to a usual hyperbolic system. First, since we are dealing with a multiphase fluid, it is difficult to deal with regions where one of the phases may vanish. This is usually solved by neglecting these regions, for instance by selecting special initial conditions. In a biofilm this choice is not possible, since it is important to model also the region where there is only the biofilm or the liquid. It turns out that this problem of vanishing phases can be solved by approximating source terms just by using an Implicit-Explicit scheme.

The other problem arises from the fact that our model is supplemented with a constraint term due to the mass conservation, which implies that the average hydrodynamic velocity of the mixture is divergence free. This constraint is needed to compute the hydrostatic pressure. To enforce the divergence free constraint, we used a fractional step approach, similar to the Chorin-Temam projection scheme [36, 161] for the Navier-Stokes equations, with a very accurate reconstruction of the pressure term.

Plan of the Thesis

This thesis is organized as follows:

in Chapter 1 we present the derivation of parabolic and hyperbolic model of chemotaxis.

At the beginning we introduce the standard Patlak-Keller-Segel model and some variations. Then we present hyperbolic models of chemotaxis showing two different possible derivations: the kinetic derivation with the moment closure method by Hillen [74] and the phenomenological derivation of a vasculogenesis model based on continuum mechanics.

In Chapter 2 we investigate the existence and the behavior for large times of global smooth solutions to the Cauchy problem on $\mathbb{R}^n$, for the semilinear hyperbolic-parabolic system (3).

Initially we introduce some properties of partially dissipative hyperbolic systems, and we present some of the results obtained by Bianchini et al. in [17] on the decomposition of the Green Kernel. Thanks to the sharp decay estimates of the Green kernel of the parabolic and hyperbolic equations, we are able to prove the results. Moreover, in Section 2.5 we prove an analogous result for perturbation of constant (non-null) stationary state.

Finally, by the same technique, we compare the large time behavior of the solution with the behavior of solution to the parabolic Keller-Segel model.

Part of these results are contained in [46].

In Chapter 3 we investigate the existence and the behavior for large times of global smooth solution to the Cauchy problem on $\mathbb{R}$ for the quasilinear hyperbolic-parabolic system (4).

Firstly we introduce hyperbolic partially dissipative systems. The global existence of solutions is proved by energy estimate, while the study of the large times behavior is based on the decay estimates of the Green Kernel of the linearized operators. We show that these results hold also for perturbation of small constant (non null) state.

Part of the results obtained are also present in [49].

Chapter 4 is devoted to the numerical approximation of the hyperbolic-parabolic models studied analytically in the previous chapters.

At the beginning we give an introduction to finite difference schemes, defining fundamental concepts like consistency, convergence, stability and monotonicity. Then we present 3-point finite difference schemes for hyperbolic conservation laws and we briefly present also some classical schemes for parabolic equations.

A section is dedicated to the relaxation method, scheme used in our simulations.

The second and the third section of this chapter are devoted to several numerical simulations in the two dimensional case of the hyperbolic-parabolic models (3), (4). With reference to the chemotaxis model we show results of pattern formation and also simulations in agreement with our analytical result. Regarding the vasculogenesis problem, we show simulations of development of vascular network with different initial data and also simulations in agreement with the analytical results.

Some of the simulations obtained are reported also in [48].

In Chapter 5, we propose a model to describe the inflammatory process which occurs during ischemic stroke [47]. Firstly, an introduction to some basic concepts about the biological phenomenon is given. Then, a detailed derivation of the model and the numerical scheme used are presented. Finally, the studies of the model robustness and sensitivity are showed and some numerical results on the time and space evolution of the process are presented and discussed.

Part of these results are contained in [47].

In the final chapter, a system of nonlinear hyperbolic partial differential equations is introduced to model the formation of biofilms. At the beginning, an introduction to some basic concepts about biofilms is given. Then a detailed derivation of the model, which is mainly based on the theory of mixtures, is presented, also in comparison with previous models. In the last sections we present an adapted numerical scheme and we discuss numerical simulations.

These results are also reported in [39, 38].

Research Perspective

In this thesis we present some global existence results on the Cauchy problem for some hyperbolic-parabolic models arising in biology assuming small initial data. However nothing is known for the moment, beyond our numerical simulations, for large initial data, bounded domains and blow-up phenomena and in particular the ability of these models to capture aggregation phenomena is unknown. Therefore, a first target could be to answer these questions: what is the asymptotic behavior of the solutions of the Cattaneo model? Do they exist globally in time or explode in finite time or may both of these situations occur with a critical threshold as for the parabolic model? We would also have to establish under which conditions on the initial data the solution remains non negative, which is an essential condition for modeling density of bacteria. To find an answer to all these analytic points, we could need also a careful and accurate scheme to simulate the multidimensional equations. These two tasks are closely related: indeed, the numerical simulations give some ideas for the behaviors of the solution we try to understand, while the analysis of the system gives us some clues on the properties the scheme has to possess. The idea could be to generalize what was proposed by [120] in the one-dimensional case, where a high order scheme on asymptotic solutions was designed and where the preservation of mass using suitable boundary conditions was enforced.

It would be also the natural first step in the analysis of the other non-linear hyperbolic models developed to describe cell movements, since the Cattaneo model is a linearized version of the non-linear Preziosi's models we will lean on. A careful comparison with the results yet proved for parabolic Patlak-Keller-Segel system would also be a significant break through. However, the analysis would be much more delicate than the one of the parabolic system and new mathematical strategies should be considered. We could get inspired from the complete study in the one-dimensional case [70], where the explicit time decay of the solutions of the linearized system was used, which for the Cauchy problem was essentially proved in [17], but then adapted to a different context, and for the Neumann case was directly analyzed in that work. We expect the system to possess equilibrium states which will make the study easier; for now on, classical techniques do not seem to work, but new perspectives may be opened thanks to pointwise estimates and combination of appropriate Lyapounov functions, like those used in chemotaxis or in population dynamics.

Concerning the biological damage of monuments, the only models that can be found until now in literature are based on the so-called kinetic theory of active particles [23] in the field of works of art conservation, or cellular automata models or ODE individual-based models [53] which lead to a huge amount of coupled ordinary differential equations. These systems are simple to be implemented and give a good description of what happens at a microscopic level. However, they have some major drawbacks: need for large computational time, difficulty to consider the effective spatial behavior of particles, difficulty to predict the possible formation of structural patterns and high sensitivity to initial data. For all these reasons, we think that a model based on PDEs, like the one

proposed in this thesis, although a bit more complicated to study, would give more reliable macroscopic results with an easier calibration, and would therefore have an impressing and immediate descriptive power. It should also enable us to work on larger space scale since PDEs simulations require less computational resources than large systems of ODEs.

Other features, as signaling mechanism, should be added and results should be compared with some experiments done on purpose. The ultimate goal of this research could be the construction of a more general model including both chemical and biological deterioration phenomena, in order to understand how they interact with each another. The natural application of this coupling could be the study of bioremediation, for which no mathematical modeling is actually known.

Chapter 1

Modeling of Chemotaxis

Chemotaxis is the influence of chemical substances present in the environment on the movement of mobile species. This influence can lead to strictly oriented movement or to partially oriented and partially tumbling movement. We have a positive/negative chemotaxis when the chemical substance attracts an organism and, in this case, the chemical factor is called chemoattractant/chemorepellent.

Chemotaxis is an important mean of cellular communication and determinates how cells arrange and organize themselves.

As shown in [114, 115], chemotaxis is important not only in animal and insect ecology, but it can also be crucial in biological processes, e.g. when a bacterial infection invades a body. The movement of cells toward the source is the result of chemotaxis. Moreover convincing evidence suggests that leukocyte cells in the blood move towards a region of bacterial inflammation, in order to counter it, by moving up a chemical gradient caused by the infection [103, 166, 165, 6].

An interesting aspect of positive oriented chemotactical movement is the formation of cells (amoebae, bacteria, etc) amounts during the responds of species population to the change of the chemical concentrations in the environment, but such aggregation patterns often require a certain threshold number of individuals [79].

Extensive research has been conducted on the mechanistic and signaling processes regulating chemotaxis in bacteria, particularly in E. coli [15], and in the life cycle of cell slime molds such as Dictyostelium discoideum [52].

In multicellular organisms, chemotaxis of cell populations plays a crucial role throughout the life cycle: during embryonic development it plays a role in organizing cell positioning, for example during gastrulation [52] and patterning of the nervous system [132]; in the adult, it directs immune cell migration to sites of inflammation [178], [47] and fibroblasts into wounded regions to initiate healing. The same mechanisms occur in cancer growth, allowing tumour cells to invade the surrounding environment [41] or stimulate the growth of new blood vessel [101].

In this chapter we present the derivation of parabolic and hyperbolic partial differential models of chemotaxis.

At the beginning we introduce the standard Patlak-Keller-Segel model, while the subsequent section is dedicated to hyperbolic models of chemotaxis. We will focus our attentions on two possible derivations: the moment closure method and the continuum mechanics approach based on phenomenological assumptions.

1.1 The Patlak-Keller-Segel Model

Chemotaxis can be described, at macroscopic level, by considering the population of the motile living species as a whole. The most famous model of partial differential equations was proposed in 1953 by Patlak [133] and subsequently in 1970 by Keller and Segel [88, 89]. Keller and Segel were interested in describing the aggregation behavior of cellular slime mold which, they interpreted as the result of an instability. The interest in slime mold morphogenesis was driven by the identification of the chemical which acts as acrasin in Dictyostelium discodeum. Then they tried to deduce the co-operative behavior of amoebae from their individual properties.

In its original form this model consists of four coupled reaction-advection-diffusion equations; we show its derivation following [141, 88]. They identified four species relevant to the process:

- $u(x, t)$ is the density of amoebae at the point x (in $\mathbb{R}$, $\mathbb{R}^2$ or $\mathbb{R}^3$) and at the time t.

- $\phi(x, t)$ is the concentration of the chemical attractant acrasin.

- $\eta(x, t)$ is the concentration of acrasinase, an enzyme that degrades the chemoattractant acrasin.

- $c(x, t)$ is the concentration of a complex that forms when acrasin and acrasinase react.

The assumptions made by Keller and Segel on the model are the following:

1. Acrasin is produced by the amoeba at a rate of $f(\phi)$ per amoebae.

2. Acrasinase is produced by the amoeba at a rate of $g(\phi, \eta)$ per amoebae.

3. Acrasin (ϕ) and acrasinase (η) react to form a complex (c) which dissociates into a free enzyme (acrasinase) and a degraded product, that is

$$\eta + \phi \underset{k_{-1}}{\overset{k_1}{\rightleftharpoons}} c \overset{k_2}{\rightarrow} \eta + \text{degraded product} \quad .$$
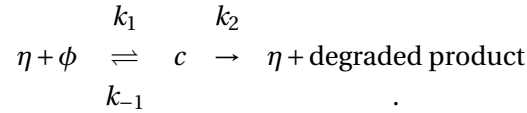
4. Acrasin (ϕ), acrasinase (η) and the complex (c) diffuse according to Fick's Law.

5. The amoebae move in the direction of increasing gradient of acrasin (ϕ) and follow a random motion analogous to diffusion.

The total number of amoebae remains fixed. In order to derive the equations of motion we consider an arbitrary fixed region and balance the mass of each species. Let V be an arbitrarily fixed region with boundary ∂V. Balance of mass requires that the amoebae density satisfies

$$\underbrace{\frac{d}{dt} \int_V u(x, t) \, dx}_{\text{change of mass in } V} = - \underbrace{\int_{\partial V} J^u \cdot n \, ds}_{\text{flux out of the boundary of } V} + \underbrace{\int_V Q^u \, dx}_{\text{birth or death in } V} \quad , \tag{1.1}$$

where J^u is the flux vector of amoeba mass, n is an outward unit normal to V, and Q^u is the net mass of amoeba created (birth - death) per unit time per unit volume.

It is possible to write equations for the other species giving rise to the analogous terms J^ϕ, Q^ϕ, J^η, Q^η, J^c, and Q^c. However, before we determine the forms based on the modeling assumptions of these terms, let us note that by the divergence theorem,

$$\int_{\partial V} J^u \cdot n \, dS = \int_V \nabla \cdot J^u \, dx,$$

and equation (1.1) can be written as

$$\int_V \partial_t u + \nabla \cdot J^u - Q^u \, dx = 0.$$

Since this equation has to hold for arbitrary V, then the integrand must vanish, yielding the differential equations

$$\partial_t u(x, t) = -\nabla \cdot J^u + Q^u.$$

It is possible to obtain similar equations for the other species, but it remains to specify the terms J^s and Q^s for $s = u, \phi, \eta$ and c. To characterize the flux and growth terms they followed the model assumptions. The flux terms ϕ, η, and c are determined by assumption 4 as a classical Fickian diffusion

$$J^s = -D_s \nabla s \quad \text{for } s = \phi, \eta, c.$$

The parameter D_s is the diffusion coefficient that they assumed to be constant. By assumption 5, the form for J^u can be determinated:

$$J^u = -D_2 \nabla u + D_1 \nabla \phi.$$

This definition of flux characterizes the model. As a matter of fact these terms describe two important aspects of the movement of the species. The term $-D_2 \nabla a$ with $D_2 > 0$ says that the organisms avoid increasing concentrations of their own kind species. It is a sort of spreading out to avoid overcrowding. The second term $D_1 \nabla \phi$ is a "Fourier" type term and illustrates the chemotaxis phenomenon of the species in the response to the chemical ϕ. When $D_1 > 0$, this term can be interpreted as the movement of amoebae from low concentrations of ϕ towards higher concentrations. It is a positive chemotaxis indicating that ϕ is a chemoattractant. If $D_1 < 0$, then we have a negative chemotaxis and ϕ is a chemoinhibitor. Keller and Segel assumed for their model $D_1 > 0$.

The last assumption implies that the total population number is constant, $Q^u = 0$.

For the other species, we assume that the chemical reactions are linear. This leads to the following forms for the growth terms:

$$
\begin{aligned}
(1) + (3) \Rightarrow Q^\phi &= u f(\phi) - k_1 \phi \eta + k_{-1} c, \\
(2) + (3) \Rightarrow Q^\eta &= u g(\phi, \eta) - k_1 \phi \eta + k_{-1} c + k_2 c, \\
(3) \Rightarrow Q^c &= k_1 \phi \eta - k_{-1} c - k_2 c.
\end{aligned}
$$

Then the system can be written as:

$$
\begin{cases}
\partial_t u &= \nabla \cdot (-D_1 \nabla \phi + D_2 \nabla u), \\
\partial_t \phi &= \nabla \cdot (D_\phi \nabla \phi) + u f(\phi) - k_1 \phi \eta + k_{-1} c, \\
\partial_t \eta &= \nabla \cdot (D_\eta \nabla \eta) + u g(\phi, \eta) - k_1 \phi \eta + k_{-1} c + k_2 c, \\
\partial_t c &= \nabla \cdot (D_c \nabla c) + k_1 \phi \eta - k_{-1} c - k_2 c.
\end{cases}
\tag{1.2}
$$

In [90] they focused their attention on the aggregation process, by considering aggregation as a manifestation of instability in a uniform distribution of amoebae and acrasin.

They assume a homogeneous population of cells. As a matter of fact, early in the life cycle of the amoebae the properties of the cells are supposed to be such that a uniform distribution is stable

and the random non-uniformities, which occur in a real system, decay. At some point in the life cycle of all cells, however, the characteristics of the individual cell change in such a way that makes a uniform distribution unstable. Any spontaneous perturbation can then trigger aggregation. Keller and Segel did not attempt to offer an explanation of the mechanisms for changes in the individual cell, but rather analyzed the effects on a population of cells which result from such changes.

In this preliminary investigation Keller and Segel considered the simplest reasonable model. So they made further simplifications which allowed the problem to be reduced to two equations for ϕ and u. These simplifications were made to avoid obscuring essential features with heavy calculations.

They made the assumption that the complex is in a steady state with regard to the chemical reaction:

$$k_1 \phi \eta - k_{-1} c - k_2 c = 0.$$

They also assumed that the total concentration of enzyme (both free and bound) is a constant η_0:

$$c + \eta = \eta_0$$

Substituting these into the system, we get a model of two equations

$$
\begin{cases}
\partial_t u & = \nabla \cdot (-D_1 \nabla \phi + D_2 \nabla u), \\[2mm]
\partial_t \phi & = \nabla \cdot (D_\phi \nabla \phi) + u f(\phi) - \phi k_\phi,
\end{cases}
\tag{1.3}
$$

where

$$k_\phi = \eta_0 k_2 K / (1 + K\phi) \text{ and } K = k_1 / (k_{-1} + k_2).$$

Let us observe that the evolution of density of bacteria and the density of chemoattractant are described by parabolic equations. The behavior of this system is quite well known now: in the one-dimensional case, the solution is always global in time. In higher-dimensional cases, if the norm of the initial datum is small enough in some norms, the solution will be global in time; on the opposite, it will explode in finite time for an initial datum which is large enough, at least for some specific initial data.

In literature there exists a lot of variations of (1.3) which differ in the choice of the chemotactic sensitivity function and the reaction terms in the mobile species equation or the chemical ones. We can write the general form of PKS model as:

$$
\begin{cases}
\partial_t u = \nabla \cdot (D(u) \nabla u - A(u) B(\phi) C(\nabla \phi)) + f(u), \\[2mm]
\partial_t \phi = \Delta \phi + u g(u) - \phi.
\end{cases}
\tag{1.4}
$$

The simplicity, the analytical tractability and the capacity to replicate key behavior of chemotactic populations are the main reasons of the success of this class of models of chemotaxis compared to discrete individual based approach. The ability to display auto-aggregation has led to its prominence as a mechanism for self-organization of biological systems. The directed movement of cells and organisms in response to chemical gradients, chemotaxis, has raised significant interest due to its critical role in a wide range of biological phenomena.

All the effects depend on the functional forms of the three main processes during chemotactical movement: the sensing of the chemoattactant which has an effect on the oriented movement of the species, the production of the chemoattractant by a mobile species or an external source and

the degradation of the chemoattractant by a mobile species or an external effect.

Patlak-Keller-Segel type equations have become widely utilized in models for chemotaxis, thanks to their ability to capture key phenomena, intuitive nature and relative tractability (analytically and numerically) as compared to discrete/ individual based approaches.

Different phenomena are described by this class of equations. Models based on the Patlak-Keller-Segel equations have also been developed to understand whether chemotaxis may underpin embryonic pattern formation processes, such as the formation and dynamics of the primitive streak [129], pigmentation patterning in snakes [116] and fish [133] and cell colonisation and neural crest migration [99]. Modeling the role of chemotaxis in pathological processes is a large field: Luca et al. [106] considered whether the chemotactic aggregation of microglia may provide a mechanistic basis for senile plaques during progression of Alzheimer's disease. Moreover, chemotaxis has been incorporated into the modeling of a number of distinct stages of tumour growth, including the migration of invasive cancer cells [136], tumour-induced angiogenesis [32, 108] and macrophage invasion into tumours [127].

In Chapter 5 we propose a model to describe the inflammatory process which occurs during ischemic stroke [47].

Further approaches, like stochastic and discrete methods, have been developed to derive these models. Horstmann's review [82] considers five different methods to describe in detail this class of system. Briefly, these are (a) arguments based on Fourier's law and Fick's law [89], (b) biased random walk approaches [126], (c) interacting particle systems [155], (d) transport equations [5] or [76], and (e) stochastic processes [133]. Recently, Byrne and Owen [25], proposed a derivation from multi-phase flow modeling.

In addition to their utilization within models for biological systems, a large body of work has emerged on the mathematical properties of the Keller-Segel equations (1.3) [82, 79] and, in particular, on the conditions under which specialisation or variations of (1.3) either form finite-time blow-up or have globally existing solutions. The majority of these papers has been devoted to a special case of (1.3), in which the function k_ϕ is assumed to have linear form [see model (M1) below]. This "minimal model" has rich and interesting properties including globally existing solutions, finite time blow-up and spatial pattern formation. Detailed reviews can be found in the survey of Horstmann [82], and in the textbooks of Suzuki [159] and Perthame [135].

A number of variations have been described based on additional biological realism; here we report some of these variations following [79]. These variations are introduced in a form that includes a single additional parameter which, under an appropriate limit, reduces the system to the minimal form. In many cases this modification regularizes the problem such that solutions exist globally in time, then the corresponding parameter for each of the extended models is called regularization parameter. This parameter allows to study in detail bifurcation conditions, pattern formation and properties of the nonuniform solutions. Below we list the ten models studied in [79].

- *The minimal model (M1)*

$$
\begin{cases}
\partial_t u + \nabla \cdot (D\nabla u - \chi u \nabla \phi) = 0, \\[2mm]
\partial_t \phi = \Delta \phi + u - \phi.
\end{cases}
$$

We shall refer to this system as the minimal model following the nomenclature of Childress and Percus [35].

- *Signal-dependent sensitivity models (M2a)-(M2b)*

  There are two versions of signal-dependent sensitivity, the "receptor" model [100, 104, 148, 149, 167],

$$\begin{cases} \partial_t u + \nabla \cdot \left(D\nabla u - \frac{\chi u}{(1+\alpha\phi)^2} \nabla\phi \right) = 0, \\\\ \partial_t \phi = \Delta\phi + u - \phi, \end{cases}$$

  where for $\alpha \to 0$ the minimal model is obtained, and the "logistic" model [123, 90]

$$\begin{cases} \partial_t u + \nabla \cdot \left(D\nabla u - \chi u \frac{1+\beta}{\phi+\beta} \nabla\phi \right) = 0, \\\\ \partial_t \phi = \Delta\phi + u - \phi, \end{cases}$$

  where for $\beta \to \infty$ the minimal model, follows and for $\beta \to 0$ the classical form of $\chi(\phi) = 1/\phi$ is obtained.

- *Density-dependent sensitivity models (M3a)-(M3b)*

  There are two models with density-dependent sensitivity, the "volume-filling" model [77, 128],

$$\begin{cases} \partial_t u + \nabla \cdot \left(D\nabla u - \chi u \left(1 - \frac{u}{\gamma}\right) \nabla\phi \right) = 0, \\\\ \partial_t \phi = \Delta\phi + u - \phi, \end{cases}$$

  where the limit of $\gamma \to \infty$ leads to the minimal model, and

$$\begin{cases} \partial_t u + \nabla \cdot \left(D\nabla u - \chi \frac{u}{1+\epsilon u} \nabla\phi \right) = 0, \\\\ \partial_t \phi = \Delta\phi + u - \phi, \end{cases}$$

  where $\epsilon \to 0$ leads to (M1).

- *The non local model (M4)*

$$\begin{cases} \partial_t u + \nabla \cdot \left(D\nabla u - \chi u \dot{\nabla}_\rho \phi \right) = 0, \\\\ \partial_t \phi = \Delta\phi + u - \phi, \end{cases}$$

  with the non-local gradient defined as

$$\dot{\nabla}_\rho \phi = \frac{n}{\omega\rho} \int_{S^{n-1}} \sigma\phi(x + \rho\sigma, t) d\sigma,$$

  where $\omega = |S^{n-1}|$ and S^{n-1} denotes the $(n-1)$ dimensional unit sphere in $\mathbb{R}^n$ [125, 78]. The non-local gradient is chosen such that the minimal model follows for $\rho \to 0$.

- *The nonlinear-diffusion model (M5)*

$$\begin{cases} \partial_t u + \nabla \cdot (D u^n \nabla u - \chi u \nabla\phi) = 0, \\\\ \partial_t \phi = \Delta\phi + u - \phi. \end{cases}$$

  where the minimal model corresponds to the limit as $n \to 0$ [25, 89, 142, 151, 152].

- *The nonlinear signal kinetics model (M6)*

$$
\begin{cases}
\partial_t u + \nabla \cdot (D\nabla u - \chi u \nabla \phi) = 0, \\[2mm]
\partial_t \phi = \Delta \phi + \frac{u}{1+\psi u} - \phi,
\end{cases}
$$

where the minimal model corresponds to the limit of $\psi \to 0$ [81, 117].

- *The nonlinear gradient model (M7)*

$$
\begin{cases}
\partial_t u + \nabla \cdot (D\nabla u - \chi u \mathbf{F}_c(\nabla \phi)) = 0, \\[2mm]
\partial_t \phi = \Delta \phi + \frac{u}{1+\psi u} - \phi,
\end{cases}
$$

where the function $\mathbf{F}_c(\nabla \phi) : \mathbb{R}^n \to \mathbb{R}^n$ is assumed

$$
\mathbf{F}_c(\nabla \phi) = \frac{1}{c}\left(\tanh\left(\frac{c\phi_{x_1}}{1+c} \right), \cdots, \tanh\left(\frac{c\phi_{x_n}}{1+c} \right) \right)
$$

and it is chosen such that the minimal model follows for $c \to 0$ [142].

- *The cells kinetics model (M8)*

$$
\begin{cases}
\partial_t u + \nabla \cdot (D\nabla u - \chi u \nabla \phi) + r u(1-u) = 0, \\[2mm]
\partial_t \phi = \Delta \phi + u - \phi,
\end{cases}
$$

which in the limit of zero growth, $r \to 0$, leads to the minimal model [128].

The models described can be summarized in the following form:

$$
\begin{cases}
\partial_t u = \nabla \cdot (D(u)\nabla u - A(u)B(\phi)C(\nabla \phi)) + f(u), \\[2mm]
\partial_t \phi = \Delta \phi + u g(u) - \phi.
\end{cases}
\tag{1.5}
$$

The specific functional choices for $D(u), A(u), B(\phi), C(\nabla \phi), f(u)$ and $g(u)$ are given in Table 1.1. Then a natural question that arises is whether solutions blow-up or exist globally in time. As mentioned earlier, the minimal model (M1) has globally existing solutions in one space dimension [122] and a threshold phenomenon with blow-up solutions in higher dimensions [82, 135, 159]. For most of the modified models (M2)-(M8), global existence of solutions is known, since they have been studied theoretically or are special cases of more general models.
The relevant results and the related references are summarized in Table 1.2.
Exploration of the literature reveals two principal methods for demonstrating the global existence of solutions; (i) finding an L^∞ a-priori estimate for the chemotaxis term in the population flux, i.e. the term $A(u)B(\phi)C(\nabla \phi)$ in (1.4), and (ii) to find a Lyapunov function.

1.2 Hyperbolic Models

The approach of Patlak-Keller-Segel model is not always sufficiently precise to describe the bacteria movements. Since this class of model describes phenomena in some large time regimes, it does

Model	$D(u)$	$A(u)$	$B(\phi)$	$C(\nabla\phi)$	$f(u)$	$g(u)$
(M1)	D	u	χ	$\nabla\phi$	0	1
(M2a)	D	u	$\frac{\chi}{(1+\alpha\phi)^2}$	$\nabla\phi$	0	1
(M2b)	D	u	$\frac{\chi(\beta+1)}{(\beta+\phi)}$	$\nabla\phi$	0	1
(M3a)	D	$u\left(1-\frac{u}{\gamma}\right)$	χ	$\nabla\phi$	0	1
(M3b)	D	$\frac{u}{1+\varepsilon u}$	χ	$\nabla\phi$	0	1
(M4)	D	u	χ	$\dot{\nabla}_\rho\phi$	0	1
(M5)	Du^n	u	χ	$\nabla_\rho\phi$	0	1
(M6)	D	u	χ	$\nabla\phi$	0	$\frac{1}{1+\psi u}$
(M7)	D	u	χ	$\frac{1}{c}\tanh\left(\frac{c\nabla\phi}{1+c}\right)$	0	1
(M8)	D	u	χ	$\nabla\phi$	$ru(1-u)$	1

Table 1.1: Summary of the models and their functional forms.

not take into account the fine structure of the cell density for short times. In order to describe phenomena at an intermediate temporal and spatial scale hyperbolic models have been introduced. They have been widely used in recent years, because they allow for analytical study and yield a realistic description of some relevant phenomena. These methods are applied to a range of different fields like population dynamics, forest fire models, bistable systems and combustion wavefronts. They are able to describe some biological mechanisms, as for instance the "run and tumble" movement of some bacteria.

Also for this class of model different derivations are possible. In [65] Fort and Mendez summarize the different approaches as follows: (a) isentropic random walk with reaction, (b) anisotropic random walks with reaction, (c) phenomenological derivation, (d) thermodynamical derivation, (e) derivation from waiting time distribution and (f) kinetic derivation. As a matter of fact, hyperbolic models can be obtained as fluid limit of transport kinetic equation with the hydrodynamic scaling $t \to \epsilon t$, $x \to \epsilon x$, as shown by Perthame et al. [59].

Another technique to reduce a kinetic transport model is the moment closure method, which leads into hyperbolic models as proved by Hillen [74]. In the next section we will show that the two-moment case reduces into models depending on Cattaneo's law of heat conduction; we will report the results of [74, 75] from which most of the contents are taken. The models obtained by this technique respect finite propagation speeds and are based on the individual movement patterns of the species.

1.2.1 The Cattaneo-Hillen Model

Velocity Jump Process and Transport Equations

As observed in experiments [1, 16], some bacteria have a characteristic movement called "run and tumble". They move in a certain direction at an almost constant speed (run), suddenly they stop and choose a new direction (tumble) to continue movement. The tumbling intervals are short compared to the mean run times. This type of individual movement pattern can be modeled by a stochastic process which is called velocity jump process [158]. The characteristic parameters are mean runtime, turning distribution and mean speed.

Model	Global existence	Reference
(M1)	Global existence in $1D$	Osaki and Yagi [122]
(M1)	Global existence in $2D$ below threshold	Calvez and Corrias [26]
(M1)	Global existence in nD below threshold	Horstmann [82]
(M2a)	Global existence in nD	Winkler [175]
(M2b) $\beta > 0$	Global existence in $2D$	Biler [18]
(M2b) $\beta = 0$	Global existence below threshold	Horstmann [82]
(M3a)	Global existence in nD	Hillen and Painter [79]; Wrzosek [177]
(M3b)	Global existence in nD	Velazquez [168]
(M4)	Global existence in nD	Hillen et al. [78]
(M5)	Global existence in nD	Kowalczyk [92]
(M6)	Global existence in nD	Horstmann [81]
(M7)	Global existence in nD	Biler [18]
(M8)	Global existence in nD	Wrzosek [176]

Table 1.2: Summary of global existence results for the model (M1)-(M8).

Let $p(x, t, v)$ denote the population density at spatial position $x \in \mathbb{R}^n$ at time $t \geq 0$ with velocity $v \in \mathbb{R}^n$. Although the most meaningful space dimensions are $n = 1, 2, 3$, the theory works for all $n \in \mathbb{N}$. Let us assume that individuals choose any direction with bounded velocity. We denote the set of possible velocities as V, where $V \subset \mathbb{R}^n$ is bounded and symmetric (i.e $v \in V \Rightarrow -v \in V$). Then the linear transport model, which bases on a velocity jump process [158, 124] reads

$$\partial_t p(x, t, v) + v \cdot \nabla p(x, t, v) = -\mu p(x, t, v) + \mu \int T(v, v') p(x, t, v') dv', \tag{1.6}$$

where μ is the turning rate or turning frequency, hence $\tau = \frac{1}{\mu}$ is the mean run time and $T(v, v')$ is the probability kernel for the new velocity v given the previous velocity was v'. Moreover the identity

$$\int T(v, v') dv = 1,$$

ensures particle conservation.

If motion is modeled by a diffusion process and birth and death are included, then a reaction-diffusion models, results [114, 115]. Similarly to the diffusion model the inclusions of birth and death bring to reaction-diffusion models. Depending on concrete experiments the reaction may depend on particle velocity, hence a nonlinear reaction-transport equation reads:

$$\partial_t p(x, t, v) + v \cdot \nabla p(x, v, t) = -\mu p(x, t, v) + \mu \int T(v, v') p(x, t, v') dv' + f(v, p, m^0), \tag{1.7}$$

where the total population density is denoted as

$$m^0(x, t) = \int_V p(x, t, v) dv. \tag{1.8}$$

Transport equations appear also in physics as models for gases e.g. Bolzmann equations [30]. In this physical application some quantities are conserved, among these are energy, momentum and mass. In biological applications in case of no birth or death reactions, the only conserved quantity is the total particle number.

The Cattaneo Law

The Cattaneo law was introduced by Cattaneo in 1949 [28] as a modification of Fourier's law of heat conduction. It is used to describe heat propagation with finite speed.

Let $\theta(x, t) \in \mathbb{R}$ be the temperature of a homogeneous medium $\Omega \cap \mathbb{R}^n$ and let $q(x, t) \in \mathbb{R}^n$ be the heat flux. Then the Cattaneo law, together with an equation for conservation of energy, leads to the following system:

$$
\begin{cases}
\partial_t \theta + \nabla \cdot q = 0, \\
\\
\tau \partial_t q + q = -D\nabla\theta.
\end{cases}
\tag{1.9}
$$

The constant $\tau > 0$ describes the adaptation time of the heat flux q to the negative gradient of the temperature θ, and the parameter $D > 0$ is the diffusion constant. This system is closely related to damped wave equation. Let us observe that for $\tau = 0$ we have Fourier's law $q = -D\nabla\theta$ and system (1.9) translates into the classical heat equation $\partial_t \theta = D\Delta\theta$.

The Cattaneo Approximation

One common feature in understanding the dynamic properties of reaction-transport equations and Boltzmann equations are moment methods. By multiplication of (1.6) with powers of v and integration, it is possible to derive an infinite sequence of equations for the moments of p.

As a matter of fact in the equation for the n-th moment the $(n+1)-$st moment appears. To close the equations for the first n moments we need an approximation of the $(n+1)-$moment. This closure problem is well know and widely discussed in transport theory. For Boltzmann equations the closure problem has been dealt with the theory of extended thermodynamics [111]. An entropy functional is maximized under the constraint of fixed first n moments. One assumes that the $(n+1)-$st moment of the minimizer approximates the $(n+1)-$st moment of the true solution, getting the desired closure.

Here we report a theory for closing the moment equations based on minimization principle proposed by Hillen [74].

In this biological context the negative $L^2(V)-$norm can be seen as an entropy as defined in thermodynamics, so it is possible to close the moment system by minimizing the L^2-norm under the constraint of fixed first $n-$moments.

We report the moment closure approach for the first two moments used by Hillen [74]; this closure leads to semilinear Cattaneo systems.

Let us consider a transport equation which corresponds to a velocity jump process with fixed speed, but variable direction (Pearson walk [134]). In this case $V = sS^{n-1}$ with $s > 0$ and we denote $\omega = |V| = s^{n-1}\omega_0$, where $\omega_0 = |S^{n-1}|$. The turn angle distribution is assumed to be constant $T(v, v') = |V|^{-1}$. Then the initial value problem for the linear transport equation reads:

$$
\partial_t p + v \cdot \nabla p = \mu\left(\frac{m^0}{\omega} - p\right),
\tag{1.10}
$$

$$
p(x, 0, v) = \varphi_0(x, v).
\tag{1.11}
$$

Let us observe that the shift operator $\Phi := -v \cdot \nabla$ on $L^2(\mathbb{R}^n \times V)$ with domain

$$
\mathscr{D}(\Phi) = \left\{\phi \in L^2(\mathbb{R}^n \times V) : \phi(\cdot, v) \in H^1(\mathbb{R}^n)\right\},
$$

is skew-adjoint. It generates a strongly continuous unitary group on $L^2(\mathbb{R}^n \times V)$ [44]. The right-hand side of (1.10) is bounded, therefore the linear transport equation defines a strongly continuous solution group on $L^2(\mathbb{R}^n \times V)$. For $\varphi_0 \in \mathscr{D}(\Phi)$ solutions $p(x, t, v)$ exist in

$$C^1([0,\infty), L^2(\mathbb{R}^n \times V)) \cap C([0,\infty), \mathscr{D}(\Phi)).$$

Let us consider the equations of the first two moments (m^0, m^i), $i \in \{1, \cdots, n\}$ of p, where m^0 is defined (1.8) and the higher moments of p are denoted by:

$$m^i(x, t) \quad = \quad \int_V v^i p(x, t, v) \, dv \quad i = 1, \ldots, n, \tag{1.12}$$

$$m^{ij}(x, t) \quad = \quad \int_V v^i v^j p(x, t, v) \, dv \quad i, j = 1, \ldots, n. \tag{1.13}$$

Let us note that m^0 is scalar, m^i is a vector and m^{ij} is a 2-tensor.

For constant turn angle distribution $T(v, v')$ in [74] is proved that the negative of the $L^2(V)-$ norm is an entropy for (1.10). The method proposed minimize the $L^2(V)-$norm under the constraint of fixed moments m^0 and m^i and then it assumes that the second moment $m^{ij}(u_{min})$ of minimizer u_{min} approximates the second moment $m^{ij}(p)$. This leads to a closed hyperbolic system for an approximate density M^0 and an approximate flow M^i.

Since the resulting system is known from heat transport theory as the Cattaneo system it is called Cattaneo approximation to (m^0, m^i). It is possible to estimate $(m^0, m^i) - (M^0, M^i)$ in $L^2(\mathbb{R}^n)$ as shown in [74], motivating the use of Cattaneo system as models for the movement of microorganisms like bacteria or amoeba.

The Cattaneo approximation can be used to approximate the transport model for all times whereas the parabolic approximations are valid for large times only.

In order to derive the equations for the first two moments m^0 and m^i we integrate (1.10) over V obtaining the conservation law

$$\partial_t m^0 + \sum_{j=1}^n \partial_j m^j = 0. \tag{1.14}$$

Multiplication of (1.10) with v_i and integration along V leads to

$$\int v^i \partial_t p \, dv = -\sum_{j=1}^n \int v^i v^j \partial_j p \, dv + \mu \frac{m^0}{\omega} \int v^i \, dv - \mu \int v^i p \, dv.$$

For the symmetry of $V = sS^{n-1}$, it follows that $\int v^i \, dv = 0$. Hence

$$\partial_t m^i + \sum_{j=1}^n \partial_j m^{ij} = -\mu m^i. \tag{1.15}$$

To close this system of $n + 1$ moment equations (1.14) and (1.15) we have to replace $m^{ij}(p)$.

The main step is to derive a function $u_{min}(x, t, v)$ which minimizes the $L^2(V)$ norm $\|u(x, t, \cdot)\|_{L^2}^2$, under the constraint that u_{min} has the same first moments m^0 and m^i as p has. Once we have obtained such a function u_{min} we have to replace $m^{ij}(p)$ by $m^{ij}(u_{min})$.

Let us introduce Lagrangian multipliers $\Lambda_0 \in \mathbb{R}$ and $\Lambda_i \in \mathbb{R}$ for $i = 1, \ldots, n$ and define

$$H(u) := \frac{1}{2} \int_V u^2 \, dv - \Lambda_0 \left(\int_V u \, dv - m^0 \right) - \sum_{i=1}^n \Lambda_i \left(v^i u \, dv - m^i \right).$$

The Euler-Lagrange equation of $H(u)$ reads $u - \Lambda_0 - \sum\limits_{i=1}^{n} \Lambda_i v^i = 0$, which gives

$$u = \Lambda_0 + \sum_{i=1}^{n} \Lambda_i v^i.$$

Then we have to use the constrains to determine Λ_0 and Λ_i:

$$m^0 = \int_V u\,dv = \int_V \Lambda_0\,dv + \sum_{i=1}^{n} \int_V \Lambda_i v^i\,dv.$$

We have $\int_V v^i\,dv\,\Lambda_i = 0$, hence

$$\Lambda_0 = \frac{m^0}{\omega},$$

$$m^i = \int_V v^i u\,dv = \int_V v^i \Lambda_0\,dv + \sum_{j=1}^{n} \int_V v^i(\Lambda_j v^j)\,dv.$$

The first integral vanishes. To evaluate the second integral let us note that

$$\int_{S^{n-1}} \sigma\sigma^T\,d\sigma = \frac{\omega_0}{n} I_n,$$

where I_n is the $n \times n$ identity matrix. Hence

$$\int_v vv^T\,dv = \int_{S^{n-1}} (s\sigma)(s\sigma)^T s^{n-1}\,d\sigma = \omega\frac{s^2}{n} I_n.$$

It follows that Λ_i is given by

$$\Lambda_i = \frac{n}{\omega s^2} m^i.$$

Then we have got an explicit form of the minimizer:

$$u_{min}(x, t, v) = \frac{1}{\omega}\left(m^0(x, t) + \sum_{i=1}^{n} \frac{n}{s^2} v_i m^i(x, t)\right).$$

To derive the moment closure we consider the second moment of the minimizer u_{min}:

$$
\begin{aligned}
m^{ij}(u_{min}) &= \sum_{j=1}^{n} \int_V v^i v^j u_{min}(x, t, v)\,dv \\
&= \frac{1}{\omega}\sum_{j=1}^{n} \int_V v^i v^j m^0\,dv + \int_V v^i v^j v_k\,dv\,m^k \\
&= \frac{s^2}{n} m^0 I, \quad\quad\quad (1.16)
\end{aligned}
$$

because the tensor $\sum\limits_{j=1}^{n} \int_v v^i v^j v_k\,dv$ vanishes.

We have chosen u_{min} such that $m^0(u) = m^0(p)$ and $m^i(u) = m^i(p)$. Let us now close the system of the first two moments by assuming that $m^{ij}(u) \approx m^{ij}(p)$. Then replacing m^{ij} in (1.15) together with (1.14) gives a linear Cattaneo system

$$\partial_t M_0 + \partial_j \sum_{j=1}^{n} M^j = 0 \quad\quad\quad (1.17)$$

$$\partial_t M^i + \frac{s^2}{n}\partial_i M^0 \;=\; -\mu M^i, \qquad (1.18)$$

with initial conditions

$$M^0(\cdot,0) = m^0(\cdot,0), \quad M^i(\cdot,0) = m^i(\cdot,0).$$

We introduce capital letters to distinguish between the moments (m^0, m^i) of p and the solutions (M^0, M^i) of the Cattaneo system. The error which appears during this approximation can be controlled, as proved in [74].

A Cattaneo Model for Chemosensitive Movement

In [74] Hillen derives also models for chemosensitive movement based on Cattaneo's law of heat propagation with finite speed. Moreover, in a work in collaboration with Dolak, he applied the model to pattern formation as observed in experiments with Dictyostelium discoideum, Salmonella typhimurium and Escherichia coli.

In case of bacterial chemotaxis it has been observed in experiments that bacteria significantly change their turning rate in response to external stimuli, but they do not change their turn angle distribution. So the turning rate should depend on the velocity v, on the concentration of the external signal ϕ and on its gradient $\nabla\phi$, then $\mu = \mu(v,\phi,\nabla\phi)$.

Since bacteria are too small to measure concentration gradients along their body axis, they measure gradients while moving through them. Then the turning rate depends not directly on $\nabla\phi$ but on the directional derivative:

$$\delta_v\phi := \partial_t\phi + v\cdot\nabla\phi.$$

Let us assume $\mu = \mu(\phi,\delta_v\phi)$. The kernel $K(v,v')$ is chosen in such a way that the total particle number is preserved.

This can be achieved by $K(v,v') = \mu(\phi,\delta_v\phi)T(v,v')$ where $\int_V T(v,v')dv = 1$. Then the transport equation for chemosensitive movement reads:

$$\partial_t p + v\cdot\nabla p = -\mu(\phi,\delta_v\phi) + \int_V \mu(\phi,\delta_v\phi)T(v,v')p(v')dv'. \qquad (1.19)$$

Let us observe that if we restrict to 1-D with two speeds $\pm s$, the model considered by Hillen and Stevens in [80] follows

$$\begin{cases} \partial_t u^+ + \gamma\partial_x u^+ = -\mu^+(\phi,\partial_x\phi)u^+ + \mu^-(\phi,\partial_x\phi)u^-, \\[2mm] \partial_t u^- - \gamma\partial_x u^- = \mu^+(\phi,\partial_x\phi)u^+ - \mu^-(\phi,\partial_x\phi)u^-, \\[2mm] \partial_t\phi - D\partial_{xx}\phi = -\beta\phi + \alpha(u^+ + u^-). \end{cases} \qquad (1.20)$$

Functions $u^\pm$ denote the densities of the right/left moving part of the total population and ϕ is the external chemotactic stimulus biasing the movement of the population itself. Parameters γ,δ,D, which are assumed to be strictly positive constants, represent characteristic speed of propagation of $u^\pm$, time-scale for the dynamics and diffusion coefficient for the chemoattractant respectively. The terms $\mu^\pm$ are called turning rates and they control the probability of transition from u^+ to u^- and vice versa, i.e. the change of direction in the movement of a single individual.

In [80], a first result of local and global existence for weak solutions under the assumption of turning rate's boundness is proved. Recently Guarguaglini et al. in [70] have proved more general results for

this model under weaker hypotheses, by showing a general result of global stability of some constant states for both the Cauchy problem on the whole real line and the Neumann problem on a bounded interval for small initial data. These results have been obtained by using the linearized operators and the accurate analysis of their nonlinear perturbations.

Let us consider now a more specific form of the turning rate

$$\mu(\phi, \delta_v \phi) = \mu_0(1 - \alpha(\phi)\delta_v \phi),$$

for some costant $\mu_0 > 0$ and an appropriate function $\alpha(\phi)$.

Let us assume moreover that $T(v, v') = \frac{1}{\omega}$, then a prototype model for chemosensitive movements reads

$$\partial_t p + v \cdot \nabla p = -\mu_0(1 - \alpha\delta_v \phi)p(v) + \frac{\mu_0}{\omega} \int_V (1 - \alpha(\phi)\delta_v)\phi T(v, v')p(v')\,dv'. \tag{1.21}$$

Using the notation of the moments m^0 and m^i we can write (1.21) as

$$\partial_t p + v \cdot \nabla p = -\mu_0(1 - \alpha(\partial_t \phi + v \cdot \nabla \phi))p(v) + \frac{\mu_0}{\omega}\left(m^0 - \alpha m^0 \partial_t \phi - \alpha m^i \partial_i \phi\right). \tag{1.22}$$

To derive the equations for the first two moments we integrate (1.22) obtaining

$$\partial_t m^0 + \sum_{j=1}^n \partial_j m^j = 0.$$

Multiplication of (1.22) with v_i and integration gives

$$m_t^i + \sum_{j=1}^n \partial_j m^{ij} = -\mu_0(1 - \alpha\partial_t \phi)m^i + \mu_0\alpha \sum_{j=1}^n \partial_j \phi m^{ij}.$$

Again with (1.16) the corresponding Cattaneo system for chemosentive movement reads

$$M_t^0 + \sum_{j=1}^n \partial_j M^j = 0$$

$$M_t^i + \frac{s^2}{n}\partial_i M^0 = -\mu_0(1 - \alpha\partial_t \phi)M^i + \frac{s^2}{n}\mu_0\alpha\partial_i \phi M^0. \tag{1.23}$$

A model for slime molds

In [51], Dolak and Hillen proposed a model of this class to describe the behavior of the slime mold Dictyostelium discoideum. This amoeba develops an extraordinary mechanism controlled by chemotaxis: upon starvation, the amoebae form tissue-like aggregates. The cells move upward gradients of the messenger molecule cAMP produced by the cells themselves. Eventually, they form a fruiting body, where spores can survive until conditions for germination are favorable. The formation of aggregates has been documented by many authors. Guided by observations of Firtel et al.[60], the aim of Dolak and Hillen simulations was not to reproduce the experimental results as precisely as possible, but to describe them qualitatively. The non-dimensionalize model is

$$\begin{cases} \partial_t u + \nabla \cdot v = 0, \\\\ \tau \partial_t v + v = -D\nabla u + u(1 - u)\nabla \phi, \\\\ \partial_t \phi = \Delta \phi + \alpha u - \phi, \end{cases} \tag{1.24}$$

Here u, v and ϕ are the particle density, the particle flux, and the signal concentration, respectively. In their study, the Cattaneo model for chemosensitive movement is well suited to describe the experimentally observed patterns. On a long time scale the same behavior for the PKS model and the Cattaneo model is expected. For short time ranges, however, one expects a better description from a Cattaneo type model, due to finite characteristic speed.

In their simulations Hillen and Dolak use realistic parameter values as given in Ford et al.[64], observing that both models, parabolic and hyperbolic, fit the data. But differences can be seen in the time range up to about 40 s. Following Ford's experiments both model types are appropriate and the model should be chosen in accordance to the available data. If spread is measured for the population as a whole (motility D or chemotactic sensitivity, χ), then a diffusion based model should be used. If individual paths are followed and turning rates and turn-angle distributions are measured, then a hyperbolic model is more appropriate. There is certainly an overlap region, where both model types can be used with equal reasons. From a more theoretical point of view, the transport and Cattaneo-models provide a convenient platform to study and understand how the behavior of a population as a whole emerges from the behavior of its individual members.

1.2.2 The Gamba-Preziosi Model

As seen for the Patlak-Keller-Segel model, it is possible get models by phenomenological derivations and continuum mechanics. In what follows we present a hyperbolic model of vasculogenesis proposed by Preziosi et al. in [150, 66].

Filbet et al. in [59] derived the model as a hydrodynamic limit of a kinetic velocity-jump process by a Chapman-Eskog expansion.

Let us start with a short biological background of this phenomenon. Vasculogenesis is the process of blood vessel formation by cells, endothelial cells and angioblasts. An analogous phenomenon is the angiogenesis, the physiological process involving the growth of new blood vessels from pre-existing vessels. It is a normal and vital process in growth and development, as well as in wound healing and in granulation tissue. However, it is also a fundamental step in the transition of tumors from a dormant state to a malignant one. Folkman in [61] hypothesized that, if it were possible to inhibit neovascularization, it might stop the growth of the tumour or at least contain its growth to a dormant mass of around 2 to 3 mm in diameter. Moreover, he suggested that such antiangiogenesis could be the basis for a new form of cancer therapy. A particularly important aspect, from a cancer therapy point of view, is that antiangiogenic therapy does not induce acquired drug resistance in experimental cancer [20] unlike chemotherapy. The field of anti-angiogenesis is now fast growing with an increasing number of areas where modeling could be of some considerable value.

In vasculogenesis, the ability to form networking capillary tubes is a cell autonomous property of the endothelial cells (ECs), which need permissive but not instructive signals from the extracellular environment. In recent years many experimental investigations have been performed on the mechanism of blood vessel formation [40].

Since in vivo studies, are prone to a variety of sensitivity problems, much of the experimental work in this area has been on in vitro (biological) model systems which avoid many of the experimental difficulties with in vivo systems. The development of in vitro angiogenesis (biological) models provides a controlled means for studying blood vessel formation [62]. The reasonable assumption is that, if the in vitro studies replicate the type of patterns observed in vivo, then these models provide information on the pattern formation mechanism which operates in vivo.

Cells are cultured on a gel matrix and their migration and aggregation are observed through videomi-

croscopy. This way, the process of formation of a vascular network starting from randomly seeded cells can be accurately tracked. Tracking of individual trajectories in some experiments [42] shows marked persistence in the direction, with a small random component superimposed. The motion is directed towards a zone of higher concentration of cells, suggesting that chemotactic factors play a role. Cells migrate over distances which are an order of magnitude larger than their radius and aggregate when they get in touch with one of their neighbors. In a time of the order of 10 h they form a continuous multicellular network which can be described as a collection of nodes connected by chords.

In the biological system the percolating property is of physiological relevance, since it is directly linked with the functionality of blood vessels.

Here we represent the theoretical model proposed by Serini et al. [150, 66] which turns out to be in good agreement with these experimental observations. In what follows we shall refer to this system as the Gamba-Preziosi model. It is able to reproduce well both the observed percolative transition and the typical scale of observed vascular networks. These structures cannot be explained by the above parabolic models, which generically lead to a fast decay or to pointwise blow-up, but are recovered by numerical experiments on hyperbolic models.

The Gamba-Preziosi model for vasculogenesis [150, 66] focuses on the early development of vascular network formation. They assume, as reported in [7], that persistence and chemotaxis are the key features to determinate the size of the structure. In their view, mechanical interaction of the cells with the matrigel can be neglected to describe the behavior of the system along the first 3-6 hours.

As shown in [7], the mathematical model is based on the following assumptions:

1. endothelial cells show persistence in their motion;

2. endothelial cells communicate via the release and absorption of a soluble growth factor. This chemical factor can reasonably identified with VEGF-A (Serini et al. [150]);

3. the chemical factors released by cells diffuse and degrade in time;

4. endothelial cells neither duplicate nor die during the process;

5. cells are slowed down by friction due to the interaction with the fixed substratum;

6. closely packed cells mechanically respond to avoid overcrowding.

Then the state variables involved in the process are:

- The density ρ of endothelial cells;

- The velocity u of the endothelial cells;

- The density ϕ of chemoattractant.

The equations are derived from the conservation laws of mass and momentum. Let us recall how get these equation in general. Proceeding in a standard way, as shown in [37], let assume that for each time t, the density ρ of endothelial cells has a well defined mass density $\rho(x, t)$ for $x \in D$, a region in the three dimensional space. Let $u(x, t)$ denote the velocity of cells that are moving

through x at time t.

Let V is an arbitrary subregion of D, then the mass of cells in V at time t is given by

$$m(V,t) = \int_V \rho(x,t)\,dx,$$

In what follows we shall assume that the function ρ and u are smooth enough so that the standard operations of calculus may be performed on them. The derivation of the equations is based on two basic principles:

i) mass is neither created nor destroyed;

ii) the rate of change of momentum of a portion of the fluid equals the force applied to it (Newton's second law);

Let V be a fixed subregion of D; the rate of change of mass in V is

$$\frac{d}{dt}m(V,t) = \frac{d}{dt}\int_V \rho(x,t)\,dx = \int_V \partial_t \rho(x,t)\,dx.$$

Let ∂V denote the boundary of V, assumed to be smooth; let n denote the unit outward normal defined at points of ∂V; and let dS denote the area element on ∂V. The volume flow rate across ∂V per unit area is $u \cdot n$ and the mass flow rate per unit area is $\rho u \cdot n$.

The principle of conservation of mass can be stated as follows: the rate of increase of mass in V equals the rate at which mass is crossing ∂V in the inward direction; i.e.,

$$\frac{d}{dt}\int_V \rho\,dx = -\int_{\partial V} \rho u \cdot dS.$$

This is the integral form of the law of conservation of mass. By the divergence theorem, this statement is equivalent to

$$\int_V \left[\partial_t \rho + \nabla \cdot (\rho u)\right] dx = 0.$$

Since this has to hold for all V, it is equivalent to

$$\partial_t \rho + \nabla \cdot (\rho u) = 0. \tag{1.25}$$

Let us observe that if ρ and u are not smooth enough to justify the steps that lead to the differential form of the law of conservation of mass, then the integral form is the one to use.

Let us call

$$\delta_u = \partial_t + u \cdot \nabla,$$

the directional derivative; it takes into account the fact that the cells are moving and that the positions of particles change with time.

For any continuum, forces acting on a piece of material are of two types.

First, there are forces of stress, whereby the piece of material is acted on by forces across its surface by the rest of the continuum. Second, there are external, or body, forces such as gravity or a magnetic field, which exert a force per unit volume on the continuum. Let us recall that, for any ideal fluid and any motion of the fluid, there is a function $p(x,t)$ called pressure such that if S is a surface in the fluid with a chosen unit normal n, the force of stress exerted across the surface S per unit area at $x \in S$ at time t is $p(x,t)n$.

Note that the force is in the direction n and that the force acts orthogonally to the surface S, then there are no tangential forces.

If V is a region in the fluid at a particular instant of time t, then the total force exerted on the fluid inside V by means of stress on its boundary is

$$f_{surf} = \{\text{force on V}\} = -\int_{\partial V} p n dS.$$

If e is any fixed vector in space, the divergence theorem gives

$$e \cdot f_{surf} = -\int_{\partial V} p e \cdot n dS = -\int_V \text{div} (pe) dx = -\int_V \nabla p \cdot e dx.$$

Thus

$$f_{surf} = -\int_V \nabla p dx. \tag{1.26}$$

If $b(x, t)$ denotes the given body force per unit mass, then the total body force is

$$B = -\int_V \rho b dx. \tag{1.27}$$

Thus, on any piece of material,

$$\text{force per unit volume} = -\nabla p + \rho b.$$

By Newton's second law we are led to the differential form of the law of balance of momentum:

$$\rho \delta_u = \overbrace{-\nabla p + \rho b}^{f}. \tag{1.28}$$

Regarding the chemoattractant we proceed as done in the Keller and Segel model, thus obtaining a linear parabolic equation.

The mathematical model then writes as

$$\begin{cases} \partial_t \rho + \nabla \cdot (\rho u) = 0, \\[2mm] \partial_t (\rho u) + \nabla \cdot (\rho u \otimes u) = f, \\[2mm] \partial_t \phi = D \Delta \phi + a\rho - \frac{1}{\tau}\phi. \end{cases} \tag{1.29}$$

The first equation in (1.29) is a mass conservation equation and corresponds to the assumption that cells do not undergo mitosis or apoptosis during the experimental phenomenon. The last equation is a diffusion equation for the chemical factor which is produced at a rate α and degrades with a half life τ.

The second equation assumes that cell motion can be obtained on the basis of a suitable force balance. Although the second term at the l.h.s. of the momentum equation reminds the convective flux of cellular matter, it should be understood as a term modeling cell persistence, their "inertia" in changing cell direction. The "force" f then models the reasons which may cause a change in cell persistence. They include

1. A chemotactic body force

$$f_{chem} = \mu \rho \nabla \phi, \tag{1.30}$$

where μ measures the intensity of cell response per unit mass. The linear dependence on ρ corresponds to the assumption that each cell experiences a similar chemotactic action. A saturation effect on the amount of chemoattractant could be included. The generalization of the model to the case of multiple species of chemical factors, characterized by different physical properties and biological actions (e.g. attraction and repulsion), is also of interest to understand how to govern the formation of the network.

2. A dissipative interaction with the substrate

$$f_{diss} = -\alpha\rho u. \tag{1.31}$$

The linear dependence of f_{diss} on ρ corresponds to the assumption that each cell is subject to the same dissipative forces.

3. As seen before a force across the surface ∇p that in this case is incompenetrability of cellular matter, to model the fact that closely packed cells resist to compression

$$f_{surf} = -\nabla[\rho\pi(\rho)], \tag{1.32}$$

where $\pi(\rho)$ is a non negative function depending on the cellular density.
After some standard algebra, it is possible to rewrite system (1.29) as

$$\begin{cases} \partial_t\rho + \nabla\cdot(\rho u) = 0, \\\\ \partial_t u + u\cdot\nabla u = \mu\nabla\phi - \alpha u - \nabla P(\rho), \\\\ \partial_t\phi = D\Delta\phi + a\rho - \frac{\phi}{\tau}, \end{cases} \tag{1.33}$$

where $P(\rho)$ is defined by

$$\rho\frac{dP}{d\rho} = \frac{d}{d\rho}(\rho\pi)$$

or

$$P = \int \frac{1}{\rho}\frac{d}{d\rho}(\rho\pi)\,d\rho,$$

and D, α, and τ, are, respectively, the diffusion coefficient, the rate of release, and the characteristic degradation time of soluble mediators.

Chapter 2

A Semilinear Hyperbolic-Parabolic Model of Chemotaxis

In this chapter we present some analytical results on a semilinear PDEs model of chemosensitive movement, which generalize the one proposed by Dolak and Hillen in [51],

$$
\begin{cases}
\partial_t u + \nabla \cdot v = 0, \\[2mm]
\partial_t v + \gamma^2 \nabla u = -b(\phi, \nabla\phi)\, v + h(\phi, \nabla\phi)\, g(u), \\[2mm]
\partial_t \phi = \Delta \phi + f(u, \phi),
\end{cases}
\tag{2.1}
$$

where $x \in \mathbb{R}^n$, $t \geq 0$, $u : \mathbb{R}^n \times \mathbb{R}^+ \to \mathbb{R}^+$ is the population density, $v = (v_1, v_2, \dots, v_n) : \mathbb{R}^n \times \mathbb{R}^+ \to \mathbb{R}^n$ are the fluxes and $\phi : \mathbb{R}^n \times \mathbb{R}^+ \to \mathbb{R}^+$ the concentration of the chemical species. The parameter γ is the characteristic speed of propagation of the cells and the source terms $b, h, g,$ and f are smooth functions.

It is a model with finite speed of propagation, based on the so-called Cattaneo system where, the typical parabolic equation for bacteria, usually used in Patlak-Keller-Segel models, is replaced by a system of hyperbolic equations. As seen in the previous chapter this model (2.1) is obtained, starting from a velocity jump process by minimizing the L^2-norm through a moment closure method.

Our aim is to study this semilinear hyperbolic-parabolic system from an analytical point of view, in order to give a rigorous analytical assessment to prototype models like (2.1), as a first step in investigation of more complex one, e.g. the quasilinear hyperbolic model for vasculogenesis studied in Chapter 3, or the model for phototrophic biofilm proposed in Chapter 6.

This chapter is focused on the study of solutions to system (2.1) with the aim to investigate their possible behavior.

With reference to the one dimensional case, a first result of local and global existence for weak solutions, under the assumption of turning rate's boundness, was proved in [80]. Recently Guarguaglini et al. in [70] have proved more general results for this model under weaker hypotheses, by showing a general result of global stability of zero constant states for the Cauchy problem and of general constant state for the Neumann problem. These results have been obtained using the linearized operators, and the accurate analysis of their nonlinear perturbations.

Proceeding along this line, in [48] we presented a global existence theorem and the asymptotic behavior for smooth solutions with small initial data to the Cauchy problem, for a simplified version

of system (2.1) in the two dimensional spatial case.

In this chapter, we will consider the multidimensional model (2.1) with generic source terms, and we will show the global existence of smooth solutions with small initial data to the Cauchy problem. Moreover we will determinate their asymptotic behavior.

The chapter is organized as follows: in the first section, we review some properties of partially dissipative hyperbolic systems, and we summarize the results obtained by Bianchini et al. in [17] about the asymptotic behavior of their smooth solutions.

In [17], the authors proposed a detailed description of the multidimensional Green function to partially dissipative system, assuming the existence of a strictly entropy and the Shizuta-Kawashima condition. The authors analyzed the behavior of the Green function for the linearized problem, decomposing it into two main terms. The first term is the diffusive one, and consists of heat kernels, while the slower term which contains the hyperbolic part.

Then in Section 2.2, we prove the local existence in time for smooth solutions to system (2.1) to the Cauchy problem, by a classical fixed point theorem, and subsequently in Section 2.4, we are able to prove the global existence result thanks to the refined decay estimates of the Green Kernel of hyperbolic equations.

We show the global existence, and we determinate the asymptotic behavior of this solutions, also for perturbation of small constant states in the case of simpler source terms. In order to prove this result, we need to slightly modified our technique to compensate the lack of polynomial decay of linear term in the hyperbolic equations.

As observed in the previous chapter, for large time hyperbolic and parabolic model are expected to have the same behavior. Then, in the last section, we first determinate the asymptotic behavior of the solutions to the parabolic Patlak-Keller-Segel model related to system (2.1), obtaining the same decay rate of the hyperbolic one. Finally, we examine the difference between solutions to the hyperbolic-parabolic system (2.1) and to the related PKS model, showing that this difference decays with a faster rate.

2.1   Partially Dissipative Hyperbolic Systems

In this first section we recall some properties of hyperbolic dissipative systems.

Let us focus our attention on the following multidimensional system of balance laws

$$
\begin{cases}
\partial_t u + \nabla \cdot v = 0, \\[2mm]
\partial_t v + \gamma^2 \nabla u = -\beta v,
\end{cases}
\tag{2.2}
$$

where $u : \mathbb{R}^n \times \mathbb{R}^+ \to \mathbb{R}^+$, $v = (v_1, v_2, \ldots, v_n) : \mathbb{R}^n \times \mathbb{R}^+ \to \mathbb{R}^n$, with initial conditions

$$u(x,0) = u_0(x), \quad v(x,0) = v_0(x).$$

We can observe that since (2.2) is equivalent to damped wave equation, the behavior of the solutions to the Cauchy problem for this system is quite well known [86]. Moreover system (2.2) belongs to the class of dissipative hyperbolic systems.

It is possible to rewrite system (2.2) in a compact form as

$$\partial_t w + \sum_{j=1}^{n} A_j \partial_{x_j} w = g(w),
\tag{2.3}$$

where $w = (u, v) \in \Omega \subseteq \mathbb{R} \times \mathbb{R}^n$, and

$$A_j = \begin{pmatrix} 0 & e_j \\ \gamma^2 e_j^t & 0 \end{pmatrix},$$

with $(A_j)_{11} \in \mathbb{R}^{1 \times 1}$, $(A_j)_{12} \in \mathbb{R}^{n \times 1}$, $(A_j)_{21} \in \mathbb{R}^{1 \times n}$, and $(A_j)_{22} \in \mathbb{R}^{n \times n}$ and e_j is the canonical j−th vector of $\mathbb{R}^n$. Here we denote the source term by

$$g(w) = \begin{pmatrix} 0 \\ q(w) \end{pmatrix} = \begin{pmatrix} 0 \\ -\beta v \end{pmatrix}, \quad \text{with } q(w) \in \mathbb{R}^n.$$

The initial condition reads

$$w(x, 0) = w_0(x). \tag{2.4}$$

By the introduction of new variables $W = (W_1, W_2)$, with

$$W_1 = u, \quad W_2 = \frac{v}{\gamma^2},$$

and a symmetric positive definite matrix A_0, defined as

$$A_0 = \begin{pmatrix} I & 0 \\ 0 & \gamma^2 I \end{pmatrix}, \tag{2.5}$$

it is possible to symmetrize system (2.3). Selecting W as new variable, our system reads

$$A_0(W)\partial_t W + \sum_{j=1}^n \bar{A}_j \partial_{x_j} W = G(\Phi(W)),$$

where

$$\bar{A}_j := A_j A_0(W) = \begin{pmatrix} 0 & \gamma^2 e_j \\ \gamma^2 e_j^t & 0 \end{pmatrix},$$

and $G(W) = g(\Phi(W)) = (0, Q(W))^t$. Let us notice that, for every $j = 1, \ldots, n$, the matrix $\bar{A}_j$ is symmetric.

In order to continue the analysis of smooth solutions for dissipative hyperbolic system let us introduce the condition of Shizuta and Kawashima [153] for hyperbolic systems.

Definition 2.1.1. *System* (2.3) *verifies condition (SK), if every eigenvector of $\sum_{j=1}^n A_j \xi_j$ is not in the null space of $Dg(0)$ for every $\xi \in \mathbb{R}^{n+1} \setminus \{0\}$.*

We can observe that system (2.3) verifies the Kawashima condition since, given an equilibrium state

$$\begin{pmatrix} u \\ 0 \end{pmatrix} \in \mathbb{R}^{n+1},$$

then the generic vector

$$\begin{pmatrix} X \\ 0 \end{pmatrix} \in \mathbb{R}^{n+1},$$

is eigenvector of $\sum_{j=1}^n A_j \xi_j$, if and only if $X = 0$.

With reference to the existence of smooth solutions to system (2.3), we recall the following result, which is a special case of the results in [17].

Theorem 2.1.2. *Let us consider the Cauchy problem* (2.3)-(2.4). *Let* $s \geq 0$. *For every* $w_0 \in H^s(\mathbb{R}^n)$, *there is a unique global solution* w *to* (2.3)-(2.4) *which verifies*

$$w \in C^0([0,\infty); H^s(\mathbb{R}^n)) \cap C^1([0,\infty); H^{s-1}(\mathbb{R}^n)),$$

and such that,

$$\sup_{0 \leq t < +\infty} \| w(t) \|_{H^s}^2 + \int_0^{+\infty} \| v(\tau) \|_{H^s}^2 \, d\tau \leq C \| w_0 \|_{H^s}^2,$$

where C *is a positive constant.*

The refined estimates of the Green Kernel of system (2.3) proposed by Bianchini et al. [17], holds for linearized dissipative system in the Conservative-Dissipative form. Then, we rewrite system (2.3) in this particular form, which will be useful in our study.

Let us consider a linear system with constant coefficients

$$w_t + \sum_{j=1}^n A_j w_{x_j} = Bw, \tag{2.6}$$

where $w = (u, v) \in \mathbb{R} \times \mathbb{R}^n$.

Definition 2.1.3. *System* (2.6) *is in Conservative-Dissipative form (C-D form) if it is symmetric, i.e.* $A_j^t = A_j$ *for all* $j = 1, \ldots, n$, *and there exists a negative definite matrix* $D \in \mathbb{R}^{n \times n}$, *such that*

$$B = \begin{pmatrix} 0 & 0 \\ 0 & D \end{pmatrix}.$$

In this case w_1 is called the conservative variable, while w_2 is the dissipative one.

Under suitable assumptions every symmetrizable dissipative system can be rewritten in the C-D form. Let us observe that system (2.3) can be easily written in the Conservative-Dissipative form by a change of variable.

Set

$$M = \begin{pmatrix} I & 0 \\ 0 & \gamma^{-1} \end{pmatrix},$$

and define the matrices of the C-D form

$$\tilde{A}_j = \begin{pmatrix} 0 & \gamma e_j \\ \gamma e_j^t & 0 \end{pmatrix}, \quad \tilde{B} = \begin{pmatrix} 0 & 0 \\ 0 & -\beta I \end{pmatrix}.$$

Setting

$$\begin{pmatrix} \tilde{w}_1 \\ \tilde{w}_2 \end{pmatrix} = M \begin{pmatrix} u \\ v \end{pmatrix} = \begin{pmatrix} u \\ \frac{v}{\gamma} \end{pmatrix}$$

and reporting in (2.2), we obtain the conservative-dissipative form for system (2.2)

$$\begin{cases} \partial_t \tilde{w}_1 + \gamma \nabla \cdot \tilde{w}_2 = 0, \\ \\ \partial_t \tilde{w}_2 + \gamma \nabla \tilde{w}_1 = -\beta \tilde{w}_2. \end{cases}$$

We will consider by now the conservative-dissipative form of system (2.2) written as:

$$\begin{cases} \partial_t u + \gamma \nabla \cdot v = 0, \\ \\ \partial_t v + \gamma \nabla u = -\beta v. \end{cases}$$

2.1.1 The Multidimensional Green Function

We present now the results on the study of the Green Kernel $\Gamma^h(x,t)$ of multidimensional dissipative hyperbolic systems done by Bianchini et al. in [17]. In their work the authors analyzed the behavior of the Green function for linearized problems, which has been decomposed into two main terms. The first term, the diffusive one, consists of heat kernel, while the slower term consists of the hyperbolic part.

In general, the form of the Green function is not explicit, but it is possible to deal with its Fourier transform. The separation of the Green kernel into various parts is done at the level of a solution operator $\Gamma(t)$ acting on $L^1 \cap L^2(\mathbb{R}^n, \mathbb{R}^{n+1})$.

They considered the Cauchy problem for the linear system in the conservative-dissipative form

$$\partial_t w + \sum_{j=1}^n A_j \partial_{x_j} w = B w, \quad w \in \mathbb{R}^{n+1}$$
$$w(0,\cdot) = w_0,$$

(2.7)

where A_j, $j = 1, \dots, n$ are symmetric matrices and

$$B = \begin{pmatrix} 0 & 0 \\ 0 & D \end{pmatrix},$$

where $D \in \mathbb{R}^{n \times n}$ is a negative definite matrix .

Set, for $\xi \in \mathbb{R}^n$,

$$A(\xi) := \sum_{j=1}^n \xi_j A_j, \quad E(i\xi) = B - i A(\xi).$$

They introduced the polar coordinates in $\mathbb{R}^n$

$$\xi = \rho\zeta, \quad \rho = |\xi|, \quad \zeta \in S^{n-1},$$

and set $E(i\rho,\zeta) = E(i\rho\zeta)$. More generally, in $\mathbb{C} \otimes S^{n-1}$,

$$E(z,\zeta) = E(z\zeta) = B - z A(\zeta).$$

Since S^{n-1} is compact, then when $E(z,\zeta)$ is considered in $\mathbb{C} \otimes S^{n-1}$, the points $z = 0$, $z = \infty$ are uniformly isolated exceptional point for all ζ, while in general there are a finite number of exceptional curves for $0 < |z| < \infty$. Exceptional points are the solutions to $det(B - zA - \lambda I)$, which is a polynomial equation with holomorphic coefficients. Thus it is possible to expand $E(z,\zeta)$ near $z = 0$ and $z = \infty$.

Since the support of Γ^h is contained in the wave cone of (2.7), then for $t \geq 0$, $\Gamma^h(\cdot,t)$ has compact support. The solution of the Cauchy problem (2.7) is given by

$$w(\cdot, t) = \Gamma^h(\cdot, t) * w_0,$$

and using the Fourier transform, we have

$$\hat{w}(\xi,t) = \widehat{\Gamma}^h(\xi,t)\hat{w}_0(\xi) = e^{E(i\xi)t}\hat{w}_0(\xi).$$

In this framework, when the condition (SK) is verified, there exists a $c > 0$ such that, if $\lambda(i\xi)$ is an eigenvalue of $E(i\xi)$, with $\xi \in \mathbb{R}^{n+1} \setminus \{0\}$, then

$$\mathscr{R}(\lambda(i\xi)) \leq -c\frac{|\xi|^2}{1 + |\xi|^2}.$$

(2.8)

Then using the previous inequaliy it is possible to obtain some decay estimates. For $a > 0$, we have

$$\|\chi(|\xi| > a)e^{E(i\xi)t}\| \le Ce^{-c\frac{a^2}{1+a^2}t},$$
$$\|\chi(|\xi| \le a)e^{E(i\xi)t}\| \le Ce^{-\frac{c}{1+a^2}|\xi|^2t}.$$

Let us introduce the following decomposition

$$w(\cdot, t) = M_a(t)w_0 + \mathcal{M}_a(t)w_0,$$

with

$$\widehat{\mathcal{M}_a}(t)w_0 = \chi(|\xi| > a)e^{E(i\xi)t}\hat{w}_0(\xi),$$

$$\widehat{M_a}(t)w_0 = \chi(|\xi| \le a)e^{E(i\xi)t}\hat{w}_0(\xi).$$

For the high frequencies it is possible to obtain

$$\|\mathcal{M}_a(t) * w_0\|_{L^2} = C\|\chi(|\xi| > a)e^{E(i\xi)t}\hat{w}_0(\xi)\|_{L^2} \le Ce^{-c\frac{a^2}{1+a^2}t}\|w_0\|_{L^2},$$

and for any derivative D^β in the space variables:

$$\|D^\beta\mathcal{M}_a(t) * w_0\|_{L^2} \le Ce^{-c\frac{a^2}{1+a^2}t}\|D^\beta w_0\|_{L^2}.$$

For the low frequencies it is possible to get,

$$
\begin{aligned}
\|D^\beta M_a(t) * w_0\|_{L^\infty} &\le& C\int_{S^{n-1}}\int_0^a e^{-\frac{c}{1+a^2}|\xi|^2t}|\xi|^\beta|\hat{w}_0(\xi)||\xi|^{n-1}d|\xi|d\zeta \\
&\le& C(a,|\beta|)\min\left\{1, t^{-\frac{n}{2}-\frac{|\beta|}{2}}\right\}\|w_0\|_{L^1} \\
\|D^\beta M_a(t) * w_0\|_{L^2} &\le& C\left(\int_{S^{n-1}}\int_0^a e^{-\frac{c}{1+a^2}|\xi|^2t}|\xi|^{2\beta}|\hat{w}_0(\xi)|^2|\xi|^{n-1}d|\xi|d\zeta\right)^{\frac{1}{2}} \\
&\le& C(a,|\beta|)\min\left\{1, t^{-\frac{n}{4}-\frac{|\beta|}{2}}\right\}\|w_0\|_{L^1}.
\end{aligned}
$$

More generally, for $\beta \in \mathbb{N}^n$ and $p \in [2, +\infty]$, the decay estimates obtained are:

$$\|D^\beta M_a(t) * w_0\|_{L^p} \le C(a,|\beta|)\min\left\{1, t^{-\frac{n}{2}(1-\frac{1}{p})-\frac{|\beta|}{2}}\right\}\|w_0\|_{L^1}.$$

In order to get more refined estimate, Bianchini et al. [17] used the Conservative-Dissipative form by expanding $E(i\xi)$ for the low frequencies.

As a matter of fact, they gave a more precise description of the behavior of the diffusive part, which is decomposed in four blocks, which decay with different decay rates. They showed that solutions have canonical projections on two different components: the conservative part and the dissipative part. The first one, which formally corresponds to the conservative part of equations in (2.7), decays in time like the heat kernel, since it corresponds to the diffusive part of the Green function. On the other side, the dissipative part is strongly influenced by the dissipation and decays at a rate $t^{-\frac{1}{2}}$ faster of the conservative one.

They studied the expansion of $E(z,\zeta) = B - zA(\zeta)$ near $z = 0$ introducing the total projector $P(z,\zeta)$ corresponding to all the eigenvalues near 0, and $P_-(z,\zeta) = I - P(z,\zeta)$ the projector corresponding to the whole family of the eigenvalues with strictly negative real part. The principal part of $P(z,\zeta)$ is

the projector $Q_0 = R_0 L_0$, the principal part of $P_-(z, \zeta)$ is $Q_- = R_- L_-$, where the projectors R_0, L_0, R_-, L_- are given by

$$L_0 = R_0^T = [I_1 \, 0], \quad L_- = R_-^T = [0 \, I_n].$$

Then they proved the following theorem, [17]:

Theorem 2.1.4. *Consider the linear PDE in the conservative-dissipative form*

$$\partial_t w + \sum_{j=1}^n A_j \partial_{x_j} w = Bw,$$

where A_j, B satisfy the assumption (SK), and let $Q_0 = R_0 L_0$, $Q_- = I - Q_0 = R_- L_-$ be the eigenprojectors on the null space and the negative definite part of B.
Then, for any function $w_0 \in L^1 \cap L^2(\mathbb{R}^n, \mathbb{R}^{n+1})$ the solution of the linear dissipative system can be decomposed as

$$w(t) = \Gamma^h(t) * w_0 = K(t) * w_0 + \mathcal{K}(t) * w_0,$$

where for any multi index β and for every $p \in [2, +\infty]$, the following estimates hold:
$K(t)$ estimates:

$$
\begin{aligned}
\|L_0 D^\beta K(t) * w_0\|_{L^p} &\leq & C(|\beta|) \min\{1, t^{-\frac{n}{2}(1-\frac{1}{p})-\frac{|\beta|}{2}}\} \|L_0 w^0\|_{L^1} \\
&+& C(|\beta|) \min\{1, t^{-\frac{n}{2}(1-\frac{1}{p})-\frac{1}{2}-\frac{|\beta|}{2}}\} \|L_- w^0\|_{L^1},
\end{aligned}
$$

$$
\begin{aligned}
\|L_- D^\beta K(t) * w_0\|_{L^p} &\leq & C(|\beta|) \min\{1, t^{-\frac{n}{2}(1-\frac{1}{p})-\frac{1}{2}-\frac{|\beta|}{2}}\} \|L_0 w^0\|_{L^1} \\
&+& C(|\beta|) \min\{1, t^{-\frac{n}{2}(1-\frac{1}{p})-1-\frac{|\beta|}{2}}\} \|L_- w^0\|_{L^1}.
\end{aligned}
$$

$\mathcal{K}(t)$ estimates:

$$\|D^\beta \mathcal{K}(t) * w_0\|_{L^2} \leq C e^{-ct} \|D^\beta w_0\|_{L^2}.$$

2.2 Local Existence of Smooth Solutions

Since our aim is to prove the global existence of smooth solutions with small initial data to the complete hyperbolic-parabolic system (2.1), a sharp results of local existence of solutions in essential for our proof. We prove this local existence of solutions to the Cauchy problem with a standard fixed point method for a more general semilinear hyperbolic-parabolic system

$$
\begin{cases}
\partial_t u + \gamma \nabla \cdot v = F_1(u, v, \phi, \nabla\phi), \\
\\
\partial_t v + \gamma \nabla u = F_2(u, v, \phi, \nabla\phi), \\
\\
\partial_t \phi = \Delta\phi + F_3(u, v, \phi, \nabla\phi),
\end{cases}
\tag{2.9}
$$

where $u, \phi : \mathbb{R}^n \times \mathbb{R}^+ \to \mathbb{R}^+$, $v = (v_1, v_2, \dots, v_n) : \mathbb{R}^n \times \mathbb{R}^+ \to \mathbb{R}^n$, $F_1, F_3 : \mathbb{R}^n \times \mathbb{R}^+ \to \mathbb{R}$ and $F_2 : (F_2^1, \dots, F_2^n) : \mathbb{R}^n \times \mathbb{R}^+ \to \mathbb{R}^n$, with $F_i(0) = 0$. We complement the system with the initial conditions

$$u(x, 0) = u_0(x), \quad v(x, 0) = v_0(x), \quad \phi(x, 0) = \phi_0(x), \tag{2.10}$$

and with the regularity assumptions

$$u_0, v_0 \in H^s(\mathbb{R}^n), \quad \phi_0 \in H^{s+1}(\mathbb{R}^n). \tag{2.11}$$

Theorem 2.2.1. *There exists $t^* > 0$, only depending on initial data, such that, under the assumptions that, for $i = 1,2,3$, F_i are locally Lipschitz maps, problem* (2.9)-(2.10)-(2.11), *has a unique local solution*

$$w = (u,v) \in C([0,t^*], H^s(\mathbb{R}^n)), \quad \phi \in C([0,t^*], H^{s+1}(\mathbb{R}^n)).$$

Proof. Thanks to the semigroup theory and the Duhamel principle it is possible to write the solutions to the hyperbolic part of (2.9) as

$$w(x,t) = S(t)w_0(x) + \int_0^t S(t-s)F(w,\phi,\nabla\phi)(s)\,ds, \tag{2.12}$$

where $w = (u,v)$, is the solution to the hyperbolic system

$$\partial_t w + \sum_{j=1}^n A_j \partial_{x_j} w = F,$$

with $F(w,\phi,\nabla\phi) = (F_1(u,v,\phi,\nabla\phi), F_2(u,v,\phi,\nabla\phi))^t$, and $\{S(t)\}_{t\geq 0}$ is the semigroup generated by the linear hyperbolic PDEs given by Theorem 2.1.2.

By the same way, the solution of the parabolic equation can be written as

$$\phi(x,t) = T(t)\phi_0(x) + \int_0^t T(t-s)F_3(w,\phi,\nabla\phi)(s)\,ds,$$

where $\{T(t)\}_{t\geq 0}$ is the semigroup generated by the linear heat equation.

Since the parabolic and hyperbolic problem have bounded solutions in $\mathbb{R}^n$ [56], we have the following estimates:

$$\|S(t)\|_{\mathscr{L}(H^s, H^s)} \leq g_1(t), \quad \|T(t)\|_{\mathscr{L}(H^{s+1}, H^{s+1})} \leq g_2(t),$$

where $g_i(t)$ are constants depending on time.

We are going to prove the local existence of solution to system (2.9) by a step procedure. At the beginning we consider smooth source terms which verify the global Lipschitz condition. In what follows we shall relax this assumption to include local Lipschitz continuity.

- Let us assume that F_i, for $i = 1,2,3$, is a smooth map which satisfies the global Lipschitz condition. Since we want to prove the existence of solutions by a fixed point method, we have to define a set where solutions will be well-defined, to prove that this is an invariant set and to built on it a contraction map.

  We will find a fixed point on (w,ϕ). Then fix $R > 0$, let us define

  $$\mathbb{K} = \left\{ \begin{array}{l} (w,\phi) \in C([0,t_0]; H^s) \times C([0,t_0]; H^{s+1}) : \|w(t) - w_0\|_{H^s} + \|\phi(t) - \phi_0\|_{H^{s+1}} \leq 2R, \\ \text{s.t.} \quad u(x,0) = u_0(x), v(x,0) = v_0(x), \phi(x,0) = \phi_0(x) \end{array} \right\}.$$

  Since we want that solutions be also in L^∞ space, by the Sobolev embedding theorem we consider H^s with $s \geq \left[\frac{n}{2}\right] + 1$.

  By assumption we know that, the source terms F_i, for $i = 1,2,3$, are C^1 functions which satisfy the global Lipschitz condition. This means,

  $$\|F_i(w_1,\phi_1,\nabla\phi_1) - F_i(w_2,\phi_2,\nabla\phi_2)\|_{H^s} \leq L(\|w_1 - w_2\|_{H^s} + \|\phi_1 - \phi_2\|_{H^s} + \|\nabla\phi_1 - \nabla\phi_2\|_{H^s}), \forall w_i, \phi_i. \tag{2.13}$$

We can observe that the set $\mathbb{K} \neq \{0\}$ because $(w_0, \phi_0) \in \mathbb{K}$. Let us now prove that $\mathbb{K}$ is an invariant set for a suitable choice of the time t_0. Taking $(w, \phi) \in \mathbb{K}$ and defining an iterative map $\Sigma(w, \phi) = (\overline{w}, \overline{\phi})$ as:

$$\overline{w}(x, t) = S(t)w_0(x) + \int_0^t S(t - s)F(w, \phi, \nabla\phi)(s)\,ds,$$

$$\overline{\phi}(x, t) = T(t)\phi_0(x) + \int_0^t T(t - s)F_3(w, \phi, \nabla\phi)(s)\,ds,$$

(2.14)

then we have to prove that $\Sigma : \mathbb{K} \to \mathbb{K}$.

Let us consider the first equality, thus

$$\|\overline{w}(t) - w_0\|_{H^s} \leq \|S(t)w_0 - w_0\|_{H^s} + \left\|\int_0^t S(t - s)F(w, \phi, \nabla\phi)(s)\,ds\right\|_{H^s}.$$

We can notice that, being $S(t)$ a strongly continuous semigroup, there exists a time t_1, small enough such that

$$\|S(t)w_0 - w_0\|_{H^s} \leq \frac{R}{2}, \quad \text{for } t \in [0, t_1].$$

By the global Lipschitz assumption follows

$$\|\overline{w}(t) - w_0\|_{H^s} \quad \leq \quad \frac{R}{2} + \left\|\int_0^t S(t - s)F(w, \phi, \nabla\phi)(s)\,ds\right\|_{H^s}$$

$$\leq \quad \frac{R}{2} + g_1(t)\, t\, L \sup_{s \in (0, t)} (\|w(s)\|_{H^s} + \|\phi(s)\|_{H^{s+1}}).$$

Since $w, \phi \in \mathbb{K}$, we deduce that

$$\|w(t)\|_{H^s} \quad \leq \quad \|w(t) - w_0\|_{H^s} + \|w_0\|_{H^s} \leq 2R + \|w_0\|_{H^s},$$

$$\|\phi(t)\|_{H^{s+1}} \quad \leq \quad \|\phi(t) - \phi_0\|_{H^{s+1}} + \|\phi_0\|_{H^{s+1}} \leq 2R + \|\phi_0\|_{H^{s+1}}.$$

Therefore

$$\|\overline{w}(t) - w_0\|_{H^s} \leq \frac{R}{2} + g_1(t)\, t L(4R + \|w_0\|_{H^s} + \|\phi_0\|_{H^{s+1}}).$$

(2.15)

Let us now estimate the parabolic equation. Since the solution can be written as

$$\overline{\phi}(x, t) = T(t)\phi_0(x) + \int_0^t T(t - s)F_3(w, \phi, \nabla\phi)(s)\,ds,$$

we can estimate

$$\|\overline{\phi}(t) - \phi_0\|_{H^{s+1}} \leq \|T(t)\phi_0 - \phi_0\|_{H^{s+1}} + \left\|\int_0^t T(t - s)F_3(w, \phi, \nabla\phi)(s)\,ds\right\|_{H^{s+1}}.$$

Let us observe that, being $T(t)$ a strongly continuous semigroup, there exists a time t_2, small enough, such that

$$\|T(t)\phi_0 - \phi_0\|_{H^{s+1}} \leq \frac{R}{2}, \text{ for } t \in [0, t_2].$$

Moreover, since for the heat kernel we have an explicit decay we get

$$\|T(t - s)F_3(w, \phi, \nabla\phi)(s)\|_{H^{s+1}} \quad \leq \quad c\|T(t - s)F_3(w, \phi, \nabla\phi)(s)\|_{L^2}$$

$$+ \sum_{|\alpha| = s+1} \|D_x^{s+1} T(t - s)F_3(w, \phi, \nabla\phi)(s)\|_{L^2}$$

$$
\begin{aligned}
&= \quad c\|T(t-s)F_3(w,\phi,\nabla\phi)(s)\|_{L^2} \\
&+ \quad \sum_{|\alpha|=s+1}\|D_x^1 T(t-s)D_x^s F_3(w,\phi,\nabla\phi)(s)\|_{L^2} \\
&\leq \quad g_2(t-s)(1+(t-s)^{-\frac{1}{2}})\|F_3(w,\phi,\nabla\phi)(s)\|_{H^s}.
\end{aligned}
$$

Then, thanks to the global Lipschitz condition we deduce

$$
\begin{aligned}
\|\overline{\phi}(t)-\phi_0\|_{H^{s+1}} &\leq \quad \frac{R}{2}+g_2(t)(t+\sqrt{t})L\sup_{s\in(0,t)}(\|w(s)\|_{H^s}+\|\phi(s)\|_{H^{s+1}}) \\
&\leq \quad \frac{R}{2}+g_2(t)(t+\sqrt{t})L(2R+\|w_0\|_{H^s}+\|\phi_0\|_{H^{s+1}}). \quad (2.16)
\end{aligned}
$$

If we sum the inequalities (2.15) and (2.16), we get

$$
\begin{aligned}
\|\overline{w}(t)-w_0\|_{H^s}+\|\overline{\phi}(t)-\phi_0\|_{H^{s+1}} &\leq \quad R+g_1(t)tL(4R+\|w_0\|_{H^s}+\|\phi_0\|_{H^{s+1}}) \\
&+ \quad g_2(t)(t+\sqrt{t})L(2R+\|w_0\|_{H^s}+\|\phi_0\|_{H^{s+1}}).
\end{aligned}
$$

Then, there will be a time $\bar{t}$, such that for $t\in(0,\bar{t}]$,

$$
\|\overline{w}(t)-w_0\|_{H^s}+\|\overline{\phi}(t)-\phi_0\|_{H^{s+1}}\leq 2R,
$$

which proves that $\mathbb{K}$ is an invariant set. We obtain our result, if we prove that the map is a contraction i.e., we need to show that:

$$
\|\Sigma(w_1,\phi_1)-\Sigma(w_2,\phi_2)\|\leq k\|(w_1,\phi_1)-(w_2,\phi_2)\| \quad \text{with } k<1.
$$

Let us define $\Sigma(w_1,\phi_1)=(\overline{w}_1,\overline{\phi}_1)$ and $\Sigma(w_2,\phi_2)=(\overline{w}_2,\overline{\phi}_2)$. Then proceeding as before

$$
\begin{aligned}
\|\overline{w}_1(t)-\overline{w}_2(t)\|_{H^s} &= \quad \left\|\int_0^t S(t-s)(F(w_1,\phi_1,\nabla\phi_1)(s)-F(w_2,\phi_2,\nabla\phi_2)(s))ds\right\|_{H^s} \\
&\leq \quad \int_0^t cg_1(t-s)L(\|w_1(s)-w_2(s)\|_{H^s}+\|\phi_1(s)-\phi_2(s)\|_{H^{s+1}})ds.
\end{aligned}
$$

Thus we obtain

$$
\|\overline{w}_1(t)-\overline{w}_2(t)\|_{H^s}\leq g_1(t)tL\sup_{s\in(0,t)}(\|w_1(s)-w_2(s)\|_{H^s}+\|\phi_1(s)-\phi_2(s)\|_{H^{s+1}}). \quad (2.17)
$$

Let us consider now the function ϕ. It is possible to estimate the difference between ϕ_1 and ϕ_2 in the H^{s+1} norms as follows

$$
\begin{aligned}
\|\overline{\phi}_1(t)-\overline{\phi}_2(t)\|_{H^{s+1}} &= \quad \left\|\int_0^t T(t-s)(F_3(w_1,\phi_1,\nabla\phi_1)(s)-F_3(w_2,\phi_2,\nabla\phi_2)(s)ds\right\|_{H^{s+1}} \\
&\leq \quad \int_0^t g_2(t-s)(1+(t-s)^{-\frac{1}{2}}L(\|w_1(s)-w_2(s)\|_{H^s}+\|\phi_1(s)-\phi_2(s)\|_{H^{s+1}})ds \\
&\leq \quad g_2(t)(t+\sqrt{t})L\sup_{s\in(0,t)}(\|w_1(s)-w_2(s)\|_{H^s}+\|\phi_1(s)-\phi_2(s)\|_{H^{s+1}}). \quad (2.18)
\end{aligned}
$$

Summing inequalities (2.17) and (2.18), we get

$$
\begin{aligned}
\|\overline{w}_1(t)&-\overline{w}_2(t)\|_{H^s}+\|\overline{\phi}_1(t)-\overline{\phi}_2(t)\|_{H^{s+1}} \\
&\leq c(g_1(t)+g_2(t))(t+\sqrt{t})L\sup_{s\in(0,t)}(\|w_1(s)-w_2(s)\|_{H^s}+\|\phi_1(s)-\phi_2(s)\|_{H^{s+1}}).
\end{aligned}
$$

Then there exists a time t^*, such that for $t \in (0, t^*)$, $L(t + \sqrt{t})(g_1(t) + g_2(t)) \le k < 1$ obtaining that:

$$\|\overline{w}_1(t) - \overline{w}_2(t)\|_{H^s} + \|\overline{\phi}_1(t) - \overline{\phi}_2(t)\|_{H^{s+1}} \le k \sup_{s \in (0,t)} (\|w_1(s) - w_2(s)\|_{H^s} + \|\phi_1(s) - \phi_2(s)\|_{H^{s+1}}).$$

Hence for small t, the contraction property of Σ holds.

Thanks to the contraction theorem, there is a fixed point of the map Σ, $\Sigma(w, \phi) = (w, \phi)$. This means that, for $t \in (0, t^*)$, system (2.9) has a smooth solution.

We can notice that, thanks to the global Lipschitz condition, it is possible to iterate this procedure obtaining a global, in time, solution to system (2.9).

- Now we will relax the condition on the source terms F_i, assuming the local Lipschitz condition, i.e.

$$\|F_i(w_1, \phi_1, \nabla\phi_1) - F_i(w_2, \phi_2, \nabla\phi_2)\|_{H^s} \le L(\|w_1 - w_2\|_{H^s} + \|\phi_1 - \phi_2\|_{H^s} + \|\nabla\phi_1 - \nabla\phi_2\|_{H^s})$$

if $\|w_i\|_{H^s}, \|\phi_i\|_{H^{s+1}} \in B_R$, for a fixed R, where $B_R := \{U = (w, \phi) : \|w\|_{H^s} + \|\phi\|_{H^{s+1}} \le R\}$.

We will consider $(w_0, \phi_0) \in B_{R_0}$, where $B_{R_0} := \{U = (w, \phi) : \|w\|_{H^s} + \|\phi\|_{H^{s+1}} \le R_0\}$ and the function $\chi \in C^\infty([0, +\infty])$, $0 \le \chi \le 1$ with $\chi = 1$ in $[0, 1)$ and supp $\chi \subseteq [0, 2]$.

Let $\varphi_R(U) = \chi(\frac{1}{R}|U|)$ and set

$$\widetilde{F}_i = \varphi(U) F_i(U) = \begin{cases} F_i & \text{on } B_R, \\ \\ 0 & \text{on } B_R^c. \end{cases}$$

We consider now the system:

$$\begin{cases} \partial_t \widetilde{u} + \gamma \nabla \cdot \widetilde{v} = \widetilde{F}_1(\widetilde{u}, \widetilde{v}, \widetilde{\phi}, \nabla\widetilde{\phi}), \\ \\ \partial_t \widetilde{v} + \gamma \nabla \widetilde{u} = \widetilde{F}_2(\widetilde{u}, \widetilde{v}, \widetilde{\phi}, \nabla\widetilde{\phi}), \\ \\ \partial_t \widetilde{\phi} = \Delta\widetilde{\phi} + \widetilde{F}_3(\widetilde{u}, \widetilde{v}, \widetilde{\phi}, \nabla\widetilde{\phi}). \end{cases} \tag{2.19}$$

Let us observe that on B_R, system (2.19) verifies a global Lipschitz condition, then from the previous proof there exists a solution $\widetilde{U} = (\widetilde{u}, \widetilde{v}, \widetilde{\phi})$ of (2.19) and it is unique for all t.

Now we want to prove that there will exists a time t_R such that $\widetilde{U}(t) \in B_R$.

Let us observe that

$$\begin{aligned} \|\widetilde{w}(t)\|_{H^s} &\le \|S(t) w_0\|_{H^s} + \left\| \int_0^t S(t-s) \widetilde{F}(\widetilde{w}, \widetilde{\phi}, \nabla\widetilde{\phi})(s) \, ds \right\|_{H^s} \\ &\le g_1(t) \|w_0\|_{H^s} + g_1(t) t L \sup_s (\|\widetilde{w}(s)\|_{H^s} + \|\widetilde{\phi}(s)\|_{H^{s+1}}). \end{aligned}$$

On the other hand, for the variable ϕ holds

$$\begin{aligned} \|\widetilde{\phi}(t)\|_{H^{s+1}} &\le \|T(t) \phi_0\|_{H^s} + \left\| \int_0^t T(t-s) \widetilde{F_3}(\widetilde{w}, \widetilde{\phi}, \nabla\widetilde{\phi}) \, ds \right\|_{H^s} \\ &\le g_2(t) \|\phi_0\|_{H^s} + g_2(t)(t + \sqrt{t}) L \sup_{s \in (0,t)} (\|\widetilde{w}(s)\|_{H^s} + \|\widetilde{\phi}(s)\|_{H^{s+1}}). \end{aligned}$$

Summing these two inequalities we obtain:

$$\|\widetilde{w}(t)\|_{H^s} + \|\widetilde{\phi}(t)\|_{H^{s+1}} \le g_1(t) \|w_0\|_{H^s} + g_2(t) \|\phi_0\|_{H^s}$$

$$+ \quad (g_1(t) + g_2(t))(t + \sqrt{t})L \sup_{s \in (0,t)} (\|\widetilde{w}(s)\|_{H^s} + \|\widetilde{\phi}(s)\|_{H^{s+1}})$$

then

$$\sup_{s \in (0,t)} (\|\widetilde{w}(s)\|_{H^s} + \|\widetilde{\phi}(s)\|_{H^{s+1}}) \quad \leq \quad \frac{1}{1 - (t + \sqrt{t})L(g_1(t) + g_2(t))}(g_1(t)\|w_0\|_{H^s} + g_2(t)\|\phi_0\|_{H^s}).$$

This implies that there will be a time t^*, such that for $t \in (0, t^*]$,

$$\sup_{s \in (0,t^*)} \|\widetilde{U}(t)\|_{H^s} = \sup_{s \in (0,t^*)} (\|\widetilde{w}(t)\|_{H^s} + \|\widetilde{\phi}(t)\|_{H^{s+1}}) \leq R.$$

Since $\widetilde{F} = F$ for $\|U\| \leq R$, by uniqueness of solution, we obtain $\widetilde{U} = U$ in $\mathbb{R}^n \times (0, t^*)$, then we have the local solution to system (2.9).

$$\square$$

2.3   Continuation Principle

In this section we prove some results which can be useful to establish the existence of global solutions to the more specific problem

$$\begin{cases} \partial_t u + \gamma \nabla \cdot v = 0, \\[2mm] \partial_t v + \gamma \nabla u = -b(\phi, \nabla\phi)v + h(\phi, \nabla\phi)g(u), \\[2mm] \partial_t \phi = \Delta\phi + f(u, \phi), \end{cases} \tag{2.20}$$

with the initial conditions

$$u(x, 0) = u_0(x), \quad v(x, 0) = v_0(x), \quad \phi(x, 0) = \phi_0(x), \tag{2.21}$$

and the regularity assumptions

$$u_0, v_0 \in H^s(\mathbb{R}^n) \cap L^1(\mathbb{R}^n), \quad \phi_0 \in H^{s+1}(\mathbb{R}^n). \tag{2.22}$$

In order to prove our results we make some assumptions on the functions b, f, g, h on the right hand side in system (2.20).

(H_b): $b \in C^{s+1}(\mathbb{R}^{n+1})$ and

$$b(z, w) = \beta + \bar{b}(z, w),$$

where $\beta > 0$, and for all fixed $K > 0$

$$|\bar{b}(z, w)| \leq B_k(|z| + |w|) \quad \text{for all } z, w \in [-K, K],$$

where B_k is a suitable constant depending on K.

(H_h): $h \in C^{s+1}(\mathbb{R}^{n+1})$ and $h(0, 0) = 0$. In particular for all fixed $K > 0$ with

$$|h(z, w)| \leq H_k(|z| + |w|) \quad \text{for all } z, w \in [-K, K],$$

where H_k is a suitable constant depending on K.

$$\overline{\overline{h(\phi, \nabla\phi) g(u)}}$$

$$\chi \nabla\phi\, u$$

$$\frac{\chi}{(1+\alpha\phi)} \nabla\phi\, u$$

$$\frac{\chi(\beta+1)}{(\beta+\phi)} \nabla\phi\, u$$

$$\chi \nabla\phi\, u(1 - \frac{u}{\gamma})$$

$$\chi \frac{1}{c} tanh(\frac{c\nabla\phi}{1+c})\, u$$

Table 2.1: Sensitivity Functions $h(\phi, \nabla\phi) g(u)$ from literature [79]. c, β, χ, γ are constants.

(H_g): $g \in C^{s+1}(\mathbb{R})$ and $g(0) = 0$. For all fixed $K > 0$ with

$$|g(z)| \le G_k |z| \quad \text{for all } z \in [-K, K],$$

where G_k is a suitable constant depending on K.

Let us notice that this general sensitivity function, $h(\phi, \nabla\phi) g(u)$, covers different possible relations between species and chemical substance present in chemotaxis models as reported in Table 2.1.

(H_f): $f \in C^{s+1}(\mathbb{R}^2)$ and

$$f(z, w) = az - bw + \bar{f}(z, w),$$

where $a, b > 0$, and for all fixed $K > 0$,

$$|\bar{f}(z, w)| \le F_k(|z|^2 + |w|^2) \quad \text{for all } z, w \in [-K, K],$$

where F_k is a suitable constant depending on K.

By these assumptions, we are led to consider the system

$$\begin{cases} \partial_t u + \gamma \nabla \cdot v = 0, \\[2mm] \partial_t v + \gamma \nabla u = -\beta v - \bar{b}(\phi, \nabla\phi) v + h(\phi, \nabla\phi) g(u), \\[2mm] \partial_t \phi = \Delta\phi + au - b\phi + \bar{f}(u, \phi). \end{cases} \quad (2.23)$$

It is possible to rewrite the above system as

$$\begin{cases} \partial_t w + \sum_{j=1}^{n} A_j \partial_{x_j} w = Bw + \bar{B}(\phi, \nabla\phi) w + H(\phi, \nabla\phi, w), \\[2mm] \partial_t \phi = \Delta\phi + au - b\phi + \bar{f}(u, \phi), \end{cases} \quad (2.24)$$

where

$$A_j = \begin{pmatrix} 0 & \gamma e_j \\ \gamma e_j^t & 0 \end{pmatrix}, \quad B = \begin{pmatrix} 0 & 0 \\ 0 & -\beta \end{pmatrix},$$

and

$$\bar{B}(\phi, \nabla\phi) = \begin{pmatrix} 0 \\ -\bar{b}(\phi, \nabla\phi) \end{pmatrix}, \quad H(\phi, \nabla\phi, w) = \begin{pmatrix} 0 \\ h(\phi, \nabla\phi)g(w) \end{pmatrix}.$$

Thanks to the regularity of source terms, the local Lipschitz condition yields. Then we can apply Theorem 2.2.1 and deduce the local existence of solution to (2.23).

Before proceeding in our study of global existence of solutions we recall some well-known inequalities in the Sobolev spaces [160].

Proposition 2.3.1. *Let* $u, v \in H^s(\mathbb{R}^n) \cap L^\infty(\mathbb{R}^n)$, $\quad s > 0$, $\quad |\beta| \leq s$, *then*

$$\|D^\beta(uv)\|_{L^2} \leq c(\|u\|_{L^\infty}\|D^\beta v\|_{L^2} + \|v\|_{L^\infty}\|D^\beta u\|_{L^2}).$$

If $u, v \in H^{s+|\beta|}(\mathbb{R}^n)$,

$$\|D^\beta(uv)\|_{H^s} \leq c(\|u\|_{L^\infty}\|D^\beta v\|_{H^s} + \|v\|_{L^\infty}\|D^\beta u\|_{H^s}),$$

if $\beta = 0$, *then*

$$\|uv\|_{L^2} \leq \|u\|_{L^2}\|v\|_{L^\infty}.$$

Proposition 2.3.2. *Let* F *be smooth and assume* $F(0) = 0$. *Then, for* $u \in H^s(\mathbb{R}^n) \cap L^\infty(\mathbb{R}^n)$

$$\|F(u)\|_{H^s} \leq C_s(\|u\|_{L^\infty})(1 + \|u\|_{H^s}).$$

Proposition 2.3.3. *Let* $u \in H^s(\mathbb{R}^n) \cap L^\infty(\mathbb{R}^n)$ $(s \geq 1)$ *such that there exists* $\gamma_0 > 0$ *that for* $(x, t) \in \mathbb{R}^n \times [0, +\infty)$,

$$|u(x, t)| \leq \gamma_0.$$

Then for every smooth function h

$$\|D^\beta h(u)\|_{L^2} \leq C_\beta \|h'\|_{C^{|\beta|-1}(|u|\leq\gamma_0)}\|u\|_{L^\infty}^{|\beta|-1}\|D^\beta u\|_{L^2},$$

with $\beta \neq 0, |\beta| \leq s$.

Now we are going to prove the existence of global solutions of perturbation to problem (2.23)-(2.21)-(2.22) using the following Continuation Principle.

Proposition 2.3.4. *Let* $T < +\infty$ *be the maximal time of existence for a local solution* (w, ϕ) *to system* (2.23)-(2.21)-(2.22). *Then*

$$\limsup_{t \to T^-} \|w(t)\|_{H^s} + \|\phi(t)\|_{H^{s+1}} = +\infty.$$

Proof. Let (w, ϕ) be a given local smooth solution on a maximal time interval $(0, T_{max})$.
Let $T > T_{max}$ and assume there exists an a priori bound

$$R := \sup_{(0,T)} \max\{\|\phi\|_{H^{s+1}}, \|w\|_{H^s}\}.$$

Let $t_R > 0$ be the maximal time of existence of solutions to the Cauchy problem, with $\|w_0\|_{H^s}$, $\|\phi_0\|_{H^{s+1}} \leq R$.
Then, there exists $\bar{t} \in (T - \frac{t_R}{2}, T)$ such that, we can consider the functions $w(x, \bar{t}) \in H^s(\mathbb{R}^n)$ and $\phi(x, \bar{t}) \in H^{s+1}(\mathbb{R}^n)$ as initial data for a new Cauchy problem, with maximal time of existence $\overline{T} = \bar{t} + t_R > T_{max}$, and we find a contradiction. $\qquad\square$

From the previous result, it is enough to estabilish an a priori H^s, H^{s+1} bound to give the global existence. Beside we can notice that to prove the global existence result, it is enough to prove the boundness of L^∞-norm of functions (w, ϕ), as proved by the following Lemma.

Lemma 2.3.5. *Let* $(w, \phi) \in C([0, t), (H^s(\mathbb{R}^n)) \times C([0, t), H^{s+1}(\mathbb{R}^n))$ *a solution of (2.23) for* $0 \le t \le T$, *where* $\|w(t)\|_{L^\infty}, \|\phi(t)\|_{W^{1,\infty}} \le K$, *then there will exist a constant* C_k *such that,*

$$\|w(t)\|_{H^s} + \|\phi(t)\|_{H^{s+1}} \le c(\|w_0\|_{H^s} + \|\phi_0\|_{H^{s+1}})e^{C_k t}, \qquad 0 \le t \le T.$$

Proof. Let $\|w(t)\|_{L^\infty}, \|\phi(t)\|_{W^{1,\infty}} \le K$, then we want to prove that H^s norms of these functions are bounded.

Thanks to the Duhamel's formula we can write the solution of the hyperbolic part as

$$w(x, t) = (\Gamma^h(t) * w_0)(x) + \int_0^t \Gamma^h(t - s) * (\bar{B}(\phi, \nabla\phi)(s)w(s) + H(\phi, \nabla\phi, w)(s))\,ds,$$

where Γ^h is the Green function of system (2.2). Then

$$
\begin{aligned}
\|w(t)\|_{H^s} &\le \|\Gamma^h(t) * w_0\|_{H^s} + \int_0^t \|\Gamma^h(t - s) * (\bar{B}(\phi, \nabla\phi)w(s) + H(\phi, \nabla\phi, w)(s))\|_{H^s}\,ds \\
&\le C\|w_0\|_{H^s} + \int_0^t C\|\bar{B}(\phi, \nabla\phi)(s)w(s)\|_{H^s} + \|H(\phi, \nabla\phi, w)(s)\|_{H^s}\,ds,
\end{aligned}
$$

by Proposition 2.3.1 we deduce

$$
\begin{aligned}
\|w(t)\|_{H^s} \le &C\|w_0\|_{H^s} + C\int_0^t (\|\bar{b}(\phi, \nabla\phi)(s)\|_{L^\infty}\|w(s)\|_{H^s} + \|w(s)\|_{L^\infty}\|\bar{b}(\phi, \nabla\phi)(s)\|_{H^s}\,ds \\
&+ C\int_0^t \|h(\phi, \nabla\phi)(s)\|_{L^\infty}\|g(w)\|_{H^s} + \|h(\phi, \nabla\phi)(s)\|_{H^s}\|g(w)\|_{L^\infty}\,ds.
\end{aligned}
$$

Let us observe that, by assumptions $(H_b),(H_f),(H_g),(H_h)$ and Proposition 2.3.3, we have

$$
\begin{aligned}
\|g(w)\|_{H^s} &\le C\|g(w)\|_{L^2} + C_{\bar{g}'}\|w\|_{L^\infty}^{s-1}\|D^s w\|_{L^2} \le CG_k\|w\|_{L^2} + C_{\bar{g}'}\|w\|_{L^\infty}^{s-1}\|w\|_{H^s}.
\end{aligned}
$$

$$
\begin{aligned}
\|h(\phi, \nabla\phi)\|_{H^s} &\le H_k(\|\phi\|_{L^2} + \|\nabla\phi\|_{L^2}) + C_{\bar{b}'}\|(\phi, \nabla\phi)\|_{L^\infty}^{s-1}\sum_{|\alpha|=s}\|D^s(\phi, \nabla\phi)\|_{L^2} \\
&\le C[H_k(\|\phi\|_{L^2} + \|\nabla\phi\|_{L^2}) + C_{\bar{h}'}K^{s-1}\|\phi\|_{H^{s+1}}].
\end{aligned}
$$

$$
\begin{aligned}
\|\bar{b}(\phi, \nabla\phi)\|_{H^s} &\le C[B_k(\|\phi\|_{L^2} + \|\nabla\phi\|_{L^2}) + C_{\bar{b}'}K^{s-1}\|\phi\|_{H^{s+1}}].
\end{aligned}
$$

$$
\begin{aligned}
\|\bar{f}(u, \phi)\|_{H^s} &\le c\|\bar{f}(u, \phi)\|_{L^2} + \sum_{|\alpha|=s}\|D_x^\alpha \bar{f}(u, \phi)\|_{L^2} \\
&\le C[F_k(\|u\|_{L^2}\|u\|_{L^\infty} + \|\phi\|_{L^2}\|\phi\|_{L^\infty}) + C_{\bar{f}'}K^{s-1}(\|\phi\|_{H^s} + \|u\|_{H^s})].
\end{aligned}
$$

By previous inequalities we get

$$
\begin{aligned}
\|w(t)\|_{H^s} \le &c(\|w_0\|_{H^s} + \int_0^t (B_k + H_k G_k)(\|\phi(s)\|_{L^\infty} + \|\nabla\phi(s)\|_{L^\infty})\|w(s)\|_{H^s}\,ds \\
&+ \int_0^t (B_k + H_k G_k)\|w(s)\|_{L^\infty}(\|\phi(s)\|_{L^2} + \|\nabla\phi(s)\|_{L^2})\,ds \\
&+ \int_0^t \|w(s)\|_{L^\infty}(C_{\bar{b}'} + C_{\bar{h}'})K^{s-1}(\|\phi\|_{H^s} + \|\nabla\phi\|_{H^s})\,ds.
\end{aligned}
$$

The last relation can be written as:

$$\|w(t)\|_{H^s} \le C\left(\|w_0\|_{H^s} + \int_0^t M_k(\|\phi\|_{H^{s+1}} + \|w(s)\|_{H^s})\,ds\right), \tag{2.25}$$

where the constant M_k depends on K and $C_{b'}$, $C_{h'}$.

Let us consider now the solution of the parabolic equation, that thanks to Duhamel's formula we can write as

$$\phi(x,t) = (e^{-bt}\Gamma^p(t) * \phi_0)(x) + \int_0^t e^{-b(t-s)}\Gamma^p(t-s) * (au(s) + \bar{f}(u,\phi)(s))\,ds.$$

Then, we can estimate the H^{s+1}-norm of ϕ as follows

$$
\begin{aligned}
\|\phi(t)\|_{H^{s+1}} &\le \|e^{-bt}\Gamma^p(t) * \phi_0\|_{H^{s+1}} + \int_0^t \|e^{-b(t-s)}\Gamma^p(t-s)*au(s) + \bar{f}(u,\phi)(s)\,ds\|_{H^{s+1}} \\
&\le C\|\phi_0\|_{H^{s+1}} + \int_0^t a\|w(s)\|_{H^s} + (1 + (t-s)^{-\frac{1}{2}})\|\bar{f}(u,\phi)(s)\|_{H^s}\,ds \\
&\le C\|\phi_0\|_{H^{s+1}} + D_k\int_0^t (1 + (t-s)^{-\frac{1}{2}})\|w(s)\|_{H^s} + \|\phi(s)\|_{H^{s+1}}\,ds,
\end{aligned}
$$

where the constant D_k depends on K and $C_{f'}$. If we sum the last inequality and (2.25) we obtain

$$
\begin{aligned}
\|w(t)\|_{H^s} + \|\phi(t)\|_{H^{s+1}} &\le C(\|\phi_0\|_{H^{s+1}} + \|w_0\|_{H^s}) \\
&\quad + \int_0^t (1 + (t-s)^{-\frac{1}{2}})(D_k + M_k)(\|w(s)\|_{H^s} + \|\phi(s)\|_{H^{s+1}})\,ds.
\end{aligned}
$$

Applying Gronwall's Lemma we easily deduce

$$\|w(t)\|_{H^s} + \|\phi(t)\|_{H^{s+1}} \le \tilde{c}(\|w_0\|_{H^s} + \|\phi_0\|_{H^{s+1}})e^{(D_k+M_k)(t+\sqrt{t})}. \tag{2.26}$$

$\square$

Moreover it is also possible to verify that the boundedness of $\|\phi\|_{W^{1,\infty}}$, implies the boundedness of $\|w\|_{L^\infty}$. Indeed we have

$$
\begin{aligned}
\|w(t)\|_{L^\infty} &= \left\|\Gamma^h(t) * w_0 + \int_0^t \Gamma^h(t-s) * (\bar{B}(\phi,\nabla\phi)(s)w(s) + H(\phi,\nabla\phi,w)(s))\right\|_{L^\infty}\,ds \\
&\le C\|w_0\|_{L^\infty} + \int_0^t C(\|\bar{B}(\phi,\nabla\phi)w(s)\|_{L^\infty} + \|H(\phi,\nabla\phi,w)(s)\|_{L^\infty})\,ds,
\end{aligned}
$$

and by assumptions (H_b), (H_h), and $\|\phi\|_{W^{1,\infty}} \le K$ we get

$$\|w(t)\|_{L^\infty} \le C\|w_0\|_{L^\infty} + \int_0^t C(B_k + H_kG_k)(\|\nabla\phi(s)\|_{L^\infty} + \|\phi(s)\|_{L^\infty})\|w(s)\|_{L^\infty}\,ds.$$

Applying as before the Gronwall's Lemma we get

$$\|w(t)\|_{L^\infty} \le \tilde{c}\|w_0\|_{L^\infty}e^{t(C(B_k+H_kG_k)K)}.$$

In the proof of global existence we are not going to use this remark, but it could be useful for more general results.

2.4 Global Existence and Asymptotic Behavior of Smooth Solutions

In this section our aim is to prove the boundedness of solutions to system (2.23) for every time t. Once that this result will be obtained, we could easily prove the global existence of solutions by Lemma 2.3.5 and Continuation Principle 2.3.4. The estimates are built up on sharp decay estimates, obtained by Theorem 2.1.4 for the Green function of the hyperbolic operator and the known decay of the heat kernel.

Let us observe that by this approach, we get simultaneously the boundedness of L^∞-norm of solutions and also their decay rates. Given $\delta > 0$, let us define for a given function g the functionals

$$M_g^\delta(t) = \sup_{(0,t)}(\max\{1, s^\delta\}\|g(s)\|_{L^2})$$

$$N_g^\delta(t) = \sup_{(0,t)}(\max\{1, s^\delta\}\|g(s)\|_{L^\infty}).$$

Moreover let us denote by D_x^s any space derivative D_x^α, such that $|\alpha| = s$.

Before starting our proof, let us recall an useful lemma [17]:

Lemma 2.4.1. *For any $\gamma, \delta \geq 0$, $t \geq 2$*

$$\nu := \min\{\gamma, \delta, \gamma + \delta - 1\},$$

it holds

$$\int_0^t \min\{1, (t-s)^{-\gamma}\}\min\{1, s^{-\delta}\}\,ds \leq C \cdot \begin{cases} \min\{1, t^{-\nu}\}, & \gamma, \delta \neq 1, \\ \min\{1, t^{-\nu}(1 + \ln t)\}, & \gamma \leq 1, \delta = 1 \text{ or } \gamma = 1, \delta \leq 1, \\ \min\{1, t^{-1}\}, & \gamma > 1, \delta = 1 \text{ or } \gamma = 1, \delta > 1, \end{cases}$$

$$\int_0^t \min\{1, s^{-\delta}\}\,ds \leq C \cdot \begin{cases} 1, & \delta > 1, \\ \ln t, & \delta = 1, \\ t^{1-\delta}, & 0 \leq \delta < 1, \end{cases}$$

$$\int_0^t e^{-c(t-s)}\min\{1, s^{-\delta}\}\,ds \leq C\min\{1, s^{-\delta}\}, \quad \gamma \geq 0.$$

2.4.1 Decay Estimates for the Chemoattractant

We can collect the estimate referred to the function ϕ in the following proposition.

Proposition 2.4.2. *Let (u, v, ϕ) be the solution of system* (2.23)-(2.21)-(2.22), *under the assumptions* $(H_b),(H_f), (H_g), (H_h)$. *Let $K, T > 0$ such that for $t \in (0, T)$, $\|u(t)\|_{L^\infty}$, $\|\phi(t)\|_{W^{1,\infty}} \leq K$. Then for $t \in (0, t)$,*

$$N_{D_x^1\phi}^{\frac{n}{2}}(t) \quad \leq \quad C\left(\|D_x\phi_0\|_{L^\infty} + (1 + F_k K)N_u^{\frac{n}{2}}(t) + F_k K N_\phi^{\frac{n}{2}}(t)\right),$$

$$M_{D_x^{s+1}\phi}^{\tilde{\delta}}(t) \quad \leq \quad C\left(\|D_x^{s+1}\phi_0\|_{L^2} + (1 + C_k)M_{D_x^s u}^{\tilde{\delta}}(t) + C_k M_{D_x^s\phi}^{\tilde{\delta}}(t)\right),$$

where $\tilde{\delta} = \min\{\frac{n}{4} + \frac{1}{2} + \frac{s}{2}, \frac{n}{2}\}$, and the constant C_k depends on K and C_f'. Moreover, if K is sufficiently small, then we have

$$N_\phi^{\frac{n}{2}}(t) \quad \leq \quad C\left(\|\phi_0\|_{L^\infty} + (1 + F_k K)N_u^{\frac{n}{2}}(t)\right),$$

$$M_\phi^{\frac{n}{4}}(t) \quad \leq \quad C\left(\|\phi_0\|_{L^2} + (1 + F_k K)M_u^{\frac{n}{4}}(t)\right),$$

$$M_{D_x^s\phi}^{\tilde{\delta}}(t) \quad \leq \quad C\left(\|D_x^s\phi_0\|_{L^2} + (1 + C_k)M_{D_x^s u}^{\tilde{\delta}}(t)\right).$$

Proof. Fix $K > 0$ large enough and let $T > 1$. Take a solution to system (2.23) such that $\|u\|_{L^\infty(\mathbb{R}^n \times (0,T))}$, $\|\phi\|_{W^{1,\infty}(\mathbb{R}^n \times (0,T))} \leq \frac{K}{2}$, this is possible provided that the initial data are suitably small. Thanks to the Duhamel's formula it is possible to write the function ϕ as

$$\phi(x, t) = (e^{-bt}\Gamma^p(t) * \phi_0)(x) + \int_0^t e^{-b(t-s)}\Gamma^p(t-s) * (\alpha u(s) + \bar{f}(u, \phi)(s)) ds. \qquad (2.27)$$

Now we proceed in estimating the function in the different norms. Let us start with the L^∞-norm

L^∞-estimate for ϕ

By the previous equations, we have

$$
\begin{aligned}
\|\phi(t)\|_{L^\infty} &\leq e^{-bt}\|\Gamma^p(t) * \phi_0\|_{L^\infty} + \int_0^t e^{-b(t-s)}\|\Gamma^p(t-s) * (\alpha u(s) + \bar{f}(u, \phi)(s))\|_{L^\infty} ds \\
&\leq e^{-bt}\|\phi_0\|_{L^\infty} + \int_0^t e^{-b(t-s)}\|\Gamma^p(t-s)\|_{L^1}\|(\alpha u(s) + \bar{f}(u, \phi)(s))\|_{L^\infty} ds \\
&\leq Ce^{-bt}\|\phi_0\|_{L^\infty} + \int_0^t Ce^{-b(t-s)}((\alpha + KF_k)\|u(s)\|_{L^\infty} + KF_k\|\phi(s)\|_{L^\infty}) ds.
\end{aligned}
$$

Let us multiply by $\min\{1, s^{-\frac{n}{2}}\}\max\{1, s^{\frac{n}{2}}\} = 1$, which yields,

$$
\begin{aligned}
\|\phi(t)\|_{L^\infty} &\leq C\left(e^{-bt}\|\phi_0\|_{L^\infty} + (1 + KF_k)N_u^{\frac{n}{2}}(t)\int_0^t e^{-b(t-s)}\min\{1, s^{-\frac{n}{2}}\} ds \right. \\
&\quad + \left. KF_k N_\phi^{\frac{n}{2}}(t)\int_0^t e^{-b(t-s)}\min\{1, s^{-\frac{n}{2}}\} ds \right).
\end{aligned}
$$

Thanks to Lemma 2.4.1, we easily deduce

$$\|\phi(t)\|_{L^\infty} \leq C\left(e^{-bt}\|\phi_0\|_{L^\infty} + (1 + F_k L)\min\{1, t^{-\frac{n}{2}}\}N_u^{\frac{n}{2}}(t) + F_k L\min\{1, t^{-\frac{n}{2}}\}N_\phi^{\frac{n}{2}}(t) \right). \qquad (2.28)$$

L^∞-estimate for $D_x^1\phi$

Proceeding in a similar way, we get

$$
\begin{aligned}
\|D_x^1\phi(t)\|_{L^\infty} &\leq \|D_x^1(e^{-bt}\Gamma^p(t) * \phi_0)\|_{L^\infty} + \int_0^t \|D_x^1(e^{-b(t-s)}\Gamma^p(t-s) * (\alpha u(s) + \bar{f}(u, \phi)(s))\|_{L^\infty} ds \\
&\leq e^{-bt}\|D_x^1(\Gamma^p(t) * \phi_0)\|_{L^\infty} + \int_0^t e^{-b(t-s)}\|D_x^1(\Gamma^p(t-s) * (\alpha u(s) + \bar{f}(u, \phi)(s))\|_{L^\infty} ds \\
&\leq e^{-bt}\|\Gamma^p(t)\|_{L^1}\|D_x^1\phi_0\|_{L^\infty} + \int_0^t e^{-b(t-s)}\|D_x^1\Gamma^p(t-s)\|_{L^1}\|\alpha u(s) + \bar{f}(u, \phi)(s)\|_{L^\infty} ds \\
&\leq Ce^{-bt}\|D_x^1\phi_0\|_{L^\infty} + \int_0^t Ce^{-b(t-s)}(t-s)^{-\frac{1}{2}}((\alpha + KF_k)\|u(s)\|_{L^\infty} + KF_k\|\phi(s)\|_{L^\infty}) ds \\
&\leq C\left[e^{-bt}\|D_x^1\phi_0\|_{L^\infty} + (1 + KF_k)N_u^{\frac{n}{2}}(t)\int_0^t e^{-b(t-s)}(t-s)^{-\frac{1}{2}}\min\{1, s^{-\frac{n}{2}}\} ds \right. \\
&\quad + \left. KF_k N_\phi^{\frac{n}{2}}(t)\int_0^t e^{-b(t-s)}(t-s)^{-\frac{1}{2}}\min\{1, s^{-\frac{n}{2}}\} ds \right].
\end{aligned}
$$

In order to complete our estimate, we need to estimate the integral

$$\int_0^t e^{-b(t-s)}(t-s)^{-\frac{1}{2}}\min\{1, s^{-\frac{n}{2}}\} ds.$$

It can be splitted in two parts as

$$\int_0^t e^{-b(t-s)}(t-s)^{-\frac{1}{2}}\min\{1,s^{-\frac{n}{2}}\}ds = \int_0^{t-1} e^{-b(t-s)}(t-s)^{-\frac{1}{2}}\min\{1,s^{-\frac{n}{2}}\}ds$$
$$+ \int_{t-1}^t e^{-b(t-s)}(t-s)^{-\frac{1}{2}}\min\{1,s^{-\frac{n}{2}}\}ds.$$

Let us start from the first integral. Since $1 \le t-s \le t$, by Lemma 2.4.1 we get

$$\int_0^{t-1} e^{-b(t-s)}(t-s)^{-\frac{1}{2}}\min\{1,s^{-\frac{n}{2}}\}ds \le \int_0^{t-1} e^{-b(t-s)}\min\{1,s^{-\frac{n}{2}}\}ds \le C\min\{1,|t-1|^{-\frac{n}{2}}\}.$$

While for the second integral, we consider the change of variable $\theta = t - s$, then

$$\int_{t-1}^t e^{-b(t-s)}(t-s)^{-\frac{1}{2}}\min\{1,s^{-\frac{n}{2}}\}ds = \int_0^1 e^{-b\theta}\theta^{-\frac{1}{2}}\min\{1,(t-\theta)^{-\frac{n}{2}}\}d\theta \le C\min\{1,|t-1|^{-\frac{n}{2}}\}.$$

Therefore, we obtain

$$\int_0^t e^{-b(t-s)}(t-s)^{-\frac{1}{2}}\min\{1,s^{-\frac{n}{2}}\}ds \le C\min\{1,|t-1|^{-\frac{n}{2}}\}.$$

Thus the estimates of the L^∞-norm of the first derivative is given by

$$\|D_x^1\phi(t)\|_{L^\infty} \le C\left(e^{-bt}\|D_x^1\phi_0\|_{L^\infty} + (1+KF_k)N_u^{\frac{n}{2}}(t)\min\{1,|t-1|^{-\frac{n}{2}}\} + KF_kN_\phi^{\frac{n}{2}}(t)\min\{1,|t-1|^{-\frac{n}{2}}\}\right).$$
$$(2.29)$$

From the last inequality and (2.28) follows that the functionals $N_\phi^{\frac{n}{2}}$ and $N_{D_x^1\phi}^{\frac{n}{2}}$, can be estimated as

$$N_\phi^{\frac{n}{2}}(t) \le C\left(\|\phi_0\|_{L^\infty} + (1+F_kK)N_u^{\frac{n}{2}}(t) + F_kKN_\phi^{\frac{n}{2}}(t)\right).$$

$$N_{D_x^1\phi}^{\frac{n}{2}}(t) \le C\left(\|D_x\phi_0\|_{L^\infty} + (1+F_kK)N_u^{\frac{n}{2}}(t) + F_kKN_\phi^{\frac{n}{2}}(t)\right). \qquad (2.30)$$

Moreover, if K is sufficiently small, then we have:

$$N_\phi^{\frac{n}{2}}(t) \le C\left(\|\phi_0\|_{L^\infty} + (1+F_kK)N_u^{\frac{n}{2}}(t)\right). \qquad (2.31)$$

L^2-estimate for ϕ

We estimate now the function ϕ and its derivatives in the L^2-norm. Let us start from the L^2 estimate for ϕ. By the Duhamel's formula (2.27), follows

$$\|\phi(t)\|_{L^2} \le \|e^{-bt}\Gamma^p(t) * \phi_0\|_{L^2} + \int_0^t \|e^{-b(t-s)}\Gamma^p(t-s) * (\alpha u(s) + \bar{f}(u,\phi)(s))\|_{L^2}ds$$

$$\le e^{-bt}\|\Gamma^p(t)\|_{L^1}\|\phi_0\|_{L^2} + \int_0^t e^{-b(t-s)}(\|\Gamma^p(t-s)\|_{L^1}\|\alpha u(s) + \bar{f}(u,\phi)(s)\|_{L^2}ds$$

$$\le C(e^{-bt}\|\phi_0\|_{L^2} + \int_0^t e^{-b(t-s)}(\|u(s)\|_{L^2} + F_kK(\|u(s)\|_{L^2} + \|\phi(s)\|_{L^2}))ds$$

$$\le C(e^{-bt}\|\phi_0\|_{L^2} + (1+F_kK)M_u^{\frac{n}{4}}(t)\int_0^t e^{-b(t-s)}\min\{1,s^{-\frac{n}{4}}\}ds$$

$$+ F_kKM_\phi^{\frac{n}{4}}(t)\int_0^t e^{-b(t-s)}\min\{1,s^{-\frac{n}{4}}\}ds).$$

Proceeding as done before, by Lemma 2.4.1 we obtain

$$\|\phi(t)\|_{L^2} \le C\left(e^{-bt}\|\phi_0\|_{L^2} + (1+F_kK)M_u^{\frac{n}{4}}(t)\min\{1,t^{-\frac{n}{4}}\} + F_kKM_\phi^{\frac{n}{4}}(t)\min\{1,t^{-\frac{n}{4}}\}\right). \quad (2.32)$$

Then, for the related functional, the following estimate yields

$$M_\phi^{\frac{n}{4}}(t) \le C\left(\|\phi_0\|_{L^2} + (1 + F_k K)M_u^{\frac{n}{4}}(t) + F_k K M_\phi^{\frac{n}{4}}(t)\right).$$

Also in this case, if K is sufficiently small, then

$$M_\phi^{\frac{n}{4}}(t) \quad \le \quad C\left(\|\phi_0\|_{L^2} + (1 + F_k K)M_u^{\frac{n}{4}}(t)\right). \tag{2.33}$$

L^2-**estimate for** $D_x^s \phi$

Let us proceed estimating the L^2−norm of the s-derivative the function ϕ. By the Duhamel's formula, we obtain in a similar way

$$
\begin{aligned}
\|D_x^s \phi(t)\|_{L^2} \quad &\le \quad e^{-bt}\|D_x^s \Gamma^p(t) * \phi_0\|_{L^2} + \int_0^t e^{-b(t-s)}\|D_x^s \Gamma^p(t-s) * (\alpha u(s) + \bar{f}(u,\phi)(s))\|_{L^2}\,ds \\
&\le \quad Ce^{-bt}\|D_x^s \phi_0\|_{L^2} + \int_0^t Ce^{-b(t-s)}(\|D_x^s u(s)\|_{L^2} + \|D_x^s \bar{f}(u,\phi)(s)\|_{L^2})\,ds \\
&\le \quad Ce^{-bt}\|D_x^s \phi_0\|_{L^2} + \int_0^t Ce^{-b(t-s)}(\|D_x^s u(s)\|_{L^2} + C_{\bar{f}'}K^{s-1}(\|D_x^s \phi(s)\|_{L^2} + \|D_x^s u(s)\|_{L^2})).
\end{aligned}
$$

Using Lemma 2.4.1 we deduce:

$$
\begin{aligned}
\|D_x^s \phi(t)\|_{L^2} \quad &\le \quad C\Big(e^{-bt}\|D_x^s \phi_0\|_{L^2} + (1 + 2C_{f'}K^{s-1})M_{D_x^s u}^{\tilde{\delta}}(t)\min\{1, t^{-\tilde{\delta}}\} \\
&\quad + \quad 2C_{f'}K^{s-1}M_{D_x^s \phi}^{\tilde{\delta}}(t)\min\{1, t^{-\tilde{\delta}}\}\Big),
\end{aligned}
$$

where $\tilde{\delta} = \min\left\{\frac{n}{4} + \frac{1}{2} + \frac{s}{2}, \frac{n}{2}\right\}$. Then, for the related functional we have

$$M_{D_x^s \phi}^{\tilde{\delta}}(t) \le C\left(\|D_x^s \phi_0\|_{L^2} + (1 + C_k)M_{D_x^s u}^{\tilde{\delta}}(t) + C_k M_{D_x^s \phi}^{\tilde{\delta}}(t)\right)$$

and, if K is sufficiently small, then

$$M_{D_x^s \phi}^{\tilde{\delta}}(t) \le C\left(\|D_x^s \phi_0\|_{L^2} + (1 + C_k)M_{D_x^s u}^{\tilde{\delta}}(t)\right). \tag{2.34}$$

L^2-**estimate for** $D_x^{s+1} \phi$

Finally we estimate the L^2-norm of the $s + 1$-derivative of ϕ. As done before

$$
\begin{aligned}
\|D_x^{s+1} \phi(t)\|_{L^2} \quad &\le \quad e^{-bt}\|D_x^{s+1}\Gamma^p(t) * \phi_0\|_{L^2} + \int_0^t e^{-b(t-s)}\|D_x^{s+1}\Gamma^p(t-s) * (\alpha u(s) + \bar{f}(u,\phi)(s))\|_{L^2}\,ds \\
&\le \quad Ce^{-bt}\|D_x^{s+1}\phi_0\|_{L^2} + \int_0^t Ce^{-b(t-s)}\|D_x^1 \Gamma^p(t-s)\|_{L^1}\|D_x^s(\alpha u(s) + \bar{f}(u,\phi)(s))\|_{L^2}\,ds \\
&\le \quad Ce^{-bt}\|D_x^{s+1}\phi_0\|_{L^2} + \int_0^t Ce^{-b(t-s)}(t-s)^{-\frac{1}{2}}\|D_x^s u(s)\|_{L^2} \\
&\quad + \quad \int_0^t 2CC_{f'}K^{s-1}e^{-b(t-s)}(t-s)^{-\frac{1}{2}}(\|D_x^s \phi(s)\|_{L^2} + \|D_x^s u(s)\|_{L^2})\,ds.
\end{aligned}
$$

Thanks to Lemma 2.4.1 we deduce,

$$
\begin{aligned}
\|D_x^{s+1}\phi(t)\|_{L^2} \quad &\le \quad C\Big(e^{-bt}\|D_x^{s+1}\phi_0\|_{L^2} + (1 + K)M_{D_x^s u}^{\tilde{\delta}}(t)\min\{1, |t-1|^{-\frac{n}{4}}\} \tag{2.35}\\
&\quad + \quad KM_{D_x^s \phi}^{\tilde{\delta}}(t)\min\{1, |t-1|^{-\tilde{\delta}}\}\Big),
\end{aligned}
$$

where $\tilde{\delta} = \min\left\{\frac{n}{4} + \frac{1}{2} + \frac{s}{2}, \frac{n}{2}\right\}$. Then, for the functional we get

$$M_{D_x^{s+1}\phi}^{\tilde{\delta}}(t) \le C\left(\|D_x^{s+1}\phi_0\|_{L^2} + (1 + C_k)M_{D_x^s u}^{\tilde{\delta}}(t) + C_k M_{D_x^s \phi}^{\tilde{\delta}}(t)\right). \tag{2.36}$$

$\square$

2.4.2 Decay Estimates for the Conservative and Dissipative Variables

Now we can prove the existence of global solutions to system (2.23) for suitably small initial data.

Theorem 2.4.3. *Under the assumptions* (H_b), (H_f), (H_g), *and* (H_h) *there exists an* $\epsilon_0 > 0$ *such that, if*

$$\|u_0\|_{H^s}, \|u_0\|_{L^1}, \|v_0\|_{H^s}, \|v_0\|_{L^1}, \|\phi_0\|_{H^{s+1}}, \|\phi_0\|_{W^{1,\infty}} \le \epsilon_0,$$

then there exists a unique global solution to the Cauchy problem (2.23)-(2.21)*:*

$$u \in C([0,\infty), H^s(\mathbb{R}^n)), \ v \in C([0,\infty), H^s(\mathbb{R}^n)), \ \phi \in C([0,\infty), H^{s+1}(\mathbb{R}^n)), \quad \text{for } s \ge \left[\frac{n}{2}\right] + 1.$$

Moreover for the solution (u, v, ϕ) *the following decay rates are satisfied*

$$\|u(t)\|_{L^\infty} \sim t^{-\frac{n}{2}}, \quad \|u(t)\|_{L^2} \sim t^{-\frac{n}{4}}, \qquad \|D_x^k u(t)\|_{L^2} \sim t^{-\delta_k}, \quad \text{for } k = 0, \dots, s;$$

$$\|v(t)\|_{L^\infty} \sim t^{-\frac{n}{2}}, \quad \|v(t)\|_{L^2} \sim t^{-\nu_0}, \qquad \|D_x^k v(t)\|_{L^2} \sim t^{-\nu_k}, \quad \text{for } k = 0, \dots, s;$$

$$\|\phi(t)\|_{L^\infty} \sim t^{-\frac{n}{2}}, \quad \|D_x^1 \phi(t)\|_{L^\infty} \sim t^{-\frac{n}{2}},,$$

$$\|\phi(t)\|_{L^2} \sim t^{-\frac{n}{4}}, \quad \|D_x^{k+1} \phi(t)\|_{L^2} \sim t^{-\delta_k}, \quad \text{for } k = 0, \dots, s;$$

where $\delta_k = \min\left\{\frac{n}{4} + \frac{1}{2} + \frac{1}{2}\left[\frac{k+1}{2}\right], \frac{n}{4} + \delta_r\right\}$, *with* $r = \left[\frac{k}{2}\right]$, $\nu_0 = \min\left\{\frac{n}{2}, \frac{n}{4} + \frac{1}{2}\right\}$, *and*
$\nu_k = \min\left\{\frac{n}{4} + 1 + \frac{1}{2}\left[\frac{k+1}{2}\right], \frac{n}{4} + \delta_r\right\}$, *with* $r = \left[\frac{k}{2}\right]$.

Remark 2.4.4. *We have defined the decay rates of the* s*-order derivative as*

$$\delta_s = \min\left\{\frac{n}{4} + \frac{1}{2} + \frac{1}{2}\left[\frac{s+1}{2}\right], \frac{n}{4} + \delta_r\right\}, \quad \text{for } s \ge 1, \tag{2.37}$$

where $r = \left[\frac{s}{2}\right]$. *Here we write the explicit form for the lower orders.*
Set $\delta_0 = \frac{n}{4}$. *Let be* $s = 1$, *then, by the relation* (2.37), *we have* $\delta_1 = \min\left\{\frac{n}{4} + 1, \frac{n}{2}\right\}$.
If $s = 2$, *then* $\delta_2 = \min\left\{\frac{n}{4} + 1, \frac{n}{4} + \delta_1\right\}$. *When* $s = 3$, *we get* $\delta_3 = \min\left\{\frac{n}{4} + \frac{3}{2}, \frac{n}{4} + \delta_1\right\}$ *and so on.*
In Figure 2.1 are illustrated the decay rates for $s = 1, \dots, 4$.

Proof. In order to prove our global existence result, we need to estimate the H^s and L^∞-norm of the solution (u, v) to system (2.23).
By the Duhamel's formula that solution w to system (2.23) can be written as

$$w(x,t) = (\Gamma^h(t) * w_0)(x) + \int_0^t \Gamma^h(t-s) * (\bar{B}(\phi, \nabla\phi)(s)\, w(s) + H(\phi, \nabla\phi, w)(s))\, ds. \tag{2.38}$$

where the function $\Gamma^h(\cdot)$ is the Green function of the dissipative hyperbolic system (2.2).
Thus for the first component of w, the conservative variable u, we have:

$$u(x,t) = (\Gamma_1^h(t) * w_0)(x) + \int_0^t \Gamma_1^h(t-s) * (\bar{B}(\phi, \nabla\phi)\, w(s) + H(\phi, \nabla\phi, w)(s))\, ds, \tag{2.39}$$
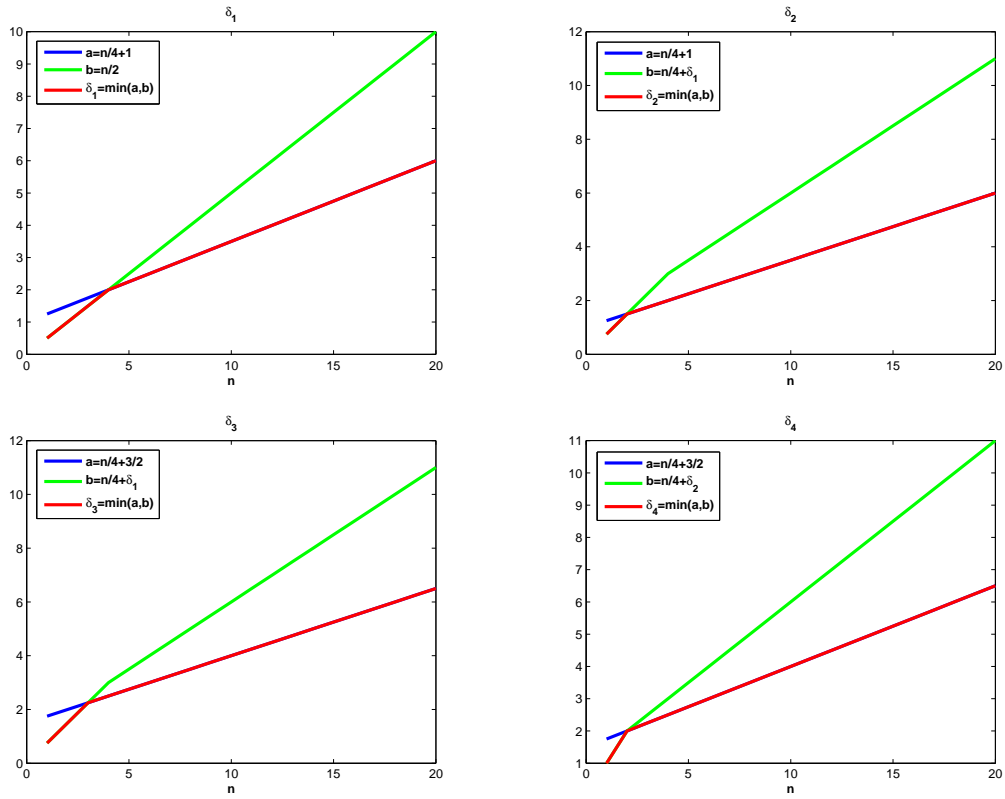
where Γ_1^h is the first row of the $(n+1) \times (n+1)$ Kernel Γ^h.
Regarding the generic dissipative component v_j, for $j = 1, \dots, n$, we have

$$v_j(x,t) = (\Gamma_{j+1}^h(t) * w_0)(x) + \int_0^t \Gamma_{j+1}^h(t-s) * (\bar{B}(\phi(s), \nabla\phi(s))\, w + H(\phi, \nabla\phi, w)(s))\, ds, \tag{2.40}$$

where Γ_{j+1}^h is the $(j+1)$-th row of Γ^h.
We take into account the expression of Γ^h and its decay rates, presented in Section 2.1.1, in order to obtain decay estimates of the conservative and dissipative variables.

Figure 2.1: Decay Rates of function ϕ, u s-derivatives for $s = 1, \ldots, 4$

L^2-estimate for u

We will start our analysis by the L^2 estimate for the function u. By equation (2.39) follows

$$\|u(t)\|_{L^2} \leq \|\Gamma_1^h(t) * w_0\|_{L^2} + \int_0^t \|\Gamma_1^h(t-s) * (\bar{B}(\phi(s), \nabla\phi(s))w + H(\phi, \nabla\phi, w))\|_{L^2} ds. \qquad (2.41)$$

In Subsection 2.1.1 we observed that, it is possible to decompose the Green Kernel, then

$$\|\Gamma_1^h(t) * w_0\|_{L^2} \leq \|K_{1,1}(t) * u_0\|_{L^2} + \sum_{i=1}^n \|K_{1,i+1}(t) * v_0^i\|_{L^2} + \|\mathcal{K}_{1,1}(t) * u_0\|_{L^2} + \sum_{i=1}^n \|\mathcal{K}_{1,i+1}(t) * v_0^i\|_{L^2}.$$

By Theorem 2.1.4 we deduce

$$\|\mathcal{K}_{1,1}(t) * u_0\|_{L^2} \leq Ce^{-ct}\|u_0\|_{L^2} \qquad \|K_{1,1}(t) * u_0\|_{L^2} \leq C\min\{1, t^{-\frac{n}{4}}\}\|u_0\|_{L^1},$$

$$\|\mathcal{K}_{1,i+1}(t) * v_0^i\|_{L^2} \leq Ce^{-ct}\|v_0^i\|_{L^2}, \qquad \|K_{1,i+1}(t) * v_0^i\|_{L^2} \leq C\min\{1, t^{-\frac{n}{4}-\frac{1}{2}}\}\|v_0^i\|_{L^1}.$$

Moreover we can decompose the integral term in (2.41) as

$$\int_0^t \|\Gamma_1^h(t-s) * (\bar{B}(\phi, \nabla\phi)(s)w(s) + H(\phi, \nabla\phi, w)(s))\|_{L^2} ds$$

$$\leq \int_0^t \|\mathcal{K}_1(t-s) * (\bar{B}(\phi, \nabla\phi)(s)w(s) + H(\phi, \nabla\phi, w)(s))\|_{L^2} ds$$

$$+ \int_0^t \|K_1(t-s) * (\bar{B}(\phi, \nabla\phi)(s)w(s) + H(\phi, \nabla\phi, w)(s))\|_{L^2} ds.$$

Let us start estimating the first integral.

$$\int_0^t \|\mathcal{K}_1(t-s) * (\bar{B}(\phi, \nabla\phi)(s) w(s) + H(\phi, \nabla\phi, w)(s))\|_{L^2}$$

$$\leq \int_0^t C e^{-c(t-s)} (\|\bar{B}(\phi, \nabla\phi)(s) w(s)\|_{L^2} + \|H(\phi, \nabla\phi, w)\|_{L^2}) ds$$

$$\leq \int_0^t C e^{-c(t-s)} (B_k(\|\nabla\phi(s)\|_{L^\infty} + \|\phi(s)\|_{L^\infty}) \|v(s)\|_{L^2} + H_k G_k(\|\nabla\phi(s)\|_{L^\infty} + \|\phi(s)\|_{L^\infty}) \|u(s)\|_{L^2} ds.$$

Proceeding as done for the estimates of the function ϕ, we arrive at

$$\int_0^t \|\mathcal{K}_1(t-s) * (\bar{B}(\phi, \nabla\phi)(s) w(s) + H(\phi, \nabla\phi, w)(s))\|_{L^2}$$

$$\leq C B_k (N_{D_x^1\phi}^{\frac{n}{2}}(t) M_v^{\nu_0}(t) + N_\phi^{\frac{n}{2}}(t) M_v^{\nu_0}(t)) \int_0^t e^{-c(t-s)} \min\{1, s^{-(\frac{n}{2}+\nu_0)}\} ds$$

$$+ C H_k G_k (M_u^{\frac{n}{4}}(t) N_\phi^{\frac{n}{2}}(t) + M_u^{\frac{n}{4}}(t) N_{D_x^1\phi}^{\frac{n}{2}}(t)) \int_0^t e^{-c(t-s)} \min\{1, s^{-\frac{3}{4}n}\} ds,$$

where $\nu_0 = \min\{\frac{n}{4} + \frac{1}{2}, \frac{n}{2}\}$. Then thanks to Lemma 2.4.1 we deduce

$$\int_0^t \|\mathcal{K}_1(t-s) * (\bar{B}(\phi, \nabla\phi)(s) w(s) + H(\phi, \nabla\phi, w)(s))\|_{L^2} \leq$$

$$+ C B_k \min\{1, t^{-(\frac{n}{2}+\nu_0)}\} (N_{D_x^1\phi}^{\frac{n}{2}}(t) M_v^{\nu_0}(t) + N_\phi^{\frac{n}{2}}(t) M_v^{\nu_0}(t))$$

$$+ C H_k G_k \min\{1, t^{-\frac{3}{4}n}\} (M_u^{\frac{n}{4}}(t) N_\phi^{\frac{n}{2}}(t) + M_u^{\frac{n}{4}}(t) N_{D_x^1\phi}^{\frac{n}{2}}(t)).$$

To complete our estimate we need to study the contribution of the hyperbolic Green function diffusive part.

$$\int_0^t \|K_1(t-s) * (\bar{B}(\phi, \nabla\phi)(s) w(s) + H(\phi, \nabla\phi, w)(s))\|_{L^2} ds$$

$$\leq \int_0^t C \min\{1, (t-s)^{-\frac{n}{4}-\frac{1}{2}}\} (\|\bar{b}(\phi, \nabla\phi)(s) v(s)\|_{L^1} + \|h(\phi, \nabla\phi) g(u)(s)\|_{L^1}) ds$$

$$\leq \int_0^t C \min\{1, (t-s)^{-\frac{n}{4}-\frac{1}{2}}\} (\|\bar{b}(\phi, \nabla\phi)(s)\|_{L^2} \|v(s)\|_{L^2} + \|h(\phi, \nabla\phi)(s)\|_{L^2} \|u(s)\|_{L^2}) ds$$

$$\leq \int_0^t C \min\{1, (t-s)^{-\frac{n}{4}-\frac{1}{2}}\} (B_k \|\phi(s)\|_{L^2} \|v(s)\|_{L^2} + B_k \|\nabla\phi(s)\|_{L^2} \|v(s)\|_{L^2}) ds$$

$$+ \int_0^t C \min\{1, (t-s)^{-\frac{n}{4}-\frac{1}{2}}\} (H_k G_k \|\phi(s)\|_{L^2} \|u(s)\|_{L^2} + H_K G_k \|\nabla\phi(s)\|_{L^2} \|u(s)\|_{L^2}) ds.$$

Introducing the functionals M^δ, we arrive at

$$\int_0^t \|K_1(t-s) * (\bar{B}(\phi, \nabla\phi)(s) w(s) + H(\phi, \nabla\phi, w)(s))\|_{L^2} ds$$

$$\leq B_K (M_\phi^{\frac{n}{4}}(t) M_v^{\nu_0}(t) + M_{D_x^1\phi}^{\frac{n}{4}}(t) M_v^{\nu_0}(t)) \int_0^t \min\{1, (t-s)^{-\frac{n}{4}-\frac{1}{2}}\} \min\{1, s^{-(\frac{n}{4}+\nu_0)}\} ds$$

$$+ H_k G_k (M_\phi^{\frac{n}{4}}(t) M_u^{\frac{n}{4}}(t) + M_{D_x^1\phi}^{\frac{n}{4}}(t) M_u^{\frac{n}{4}}(t)) \int_0^t \min\{1, (t-s)^{-\frac{n}{4}-\frac{1}{2}}\} \min\{1, s^{-\frac{n}{2}}\} ds,$$

and by Lemma 2.4.1 we deduce

$$\int_0^t \|K_1(t-s) * (\bar{B}(\phi, \nabla\phi) w(s) + H(\phi, \nabla\phi, w)(s))\|_{L^2}$$

$$\leq \min\{1, t^{-\nu_0}\}(B_K M_\phi^{\frac{n}{4}}(t) M_v^{\nu_0}(t) + B_K M_{D_x^1\phi}^{\frac{n}{4}}(t) M_v^{\nu_0}(t)) \tag{2.42}$$

$$+ \min\{1, t^{-\theta}\}(H_k G_k M_u^{\frac{n}{4}}(t) M_\phi^{\frac{n}{4}}(t) + H_k G_k M_u^{\frac{n}{4}}(t) M_{D_x^1\phi}^{\frac{n}{4}}(t)).$$

where $\theta = \frac{1}{4}$ if $n = 1$ otherwise $\theta = \frac{n}{4} + \frac{1}{2}$.

Then we obtain the L^2-norm of the function u summing the previous inequalities.

$$
\begin{aligned}
\|u(t)\|_{L^2} \leq\ & C\left[e^{-ct}(\|u_0\|_{L^2} + \sum_{i=1}^n \|v_0^i\|_{L^2}) + \min\{1, t^{-\frac{n}{4}}\}\|u_0\|_{L^1} + \min\{1, t^{-\frac{n}{4}-\frac{1}{2}}\}\sum_{i=1}^n \|v_i^0\|_{L^1}\right] \\
& + C_k\left[\min\{1, t^{-(\frac{n}{2}+\nu_0)}\}(N_{D_x^1\phi}^{\frac{n}{2}}(t) M_v^{\nu_0}(t) + N_\phi^{\frac{n}{2}}(t) M_v^{\nu_0}(t))\right. \\
& \quad + \min\{1, t^{-\frac{3}{4}n}\}(M_u^{\frac{n}{4}}(t) N_\phi^{\frac{n}{2}}(t) + M_u^{\frac{n}{4}}(t) N_{D_x^1\phi}^{\frac{n}{2}}(t)) \\
& \quad + \min\{1, t^{-\nu_0}\}(M_\phi^{\frac{n}{4}}(t) M_v^{\nu_0}(t) + M_{D_x^1\phi}^{\frac{n}{4}}(t) M_v^{\nu_0}(t)) \\
& \quad \left. + \min\{1, t^{-\theta}\}(M_u^{\frac{n}{4}}(t) M_\phi^{\frac{n}{4}}(t) + M_u^{\frac{n}{4}}(t) M_{D_x^1\phi}^{\frac{n}{4}}(t))\right],
\end{aligned}
\tag{2.43}
$$

where the constant C_k depends on K.

L^2-**estimate for** $D_x^s u$

The next step is the estimate of s-order derivative of function u. From the Duhamel's formula, it follows that

$$\|D_x^s u(t)\|_{L^2} \leq \|D_x^s \Gamma_1^h(t) * w_0\|_{L^2} + \int_0^t \|D_x^s \Gamma_1^h(t-s) * (\bar{B}(\phi, \nabla\phi)(s) w(s) + H(\phi, \nabla\phi, w)(s))\|_{L^2} ds.$$
$$\tag{2.44}$$

Decomposing the Green Kernel, the first term in the previous inequality can be estimated as

$$
\begin{aligned}
\|D_x^s \Gamma_1^h(t) * w_0\|_{L^2} \leq\ & \|D_x^s K_{1,1}(t) * u_0\|_{L^2} + \sum_{i=1}^n \|D_x^s K_{1,i+1}(t) * v_0^i\|_{L^2} + \|D_x^s \mathscr{K}_{1,1}(t) * u_0\|_{L^2} \\
& + \sum_{i=1}^n \|D_x^s \mathscr{K}_{1,i+1}(t) * v_0^i\|_{L^2}.
\end{aligned}
$$

Therefore, by Theorem 2.1.4, we have

$$\|D_x^s \mathscr{K}_{1,1}(t) * u_0\|_{L^2} \leq C e^{-ct}\|D_x^s u_0\|_{L^2}, \qquad \|D_x^s K_{1,1}(t) * u_0\|_{L^2} \leq C\min\{1, t^{-\frac{n}{4}-\frac{s}{2}}\}\|u_0\|_{L^1},$$

$$\|D_x^s \mathscr{K}_{1,i+1}(t) * v_0^i\|_{L^2} \leq C e^{-ct}\|D_x^s v_0^i\|_{L^2}, \qquad \|D_x^s K_{1,i+1}(t) * v_0^i\|_{L^2} \leq C\min\{1, t^{-\frac{n}{4}-\frac{1}{2}-\frac{s}{2}}\}\|v_0^i\|_{L^1}.$$

Moreover we can decompose the integral term in (2.44) as

$$\int_0^t \|D_x^s \Gamma_1^h(t-s) * (\bar{B}(\phi, \nabla\phi) w(s) + H(\phi, \nabla\phi, w)(s))\|_{L^2} ds$$

$$\leq \int_0^t \|D_x^s \mathscr{K}_1(t-s) * (\bar{B}(\phi, \nabla\phi) w(s) + H(\phi, \nabla\phi, w)(s))\|_{L^2} ds$$

$$+ \int_0^t \|D_x^s K_1(t-s) * (\bar{B}(\phi, \nabla\phi) w(s) + H(\phi, \nabla\phi, w))\|_{L^2} ds.$$

Let us start estimating the first integral.

$$\int_0^t \|D_x^s \mathscr{K}_1(t-s) * (\bar{B}(\phi, \nabla\phi) w(s) + H(\phi, \nabla\phi, w)(s))\|_{L^2}$$

$$\leq \int_0^t C e^{-c(t-s)} \|D_x^s \bar{B}(\phi,\nabla\phi) w(s)\|_{L^2} + \|D_x^s H(\phi,\nabla\phi,w)(s)\|_{L^2} \, ds$$

$$\leq \int_0^t C e^{-c(t-s)} (\|D_x^s \bar{b}(\phi,\nabla\phi)\|_{L^2} \|v(s)\|_{L^\infty} + \|\bar{b}(\phi,\nabla\phi)\|_{L^2} \|D_x^s v(s)\|_{L^\infty}) \, ds$$

$$+ \int_0^t C e^{-c(t-s)} (\|D_x^s h(\phi,\nabla\phi)\|_{L^2} \|g(u)(s)\|_{L^\infty} + \|\bar{b}(\phi,\nabla\phi)\|_{L^\infty}) \|D_x^s g(u)(s)\|_{L^\infty}) \, ds$$

$$\leq \int_0^t e^{-c(t-s)} 2C_{b'} K^{s-1} (\|D_x^{s+1}\phi(s)\|_{L^2} + \|D_x^s \phi(s)\|_{L^2}) \|v(s)\|_{L^\infty} \, ds$$

$$+ \int_0^t e^{-c(t-s)} B_k (\|\nabla\phi(s)\|_{L^\infty} + \|\phi(s)\|_{L^\infty}) \|D_x^s v(s)\|_{L^2} \, ds$$

$$+ \int_0^t e^{-c(t-s)} 2C_{h'} K^{s-1} G_k (\|D_x^{s+1}\phi(s)\|_{L^2} + \|D_x^s \phi(s)\|_{L^2}) \|u(s)\|_{L^\infty} \, ds$$

$$+ \int_0^t e^{-c(t-s)} H_k G_k (\|\nabla\phi(s)\|_{L^\infty} + \|\phi(s)\|_{L^\infty}) \|D_x^s u(s)\|_{L^2} \, ds.$$

Then, by Lemma 2.4.1 we get

$$\int_0^t \|D_x^s \mathcal{K}_1(t-s) * (\bar{B}(\phi,\nabla\phi) w(s) + H(\phi,\nabla\phi,w)(s))\|_{L^2}$$

$$\leq 2C_{b'} K^{s-1} \min\{1, t^{-(\tilde{\delta}+\frac{n}{2})}\} (M^{\tilde{\delta}}_{D_x^s\phi}(t) N_v^{\frac{n}{2}}(t) + M^{\tilde{\delta}}_{D_x^{s+1}\phi}(t) N_v^{\frac{n}{2}}(t))$$

$$+ B_k \min\{1, t^{-(\frac{n}{2}+\tilde{\nu})}\} (N^{\frac{n}{2}}_{D_x^1\phi}(t) M^{\tilde{\nu}}_{D_x^s v}(t) + N_\phi^{\frac{n}{2}}(t) M^{\tilde{\nu}}_{D_x^s v}(t))$$

$$+ G_k C_{h'} K^{s-2} \min\{1, t^{-(\tilde{\delta}+\frac{n}{2})}\} (M^{\tilde{\delta}}_{D_x^s\phi}(t) N_u^{\frac{n}{2}}(t) + M^{\tilde{\delta}}_{D_x^s\phi}(t) N_u^{\frac{n}{2}}(t))$$

$$+ H_k G_k \min\{1, t^{-(\tilde{\delta}+\frac{n}{2})}\} (M^{\tilde{\delta}}_{D_x^s u}(t) N_\phi^{\frac{n}{2}}(t) + M^{\tilde{\delta}}_{D_x^s u}(t) N^{\frac{n}{2}}_{D_x^1\phi}(t)),$$

where $\tilde{\delta} = \min\{\frac{n}{4} + \frac{1}{2} + \frac{s}{2}, \frac{n}{2}\}$ and $\tilde{\nu} = \min\{\frac{n}{4} + 1 + \frac{s}{2}, \frac{n}{2}\}$.

In order to complete our estimate, we need to study the contribution of the hyperbolic Green function diffusive part

$$\int_0^t \|D_x^s K_1(t-s) * (\bar{B}(\phi,\nabla\phi)(s) w(s) + H(\phi,\nabla\phi,w)(s))\|_{L^2} \, ds.$$

Proceeding as before,

$$\int_0^t \|D_x^s K_1(t-s) * (\bar{B}(\phi,\nabla\phi)(s) w(s) + H(\phi,\nabla\phi,w)(s))\|_{L^2} \, ds$$

$$\leq \int_0^t \|\sum_{i=1}^n D_x^s K_{1,i+1}(t-s) * (\bar{B}(\phi,\nabla\phi)(s) v_i(s) + h_i(\phi,\nabla\phi,u)(s))\|_{L^2} \, ds$$

$$\leq \int_0^t C \min\{1, (t-s)^{-\frac{n}{4}-\frac{1}{2}-\frac{s}{2}}\} \|\bar{B}(\phi,\nabla\phi)(s) v(s)\|_{L^1} + \|h(\phi,\nabla\phi) g(u)(s)\|_{L^1} \, ds$$

$$\leq \int_0^t C \min\{1, (t-s)^{-\frac{n}{4}-\frac{1}{2}-\frac{s}{2}}\} B_K (\|\phi(s)\|_{L^2} \|v(s)\|_{L^2} + \|\nabla\phi(s)\|_{L^2} \|v(s)\|_{L^2}) \, ds$$

$$+ \int_0^t C \min\{1, (t-s)^{-\frac{n}{4}-\frac{1}{2}-\frac{s}{2}}\} G_k H_k (\|\phi(s)\|_{L^2} \|u(s)\|_{L^2} + \|\nabla\phi(s)\|_{L^2} \|u(s)\|_{L^2}) \, ds.$$

Moreover

$$\int_0^t \|D_x^s K_1(t-s) * (\bar{B}(\phi,\nabla\phi)(s) w(s) + H(\phi,\nabla\phi,w)(s))\|_{L^2} \, ds$$

$$\leq C B_K (M_\phi^{\frac{n}{4}}(t) M_v^{\nu_0}(t) + M^{\frac{n}{4}}_{D_x^1\phi}(t) M_v^{\nu_0}(t)) \int_0^t \min\{1, (t-s)^{-\frac{n}{4}-\frac{1}{2}-\frac{s}{2}}\} \min\{1, s^{-(\frac{n}{4}+\nu_0)}\} \, ds$$

$$+ CH_k G_k (M_\phi^{\frac{n}{4}}(t) M_u^{\frac{n}{4}}(t) + M_{D_x^1\phi}^{\frac{n}{4}} M_u^{\frac{n}{4}}(t)) \int_0^t \min\{1, (t-s)^{-\frac{n}{4}-\frac{1}{2}-\frac{s}{2}}\} \min\{1, s^{-\frac{n}{2}}\} ds.$$

Then, by Lemma 2.4.1 we get

$$\int_0^t \|D_x^1 K_1(t-s) * (\bar{B}(\phi(s), \nabla\phi(s)) w + H(\phi, \nabla\phi, w)(s))\|_{L^2}$$
$$\leq C_k \min\{1, t^{-\tilde{\delta}}\} \left(M_\phi^{\frac{n}{4}}(t) M_v^{\nu_0}(t) + M_{D_x^1\phi}^{\frac{n}{4}}(t) M_v^{\nu_0}(t) + M_{D_x^1\phi}^{\frac{n}{4}}(t) M_u^{\frac{n}{4}}(t) + M_\phi^{\frac{n}{4}}(t) M_u^{\frac{n}{4}}(t) \right),$$

where $\tilde{\delta} = \min\left\{\frac{n}{4} + \frac{1}{2} + \frac{s}{2}, \frac{n}{2}\right\}$, and $\tilde{\nu} = \min\left\{\frac{n}{4} + 1 + \frac{s}{2}, \frac{n}{2}\right\}$.

Finally the L^2 norm of the s-derivative of function u, can be estimated as follows:

$$
\begin{aligned}
\|D_x^s u(t)\|_{L^2} \leq & \; C\left[e^{-ct}(\|D_x^s u_0\|_{L^2} + \sum_{i=1}^n \|D_x^s v_0^i\|_{L^2}) + \min\{1, t^{-\frac{n}{4}-\frac{1}{2}-\frac{s}{2}}\} \sum_{i=1}^n \|v_0^i\|_{L^1} \right. \\
& + \min\{1, t^{-\frac{n}{4}-\frac{s}{2}}\} \|u_0\|_{L^1} \right] + C_k \left[\min\{1, t^{-(\tilde{\delta}+\frac{n}{2})}\}(M_{D_x^s\phi}^{\tilde{\delta}}(t) N_v^{\frac{n}{2}}(t) + M_{D_x^{s+1}\phi}^{\tilde{\delta}}(t) N_v^{\frac{n}{2}}(t)) \right. \\
& + \min\{1, t^{-(\tilde{\nu}+\frac{n}{2})}\}(N_{D_x^1\phi}^{\frac{n}{2}}(t) M_{D_x^s v}^{\tilde{\nu}}(t) + N_\phi^{\frac{n}{2}}(t) M_{D_x^s v}^{\tilde{\nu}}(t)) \\
& + \min\{1, t^{-(\tilde{\delta}+\frac{n}{2})}\}(M_{D_x^s\phi}^{\tilde{\delta}}(t) N_u^{\frac{n}{2}}(t) + M_{D_x^s\phi}^{\tilde{\delta}}(t) N_u^{\frac{n}{2}}(t)) + M_{D_x^s u}^{\tilde{\delta}}(t) N_\phi^{\frac{n}{2}}(t) + M_{D_x^s u}^{\tilde{\delta}}(t) N_{D_x^1\phi}^{\frac{n}{2}}(t) \\
& \left. + \min\{1, t^{-\tilde{\delta}}\}(M_\phi^{\frac{n}{4}}(t) M_v^{\nu_0}(t) + M_{D_x^1\phi}^{\frac{n}{4}}(t) M_v^{\nu_0}(t) + M_{D_x^1\phi}^{\frac{n}{4}}(t) M_u^{\frac{n}{4}}(t) + M_\phi^{\frac{n}{4}}(t) M_u^{\frac{n}{4}}(t)) \right].
\end{aligned}
\tag{2.45}
$$

L^∞ estimate for u

Let us focus now on the L^∞ norm of the function u.

$$\|u(t)\|_{L^\infty} \leq \|\Gamma_1^h(t) * w_0\|_{L^\infty} + \int_0^t \|\Gamma_1^h(t-s) * (\bar{B}(\phi, \nabla\phi)(s) w(s) + H(\phi, \nabla\phi, w)(s))\|_{L^\infty} ds. \tag{2.46}$$

By the decomposition of the Green Kernel, we can estimate the first term in the previous inequality as

$$\|\Gamma_1^h(t) * w_0\|_{L^\infty} \leq \|K_{1,1}(t) * u_0\|_{L^\infty} + \sum_{i=1}^n \|K_{1,i+1}(t) * v_0^i\|_{L^\infty} + \|\mathcal{K}_{1,1}(t) * u_0\|_{L^\infty} + \sum_{i=1}^n \|\mathcal{K}_{1,i+1}(t) * v_0^i\|_{L^\infty}.$$

Thanks to Theorem 2.1.4, we have

$$\|\mathcal{K}_{11}(t) * u_0\|_{L^\infty} \leq \|K_{1,1}(t) * u_0\|_{H^s} \leq C e^{-ct} \|u_0\|_{H^s}, \qquad \|K_{1,1}(t) * u_0\|_{L^\infty} \leq C \min\{1, t^{-\frac{n}{2}}\} \|u_0\|_{L^1},$$

$$\|\mathcal{K}_{1,i+1}(t) * v_0^i\|_{L^2} \leq C e^{-ct} \|v_0^i\|_{H^s}, \qquad\qquad\qquad \|K_{1,i+1}(t) * v_0^i\|_{L^2} \leq C \min\{1, t^{-\frac{n}{2}-\frac{1}{2}}\} \|v_0^i\|_{L^1}.$$

Let us decompose the integral term.

$$\int_0^t \|\Gamma_1^h(t-s) * (\bar{B}(\phi, \nabla\phi)(s) w(s) + H(\phi, \nabla\phi, w)(s))\|_{L^\infty} ds$$
$$\leq \int_0^t \|\mathcal{K}_1(t-s) * (\bar{B}(\phi, \nabla\phi)(s) w(s) + H(\phi, \nabla\phi, w)(s))\|_{L^\infty} ds$$
$$+ \int_0^t \|K_1(t-s) * (\bar{B}(\phi, \nabla\phi)(s) w(s) + H(\phi, \nabla\phi, w)(s))\|_{L^\infty} ds.$$

We can estimate the first integral as

$$\int_0^t \|\mathcal{K}_1(t-s) * (\bar{B}(\phi, \nabla\phi)(s) w(s) + H(\phi, \nabla\phi, w)(s))\|_{L^\infty}$$

$$\leq C \int_0^t \|\mathcal{K}_1(t-s) * (\bar{B}(\phi, \nabla\phi)(s)\, w(s) + H(\phi, \nabla\phi, w)(s))\|_{L^2}\, ds$$

$$+ C \int_0^t \sum_{|\alpha|=s} \|D_x^s \mathcal{K}_1(t-s) * (\bar{B}(\phi, \nabla\phi)(s)\, w(s) + H(\phi, \nabla\phi, w)(s))\|_{L^2}\, ds.$$

Then, thanks to the L^2-estimate calculated previously, we easily obtain

$$\int_0^t \|\mathcal{K}_1(t-s) * (\bar{B}(\phi, \nabla\phi)(s)\, w(s) + H(\phi, \nabla\phi, w)(s))\|_{L^\infty}$$

$$\leq C B_k \min\{1, t^{-(\frac{n}{2}+\nu_0)}\}(N_{D_x^1\phi}^{\frac{n}{2}}(t) M_\nu^{\nu_0}(t) + N_\phi^{\frac{n}{2}}(t) M_\nu^{\nu_0}(t))$$

$$+ C H_k G_k \min\{1, t^{-\frac{3}{4}n}\}(M_u^{\frac{n}{4}}(t) N_\phi^{\frac{n}{2}}(t) + M_u^{\frac{n}{4}}(t) N_{D_x^1\phi}^{\frac{n}{2}}(t))$$

$$+ 2 C_{b'} K^{s-1} \min\{1, t^{-(\tilde{\delta}+\frac{n}{2})}\}(M_{D_x^s\phi}^{\tilde{\delta}}(t) N_\nu^{\frac{n}{2}}(t) + M_{D_x^{s+1}\phi}^{\tilde{\delta}}(t) N_\nu^{\frac{n}{2}}(t))$$

$$+ B_k \min\{1, t^{-(\frac{n}{2}+\tilde{\nu})}\}(N_{D_x^1\phi}^{\frac{n}{2}}(t) M_{D_x^s\nu}^{\tilde{\nu}}(t) + N_\phi^{\frac{n}{2}}(t) M_{D_x^s\nu}^{\tilde{\nu}}(t))$$

$$+ G_k C_{h'} K^{s-2} \min\{1, t^{-(\tilde{\delta}+\frac{n}{2})}\}(M_{D_x^s\phi}^{\tilde{\delta}}(t) N_u^{\frac{n}{2}}(t) + M_{D_x^s\phi}^{\tilde{\delta}}(t) N_u^{\frac{n}{2}}(t))$$

$$+ H_k G_k \min\{1, t^{-(\tilde{\delta}+\frac{n}{2})}\}(M_{D_x^s u}^{\tilde{\delta}}(t) N_\phi^{\frac{n}{2}}(t) + M_{D_x^s u}^{\tilde{\delta}}(t) N_{D_x^1\phi}^{\frac{n}{2}}(t)).$$

In order to complete our study on the L^∞ norm of function u, we estimate the contribution of the hyperbolic Green function diffusive part.

$$\int_0^t \|K_1(t-s) * (\bar{B}(\phi, \nabla\phi)(s)\, w(s) + H(\phi, \nabla\phi, w)(s)(s))\|_{L^\infty}\, ds$$

$$\leq \int_0^t \min\{1, (t-s)^{-\frac{n}{2}-\frac{1}{2}}\} \|\bar{B}(\phi, \nabla\phi)(s)\, v(s)\|_{L^1} + \|\bar{h}(\phi, \nabla\phi) g(u)(s)\|_{L^1}\, ds$$

$$\leq \int_0^t \min\{1, (t-s)^{-\frac{n}{2}-\frac{1}{2}}\} B_k (\|\phi(s)\|_{L^2} \|v(s)\|_{L^2} + \|\nabla\phi(s)\|_{L^2} \|v(s)\|_{L^2})\, ds$$

$$+ \int_0^t \min\{1, (t-s)^{-\frac{n}{2}-\frac{1}{2}}\} H_k G_k (\|\phi(s)\|_{L^2} \|u(s)\|_{L^2} + \|\nabla\phi(s)\|_{L^2} \|u(s)\|_{L^2})\, ds$$

$$\leq B_K (M_\phi^{\frac{n}{4}}(t) M_\nu^{\nu_0}(t) + M_{D_x^1\phi}^{\frac{n}{4}}(t) M_\nu^{\nu_0}(t)) \int_0^t \min\{1, (t-s)^{-\frac{n}{2}-\frac{1}{2}}\} \min\{1, s^{-(\frac{n}{4}+\nu_0)}\}\, ds$$

$$+ H_k G_k (M_\phi^{\frac{n}{4}}(t) M_u^{\frac{n}{4}}(t) + M_{D_x^1\phi}^{\frac{n}{4}}(t) M_u^{\frac{n}{4}}(t)) \int_0^t \min\{1, (t-s)^{-\frac{n}{2}-\frac{1}{2}}\} \min\{1, s^{-\frac{n}{2}}\}\, ds.$$

Thanks to Lemma 2.4.1 we deduce

$$\int_0^t \|K_1(t-s) * (\bar{B}(\phi, \nabla\phi)\, w(s) + H(\phi, \nabla\phi, w)(s))\|_{L^\infty}$$

$$\leq C_k \min\{1, t^{-\frac{n}{2}}\} \left(M_\phi^{\frac{n}{4}}(t) M_\nu^{\nu_0}(t) + M_{D_x^1\phi}^{\frac{n}{4}}(t) M_\nu^{\nu_0}(t) + M_\phi^{\frac{n}{4}}(t) M_u^{\frac{n}{4}}(t) + M_{D_x^1\phi}^{\frac{n}{4}}(t) M_u^{\frac{n}{4}}(t) \right).$$

We can collect the previous estimates in the following inequality

$$
\begin{aligned}
\|u(t)\|_{L^\infty} \leq{}& C \left[e^{-ct}(\|u_0\|_{H^s} + \sum_{i=1}^n \|v_0^i\|_{H^s}) + \min\{1, t^{-\frac{n}{2}}\} \|u^0\|_{L^1} + \min\{1, t^{-\frac{n}{2}-\frac{1}{2}}\} \sum_{i=1}^n \|v_0^i\|_{L^1} \right] \\
&+ C_k \left[\min\{1, t^{-(\frac{n}{2}+\nu_0)}\}(N_{D_x^1\phi}^{\frac{n}{2}}(t) M_\nu^{\nu_0}(t) + N_\phi^{\frac{n}{2}}(t) M_\nu^{\nu_0}(t)) \right. \\
&+ \min\{1, t^{-\frac{3}{4}n}\}(M_u^{\frac{n}{4}}(t) N_\phi^{\frac{n}{2}}(t) + M_u^{\frac{n}{4}}(t) N_{D_x^1\phi}^{\frac{n}{2}}(t)) \\
&+ \min\{1, t^{-(\tilde{\delta}+\frac{n}{2})}\}(M_{D_x^s\phi}^{\tilde{\delta}}(t) N_\nu^{\frac{n}{2}}(t) + M_{D_x^{s+1}\phi}^{\tilde{\delta}}(t) N_\nu^{\frac{n}{2}}(t))
\end{aligned}
\tag{2.47}
$$

$$+ \quad \min\{1, t^{-(\frac{n}{2}+\tilde{\nu})}\}(N_{D_x^1\phi}^{\frac{n}{2}}(t)M_{D_x^s\nu}^{\tilde{\nu}}(t) + N_\phi^{\frac{n}{2}}(t)M_{D_x^s\nu}^{\tilde{\nu}}(t))$$

$$+ \quad \min\{1, t^{-(\tilde{\delta}+\frac{n}{2})}\}(M_{D_x^s\phi}^{\tilde{\delta}}(t)N_u^{\frac{n}{2}}(t) + M_{D_x^s\phi}^{\tilde{\delta}}(t)N_u^{\frac{n}{2}}(t)) + M_{D_x^s u}^{\tilde{\delta}}(t)N_\phi^{\frac{n}{2}}(t) + M_{D_x^s u}^{\tilde{\delta}}(t)N_{D_x^1\phi}^{\frac{n}{2}}(t))$$

$$+ \quad \min\{1, t^{-\frac{n}{2}}\}(M_\phi^{\frac{n}{4}}(t)M_\nu^{\nu_0}(t) + M_{D_x^1\phi}^{\frac{n}{4}}(t)M_\nu^{\nu_0}(t)) + M_\phi^{\frac{n}{4}}(t)M_u^{\frac{n}{4}}(t) + M_{D_x^1\phi}^{\frac{n}{4}}(t)M_u^{\frac{n}{4}}(t)) \Big],$$

where the constant C_k depends on K.

In order to complete our proof we need to estimate, by the same technique, the dissipative variable v.

L^2-estimate for v

Let us start with the L^2 norm of a generic component v_j, with $j = 1, \dots, n$.
By the Duhamel's formula (2.40) we get

$$\|v_j(t)\|_{L^2} \le \|\Gamma_{j+1}^h(t) * w_0\|_{L^2} + \int_0^t \|\Gamma_{j+1}^h(t-s) * (\bar{B}(\phi, \nabla\phi)(s)w(s) + H(\phi, \nabla\phi, w)(s))\|_{L^2} ds. \quad (2.48)$$

Then by the decomposition of the Green kernel we have

$$\|\Gamma_{j+1}^h(t) * w_0\|_{L^2} \quad \le \quad \|K_{j+1,1}(t) * u_0\|_{L^2} + \sum_{i=1}^n \|K_{j+1,i+1}(t) * v_0^i\|_{L^2} + \|\mathcal{K}_{j+1,1}(t) * u_0\|_{L^2}$$

$$+ \quad \sum_{i=1}^n \|\mathcal{K}_{j+1,i+1}(t) * v_0^i\|_{L^2},$$

and by Theorem 2.1.4 we get the following estimates

$$\|\mathcal{K}_{j+1,1}(t) * u_0\|_{L^2} \le Ce^{-ct}\|u_0\|_{L^2}, \qquad \|K_{j+1,1}(t) * u_0\|_{L^2} \le C\min\{1, t^{-\frac{n}{4}-\frac{1}{2}}\}\|u_0\|_{L^1},$$

$$\|\mathcal{K}_{j+1,i+1}(t) * v_0^i\|_{L^2} \le Ce^{-ct}\|v_0^i\|_{L^2}, \qquad \|K_{j+1,i+1}(t) * v_0^i\|_{L^2} \le C\min\{1, t^{-\frac{n}{4}-1}\}\|v_0^i\|_{L^1}.$$

We pass now to estimate the second term in (2.48). Decomposing the integral term, we get

$$\int_0^t \|\Gamma_{j+1}^h(t-s) * (\bar{B}(\phi, \nabla\phi)(s)w(s) + H(\phi, \nabla\phi, w)(s))\|_{L^2} ds$$

$$\le \int_0^t \|\mathcal{K}_{j+1}(t-s) * (\bar{B}(\phi, \nabla\phi)(s)w(s) + H(\phi, \nabla\phi, s)(s))\|_{L^2} ds$$

$$+ \int_0^t \|K_{j+1}(t-s) * (\bar{B}(\phi(s), \nabla\phi(s))w(s) + H(\phi, \nabla\phi, u)(s))\|_{L^2} ds.$$

Let us focus on the first integral on the right-hand side. We can notice that, since the singular part of the Green Kernel has the same decay rate for both conservative and dissipative variable, we can estimate this term, as done previously in the estimate of function u. Then,

$$\int_0^t \|\mathcal{K}_{i+1}(t-s) * (\bar{B}(\phi, \nabla\phi)w + H(\phi, \nabla\phi, w)(s))\|_{L^2} ds$$

$$\le CB_k \min\{1, t^{-(\frac{n}{2}+\nu_0)}\} \left(N_{D_x^1\phi}^{\frac{n}{2}}(t)M_\nu^{\nu_0}(t) + N_\phi^{\frac{n}{2}}(t)M_\nu^{\nu_0}(t) \right)$$

$$+ CH_k G_k \min\{1, t^{-(\frac{n}{4}+\frac{n}{2})}\} \left(M_u^{\frac{n}{4}}(t)N_\phi^{\frac{n}{2}}(t) + M_u^{\frac{n}{4}}(t)N_{D_x^1\phi}^{\frac{n}{2}}(t) \right),$$

where $\nu_0 = \min\left\{\frac{n}{4} + \frac{1}{2}, \frac{n}{2}\right\}$. On the other hand, when estimating the dissipative term of Green Kernel diffusive part, we get a faster decay, with respect to the conservative variable u. The dissipative part,

being strongly influenced by the dissipation, decays at the rate $t^{-\frac{1}{2}}$ faster of the conservative one. Proceeding as done before,

$$\int_0^t \|K_{j+1}(t-s) * (\bar{B}(\phi, \nabla\phi)(s)\, w(s) + H(\phi, \nabla\phi, w)(s))\|_{L^2}\, ds$$

$$\leq \int_0^t C\min\{1, (t-s)^{-\frac{n}{4}-1}\}\|(\bar{B}(\phi, \nabla\phi)(s)\, w(s) + H(\phi, \nabla\phi, w)(s))\|_{L^1}\, ds$$

$$\leq \int_0^t C\min\{1, (t-s)^{-\frac{n}{4}-1}\}B_k(\|\phi(s)\|_{L^2}\|v(s)\|_{L^2} + \|\nabla\phi(s)\|_{L^2}\|v(s)\|_{L^2})\, ds$$

$$+ \int_0^t C\min\{1, (t-s)^{-\frac{n}{4}-1}\}H_k G_k(\|\phi(s)\|_{L^2}\|u(s)\|_{L^2} + \|\nabla\phi(s)\|_{L^2}\|u(s)\|_{L^2})\, ds$$

$$\leq B_K(M_\phi^{\frac{n}{4}}(t)M_v^{\nu_0}(t) + M_{D_x^1\phi}^{\frac{n}{4}}(t)M_v^{\nu_0}(t))\int_0^t C\min\{1, (t-s)^{-\frac{n}{4}-1}\}\min\{1, s^{-(\frac{n}{4}+\nu_0)}\}\, ds$$

$$+ H_k G_k(M_\phi^{\frac{n}{4}}(t)M_u^{\frac{n}{4}}(t) + M_{D_x^1\phi}^{\frac{n}{4}}(t)M_u^{\frac{n}{4}}(t))\int_0^t C\min\{1, (t-s)^{-\frac{n}{4}-1}\}\min\{1, s^{-\frac{n}{2}}\}\, ds.$$

Thanks to Lemma 2.4.1 we deduce

$$\int_0^t \|K_{j+1}(t-s) * (\bar{B}(\phi, \nabla\phi)(s)\, w(s) + H(\phi, \nabla\phi, w)(s))\|_{L^2}$$

$$\leq \min\{1, t^{-\nu_0}\}C_k(M_\phi^{\frac{n}{4}}(t)M_v^{\nu_0}(t) + M_{D_x^1\phi}^{\frac{n}{4}}(t)M_v^{\nu_0}(t) + M_\phi^{\frac{n}{4}}(t)M_u^{\frac{n}{4}}(t) + M_{D_x^1\phi}^{\frac{n}{4}}(t)M_u^{\frac{n}{4}}(t)).$$

where $\nu_0 = \min\{\frac{n}{2}, \frac{n}{4}+1\}$. Then, summing the previous inequalities we obtain the L^2-norm of the function v.

$$
\begin{aligned}
\|v_j(t)\|_{L^2} \;\leq\; & C\left[e^{-ct}(\|u_0\|_{L^2} + \sum_i \|v_0^i\|_{L^2}) + \min\{1, t^{-\frac{n}{4}-\frac{1}{2}}\}\|u^0\|_{L^1} + \min\{1, t^{-\frac{n}{4}-1}\}\sum_i \|v_0^i\|_{L^1}\right] \\
& + C_k\left[\min\{1, t^{-(\frac{n}{2}+\nu_0)}\}(N_{D_x^1\phi}^{\frac{n}{2}}(t)M_v^{\nu_0}(t) + N_\phi^{\frac{n}{2}}(t)M_v^{\nu_0}(t))\right. \qquad\qquad\qquad (2.49) \\
& + \min\{1, t^{-\frac{3}{4}n}\}(M_u^{\frac{n}{4}}(t)N_\phi^{\frac{n}{2}}(t) + M_u^{\frac{n}{4}}(t)N_{D_x^1\phi}^{\frac{n}{2}}(t)) \\
& + \left.\min\{1, t^{-\nu_0}\}(M_\phi^{\frac{n}{4}}(t)M_v^{\nu_0}(t) + M_{D_x^1\phi}^{\frac{n}{4}}(t)M_v^{\nu_0}(t) + M_\phi^{\frac{n}{4}}(t)M_u^{\frac{n}{4}}(t) + M_{D_x^1\phi}^{\frac{n}{4}}(t)M_u^{\frac{n}{4}}(t))\right].
\end{aligned}
$$

In order to complete our study we need to estimate the L^2 norm of the s-derivative of function v and its L^∞ norm.

L^2-estimate for $D_x^s v$

Regarding the s-order estimate for v_j, we have

$$
\begin{aligned}
\|D_x^s v_j(t)\|_{L^2} \;\leq\; & C\left[e^{-ct}(\|D_x^s u_0\|_{L^2} + \sum_{i=1}^n \|D_x^s v_0^i\|_{L^2} + \min\{1, t^{-\frac{n}{4}-\frac{1}{2}-\frac{s}{2}}\}\|u_0\|_{L^1}\right. \\
& + \left.\min\{1, t^{-\frac{n}{4}-1-\frac{s}{2}}\}\sum_{i=1}^n \|v_0^i\|_{L^1}\right] + C_k\left[\min\{1, t^{-(\tilde{\delta}+\frac{n}{2})}\}(M_{D_x^s\phi}^{\tilde{\delta}}(t)N_v^{\frac{n}{2}}(t) + M_{D_x^{s+1}\phi}^{\tilde{\delta}}(t)N_v^{\frac{n}{2}}(t))\right. \\
& + \min\{1, t^{-(\frac{n}{2}+\tilde{v})}\}(N_{D_x^1\phi}^{\frac{n}{2}}(t)M_{D_x^s v}^{\tilde{v}}(t) + N_\phi^{\frac{n}{2}}(t)M_{D_x^s v}^{\tilde{v}}(t)) \qquad\qquad (2.50) \\
& + \min\{1, t^{-(\tilde{\delta}+\frac{n}{2})}\}(M_{D_x^s\phi}^{\tilde{\delta}}(t)N_u^{\frac{n}{2}}(t) + M_{D_x^s\phi}^{\tilde{\delta}}(t)N_u^{\frac{n}{2}}(t) + M_{D_x^s u}^{\tilde{\delta}}(t)N_\phi^{\frac{n}{2}}(t) + M_{D_x^s u}^{\tilde{\delta}}(t)N_{D_x^1\phi}^{\frac{n}{2}}(t) \\
& + \left.\min\{1, t^{-\tilde{v}}\}(M_\phi^{\frac{n}{4}}(t)M_v^{\nu_0}(t) + M_{D_x^1\phi}^{\frac{n}{4}}(t)M_v^{\nu_0}(t) + M_\phi^{\frac{n}{4}}(t)M_v^{\nu_0}(t) + M_{D_x^1\phi}^{\frac{n}{4}}(t)M_v^{\nu_0}(t)\right].
\end{aligned}
$$

Let us recall that $\tilde{v} = \min\{\frac{n}{4}+1+\frac{s}{2}, \frac{n}{2}\}$.

L^∞-**estimate for** v

On the other hand, for the L^∞ norm of function v_j, we get the following estimates

$$
\begin{aligned}
\|v_j(t)\|_{L^\infty} \;\leq\; & C\left[e^{-ct}(\|u_0\|_{H^s} + \sum_{i=1}^{n}\|v_0^i\|_{H^s}) + \min\{1, t^{-\frac{n}{2}-\frac{1}{2}}\}\|u_0\|_{L^1} + \min\{1, t^{-\frac{n}{2}-1}\}\sum_{i=1}^{n}\|v_0^n\|_{L^1}\right] \\
& + C_k\left[\min\{1, t^{-(\frac{n}{2}+v_0)}\}(N_{D_x^1\phi}^{\frac{n}{2}}(t)M_v^{v_0}(t) + N_\phi^{\frac{n}{2}}(t)M_v^{v_0}(t))\right. \\
& + \min\{1, t^{-\frac{3}{4}n}\}(M_u^{\frac{n}{4}}(t)N_\phi^{\frac{n}{2}}(t) + M_u^{\frac{n}{4}}(t)N_{D_x^1\phi}^{\frac{n}{2}}(t)) \\
& + \min\{1, t^{-(\tilde\delta+\frac{n}{2})}\}(M_{D_x^s\phi}^{\tilde\delta}(t)N_v^{\frac{n}{2}}(t) + M_{D_x^{s+1}\phi}^{\tilde\delta}(t)N_v^{\frac{n}{2}}(t)) \\
& + \min\{1, t^{-(\frac{n}{2}+\tilde v)}\}(N_{D_x^1\phi}^{\frac{n}{2}}(t)M_{D_x^s v}^{\tilde v}(t) + N_\phi^{\frac{n}{2}}(t)M_{D_x^s v}^{\tilde v}(t)) \\
& + \min\{1, t^{-(\tilde\delta+\frac{n}{2})}\}(M_{D_x^s\phi}^{\tilde\delta}(t)N_u^{\frac{n}{2}}(t) + M_{D_x^s\phi}^{\tilde\delta}(t)N_u^{\frac{n}{2}}(t) + M_{D_x^s u}^{\tilde\delta}(t)N_\phi^{\frac{n}{2}}(t) + M_{D_x^s u}^{\tilde\delta}(t)N_{D_x^1\phi}^{\frac{n}{2}}(t)) \\
& \left. + \min\{1, t^{-\frac{n}{2}}\}(M_\phi^{\frac{n}{4}}(t)M_v^{v_0}(t) + M_{D_x^1\phi}^{\frac{n}{4}}(t)M_v^{v_0}(t)) + M_\phi^{\frac{n}{4}}(t)M_u^{\frac{n}{4}}(t) + M_{D_x^1\phi}^{\frac{n}{4}}(t)M_u^{\frac{n}{4}}(t)\right].
\end{aligned}
\tag{2.51}
$$

Once that, decay rates of variable have been determined by inequalities (2.43), (2.45), (2.47), (2.49), (2.50), (2.51), we apply Proposition 2.4.2 to get the following estimates for the functionals related to the solution (u, v). For $t > \epsilon > 0$,

$$
\begin{aligned}
M_u^{\frac{n}{4}}(t) \;\leq\; & C_1\left[E_0 + D_0 + D_0\left(M_u^{\frac{n}{4}}(t) + N_u^{\frac{n}{2}}(t) + M_v^{v_0}(t) + N_v^{\frac{n}{2}}(t)\right) + (N_u^{\frac{n}{2}}(t))^2\right. \\
& \left. + M_u^{\frac{n}{4}}(t)N_v^{\frac{n}{2}}(t) + N_u^{\frac{n}{2}}(t)M_u^{\frac{n}{4}}(t) + (M_u^{\frac{n}{4}}(t))^2 + M_u^{\frac{n}{4}}(t)M_v^{v_0}(t)\right],
\end{aligned}
$$

where $v_0 = \min\{\frac{n}{2}, \frac{n}{4}+\frac{1}{2}\}$.

$$
\begin{aligned}
M_{D_x^s u}^{\tilde\delta}(t) \;\leq\; & C_2\left[E_0 + D_0 + D_0\left(M_u^{\frac{n}{4}}(t) + N_u^{\frac{n}{2}}(t) + M_{D_x^s u}^{\tilde\delta}(t) + M_v^{v_0}(t) + N_v^{\frac{n}{2}}(t) + M_{D_x^s v}^{\tilde v}(t)\right)\right. \\
& \left. + N_u^{\frac{n}{2}}(t)M_{D_x^s v}^{\tilde v}(t) + (M_u^{\frac{n}{4}}(t))^2 + M_{D_x^s u}^{\tilde\delta}(t)N_v^{\frac{n}{2}}(t) + N_u^{\frac{n}{2}}(t)M_{D_x^s u}^{\tilde\delta}(t) + M_u^{\frac{n}{4}}(t)M_v^{v_0} + (M_{D_x^s u}^{\tilde\delta}(t))^2\right],
\end{aligned}
$$

where $\tilde\delta = \min\{\frac{n}{4}+\frac{1}{2}+\frac{s}{2}, \frac{n}{2}\}$, and $\tilde v = \min\{\frac{n}{4}+1+\frac{s}{2}, \frac{n}{2}\}$.

$$
\begin{aligned}
N_u^{\frac{n}{2}}(t) \;\leq\; & C_3\left[E_0 + D_0 + D_0\left(M_u^{\frac{n}{4}}(t) + N_u^{\frac{n}{2}}(t) + M_{D_x^s u}^{\tilde\delta}(t) + M_v^{v_0}(t) + N_v^{\frac{n}{2}}(t) + M_{D_x^s v}^{\tilde v}(t)\right)\right. \\
& + M_u^{\frac{n}{4}}(t)N_v^{\frac{n}{2}}(t) + N_u^{\frac{n}{2}}(t)M_v^{v_0}(t) + N_u^{\frac{n}{2}}(t)M_u^{\frac{n}{4}}(t) + (M_u^{\frac{n}{4}}(t))^2 + M_{D_x^s u}^{\tilde\delta}(t)N_v^{\frac{n}{2}}(t) \\
& \left. + N_u^{\frac{n}{2}}(t)M_{D_x^s u}^{\tilde\delta}(t) + M_u^{\frac{n}{4}}(t)M_v^{v_0}(t) + M_{D_x^s v}^{\tilde v}(t)N_u^{\frac{n}{2}}(t) + (M_{D_x^s u}^{\tilde v}(t))^2 + M_{D_x^s u}^{\frac{n}{2}}(t)N_u^{\frac{n}{2}}(t)\right].
\end{aligned}
$$

$$M_v^{v_0}(t) \leq C_4 \left[E_0 + D_0 + D_0 \, (M_u^{\frac{n}{4}}(t) + N_u^{\frac{n}{2}}(t) + M_v^{v_0}(t) + N_v^{\frac{n}{2}}(t)) \, (N_u^{\frac{n}{2}}(t))^2 \right.$$

$$\left. + \ M_u^{\frac{n}{4}}(t) N_v^{\frac{n}{2}}(t) + N_u^{\frac{n}{2}}(t) M_u^{\frac{n}{4}}(t) + (M_u^{\frac{n}{4}}(t))^2 + M_u^{\frac{n}{4}}(t) M_v^{v_0}(t) \right].$$

$$M_{D_x^s v}^{\tilde{v}}(t) \leq C_5 \left[E_0 + D_0 + D_0 \left(M_u^{\frac{n}{4}}(t) + N_u^{\frac{n}{2}}(t) + M_{D_x^s u}^{\tilde{\delta}}(t) + M_v^{v_0}(t) + N_v^{\frac{n}{2}}(t) + M_{D_x^s v}^{\tilde{v}}(t) \right) \right.$$

$$\left. + \ N_u^{\frac{n}{2}}(t) M_{D_x^s v}^{\tilde{v}}(t) + (M_u^{\frac{n}{4}}(t))^2 + M_{D_x^s u}^{\tilde{\delta}}(t) N_v^{\frac{n}{2}}(t) + N_u^{\frac{n}{2}}(t) M_{D_x^s u}^{\tilde{\delta}}(t) + M_u^{\frac{n}{4}}(t) M_v^{v_0} + (M_{D_x^s u}^{\tilde{\delta}}(t))^2 \right].$$

$$N_v^{\frac{n}{2}}(t) \leq C_6 \left[E_0 + D_0 + D_0 \left(M_u^{\frac{n}{4}}(t) + N_u^{\frac{n}{2}}(t) + M_{D_x^s u}^{\tilde{\delta}}(t) + M_v^{v_0}(t) + N_v^{\frac{n}{2}}(t) + M_{D_x^s v}^{\tilde{v}}(t) \right) \right.$$

$$+ \ M_u^{\frac{n}{4}}(t) N_v^{\frac{n}{2}}(t) + N_u^{\frac{n}{2}}(t) M_v^{v_0}(t) + N_u^{\frac{n}{2}}(t) M_u^{\frac{n}{4}}(t) + (M_u^{\frac{n}{4}}(t))^2 + M_{D_x^s u}^{\tilde{\delta}}(t) N_v^{\frac{n}{2}}(t)$$

$$\left. + \ N_u^{\frac{n}{2}}(t) M_{D_x^s u}^{\tilde{\delta}}(t) + M_u^{\frac{n}{4}}(t) M_v^{v_0}(t) + M_{D_x^s v}^{\tilde{v}}(t) N_u^{\frac{n}{2}}(t) + (M_{D_x^s u}^{\tilde{v}}(t))^2 + M_{D_x^s u}^{\frac{n}{2}}(t) N_u^{\frac{n}{2}}(t) + (N_u^{\frac{n}{2}}(t))^2 \right].$$

where $D_0 = \|\phi_0\|_{H^{s+1}}$, $E_0 = \max\{\|u_0\|_{H^s}, \|u_0\|_{L^1}, \|v_0\|_{H^s}, \|v_0\|_{L^1}\}$ and the constant $C_i = C_i(F_k, K, C_{b'}, C_{h'})$.

Let us define

$$P(t) := M_u^{\frac{n}{4}}(t) + N_u^{\frac{n}{2}}(t) + M_{D_x^s u}^{\tilde{\delta}}(t) + M_v^{v_0}(t) + N_v^{\frac{n}{2}}(t) + M_{D_x^s v}^{\tilde{v}}(t).$$

We can notice that all the previous estimates are linear combinations of sums of type: $A_0 F_w^\delta(t) + F_w^\delta(t) F_{w_1}^{\delta_1}(t)$ where $F_w^\delta, F_{w_1}^{\delta_1}$ are terms of $P(t)$. Then it is possible to estimate each of them with $A_0 P(t) + P(t)^2$. It follows that if initial data are small, we have

$$C_k P(t)^2 - (1 - C_{k0}) P(t) + C_0 \geq 0, \tag{2.52}$$

where C_k is a positive constant depending on K, C_{k0} is a positive constant depending on K and on data, and C_0 also is a positive constant depending on data. For suitably small initial data, this inequality implies that $M_u^{\frac{n}{4}}(t)$, $N_u^{\frac{n}{2}}(t)$, $M_{D_x^s u}^{\tilde{\delta}}(t)$, $M_v^{v_0}(t)$, $N_v^{\frac{n}{2}}(t)$, $M_{D_x^s v}^{\tilde{v}}(t)$ remain bounded, as far as $\|u, v\|_{L^\infty} \leq K$ and $\|\phi\|_{W^{1,\infty}} \leq K$. When $t > 1$ this implies that $\|w(t)\|_{L^\infty}$ does not increase. Thanks to the Proposition 2.4.2 the same is true for $N_\phi^{\frac{n}{2}}$ and $N_{D_x^1 \phi}^{\frac{n}{2}}$.

Since we have also obtained that $\|\phi(t)\|_{W^{1,\infty}}$ is bounded, from Lemma 2.3.5 and the continuation principle we have the global existence of smooth solutions to system (2.1).

Optimal Decay Rates

In order to complete our proof, we need to improve the decay rates of $D_x^s u$, $D_x^s v$, $D_x^s \phi$ in the L^2 norm.

By the previous estimates, we got that, independently from the derivative order s, the decays rates of these function are equal to $\tilde{\delta} = \min\{\frac{n}{4} + \frac{1}{2} + \frac{s}{2}, \frac{n}{2}\}$, for u, ϕ and equal to $\tilde{v} = \min\{\frac{n}{4} + 1 + \frac{s}{2}, \frac{n}{2}\}$ for v. This implies that, for small n, even if the derivative order is high, we get always the decay $t^{-\frac{n}{2}}$, as illustrated by the blue line in Figure 2.2 for $n = 2$.
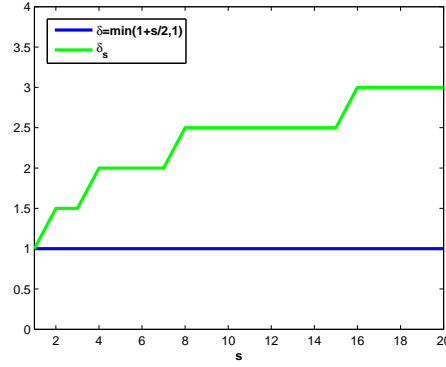
Figure 2.2: Comparison between $\tilde{\delta} = \min\left\{1 + \frac{s}{2}, 1\right\}$ and $\delta_s = \min\left\{1 + \frac{1}{2}\left[\frac{s+1}{2}\right], \frac{1}{2} + \delta_r\right\}$, with $r = \left[\frac{s}{2}\right]$ for $n = 2$.

Looking at inequality (2.45) we notice that these decays come from the estimates related to Green Kernel diffusive part.

Then, we need to adopt a different strategy to estimate these terms and overcome the difficulty, i.e. split the derivatives on both terms.

We show this procedure by induction on a simple source term ϕu.

- Let $s = 1$. Since in this case we cannot split the order of derivative, we proceed as done before keeping the derivative on the Green Kernel. Then,

$$
\begin{aligned}
\int_0^t \|D_x^1 K_{12}(t-s) * (u(s)\phi(s))\|_{L^2} ds &\leq \int_0^t C\min\{1, (t-s)^{-\frac{n}{4}-1}\}\|\phi)(s)u(s)\|_{L^1} ds \\
&\leq \int_0^t C\min\{1, (t-s)^{-\frac{n}{4}-1}\}\|\phi(s)\|_{L^2}\|u(s)\|_{L^2} ds \\
&\leq CM_\phi^{\frac{n}{4}}(t)M_u^{\frac{n}{4}}(t)\int_0^t \min\{1, (t-s)^{-\frac{n}{4}-1}\}\min\{1, s^{-\frac{n}{2}}\} ds \\
&\leq \min\{1, t^{-\delta_1}\}CM_\phi^{\frac{n}{4}}(t)M_u^{\frac{n}{4}}(t),
\end{aligned}
$$

where $\delta_1 = \min\left\{\frac{n}{4} + 1, \frac{n}{2}\right\}$.

- Let us consider the second order derivative, i.e. $s = 2$. Now we split the derivative both on the Green Kernel and the source term, proceeding as follows,

$$
\begin{aligned}
\int_0^t \|D_x^2 K_{12}(t-s) * (\phi(s)u(s)\|_{L^2} ds &= \int_0^t \|D_x^1 K_{12}(t-s) * D_x^1(\phi(s)u(s))\|_{L^2} ds \\
&\leq \int_0^t C\min\{1, (t-s)^{-\frac{n}{4}-1}\}\|D_x^1\phi(s)u(s)\|_{L^1} ds \\
&\leq \int_0^t C\min\{1, (t-s)^{-\frac{n}{4}-1}\}(\|D_x^1\phi\|_{L^2}\|u(s)\|_{L^2} + \|\phi(s)\|_{L^2}\|D_x^1 u(s)\|_{L^2}) \\
&\quad + C(M_{D_x^1\phi}^{\delta_1}M_u^{\frac{n}{4}}(t) + M_\phi^{\frac{n}{4}}M_{D_x^1 u}^{\delta}(t))\int_0^t \min\{1, (t-s)^{-\frac{n}{4}-1}\}\min\{1, s^{-\frac{n}{4}-\delta_1}\} ds \\
&\leq \min\{1, t^{-\delta_2}\}C(M_\phi^{\frac{n}{4}}(t)M_{D_x^1 u}^{\delta_1}(t) + M_{D_x^1\phi}^{\delta_1}(t)M_u^{\frac{n}{4}}(t)),
\end{aligned}
$$

where $\delta_2 = \min\left\{\frac{n}{4} + 1, \frac{n}{4} + \delta_1\right\}$.

- Finally, we iterate the procedure for a generic s, splitting the derivatives as follows. We left $\left[\frac{s+1}{2}\right]$ derivatives on the Green Kernel, and the remaining ones $\left[\frac{s}{2}\right]$, on the source terms. By this way we get

$$\int_0^t \|D_x^s K_{12}(t-s) * (\phi(s)u(s))\|_{L^2} \le \int_0^t \|D_x^{\left[\frac{s+1}{2}\right]} K_{12}(t-s) * D_x^{\left[\frac{s}{2}\right]}(\phi(s)u(s))\|_{L^2} ds$$

$$\le \min\{1, t^{-\delta_s}\} C(M_\phi^{\frac{n}{4}}(t) M_{D_x^r u}^{\delta_r}(t) + M_{D_x^r \phi}^{\delta_r}(t) M_u^{\frac{n}{4}}(t)),$$

where $\delta_s = \min\left\{\frac{n}{4} + \frac{1}{2} + \frac{1}{2}\left[\frac{s+1}{2}\right], \frac{n}{4} + \delta_r\right\}$, with $r = \left[\frac{s}{2}\right]$.

Thus, through this simple procedure, we are able to obtain faster decays rates for the s derivative of the functions u, v and ϕ. More precisely for the $s-$derivative of function v, since the Green Kernel has a faster decay, we get the rate $v_s = \min\left\{\frac{n}{4} + 1 + \frac{1}{2}\left[\frac{s+1}{2}\right], \frac{n}{4} + \delta_r\right\}$.

$\square$

2.5 Global Existence and Asymptotic Behavior of Perturbations of Constant Stationary States

The aim of this section is to investigate the behavior of small constant states. For the sake of simplicity we will consider the system with a simpler source term,

$$\begin{cases} \partial_t \tilde{u} + \nabla \cdot \tilde{v} = 0, \\\\ \partial_t \tilde{v} + \nabla \tilde{u} = -\tilde{v} + \tilde{u} \nabla \tilde{\phi}, \\\\ \partial_t \tilde{\phi} = \Delta \tilde{\phi} + a \tilde{u} - b \tilde{\phi}, \end{cases}$$

where $(\tilde{u}, \tilde{v}, \tilde{\phi}) = (\bar{u} + u, v, \bar{\phi} + \phi)$, $(\bar{u}, 0, \bar{\phi})$ is a stationary solution with $\bar{\phi} = \frac{a}{b} \bar{u}$, and (u, v, ϕ) is a perturbation. Therefore we can rewrite the previous system as follows

$$\begin{cases} \partial_t u + \nabla \cdot v = 0, \\\\ \partial_t v + \nabla u = -v + (u + \bar{u}) \nabla \phi, \\\\ \partial_t \phi = \Delta \phi + a u - b \phi. \end{cases} \tag{2.53}$$

This system is supplemented by the initial conditions

$$u_0, v_0 \in H^s(\mathbb{R}^n) \cap L^1(\mathbb{R}^n), \quad \phi_0 \in H^{s+1}(\mathbb{R}^n) \cap L^1(\mathbb{R}^n). \tag{2.54}$$

In order to prove the global existence result and the decay of solutions to (2.53) we will proceed along the lines of the previous sections. Then starting from a local solution to (2.53), which is guaranteed by Theorem 2.2.1, we will get estimates and decay rates of the H^s and L^∞ norm. Then by the continuation principle 2.3.4 we will obtain our existence result.

To get the decay of solutions we need to adapt the technique used in the above proof of stability for the zero constant state, to treat the linear term $\bar{u} \nabla \phi$, which does not present enough polynomial decay.

Existence of global solutions to system (2.53) is given by the following theorem.

Theorem 2.5.1. *There exists an $\epsilon_0 > 0$ such that, if*

$$\|u_0\|_{H^s}, \|u_0\|_{L^1}, \|v_0\|_{H^s}, \|v_0\|_{L^1}, \|\phi_0\|_{H^{s+1}}, \|\phi_0\|_{L^1}, \bar{u} \le \epsilon_0,$$

then there exists a unique global solution to the Cauchy problem (2.53)-(2.54)

$$u \in C([0,\infty); H^s(\mathbb{R}^n)), \; v \in C([0,\infty); H^s(\mathbb{R}^n)), \; \phi \in C([0,\infty); H^{s+1}(\mathbb{R}^n)), \quad for \; s \ge \left[\frac{n}{2}\right] + 1. \qquad (2.55)$$

Moreover, for the solution (u, v, ϕ) the following decay rates are satisfied

$$\|u(t)\|_{L^\infty} \sim t^{-\frac{n}{4}}, \quad \|u(t)\|_{L^2} \sim t^{-\frac{n}{4}}, \qquad \|D_x^k u(t)\|_{L^2} \sim t^{-\delta_k}, \quad for \; k = 0,\dots,s;$$

$$\|v(t)\|_{L^\infty} \sim t^{-\frac{n}{4}}, \quad \|v(t)\|_{L^2} \sim t^{-\frac{n}{4}}, \qquad \|D_x^k v(t)\|_{L^2} \sim t^{-\delta_k}, \quad for \; k = 0,\dots,s; \qquad (2.56)$$

$$\|\phi(t)\|_{L^\infty} \sim t^{-\frac{n}{4}}, \quad \|D_x^1 \phi(t)\|_{L^\infty} \sim t^{-\frac{n}{4}},$$

$$\|\phi(t)\|_{L^2} \sim t^{-\frac{n}{4}}, \quad \|D_x^{k+1} \phi(t)\|_{L^2} \sim t^{-\delta_k}, \quad for \; k = 0,\dots,s;$$

where $\delta_k = \min\left\{\frac{n}{4} + \frac{1}{2} + \frac{s}{2}, \frac{n}{2}\right\}$.

Proof. Let us consider a local solution to system (2.53). Taking into account the expressions for the Green function, we are going to estimates the norm of solutions.

Let us notice that for the solution to the linear parabolic equation the estimates of the previous case still hold. Moreover it is possible to get the following estimate for the function ϕ in the L^1 norm,

$$\|\phi(t)\|_{L^1} \le e^{-bt}\|\phi_0\|_{L^1} + c \sup_{s \in (0,t)} \|u(s)\|_{L^1} = e^{-bt}\|\phi_0\|_{L^1} + c\|u_0\|_{L^1}, \qquad (2.57)$$

where thanks to the conservation of the mass $\sup_{s \in (0,t)} \|u(s)\|_{L^1} = \|u_0\|_{L^1}$.

2.5.1   Decay Estimates for the Conservative and Dissipative Variables

As before we proceed by estimating the norm of the is conservative and dissipative variables of the hyperbolic part, starting from the function u.

L^2-estimate for u

By the Duhamel's formula we can write this solution as

$$u(x,t) = (\Gamma_1^h(t) * w_0)(x) + \int_0^t \Gamma_1^h(t-s) * [0, (u + \bar{u})\nabla\phi(s)] \, ds, \qquad (2.58)$$

where Γ_1^h is the first row of the $(n+1) \times (n+1)$ matrix Γ^h.

Then

$$\|u(t)\|_{L^2} \le \|\Gamma_1^h(t) * w_0\|_{L^2} + \int_0^t \|\Gamma_1^h(t-s) * [0, (u + \bar{u})\nabla\phi(s)]\|_{L^2} \, ds, \qquad (2.59)$$

From the decomposition of the Green Kernel we know that

$$\|\Gamma_1^h(t) * w_0\|_{L^2} \le \|K_{1,1}(t) * u_0\|_{L^2} + \sum_{i=1}^n \|K_{1,i+1}(t) * v_0^i\|_{L^2} + \|\mathcal{K}_{1,1}(t) * u_0\|_{L^2} + \sum_{i=1}^n \|\mathcal{K}_{1,i+1}(t) * v_0^i\|_{L^2},$$

and by Theorem 2.1.4 we get

$$\|\mathcal{K}_{1,1}(t) * u_0\|_{L^2} \le C e^{-ct} \|u_0\|_{L^2}, \qquad \|K_{1,1}(t) * u_0\|_{L^2} \le C \min\{1, t^{-\frac{n}{4}}\} \|u_0\|_{L^1},$$

$$\|\mathcal{K}_{1,i+1}(t) * v_0^i\|_{L^2} \le C e^{-ct} \|v_0^i\|_{L^2}, \qquad \|K_{1,i+1}(t) * v_0^i\|_{L^2} \le C \min\{1, t^{-\frac{n}{4}-\frac{1}{2}}\} \|v_0^i\|_{L^1}, \quad \text{for } i = 1, \dots, n.$$
$$\tag{2.60}$$

The integral term can be decomposed as

$$\int_0^t \|\Gamma_1^h(t-s) * [0, (u(s)+\bar{u})\nabla\phi(s)]\|_{L^2} \, ds \le \int_0^t \|\mathcal{K}_1(t-s) * [0, (u(s)+\bar{u})\nabla\phi(s)]\|_{L^2} \, ds$$
$$+ \int_0^t \|K_1(t-s) * [0, (u(s)+\bar{u})\nabla\phi(s)]\|_{L^2} \, ds.$$

Let us start with the first integral of the previous inequality.

$$\int_0^t \|\mathcal{K}_1(t-s) * ([0, (u(s)+\bar{u})\nabla\phi(s)])\|_{L^2} \le \int_0^t c e^{-c(t-s)} \|(u(s)+\bar{u})\nabla\phi(s)\|_{L^2} \, ds$$
$$\le \int_0^t c e^{-c(t-s)} (\|\nabla\phi(s)\|_{L^2} \|u(s)\|_{L^\infty} + \bar{u}\|\nabla\phi(s)\|_{L^2}) \, ds,$$

then

$$\int_0^t \|\mathcal{K}_1(t-s) * ([0, (u+\bar{u})\nabla\phi(s)])\|_{L^2} \le C M_{D_x^1\phi}^{\frac{n}{4}}(t) N_u^{\frac{n}{4}}(t) \int_0^t e^{-c(t-s)} \min\{1, s^{-\frac{n}{2}}\} \, ds$$
$$+ C\bar{u} M_{D_x^1\phi}^{\frac{n}{4}}(t) \int_0^t e^{-c(t-s)} \min\{1, s^{-\frac{n}{4}}\} \, ds.$$

By Lemma 2.4.1 we deduce that

$$\int_0^t \|\mathcal{K}_1(t-s) * ([0, (u(s)+\bar{u})\nabla\phi(s)]) \, ds\|_{L^2} \le C \left[\min\{1, t^{-\frac{n}{2}}\} M_{D_x^1\phi}^{\frac{n}{4}}(t) N_u^{\frac{n}{4}}(t) + \min\{1, t^{-\frac{n}{4}}\} \bar{u} M_{D_x^1\phi}^{\frac{n}{4}}(t) \right].$$
$$\tag{2.61}$$

To complete our estimate we need to study the dissipative part. Due to the presence of the linear term $\bar{u} D_x^1\phi$, we do not have enough polynomial decay. In order to overcome this difficulty we apply the derivative of the linear term to the Green function, getting a faster decay.

Thanks to this modification, we are able to estimate this term as follows

$$\int_0^t \|K_1(t-s) * ([0, (u(s)+\bar{u})\nabla\phi(s)])\|_{L^2} \, ds \le \int_0^t \sum_{i=1}^n \|K_{1,i+1}(t-s) * ([0, (u(s)+\bar{u})\partial_{x_i}\phi(s)])\|_{L^2} \, ds$$

$$\le \int_0^t \sum_{i=1}^n \|K_{1,i+1}(t-s) * ([0, u\partial_{x_i}\phi(s)])\|_{L^2} \, ds + \int_0^t \sum_{i=1}^n \|D_{x_i}^1 K_{1,i+1}(t-s) * ([0, \bar{u}\phi(s)])\|_{L^2} \, ds$$

$$\le C \int_0^t \min\{1, (t-s)^{-\frac{n}{4}-\frac{1}{2}}\} (\|u(s)\nabla\phi(s)\|_{L^1} \, ds + C \int_0^t \min\{1, (t-s)^{-\frac{n}{4}-1}\} (\|\bar{u}\phi(s)\|_{L^1} \, ds$$

$$\le C \int_0^t \min\{1, (t-s)^{-\frac{n}{4}-\frac{1}{2}}\} \|\nabla\phi(s)\|_{L^2} \|u(s)\|_{L^2} \, ds + C \int_0^t \min\{1, (t-s)^{-\frac{n}{4}-1}\} \bar{u}(e^{-bt}\|\phi_0\|_{L^1} + c\|u_0\|_{L^1}) \, ds.$$

Then we obtain the estimate

$$\int_0^t \|K_1(t-s) * ([0, (u+\bar{u})\nabla\phi(s)])\|_{L^2} \, ds \le C M_{D_x^1\phi}^{\frac{n}{4}}(t) M_u^{\frac{n}{4}}(t) \int_0^t \min\{1, (t-s)^{-\frac{n}{4}-\frac{1}{2}}\} \min\{1, s^{-\frac{n}{2}}\} \, ds$$
$$+ C\bar{u} \min\{1, t^{-\frac{n}{4}-1}\} \|\phi_0\|_{L^1} + c\bar{u} t^{-\frac{n}{4}} \|u_0\|_{L^1}$$
$$\le C \left(\min\{1, t^{-\nu}\} M_{D_x^1\phi}^{\frac{n}{4}}(t) M_u^{\frac{n}{4}}(t) + \bar{u} \min\{1, t^{-\frac{n}{4}-1}\} \|\phi_0\|_{L^1} \right)$$

$$+ \quad \bar{u} t^{-\frac{n}{4}} \|u_0\|_{L^1} \Big).$$

where $\nu = \frac{1}{4}$ if $n = 1$, otherwise $\nu = \frac{n}{4} + \frac{1}{2}$. Summing the last inequality and (2.60), (2.61) we obtain

$$
\begin{aligned}
\|u(t)\|_{L^2} \quad \leq \quad & C\Big(e^{-ct}(\|u_0\|_{L^2} + \sum_{i=1}^n \|v_0^i\|_{L^2} + \min\{1, t^{-\frac{n}{4}}\}\|u_0\|_{L^1} + \min\{1, t^{-\frac{n}{4}-\frac{1}{2}}\}\sum_{i=1}^n \|v_0^i\|_{L^1} \\
& + \quad \min\{1, t^{-\frac{n}{2}}\}(M_{D_x^1\phi}^{\frac{n}{4}}(t)N_u^{\frac{n}{4}}(t) + \min\{1, t^{-\frac{n}{4}}\}\bar{u}M_{D_x^1\phi}^{\frac{n}{4}}(t) \\
& + \quad \min\{1, t^{-\nu}\}M_{D_x^1\phi}^{\frac{n}{4}}(t)M_u^{\frac{n}{4}}(t) + \bar{u}\min\{1, t^{-\frac{n}{4}-1}\}\|\phi_0\|_{L^1} + \bar{u}t^{-\frac{n}{4}}\|u_0\|_{L^1}\Big). \quad (2.62)
\end{aligned}
$$

L^2 **estimate for** $D_x^s u$

In a similar way it is possible obtain the s-order estimate for the conservative variable. From the Duhamel's formula we know that

$$\|D_x^s u(t)\|_{L^2} \leq \|D_x^s \Gamma_1^h(t) * w_0\|_{L^2} + \int_0^t \|D_x^s \Gamma_1^h(t-s) * ([0, (u(s) + \bar{u})\nabla\phi(s)])\|_{L^2} \, ds. \quad (2.63)$$

Let us start considering the first term that we can decompose as

$$
\begin{aligned}
\|D_x^s \Gamma_1^h(t) * w_0\|_{L^2} \quad \leq \quad & \|D_x^s K_{1,1}(t) * u_0\|_{L^2} + \sum_{i=1}^n \|D_x^s K_{1,i+1}(t) * v_0^i\|_{L^2} + \|D_x^s \mathcal{K}_{1,1}(t) * u_0\|_{L^2} \\
& + \quad \sum_{i=1}^n \|D_x^s \mathcal{K}_{1,i+1}(t) * v_0^i\|_{L^2}, \quad \text{for } i = 1, \ldots, n,
\end{aligned}
$$

then by Theorem 2.1.4 we have

$$\|D_x^s \mathcal{K}_{1,1}(t) * u_0\|_{L^2} \leq Ce^{-ct}\|D_x^s u_0\|_{L^2}, \qquad \|D_x^s K_{1,1}(t) * u_0\|_{L^2} \leq C\min\{1, t^{-\frac{n}{4}-\frac{s}{2}}\}\|u_0\|_{L^1},$$

$$\|D_x^s \mathcal{K}_{1,i+1}(t) * v_0^i\|_{L^2} \leq Ce^{-ct}\|D_x^s v_0^i\|_{L^2}, \qquad \|D_x^s K_{1,i+1}(t) * v_0^i\|_{L^2} \leq C\min\{1, t^{-\frac{n}{4}-\frac{1}{2}-\frac{s}{2}}\}\|v_0^i\|_{L^1}.$$

Let us focus now on the integral term that we can decompose as

$$
\begin{aligned}
\int_0^t \|D_x^s \Gamma_1^h(t-s) * ([0, (u+\bar{u})\nabla\phi(s)])\|_{L^2} \, ds \quad \leq \quad & \int_0^t \|D_x^s \mathcal{K}_1(t-s) * ([0, (u(s)+\bar{u})\nabla\phi(s)])\|_{L^2} \, ds \\
& + \quad \int_0^t \|D_x^s K_1(t-s) * ([0, (u(s)+\bar{u})\nabla\phi(s)])\|_{L^2} \, ds.
\end{aligned}
$$

We estimate the first integral as

$$
\begin{aligned}
\int_0^t \|D_x^s \mathcal{K}_1(t-s) * ([0, (u(s)+\bar{u})\nabla\phi(s)])\|_{L^2} &\leq \int_0^t Ce^{-c(t-s)}\|D_x^s[(u(s)+\bar{u})\nabla\phi(s)]\|_{L^2} \\
&\leq \int_0^t Ce^{-c(t-s)}(\|\bar{u}D_x^s(\nabla\phi(s))\|_{L^2} + \|D_x^s(u\nabla\phi(s))\|_{L^2}) \\
&\leq \int_0^t Ce^{-c(t-s)}(\bar{u}\|D_x^{s+1}\phi(s)\|_{L^2} + \|u(s)\|_{L^\infty}\|D_x^{s+1}\phi(s)\|_{L^2} + \|\nabla\phi(s)\|_{L^\infty}\|D_x^s u(s)\|_{L^2}.
\end{aligned}
$$

Thanks to Lemma 2.4.1 we deduce that:

$$
\begin{aligned}
\int_0^t \|D_x^s \mathcal{K}_1(t-s) * ([0, (u+\bar{u})\nabla\phi(s)])\|_{L^2} \quad \leq \quad & C\bar{u}\min\{1, t^{-\delta_s}\}M_{D_x^{s+1}\phi}^{\delta_s}(t) \\
& + \quad C\min\{1, t^{-\delta_s+\frac{n}{4}}\}(N_u^{\frac{n}{4}}(t)M_{D_x^{s+1}\phi}^{\delta_s}(t) + N_{D_x^1\phi}^{\frac{n}{4}}(t)M_{D_x^s u}^{\delta_s}(t)).
\end{aligned}
$$

To complete our estimate, we need to study the dissipative part,

$$\int_0^t \|D_x^s K_1(t-s) * ([0,(u+\bar{u})\nabla\phi(s)])\|_{L^2}\,ds \leq \int_0^t \sum_{i=1}^n \|D_x^s K_{1,i+1}(t-s) * ([0,(u+\bar{u})\partial_{x_i}\phi(s)])\|_{L^2}\,ds$$

$$\leq \int_0^t \sum_{i=1}^n \|D_x^s \mathcal{K}_{1,i+1}(t-s) * u(s)\partial_{x_i}\phi(s)\|_{L^2}\,ds + \int_0^t \sum_{i=1}^n \|D_x^{s+1} K_{1,i+1}(t-s) * \bar{u}\phi(s)\|_{L^2}\,ds.$$

We proceed as done before and by Lemma 2.4.1 we obtain

$$\int_0^t \|K_1(t-s) * ([0,(u(s)+\bar{u})\nabla\phi(s)])\|_{L^2} \leq C\left[\min\{1, t^{-\delta_s}\}(M_{D_x^1\phi}^{\frac{n}{4}}(t)M_u^{\frac{n}{4}}(t) + M_u^{\frac{n}{4}}(t)M_{D_x^1\phi}^{\frac{n}{4}}(t))\right.$$

$$\left. + \bar{u}t^{-\frac{n}{4}-\frac{s}{2}}\|u_0\|_{L^1} + \bar{u}\min\{1, t^{-\frac{n}{4}-1-\frac{s}{2}}\}\|\phi_0\|_{L^1}\right].$$

where $\delta_s = \min\left\{\frac{n}{4}+\frac{1}{2}+\frac{s}{2}, \frac{n}{2}\right\}$. Then we can write the estimate in the L^2 norm of the s−derivative of the conservative variable u as

$$
\begin{aligned}
\|D_x^s u(t)\|_{L^2} \leq\ & C\Big[e^{-ct}(\|D_x^s u_0\|_{L^2} + \|D_x^s v_0\|_{L^2} + \min\{1, t^{-\frac{n}{4}-\frac{s}{2}}\}\|u^0\|_{L^1} + \min\{1, t^{-\frac{n}{4}-\frac{1}{2}-\frac{s}{2}}\}\|v_0\|_{L^1})) \\
& + \bar{u}\min\{1, t^{-\delta_s}\}(M_{D_x^{s+1}\phi}^{\delta_s}(t) + \min\{1, t^{-\delta_s+\frac{n}{2}}\}(N_u^{\frac{n}{4}}(t)M_{D_x^{s+1}\phi}^{\delta_s}(t) + N_{D_x^1\phi}^{\frac{n}{4}}(t)M_{D_x^s u}^{\delta_s}(t))) \\
& + \min\{1, t^{-\delta_s}\}(M_{D_x^1\phi}^{\frac{n}{4}}(t)M_u^{\frac{n}{4}}(t) + M_u^{\frac{n}{4}}(t)M_{D_x^1\phi}^{\frac{n}{4}}(t)) \qquad\qquad (2.64)\\
& + \bar{u}t^{-\frac{n}{4}-\frac{s}{2}}\|u_0\|_{L^1} + \bar{u}\min\{1, t^{-\frac{n}{4}-1-\frac{s}{2}}\}\|\phi_0\|_{L^1}\Big].
\end{aligned}
$$

L^∞-estimate for u

Finally with the same approach, we estimate the L^∞ norm of the function u. By the Duhamel's formula we know that

$$\|u(t)\|_{L^\infty} \leq \|\Gamma_1^h(t) * w_0\|_{L^\infty} + \int_0^t \|\Gamma_1^h(t-s) * ([0,(u(s)+\bar{u})\nabla\phi(s)])\|_{L^\infty}\,ds, \qquad (2.65)$$

and by the decomposition of the Green Kernel, we get

$$\|\Gamma_1^h(t) * w_0\|_{L^\infty} \leq \|K_{1,1}(t) * u_0\|_{L^\infty} + \sum_{i=1}^n \|K_{1,i+1}(t) * v_0^i\|_{L^\infty} + \|\mathcal{K}_{1,1}(t) * u_0\|_{L^\infty} + \sum_{i=1}^n \|\mathcal{K}_{1,i+1}(t) * v_0^i\|_{L^\infty}.$$

By Theorem 2.1.4, we deduce that

$$\|\mathcal{K}_{1,1}(t) * u_0\|_{L^\infty} \leq Ce^{-ct}\|u_0\|_{H^s}, \qquad \|K_{1,1}(t) * u_0\|_{L^\infty} \leq C\min\{1, t^{-\frac{n}{2}}\}\|u_0\|_{L^1},$$

$$\|\mathcal{K}_{1,i+1}(t) * v_0^i\|_{L^2} \leq Ce^{-ct}\|v_0^i\|_{H^s}, \qquad \|K_{1,i+1}(t) * v_0^i\|_{L^2} \leq C\min\{1, t^{-\frac{n}{2}-\frac{1}{2}}\}\|v_0^i\|_{L^1}.$$

We can decompose the integral term as,

$$
\begin{aligned}
\int_0^t \|\Gamma_1^h(t-s) * ([0,(u(s)+\bar{u})\nabla\phi(s)])\|_{L^\infty}\,ds \leq\ & \int_0^t \sum_{i=1}^n \|\mathcal{K}_{1,i+1}(t-s) * ([0,(u+\bar{u})\partial_{x_i}\phi(s)])\|_{L^\infty}\,ds \\
& + \int_0^t \sum_{i=1}^n \|K_{1,i+1}(t-s) * ([0,(u(s)+\bar{u})\partial_{x_i}\phi(s)])\|_{L^\infty}\,ds.
\end{aligned}
$$

Let us estimate the first term in the previous inequality,

$$\int_0^t \sum_{i=1}^n \|\mathcal{K}_{1,i+1}(t-s) * ([0,(u(s)+\bar{u})\partial_{x_i}\phi(s)])\|_{L^\infty}\,ds \leq \int_0^t \sum_{i=1}^n C\|\mathcal{K}_{1,i+1}(t-s) * ([0,(u+\bar{u})\partial_{x_i}\phi(s)])\|_{L^2}\,ds$$

$$+C\int_0^t \sum_{|\alpha|=s} \|D_x^s \sum_{i=1}^n \mathcal{K}_{1,i+1}(t-s) * ([0,(u+\bar{u})\partial_{x_i}\phi(s)])\|_{L^2} \, ds$$

Then, by the estimates of the function u and its derivatives in the L^2 norm, we have

$$\int_0^t \sum_{i=1}^n \|\mathcal{K}_{1,i+1}(t-s) * ([0,(u+\bar{u})\partial_{x_i}\phi(s)])\|_{L^\infty} \, ds$$

$$\leq C\Big(\min\{1,t^{-\frac{n}{2}}\}(M_{D_x^1\phi}^{\frac{n}{4}}(t)N_u^{\frac{n}{4}}(t) + \min\{1,t^{-\frac{n}{4}}\}\bar{u}M_{D_x^1\phi}^{\frac{n}{4}}(t)$$

$$+ \bar{u}\min\{1,t^{-\delta_s}\}(M_{D_x^{s+1}\phi}^{\delta_s}(t) + \min\{1,t^{-\delta_s+\frac{n}{4}}\}(N_u^{\frac{n}{4}}(t)M_{D_x^{s+1}\phi}^{\delta_s}(t) + N_{D_x^1\phi}^{\frac{n}{4}}(t)M_{D_x^s u}^{\delta_s}(t))\Big).$$

As the final step we need to estimate the dissipative part:

$$\int_0^t \|K_1(t-s) * ([0,(u+\bar{u})\nabla\phi(s)])\|_{L^\infty} \, ds \leq \int_0^t C\min\{1,(t-s)^{-\frac{n}{2}-\frac{1}{2}}\}\|(u+\bar{u})\nabla\phi(s)])\|_{L^1} \, ds$$

$$\leq \int_0^t C\min\{1,(t-s)^{-\frac{n}{2}-\frac{1}{2}}\}\|\nabla\phi(s)\|_{L^2}\|u(s)\|_{L^2} \, ds$$

$$+ \int_0^t C\min\{1,(t-s)^{-\frac{n}{2}-1}\}\bar{u}\|\phi(s)\|_{L^1} \, ds$$

$$\leq C\Big[\min\{1,t^{-\frac{n}{2}}\}M_{D_x^1\phi}^{\frac{n}{4}}(t)M_u^{\frac{n}{4}}(t) + \bar{u}t^{-\frac{n}{2}}\|u_0\|_{L^1}$$

$$+ \bar{u}\min\{1,t^{-\frac{n}{2}-1}\}\|\phi_0\|_{L^1}\Big].$$

Thus we can estimate the L^∞ norm of the function u as follows.

$$\begin{aligned}
\|u(t)\|_{L^\infty} &\leq C\Big[e^{-ct}(\|u_0\|_{H^s} + \sum_{i=1}^n \|v_0^i\|_{H^s}) + \min\{1,t^{-\frac{n}{2}}\}\|u^0\|_{L^1} + \min\{1,t^{-\frac{n}{2}-\frac{1}{2}}\}\sum_{i=1}^n \|v_0^i\|_{L^1} \\
&+ \min\{1,t^{-\frac{n}{2}}\}(M_{D_x^1\phi}^{\frac{n}{4}}(t)N_u^{\frac{n}{4}}(t) + \min\{1,t^{-\frac{n}{4}}\}\bar{u}M_{D_x^1\phi}^{\frac{n}{4}}(t) \\
&+ \bar{u}\min\{1,t^{-\delta_s}\}M_{D_x^{s+1}\phi}^{\delta_s}(t) + \min\{1,t^{-\delta_s+\frac{n}{4}}\}(N_u^{\frac{n}{2}}(t)M_{D_x^{s+1}\phi}^{\delta_s}(t) + N_{D_x^1\phi}^{\frac{n}{4}}(t)M_{D_x^s u}^{\delta_s}(t)) \\
&+ \min\{1,t^{-\frac{n}{2}}\}M_{D_x^1\phi}^{\frac{n}{4}}(t)M_u^{\frac{n}{4}}(t) + \bar{u}t^{-\frac{n}{2}}\|u_0\|_{L^1} + \bar{u}\min\{1,t^{-\frac{n}{2}-1}\}\|\phi_0\|_{L^1}\Big]. \qquad (2.66)
\end{aligned}$$

Next subsection is devoted to the estimates of the L^2 and L^∞ norms of the function v.

L^2-**estimate for v**

By the Duhamel's formula we can write the generic component v_j, with $j = 1,\dots,n$, as

$$v_j(x,t) = (\Gamma_{j+1}^h(t) * w_0)(x) + \int_0^t \Gamma_{j+1}^h(t-s) * ([0,(u(s)+\bar{u})\nabla\phi(s)]) \, ds,$$

then

$$\|v_j(t)\|_{L^2} \leq \|\Gamma_{j+1}^h(t) * w_0\|_{L^2} + \int_0^t \|\Gamma_{j+1}^h(t-s) * ([0,(u+\bar{u})\nabla\phi(s)])\|_{L^2} \, ds. \qquad (2.67)$$

By the decomposition of the Green kernel we have that

$$\begin{aligned}
\|\Gamma_{j+1}^h(t) * w_0\|_{L^2} &\leq \|K_{j+1,1}(t) * u_0\|_{L^2} + \sum_{i=1}^n \|K_{j+1,i+1}(t) * v_0^i\|_{L^2} + \|\mathcal{K}_{j+1,1}(t) * u_0\|_{L^2} \\
&+ \sum_{i=1}^n \|\mathcal{K}_{j+1,i+1}(t) * v_0^i\|_{L^2}.
\end{aligned}$$

Thus, thanks to Theorem 2.1.4 we deduce

$$\|\mathcal{K}_{j+1,1}(t) * u_0\|_{L^2} \le Ce^{-ct}\|u_0\|_{L^2}, \qquad \|K_{j+1,1}(t) * u_0\|_{L^2} \le C\min\{1, t^{-\frac{n}{4}-\frac{1}{2}}\}\|u_0\|_{L^1},$$

$$\|\mathcal{K}_{j+1,i+1}(t) * v_0^i\|_{L^2} \le Ce^{-ct}\|v_0^i\|_{L^2}, \qquad \|K_{j+1,i+1}(t) * v_0^i\|_{L^2} \le C\min\{1, t^{-\frac{n}{4}-1}\}\|v_0^i\|_{L^1} \quad \text{for } i = 1, \dots, n. \tag{2.68}$$

As done before we can decompose the integral term in (2.67) as

$$\int_0^t \|\Gamma_{j+1}^h(t-s) * ([0,(u(s)+\bar{u})\nabla\phi(s)])\|_{L^2}\,ds \quad \le \quad \int_0^t \|\mathcal{K}_{j+1}(t-s) * ([0,(u+\bar{u})\nabla\phi(s)])\|_{L^2}\,ds$$

$$+ \quad \int_0^t \|K_{j+1}(t-s) * ([0,(u+\bar{u})\nabla\phi(s)])\|_{L^2}\,ds.$$

Let us start estimating the first integral

$$\int_0^t \|\mathcal{K}_{j+1}(t-s) * ([0,(u(s)+\bar{u})\nabla\phi(s)])\|_{L^2}\,ds \quad \le \quad \int_0^t Ce^{-c(t-s)}\|(u(s)+\bar{u})\nabla\phi(s)\|_{L^2}\,ds$$

$$\le \quad \int_0^t Ce^{-c(t-s)}(\|\nabla\phi(s)\|_{L^2}\|u(s)\|_{L^\infty} + \bar{u}\|\nabla\phi(s)\|_{L^2}\,ds$$

$$+ \quad CM_{D_x^1\phi}^{\frac{n}{4}}(t)N_u^{\frac{n}{4}}(t)\int_0^t e^{-c(t-s)}\min\{1, s^{-\frac{n}{2}}\}\,ds$$

$$+ \quad C\bar{u}M_{D_x^1\phi}^{\frac{n}{4}}(t)\int_0^t e^{-c(t-s)}\min\{1, s^{-\frac{n}{4}}\}\,ds.$$

Thanks to Lemma 2.4.1 we obtain:

$$\int_0^t \|\mathcal{K}_{j+1}(t-s) * ([0,(u+\bar{u})\nabla\phi(s)])\|_{L^2} \le C\min\{1, t^{-\frac{n}{2}}\}(M_{D_x^1\phi}^{\frac{n}{4}}(t)N_u^{\frac{n}{4}}(t) + \bar{u}\min\{1, t^{-\frac{n}{4}}\}M_{D_x^1\phi}^{\frac{n}{4}}(t). \tag{2.69}$$

In order to complete our estimate we need to study the dissipative part, then

$$\int_0^t \|K_{j+1}(t-s) * ([0,(u(s)+\bar{u})\nabla\phi(s)])\|_{L^2}\,ds \le \int_0^t C\min\{1,(t-s)^{-\frac{n}{4}-1}\}\|\nabla\phi(s)\|_{L^2}\|u(s)\|_{L^2}\,ds$$

$$+ \int_0^t C\min\{1,(t-s)^{-\frac{n}{4}-\frac{3}{2}}\}\bar{u}\|\phi(s)\|_{L^1}\,ds$$

$$\le C(\min\{1, t^{-\nu}\}M_{D_x^1\phi}^{\frac{n}{4}}(t)M_u^{\frac{n}{4}}(t) + \bar{u}\min\{1, t^{-\frac{n}{4}-\frac{3}{2}}\}\|\phi_0\|_{L^1}$$

$$+ \bar{u}t^{-\frac{n}{4}-\frac{1}{2}}\|u_0\|_{L^1}).$$

where $\nu = \min\left\{\frac{n}{4}+1, \frac{n}{2}\right\}$. Finally if we sum the last inequality and (2.68), (2.69) we get the L^2-norm of the function v

$$\|v(t)\|_{L^2} \quad \le \quad C\left[e^{-ct}(\|u_0\|_{L^2} + \sum_{i=1}^n \|v_0^i\|_{L^2}) + \min\{1, t^{-\frac{n}{4}-\frac{1}{2}}\}\|u_0\|_{L^1} + \min\{1, t^{-\frac{n}{4}-1}\}\sum_{i=1}^n \|v_0^i\|_{L^1}\right.$$

$$+ \quad \min\{1, t^{-\frac{n}{2}}\}(M_{D_x^1\phi}^{\frac{n}{4}}(t)N_u^{\frac{n}{4}}(t) + \min\{1, t^{-\frac{n}{4}}\}\bar{u}M_{D_x^1\phi}^{\frac{n}{4}}(t) + \min\{1, t^{-\nu}\}M_{D_x^1\phi}^{\frac{n}{4}}(t)M_u^{\frac{n}{4}}(t)$$

$$+ \quad \bar{u}\min\{1, t^{-\frac{n}{4}-\frac{3}{2}}\}\|\phi_0\|_{L^1} + \bar{u}t^{-\frac{n}{4}-\frac{1}{2}}\|u_0\|_{L^1}\right]. \tag{2.70}$$

L^2-estimate for $D_x^s v$

Proceeding along the lines of the conservative variable estimates, we get the estimate of the s−derivative of v in L^2,

$$\|D_x^s v_j(t)\|_{L^2} \quad \le \quad C\left[e^{-ct}(\|D_x^s u_0\|_{L^2} + \sum_{i=1}^n \|D_x^s v_0^i\|_{L^2} + \min\{1, t^{-\frac{n}{4}-\frac{1}{2}-\frac{s}{2}}\}\|u^0\|_{L^1}\right.$$

$$+ \quad \min\{1, t^{-\frac{n}{4}-1-\frac{s}{2}}\} \sum_{i=1}^{n} \|v_0^i\|_{L^1}) + \bar{u} \min\{1, t^{-\delta_s}\}(M_{D_x^{s+1}\phi}^{\delta_s}(t)$$

$$+ \quad \min\{1, t^{-\delta_s+\frac{n}{2}}\}(N_u^{\frac{n}{4}}(t) M_{D_x^{s+1}\phi}^{\delta_s}(t) + N_{D_x^1\phi}^{\frac{n}{4}}(t) M_{D_x^s u}^{\delta_0}(t)) \tag{2.71}$$

$$+ \quad \min\{1, t^{-\nu_s}\}(M_{D_x^1\phi}^{\frac{n}{4}}(t) M_u^{\frac{n}{4}}(t) + M_u^{\frac{n}{4}}(t) M_{D_x^1\phi}^{\frac{n}{4}}(t))$$

$$+ \quad \bar{u} t^{-\frac{n}{4}-\frac{s}{2}} \|u_0\|_{L^1} + \bar{u} \min\{1, t^{-\frac{n}{4}-1-\frac{s}{2}}\}\|\phi_0\|_{L^1} \Big],$$

where $\nu_s = \min\left\{\frac{n}{4}+1+\frac{s}{2}, \frac{n}{2}\right\}$.

L^∞ estimates for v

In a similar way we obtain the estimate of the L^∞ norm of v_j,

$$\|v_j(t)\|_{L^\infty} \leq C \Big[e^{-ct}(\|u_0\|_{H^s} + \sum_{i=1}^{n} \|v_0^i\|_{H^s}) + \min\{1, t^{-\frac{n}{2}-\frac{1}{2}}\}\|u^0\|_{L^1} + \min\{1, t^{-\frac{n}{2}-1}\} \sum_{i=1}^{n} \|v_0^n\|_{L^1}$$

$$+ \quad \min\{1, t^{-\frac{n}{2}}\} M_{D_x^1\phi}^{\frac{n}{4}}(t) N_u^{\frac{n}{2}}(t) + \bar{u} \min\{1, t^{-\frac{n}{4}}\} M_{D_x^1\phi}^{\frac{n}{4}}(t) + \min\{1, t^{-\frac{n}{2}}\} M_{D_x^1\phi}^{\frac{n}{4}}(t) M_u^{\frac{n}{4}}(t)$$

$$+ \quad \bar{u} \min\{1, t^{-\frac{n}{2}-\frac{3}{2}}\}\|\phi_0\|_{L^1} + \bar{u} t^{-\frac{n}{2}-\frac{1}{2}}\|u_0\|_{L^1} + \bar{u} \min\{1, t^{-\delta_s}\} M_{D_x^{s+1}\phi}^{\delta_s}(t) \Big]. \tag{2.72}$$

Decay rates of variables

Thanks to Proposition (2.4.2) and inequalities in (2.62), (2.64), (2.66), (2.70), (2.71), (2.72), we obtain, for $t > \epsilon > 0$ the following estimates for functionals:

$$M_u^{\frac{n}{4}}(t) \quad \leq \quad C\bar{u}(E_0 + D_0) + C_1 \Big[\bar{u} D_0 \Big(M_u^{\frac{n}{4}}(t) + N_u^{\frac{n}{4}}(t) \Big) + (N_u^{\frac{n}{4}}(t))^2 + N_u^{\frac{n}{4}}(t) M_u^{\frac{n}{4}}(t) + (M_u^{\frac{n}{4}}(t))^2 \Big]$$

$$M_{D_x^s u}^{\delta_s}(t) \quad \leq \quad C\bar{u}(E_0 + D_0) + C_2 \Big[\bar{u} D_0 \Big(M_u^{\frac{n}{4}}(t) + N_u^{\frac{n}{4}}(t) + M_{D_x^s u}^{\frac{n}{2}}(t) \Big) + (M_u^{\frac{n}{4}}(t))^2$$

$$+ \quad N_u^{\frac{n}{4}}(t) M_{D_x^s u}^{\delta_s}(t) + (M_{D_x^s u}^{\delta_s}(t))^2 \Big].$$

$$N_u^{\frac{n}{4}}(t) \quad \leq \quad C\bar{u}(E_0 + D_0) + C_3 \Big[\bar{u} D_0 \Big(M_u^{\frac{n}{4}}(t) + N_u^{\frac{n}{4}}(t) + M_{D_x^s u}^{\delta_s}(t) \Big) + N_u^{\frac{n}{4}}(t) M_u^{\frac{n}{4}}(t) + (M_u^{\frac{n}{4}}(t))^2$$

$$+ \quad N_u^{\frac{n}{4}}(t) M_{D_x^s u}^{\delta_s}(t) + (M_{D_x^s u}^{\delta_s}(t))^2 + M_{D_x^s u}^{\delta_s}(t) N_u^{\frac{n}{2}}(t) + (N_u^{\frac{n}{4}}(t))^2 \Big].$$

$$M_v^{\frac{n}{4}}(t) \quad \leq \quad C\bar{u}(E_0 + D_0) + C_4 \Big[\bar{u} D_0 \Big(M_u^{\frac{n}{4}}(t) + N_u^{\frac{n}{4}}(t) \Big) + (N_u^{\frac{n}{4}}(t))^2 + N_u^{\frac{n}{4}}(t) M_u^{\frac{n}{4}}(t) + (M_u^{\frac{n}{4}}(t))^2 \Big].$$

$$M_{D_x^s v}^{\delta_s}(t) \quad \leq \quad C\bar{u}(E_0 + D_0) + C_5 \Big[\bar{u} D_0 \Big(M_u^{\frac{n}{4}}(t) + N_u^{\frac{n}{4}}(t) + M_{D_x^s u}^{\delta_s}(t) \Big) + (M_u^{\frac{n}{4}}(t))^2$$

$$+ \quad N_u^{\frac{n}{4}}(t) M_{D_x^s u}^{\delta_s}(t) + (M_{D_x^s u}^{\delta_s}(t))^2 \Big].$$

$$N_v^{\frac{n}{4}}(t) \quad \leq \quad C\bar{u}(E_0 + D_0) + C_6 \Big[\bar{u} D_0 \Big(M_u^{\frac{n}{4}}(t) + N_u^{\frac{n}{4}}(t) + M_{D_x^s u}^{\delta_s}(t) \Big) + N_u^{\frac{n}{4}}(t) M_u^{\frac{n}{4}}(t) + (M_u^{\frac{n}{4}}(t))^2$$

$$+ \quad N_u^{\frac{n}{4}}(t) M_{D_x^s u}^{\frac{n}{2}}(t) + (M_{D_x^s u}^{\delta_s}(t))^2 + M_{D_x^s u}^{\delta_s}(t) N_u^{\frac{n}{4}}(t) + (N_u^{\frac{n}{4}}(t))^2 \Big],$$

where $\delta_s = \min\{\frac{n}{4} + \frac{1}{2} + \frac{s}{2}, \frac{n}{2}\}$. Moreover $D_0 = \max\{\|\phi_0\|_{H^{s+1}}, \|\phi_0\|_{L^1}\}$ $E_0 = \max\{\|w_0\|_{H^s}, \|w_0\|_{L^1}\}$, while the constant $C_i = C_i(F_k, K, C_{b'}, C_{h'})$ for $i = 1, \ldots, 6$.

Let us proceed as in the previous section setting

$$P(t) := M_u^{\frac{n}{4}}(t) + N_u^{\frac{n}{2}}(t) + M_{D_x^s u}^{\delta_s}(t) + M_v^{\frac{n}{4}}(t) + N_v^{\frac{n}{2}}(t) + M_{D_x^s v}^{\delta_s}(t).$$

It follows that, if initial data and the constant state are small, we have

$$CP(t)^2 - (1 - C_{k0})P(t) + C_0 \geq 0, \tag{2.73}$$

where C_0 and C_{k0} are positive constants depending on initial data and constant state and C is a positive constant depending on estimates of Green function. For suitably small data, this inequality implies that $M_u^{\frac{n}{4}}(t)$, $N_u^{\frac{n}{2}}(t)$, $M_{D_x^s u}^{\delta_s}(t)$, $M_v^{\frac{n}{4}}(t)$, $N_v^{\frac{n}{2}}(t)$, $M_{D_x^s v}^{\delta_s}(t)$ remain bounded. On the other hand, when $t > 1$, this implies that L^∞-norm of solution (u, v) do not increase with t. Thanks to the Proposition 2.4.2 the same holds for $N_\phi^{\frac{n}{2}}$ and $N_{D_x^1 \phi}^{\frac{n}{2}}$. Then by Lemma 2.3.5 and the continuation principle we get the global existence of solution. □

2.6 Comparison with the Patlak-Keller-Segel Model

As observed in Chapter 1, hyperbolic and parabolic model are expected to have the same behavior for large times. In this section we investigate this aspect by studying the decay estimates for the analogous Patlak-Keller-Segel (PKS) model, and comparing these results with the ones obtained in the previous section for the Cattaneo-Hillen model. For the sake of simplicity we consider a simplified version of system (2.1), namely

$$\begin{cases} \partial_t u + \nabla \cdot v = 0, \\ \\ \partial_t v + \nabla u = -\beta v + h(\phi, \nabla\phi)g(u), \\ \\ \partial_t \phi = \Delta\phi + f(u, \phi). \end{cases} \tag{2.74}$$

Thus, assuming $b(\phi, \nabla\phi) \equiv \beta$ and formally disregarding the term $\partial_t v$ in the second equation of (2.74), we get $v = \frac{1}{\beta}(h(\phi, \nabla\phi)g(u) - \nabla u)$, then the system reduces to the PKS parabolic system:

$$\begin{cases} \beta\partial_t \tilde{u} - \Delta\tilde{u} + \nabla \cdot (h(\tilde{\phi}, \nabla\tilde{\phi}), g(\tilde{u})) = 0, \\ \\ \partial_t \tilde{\phi} = \Delta\tilde{\phi} + f(\tilde{u}, \tilde{\phi}), \end{cases}$$

where the functions f, g, h satisfy the assumptions (H_g), (H_f), (H_h). Then we are led to consider the system

$$\begin{cases} \beta\partial_t \tilde{u} - \Delta\tilde{u} + \nabla \cdot (h(\tilde{\phi}, \nabla\tilde{\phi})g(\tilde{u})) = 0, \\ \\ \partial_t \tilde{\phi} = \Delta\tilde{\phi} + a\tilde{u} - b\tilde{\phi} + \bar{f}(\tilde{u}, \tilde{\phi}), \end{cases} \tag{2.75}$$

with initial condition

$$\tilde{u}(x, 0) = \tilde{u}_0(x), \quad \tilde{\phi}(x, 0) = \tilde{\phi}_0(x). \tag{2.76}$$

It is known that, for small initial data the solution of the above problem decay in time in L^2-norm in the same way as the solutions to problem (2.74) [94].

Our aim is to prove that under the assumption of small initial data, if

$$u_0(x) = \tilde{u}_0(x), \quad \phi_0(x) = \tilde{\phi}_0(x), \tag{2.77}$$

then $\|u(t) - \tilde{u}(t)\|_{L^2}$ and $\|\phi(t) - \tilde{\phi}(t)\|_{L^2}$ for large t, approach zero faster than the decay of $\|u(t)\|_{L^2}$, $\|\tilde{u}(t)\|_{L^2}$, $\|\phi(t)\|_{L^2}$ and $\|\tilde{\phi}(t)\|_{L^2}$

2.6.1 Asymptotic Behavior of the Patlak-Keller-Segel Model Solutions

First of all we prove the following theorem on the asymptotic behavior of global smooth solutions to system (2.75).

Theorem 2.6.1. *Let* $(\tilde{u}, \tilde{\phi})$ *a global solution to the Cauchy problem* (2.75)-(2.76), *with regularity assumptions*

$$\|\tilde{u}_0\|_{H^s}, \|\tilde{u}_0\|_{L^\infty}, \|\tilde{\phi}_0\|_{H^{s+1}}, \|\tilde{\phi}_0\|_{W^{1,\infty}} \le \epsilon_0$$

Then the following decay estimate holds,

$$\|\tilde{u}(t)\|_{L^\infty} \sim t^{-\frac{n}{2}}, \quad \|\tilde{u}(t)\|_{L^2} \sim t^{-\frac{n}{4}},$$

$$\|\tilde{\phi}(t)\|_{L^\infty} \sim t^{-\frac{n}{2}}, \quad \|D_x^1 \tilde{\phi}(t)\|_{L^\infty} \sim t^{-\frac{n}{2}},$$

$$\|\tilde{\phi}(t)\|_{L^2} \sim t^{-\frac{n}{4}}, \quad \|D_x^1 \tilde{\phi}(t)\|_{L^2} \sim t^{-\frac{n}{4}}.$$

To prove the theorem we use the same approach of the previous section. Let us observe that we can easily obtain the local existence of solution to system (2.75) by the semigroup theory and fixed point method [160]. While for a global existence result for small initial data see [26] and reference therein.

Proof. Fix $K > 0$ large enough and let $T > 1$. Take a solution to system (2.75) such that $\|\tilde{u}\|_{L^\infty(\mathbb{R}^n \times (0,T))} \le \frac{K}{2}$, $\|\tilde{\phi}, D_x^1 \tilde{\phi}\|_{L^\infty(\mathbb{R}^n \times (0,T))} \le \frac{K}{2}$, this is possible provided that the initial data are suitably small.

By the Duhamel's formula we can write solution to (2.75) as

$$\tilde{u}(x,t) = \Gamma^{\frac{1}{\beta}}(t) * \tilde{u}_0(x) + \int_0^t \Gamma^{\frac{1}{\beta}}(t-s) * (\nabla \cdot (h(\tilde{\phi}, \nabla\tilde{\phi}) g(\tilde{u})(s)) ds,$$

$$\tilde{\phi}(x,t) = (e^{-bt} \Gamma^p(t) * \tilde{\phi}_0)(x) + \int_0^t e^{-b(t-s)} \Gamma^p(t-s) * (\alpha \tilde{u}(s) + \bar{f}(\tilde{u}, \tilde{\phi})) ds.$$

Let us focus on the function $\tilde{u}$, then we can estimate the L^2-norm as

$$
\begin{aligned}
\|\tilde{u}(t)\|_{L^2} &\le \|\Gamma^{\frac{1}{\beta}}(t) * \tilde{u}_0\|_{L^2} + \int_0^t \|\Gamma^{\frac{1}{\beta}}(t-s) * (\nabla \cdot (\bar{h}(\tilde{\phi}, \nabla\tilde{\phi}) g(\tilde{u})(s)))\|_{L^2} ds, \\
&\le C t^{-\frac{n}{4}} \|\tilde{u}_0\|_{L^1} + G_k H_k \int_0^t (t-s)^{-\frac{1}{2}} (\|\tilde{u}(s)\|_{L^\infty} (\|\tilde{\phi}(s)\|_{L^2} + \|\nabla\tilde{\phi}(s)\|_{L^2}) ds, \\
&\le C t^{-\frac{n}{4}} \|\tilde{u}_0\|_{L^1} + C \min\{1, t^{-(\frac{n}{4}+\frac{n}{2})+\frac{1}{2}}\} (M_{\tilde{\phi}}^{\frac{n}{4}}(t) N_{\tilde{u}}^{\frac{n}{2}}(t) + M_{D_x^1 \tilde{\phi}}^{\frac{n}{4}}(t) N_{\tilde{u}}^{\frac{n}{2}}(t)).
\end{aligned}
$$

Then for the functional the following estimates yields,

$$M_{\tilde{u}}^{\frac{n}{4}}(t) \le C \left(\|\tilde{u}_0\|_{L^1} + M_{\tilde{\phi}}^{\frac{n}{4}}(t) N_{\tilde{u}}^{\frac{n}{2}}(t) + M_{D_x^1 \tilde{\phi}}^{\frac{n}{4}}(t) N_{\tilde{u}}^{\frac{n}{2}}(t) \right). \tag{2.78}$$

Proceeding in a similar way, we get the estimate of the function in the L^∞-norm

$$
\begin{aligned}
\|\tilde{u}(t)\|_{L^\infty} &\leq \|\Gamma^{\frac{1}{\beta}}(t) * \tilde{u}_0\|_{L^\infty} + \int_0^t \|\Gamma^{\frac{1}{\beta}}(t-s) * (\nabla \cdot (\bar{h}(\tilde{\phi}, \nabla \tilde{\phi}) g(\tilde{u})(s)))\|_{L^\infty} ds, \\
&\leq ct^{-\frac{n}{2}} \|\tilde{u}_0\|_{L^1} + G_k H_k \int_0^t (t-s)^{-\frac{1}{2}} \|\tilde{u}(s)\|_{L^\infty} (\|\tilde{\phi}(s)\|_{L^\infty} + \|\nabla \tilde{\phi}(s)\|_{L^\infty}) ds, \\
&\leq ct^{-\frac{n}{2}} \|\tilde{u}_0\|_{L^1} + \min\{1, t^{-n+\frac{1}{2}}\} N_{\tilde{u}}^{\frac{n}{2}}(t) (N_{\tilde{\phi}}^{\frac{n}{2}}(t) + N_{D_x^1 \tilde{\phi}}^{\frac{n}{2}}(t)).
\end{aligned}
$$

This implies

$$
N_{\tilde{u}}^{\frac{n}{2}}(t) \leq C \left(\|\tilde{u}_0\|_{L^1} + N_{\tilde{u}}^{\frac{n}{2}}(t) (N_{\tilde{\phi}}^{\frac{n}{2}}(t) + N_{D_x^1 \tilde{\phi}}^{\frac{n}{2}}(t)) \right). \tag{2.79}
$$

Now we consider the solution to the second parabolic equation of (2.75), ϕ. Thanks to Proposition 2.4.2 we have

$$
\begin{aligned}
M_{\tilde{\phi}}^{\frac{n}{4}}(t) &\leq C \left(\|\tilde{\phi}_0\|_{L^2} + (1 + F_k L) M_{\tilde{u}}^{\frac{n}{4}}(t) \right), \\
M_{D_x^1 \phi}^{\frac{n}{4}}(t) &\leq C \left(\|D_x^1 \phi_0\|_{L^2} + (1 + F_k K) M_{\tilde{u}}^{\frac{n}{4}}(t) + F_k K M_{\tilde{\phi}}^{\frac{n}{4}}(t) \right), \\
N_{\tilde{\phi}}^{\frac{n}{2}}(t) &\leq C \left(\|\tilde{\phi}_0\|_{L^\infty} + (1 + F_k L) N_{\tilde{u}}^{\frac{n}{2}}(t) \right), \\
N_{D_x^1 \phi}^{\frac{n}{2}}(t) &\leq C \left(\|D_x \tilde{\phi}_0\|_{L^\infty} + (1 + F_k K) N_{\tilde{u}}^{\frac{n}{2}}(t) + F_k K N_{\tilde{\phi}}^{\frac{n}{2}}(t) \right).
\end{aligned}
$$

Then substituting these inequalities in (2.78), (2.79) we get

$$
M_{\tilde{u}}^{\frac{n}{4}}(t) \leq C_0 + B_0 (M_{\tilde{u}}^{\frac{n}{4}}(t) + N_{\tilde{u}}^{\frac{n}{2}}(t)) + C_k M_{\tilde{u}}^{\frac{n}{4}}(t) N_{\tilde{u}}^{\frac{n}{2}}(t), \tag{2.80}
$$

$$
N_{\tilde{u}}^{\frac{n}{2}}(t) \leq C_0 + B_0 N_{\tilde{u}}^{\frac{n}{2}}(t) + C_k (N_{\tilde{u}}^{\frac{n}{2}}(t))^2, \tag{2.81}
$$

where C_k is a positive constant depending on K, B_0 is a positive constant depending on K and data and C_0 is also a positive constant depending on data. Let us sum these last relations, and define $P(t) := M_{\tilde{u}}^{\frac{n}{4}}(t) + N_{\tilde{u}}^{\frac{n}{2}}(t)$.
Then we obtain the following inequality

$$
2C_k P(t)^2 - (1 - 2B_0) P(t) + 2C_0 \geq 0.
$$

This formula, implies that for suitably small data, $M_{\tilde{u}}^{\frac{n}{4}}(t), N_{\tilde{u}}^{\frac{n}{2}}(t)$ remain bounded. Moreover when $t > 1$ this implies that the norm of u do not increase. Thanks to Proposition 2.4.2 the same holds for the L^∞-norm of ϕ and $\nabla \phi$. □

2.6.2 Decay Estimate of the Difference of Solutions

In this section we compare the large times behavior of solution u to system (2.74) with the solution to the parabolic PKS model (2.75). We have proved, in the previous section that for small initial data, the solutions to the problem (2.75) decay in time, in L^∞ and L^2-norms, as the solutions to the hyperbolic system (2.74).
Let us recall that it is possible to give a more precise expansion of the diffusive part $K(x,t)$ of the Green Kernel of the dissipative hyperbolic system. As a matter of fact, in [17] it is shown that in the linearized isentropic Euler equations with damping for a generic n, $K(x,t)$ can be decomposed as:

$$
K(x,t) = \begin{bmatrix} \Gamma^p & (\nabla \Gamma^p)^T \\ \nabla \Gamma^p & \nabla^2 \Gamma^p \end{bmatrix} + R_1(x,t), \tag{2.82}
$$

where Γ^p is the heat kernel for $u_t = \Delta u$, and the rest term $R_1(x, t)$ satisfies the bound

$$R_1(x, t) = \frac{e^{-c|x|^2/t}}{(1+t)^{\frac{n}{2}+\frac{1}{2}}} \begin{bmatrix} O(1) & O(1)(1+t)^{-\frac{1}{2}} \\ O(1)(1+t)^{-\frac{1}{2}} & O(1)(1+t)^{-1} \end{bmatrix}.$$

Our aim is to show that, under the assumption of small initial data, if

$$u_0(x) = \tilde{u}_0(x), \quad \phi_0(x) = \tilde{\phi}_0(x), \tag{2.83}$$

then $\|u(t) - \tilde{u}(t)\|_{L^2}$, and $\|\phi(t) - \tilde{\phi}(t)\|_{L^2}$, for large t, approach zero faster than $\|u(t)\|_{L^2}$, $\|\tilde{u}(t)\|_{L^2}$, $\|\phi(t)\|_{L^2}$ and $\|\tilde{\phi}(t)\|_{L^2}$.

Theorem 2.6.2. *Let (u, v, ϕ) and $(\tilde{u}, \tilde{\phi})$ be the global solutions respectively to system* (2.74) *and* (2.75) *under the assumptions* (H_f), (H_g), (H_h) *and* (2.83). *Then there exist $\epsilon_0, L > 0$ such that, if*

$$\|u_0\|_{H^s}, \|u_0\|_{L^1}, \|v_0\|_{H^s}, \|v_0\|_{L^1}, \|\phi_0\|_{H^{s+1}}, \|\phi_0\|_{W^{1,\infty}} \le \epsilon_0$$

then, for all $t > 0$,

$$\sup_{(0,t)} \left\{ \max\{1, s^\delta\} \|u(s) - \tilde{u}(s)\|_{L^2} \right\} \le L, \quad \sup_{(0,t)} \left\{ \max\{1, s^\delta\} \|\phi(s) - \tilde{\phi}(s)\|_{L^2} \right\} \le L,$$

where $\delta = \min\{\frac{n}{4} + \frac{1}{2}, \frac{n}{2}\}$.

Proof. Let $K > 0$ such that $\|u, v, \phi, \nabla\phi, \tilde{u}, \tilde{v}, \tilde{\phi}, \nabla\tilde{\phi}\|_{L^\infty(\mathbb{R}^n \times (0,\infty))} \le K$. The difference between u and $\tilde{u}$ can be expressed as follows

$$\begin{aligned}
|u - \tilde{u}| &\le |(\Gamma_{11}^h(t) - \Gamma^{\frac{1}{\beta}}(t)) * u_0| + \left| \sum_{i=1}^n \Gamma_{1,i+1}^h(t) * v_0^i \right| \\
&\quad + \left| \int_0^t \Gamma_1^h(t-s) * (\bar{B}(\phi, \nabla\phi)v(s) + H(\phi, \nabla\phi, u)(s))\, ds \right. \\
&\quad \left. - \frac{1}{\beta} \int_0^t \nabla\Gamma^{\frac{1}{\beta}}(t-s) * (H(\tilde{\phi}, \nabla\tilde{\phi}, \tilde{u}))\, ds \right|.
\end{aligned}$$

By equation (2.82), for $t > 1$, we have

$$\begin{aligned}
|u - \tilde{u}| &\le |(\mathcal{K}_{11}(t) + R_{11}(t)) * u_0| + \left| \sum_{i=1}^n \Gamma_{1,i+1}^h(t) * v_0^i \right| \\
&\quad + \left| \frac{1}{\beta} \int_0^t \nabla\Gamma^{\frac{1}{\beta}}(t-s) * (H(\phi, \nabla\phi, u) - H(\tilde{\phi}, \nabla\tilde{\phi}, \tilde{u}))\, ds \right| \\
&\quad + \left| \int_0^t (\mathcal{K}_1(t-s) + R_1(t-s)) * H(\phi, \nabla\phi, u)\, ds \right| \\
&\quad + \left| \int_0^t \Gamma_1^h(t-s) * \bar{B}(\phi, \nabla\phi)v(s)\, ds \right|.
\end{aligned}$$

Proceeding as in the proof of Theorem 2.4.3, we are able to estimate $\|u - \tilde{u}\|_{L^2}$ for large t:

$$\begin{aligned}
\|u(t) - \tilde{u}(t)\|_{L^2} &\le \|(\mathcal{K}_{11}(t) + R_{11}(t)) * u_0\|_{L^2} + \left\| \sum_{i=1}^n \Gamma_{1,i+1}^h(t) * v_0^i \right\|_{L^2} \\
&\quad + \frac{1}{\beta} \int_0^{t-1} \|\nabla\Gamma^{\frac{1}{\beta}}(t-s) * (H(\phi, \nabla\phi, u)(s) - H(\tilde{\phi}, \nabla\tilde{\phi}, \tilde{u})(s))\|_{L^2}\, ds \\
&\quad + \int_0^t \|(\mathcal{K}_1(t-s) + R_1(t-s)) * H(\phi, \nabla\phi, u)(s)\|_{L^2}\, ds \tag{2.84}
\end{aligned}$$

$$+ \quad \int_0^t \|\Gamma_1^h(t-s) * \bar{B}(\phi, \nabla\phi) v(s)\|_{L^2} \, ds$$

$$+ \quad \frac{1}{\beta} \int_{t-1}^t \|\nabla\Gamma^{\frac{1}{\beta}}(t-s) * (H(\phi, \nabla\phi, u)(s) - H(\tilde{\phi}, \nabla\tilde{\phi}, \tilde{u})(s))\|_{L^2} \, ds.$$

For the first two terms on the right hand side we have,

$$\|(\mathscr{K}_{11}(t) + R_{11}(t)) * u_0\|_{L^2} \le e^{-ct} \|u_0\|_{L^2} + t^{-(\frac{n}{4}+\frac{1}{2})} \|u_0\|_{L^1}$$

$$\|\sum_{i=1}^n \Gamma_{1,i+1}^h(t) * v_0^i\|_{L^2} \le e^{-ct} \sum_{i=1}^n \|v_0^i\|_{L^2} + \min\{1, t^{-(\frac{n}{4}+\frac{1}{2})}\} \sum_{i=1}^n \|v_0^i\|_{L^1}.$$

Let us now estimate the first integral as

$$\frac{1}{\beta} \int_0^{t-1} \|\nabla\Gamma^{\frac{1}{\beta}}(t-s) * (H(\phi, \nabla\phi, u)(s) - H(\tilde{\phi}, \nabla\tilde{\phi}, \tilde{u})(s))\|_{L^2} \, ds$$

$$\le \frac{1}{\beta} \int_0^{t-1} \|\nabla\Gamma^{\frac{1}{\beta}}(t-s)\|_{L^2} \|h(\phi, \nabla\phi)(s) g(u)(s) - h(\tilde{\phi}, \nabla\tilde{\phi})(s) g(\tilde{u})(s)\|_{L^1} \, ds$$

$$\le \frac{1}{\beta} \int_0^{t-1} C \min\{1, t-s^{-(\frac{n}{4}+\frac{1}{2})}\} \|h(\phi, \nabla\phi)(s) g(u)(s) - h(\tilde{\phi}, \nabla\tilde{\phi})(s) g(\tilde{u})(s)\|_{L^1} \, ds$$

$$+ C H_k G_k (M_{D_x^1\phi}^{\frac{n}{4}}(t) + M_\phi^{\frac{n}{4}}(t)) M_{u-\tilde{u}}^\delta \frac{1}{\beta} \int_0^{t-1} \min\{1, t-s^{-(\frac{n}{4}+\frac{1}{2})}\} \min\{1, s^{-\frac{n}{4}-\delta)}\} \, ds$$

$$+ C H_k G_k M_{\tilde{u}}^{\frac{n}{4}}(t) M_{\phi-\tilde{\phi}}^\delta \frac{1}{\beta} \int_0^{t-1} \min\{1, t-s^{-(\frac{n}{4}+\frac{1}{2})}\} \min\{1, s^{-\frac{n}{4}-\delta)}\} \, ds$$

$$+ C H_k G_k M_{\tilde{u}}^{\frac{n}{4}}(t) M_{D_x^1\phi-D_x^1\tilde{\phi}}^\delta \frac{1}{\beta} \int_0^{t-1} \min\{1, t-s^{-(\frac{n}{4}+\frac{1}{2})}\} \min\{1, s^{-\frac{n}{4}-\delta)}\} \, ds,$$

where $\delta = \min\{\frac{n}{4} + \frac{1}{2}, \frac{n}{2}\}$.
Then, thanks to Lemma 2.4.1 we deduce

$$\frac{1}{\beta} \int_0^{t-1} \|\nabla\Gamma^{\frac{1}{\beta}}(t-s) * (H(\phi, \nabla\phi, u)(s) - H(\tilde{\phi}, \nabla\tilde{\phi}, \tilde{u})(s))\|_{L^2} \, ds$$

$$\le C_1 (\min\{1, t^{-\theta_1}\} (H_k G_k (M_\phi^{\frac{n}{4}}(t) + M_{D_x^1\phi}^{\frac{n}{4}}(t)) M_{u-\tilde{u}}^\delta + M_{\tilde{u}}^{\frac{n}{4}}(t) M_{\phi-\tilde{\phi}}^\delta + M_{\tilde{u}}^{\frac{n}{4}}(t) M_{D_x^1\phi-D_x^1\tilde{\phi}}^\delta).$$

where $\theta_1 = \min\{\frac{n}{4} + \frac{1}{2}, \frac{n}{4} + \delta, \frac{n}{2} + \delta - \frac{1}{2}\}$. The second part of the integral can be estimated as follows

$$\frac{1}{\beta} \int_{t-1}^t \|\nabla\Gamma^{\frac{1}{\beta}}(t-s) * (H(\phi, \nabla\phi, u)(s) - H(\tilde{\phi}, \nabla\tilde{\phi}, \tilde{u})(s))\|_{L^2} \, ds$$

$$\le \frac{1}{\beta} \int_{t-1}^t (t-s)^{-\frac{1}{2}} \|h(\phi, \nabla\phi) g(u)(s) - h(\tilde{\phi}, \nabla\tilde{\phi}) g(\tilde{u})(s)\|_{L^2} \, ds$$

$$+ H_k G_k C \min\{1, t^{-(\delta+\frac{n}{2})}\} (M_{u-\tilde{u}}^\delta(t) N_{\tilde{\phi}}^{\frac{n}{2}}(t) + M_{u-\tilde{u}}^\delta(t) N_{D_x^1\tilde{\phi}}^{\frac{n}{2}}(t))$$

$$+ H_k G_k C \min\{1, t^{-(\delta+\frac{n}{2})}\} (M_{\phi-\tilde{\phi}}^\delta(t) N_{\tilde{u}}^{\frac{n}{2}}(t) + M_{D_x^1\phi-D_x^1\tilde{\phi}}^\delta(t) N_{\tilde{u}}^{\frac{n}{2}}(t)).$$

We estimate now the fourth term in (2.84) as,

$$\int_0^t \|(\mathscr{K}_1(t-s) + R_1(t-s)) * H(\phi, \nabla\phi, u)(s)\|_{L^2} \, ds$$

$$\le \int_0^t C e^{-c(t-s)} \|h(\phi, \nabla\phi) g(u)\|_{L^2} + C \min\{1, (t-s)^{-(\frac{n}{4}+1)}\} \|h(\phi, \nabla\phi) g(u)(s)\|_{L^1} \, ds.$$

On the other hand the first term can be estimated as

$$
\int_0^t Ce^{-c(t-s)}\|h(\phi,\nabla\phi)g(u)\|_{L^2}\,ds \;\;\leq\;\; \int_0^t Ce^{-c(t-s)}H_kG_k(\|\phi(s)\|_{L^2}\|u(s)\|_{L^\infty}+\|\nabla\phi(s)\|_{L^2}\|u(s)\|_{L^\infty})\,ds
$$

$$
\leq\;\; C\min\{1,t^{-\frac{3}{4}n}\}(G_kH_kM_{D_x^1}^{\frac{n}{4}}(t)N_u^{\frac{n}{2}}(t)+M_\phi^{\frac{n}{4}}(t)N_u^{\frac{n}{2}}(t)).
$$

While the second term is estimate by

$$
\int_0^t C\min\{1,(t-s)^{-(\frac{n}{4}+1)}\}\|h(\phi,\nabla\phi)(s)g(u)(s)\|_{L^1}\,ds
$$

$$
\leq \int_0^t C\min\{1,(t-s)^{-(\frac{n}{4}+1)}\}G_kH_k(\|\phi(s)\|_{L^2}+\|\nabla\phi(s)\|_{L^2})\|u(s)\|_{L^2})\,ds
$$

$$
\leq C_2\min\{1,t^{-\theta_2}\}H_kG_k(M_u^{\frac{n}{4}}(t)M_\phi^{\frac{n}{4}}(t)+M_u^{\frac{n}{4}}(t)M_{D_x^1\phi}^{\frac{n}{4}}(t)),
$$

where $\theta_2=\min\{\frac{n}{4}+1,\frac{n}{2}\}$. In order to complete our estimate, we need to study the fifth integral term in (2.84), then proceeding as done before,

$$
\int_0^t \|\Gamma_1^h(t-s)*\bar{B}(\phi,\nabla\phi)w(s)\|_{L^2}\,ds \;\;\leq\;\; \int_0^t \|K_1(t-s)*\bar{b}(\phi,\nabla\phi)v(s)\|_{L^2}\,ds
$$

$$
+\;\; \int_0^t \|\mathscr{K}_1(t-s)*\bar{b}(\phi,\nabla\phi)v(s)\|_{L^2}\,ds
$$

$$
\leq\;\; B_k\min\{1,t^{-(\frac{n}{4}+\frac{n}{2})}\}(M_\phi^{\frac{n}{4}}(t)N_v^{\frac{n}{2}}(t)+M_{D_x^1\phi}^{\frac{n}{4}}(t)N_v^{\frac{n}{2}}(t))
$$

$$
+\;\; B_k\min\{1,t^{-\theta_3}\}B_K(M_\phi^{\frac{n}{4}}(t)M_v^{\nu_0}(t)+M_{D_x^1\phi}^{\frac{n}{4}}(t)M_v^{\nu_0}(t)),
$$

where $\theta_3=\min\{\frac{n}{4}+\frac{1}{2},\frac{n}{2}\}$.

If we sum all the previous estimates, we get the following estimate for the difference of function u and function $\tilde{u}$ in the L^2-norm.

$$
\|u(t)-\tilde{u}(t)\|_{L^2} \;\;\leq\;\; C\left[e^{-ct}\|u_0\|_{L^2}+t^{-(\frac{n}{4}+\frac{1}{2})}\|u_0\|_{L^1}+e^{-ct}\sum_{i=1}^n\|v_0^i\|_{L^2}+\min\{1,t^{-(\frac{n}{4}+\frac{1}{2})}\}\sum_{i=1}^n\|v_0^i\|_{L^1}\right]
$$

$$
+\;\; C_k\left[\min\{1,t^{-\theta_1}\}((M_\phi^{\frac{n}{4}}(t)+M_{D_x^1\phi}^{\frac{n}{4}}(t))M_{u-\tilde{u}}^\delta(t)+M_{\tilde{u}}^{\frac{n}{4}}(t)(M_{\phi-\tilde\phi}^\delta(t)+M_{D_x^1\phi-D_x^1\tilde\phi}^\delta(t))\right.
$$

$$
+\;\; \min\{1,t^{-(\frac{n}{4}+\delta)}\}(M_{u-\tilde{u}}^\delta(t)N_{D_x^1\tilde\phi}^{\frac{n}{2}}(t)+M_{u-\tilde{u}}^\delta(t)N_{\tilde\phi}^{\frac{n}{2}}(t))
$$

$$
+\;\; \min\{1,t^{-(\frac{n}{4}+\delta)}\}(M_{\phi-\tilde\phi}^\delta(t)N_u^{\frac{n}{2}}(t)+M_{D_x^1\phi-D_x^1\tilde\phi}^\delta(t)N_u^{\frac{n}{2}}(t))
$$

$$
+\;\; \min\{1,t^{-\frac{3}{4}n}\}(M_\phi^{\frac{n}{4}}(t)N_u^{\frac{n}{2}}(t)+M_{D_x^1\phi}^{\frac{n}{4}}(t)N_u^{\frac{n}{2}}(t))
$$

$$
+\;\; \min\{1,t^{-\theta_2}\}(M_u^{\frac{n}{4}}M_\phi^{\frac{n}{4}}+M_u^{\frac{n}{4}}M_{D_x^1\phi}^{\frac{n}{4}})+\min\{1,t^{-\theta_3}\}(M_\phi^{\frac{n}{4}}M_v^{\nu_0}(t)+M_{D_x^1\phi}^{\frac{n}{4}}M_v^{\nu_0}(t))\,,
$$

where $\delta=\min\{\frac{n}{4}+\frac{1}{2},\frac{n}{2}\}$, $\theta_1=\min\{\frac{n}{4}+\frac{1}{2},\frac{n}{4}+\delta,\frac{n}{2}-\frac{1}{2}+\delta\}$, $\theta_2=\min\{\frac{n}{4}+1,\frac{n}{2}\}$, and $\theta_3=\min\{\frac{n}{4}+\frac{1}{2},\frac{n}{2}\}$. Let us now focus on the function ϕ. Arguing as in Proposition 2.4.2, it is easy to show that the difference of the second variables is given by

$$
\|\phi(t)-\tilde\phi(t)\|_{L^2} \;\;\leq\;\; \int_0^t \|e^{-b(t-s)}\Gamma^p(t-s)*(au(s)-a\tilde{u}(s)+\bar{f}(u,\phi)(s)-\bar{f}(\tilde{u},\tilde\phi)(s))\|_{L^2}\,ds
$$

$$
\leq\;\; \int_0^t Ce^{-b(t-s)}(\|au(s)-a\tilde{u}(s)\|_{L^2}+\|\bar{f}(u,\phi)(s)-\bar{f}(\tilde{u},\tilde\phi)(s)\|_{L^2}\,ds
$$

$$
\leq\;\; \int_0^t e^{-b(t-s)}C_k(\|u(s)-\tilde{u}(s)\|_{L^2}+\|\phi(s)-\tilde\phi(s)\|_{L^2})\,ds
$$

$$
\begin{aligned}
&\leq \quad C_k(M^\delta_{u-\tilde{u}}(t) + M^\delta_{\phi-\tilde{\phi}}(t)) \int_0^t e^{-b(t-s)} \min\{1, s^{-\delta}\} ds \\
&\leq \quad C_k \min\{1, t^{-\delta}\}(M^\delta_{u-\tilde{u}}(t) + M^\delta_{\phi-\tilde{\phi}}(t)).
\end{aligned}
$$

Then, for small initial data we have

$$
M^\delta_{\phi-\tilde{\phi}}(t) \leq C_{1k} M^\delta_{u-\tilde{u}}(t). \tag{2.85}
$$

Proceeding in a similar way we get also

$$
M^\delta_{D^1_x\phi - D^1_x\tilde{\phi}} \leq C_{2K} M^\delta_{u-\tilde{u}}. \tag{2.86}
$$

Then by using the known decays of the L^2-norm and L^∞-norm of $u, \tilde{u}, \phi, \tilde{\phi}, \nabla\phi, \nabla\tilde{\phi}$, from inequalities in (2.85) and (2.86) we obtain

$$
\begin{aligned}
M^\delta_{u-\tilde{u}}(t) \quad \leq \quad & C_0 \left(\|u_0\|_{L^2} + \sum_{i=1}^n \|v_0^i\|_{L^2} + \|u_0\|_{L^1} + \sum_i \|v_0^i\|_{L^1} \right) \\
+ \quad & C_{1k} \left[M^\delta_{u-\tilde{u}}(t)(M^{\frac{n}{4}}_\phi(t) + M^{\frac{n}{4}}_{D^1_x\phi}(t) + M^{\frac{n}{4}}_{\tilde{u}}(t)) \right] \\
+ \quad & C_{2k} \left[M^{\frac{n}{4}}_{D^1_x\tilde{\phi}}(t) N^{\frac{n}{2}}_{D^1_x\tilde{\phi}}(t)) + M^{\frac{n}{4}}_\phi(t) N^{\frac{n}{2}}_{\tilde{\phi}}(t) + M^{\frac{n}{4}}_{\tilde{u}}(t) N^{\frac{n}{2}}_{\tilde{u}}(t) \right. \\
+ \quad & M^{\frac{n}{4}}_{D^1_x\phi}(t) N^{\frac{n}{2}}_{D^1_x\phi}(t) + M^{\frac{n}{4}}_\phi(t) N^{\frac{n}{2}}_{\tilde{\phi}}(t) + M^{\frac{n}{4}}_u(t) N^{\frac{n}{2}}_u(t) \\
+ \quad & M^{\frac{n}{4}}_u(t) N^{\frac{n}{2}}_u(t) + M^{\frac{n}{4}}_\phi(t) N^{\frac{n}{2}}_u(t) + M^{\frac{n}{4}}_{D^1_x\phi}(t) N^{\frac{n}{2}}_u(t) + M^{\frac{n}{4}}_\phi(t) M^{\frac{n}{4}}_u(t) \\
+ \quad & \left. M^{\frac{n}{4}}_{D^1_x\phi}(t) M^{\frac{n}{4}}_u(t) + M^{\frac{n}{4}}_\phi(t) M^{v_0}_v(t) + M^{\frac{n}{4}}_{D^1_x\phi}(t) M^{v_0}_v(t) \right],
\end{aligned}
$$

where C_{1k} and C_{2k} are positive constant depending on K.

Now for small $M^{\frac{n}{4}}_\phi(t)$, $M^{\frac{n}{4}}_{D^1_x\phi}(t)$ and $M^{\frac{n}{4}}_{\tilde{u}}(t)$, or K, i.e. for small initial data, we have a global bound for $M^\delta_{u-\tilde{u}}(t)$, with $\delta = \min\{\frac{n}{4} + \frac{1}{2}, \frac{n}{2}\}$, and of course for the functional $M^\delta_{\phi-\tilde{\phi}}(t)$. $\qquad\square$

Chapter 3

A Quasilinear Hyperbolic-Parabolic Model of Vasculogenesis

In this chapter we present some analytical results on the PDEs model of vasculogenesis proposed by Gamba el al. [150, 66]

$$
\begin{cases}
\partial_t \rho + \nabla \cdot (\rho u) = 0, \\[2mm]
\partial_t (\rho u) + \nabla \cdot (\rho u \otimes u) + \nabla P(\rho) = -\alpha \rho u + \mu \rho \nabla \phi, \\[2mm]
\partial_t \phi = D \Delta \phi + a \rho - \frac{\phi}{\tau}.
\end{cases}
\tag{3.1}
$$

Here ρ is the density of endothelial cells, u their velocity, and ϕ the density of chemoattractant. The parameters D, a, and τ are, respectively, the diffusion coefficient, the rate of release, and the characteristic degradation time of soluble mediators, while α is a drift coefficient and μ measures the strength of cell response.

As seen in Chapter 1, this system is derived in a classical way by continuum mechanics and describes the early stages of vasculogenesis taking into account migration and chemotaxis.

It is based on the following assumptions:

1. endothelial cells show persistence in their motion;

2. endothelial cells communicate via the release and absorption of a soluble growth factor. This chemical factor can reasonably identified with VEGF-A (Serini et al. [150]);

3. the chemical factors released by cells diffuse and degrade in time;

4. endothelial cells neither duplicate nor die during the process;

5. cells are slowed down by friction due to the interaction with the fixed substratum;

6. closely packed cells mechanically respond to avoid overcrowding.

The model in (3.1) is able to reproduce several experimentally observed facts, e.g. the mean chord length is approximately independent on the initial cell density and connected networks are formed only above a critical threshold for density, as shown in [150, 66]. Moreover, through biological experiment, theoretical insights and numerical simulations, the authors provided a strong evidence that endothelial cell number and the range of activity of a chemoattractant factor regulate vascular

network formation.

Since we are interested in the behavior of system (3.1) from an analytical point of view, we focus our attention on the study of solutions to the hyperbolic-parabolic systems, aiming at investigating the different behaviors which can arise. Our purpose is to give a rigorous analytical assessment of a prototype model, like system (3.1), which can be used as a first step in the understanding of more complete systems.

A first analytical study of this model was proposed by Kowalczyk et al. in [93]. In their work, the authors introduced a viscous term $\gamma \nabla^2 (\rho u)$ in the second equation, in order to reproduce an energy mechanism that models the slowing down of cells in the proximity of network structure. They performed a detailed linear stability analysis of the model in the two dimensional case, aiming at checking its potential for structure formation. They found that, in the case of initial data representing a continuum cell monolayer, this is unstable at low cell densities, while pressure stabilizes it at high densities.

In this chapter we study the model in (3.1) from the analytical point of view by considering the one-dimensional case. In particular, we focus on solutions that can be written as perturbation of a non null constant state [49]. We will prove a global existence theorem and then we will study the asymptotic behavior of smooth solutions to the Cauchy problem in H^s.

Let us observe that system (3.1), as the semilinear Cattaneo-Hillen model analyzed in the previous chapter, does not enter in the framework of hyperbolic-parabolic system studied by Shizuta and Kawashima, [86, 153, 87]. Indeed, due to the presence of the source term $a\rho$, the dissipative condition fails.

In order to prove our results we use a different technique with respect to Chapter 2, where we proved these analytical results for the linearization of the differential part of system (3.1). As a matter of fact, the nonlinearity of the fluxes precludes the direct use of the decay estimate of the linearized Green operator.

In the first section we recall some basic results concerning quasilinear hyperbolic systems with entropy dissipation and the Shizuta-Kawashima (SK) condition. Indeed in [73], Hanouzet and Natalini determined these as sufficient conditions which guarantee the global existence in time of smooth solutions. The entropy dissipation is a condition for system which are endowed with a strictly convex entropy, but it is to weak to prevent the formation of singularities. In fact there exist systems, which even if satisfy this condition, do not admit a global solution. The condition (SK) guarantees the necessary coupling between conserved and non conserved quantities to have dissipation in both the state variables. Moreover additional energy estimates, based on condition (SK), permit one to close the analysis.

Since the hyperbolic part of system (3.1), i.e. isentropic Euler equations, verifies these conditions, we prove our result of global solution for system (3.1) by combining in a suitable way energy estimates for the parabolic and hyperbolic parts.

Finally we focus on the study of the decay property of the quasilinear system. We prove some estimates that describe the asymptotic behavior of solution in L^∞ and H^s−norm.

3.1 Partially Dissipative Hyperbolic Systems

Let us consider the Cauchy problem for the following hyperbolic-parabolic system

$$
\begin{cases}
\partial_t \tilde{\rho} + \partial_x(\tilde{\rho}\tilde{u}) = 0, \\[2mm]
\partial_t(\tilde{\rho}\tilde{u}) + \partial_x(\tilde{\rho}\tilde{u}^2 + P(\tilde{\rho})) = -\alpha\tilde{\rho}\tilde{u} + \mu\tilde{\rho}\partial_x\tilde{\phi}, \\[2mm]
\partial_t\tilde{\phi} = D\partial_{xx}\tilde{\phi} + a\tilde{\rho} - \frac{\tilde{\phi}}{\tau},
\end{cases}
\tag{3.2}
$$

where $\tilde{\rho}, \tilde{u}, \tilde{\phi} : \mathbb{R} \times \mathbb{R}^+ \to \mathbb{R}^+$, with initial conditions

$$
\tilde{\rho}(x,0) = \rho_0(x), \quad \tilde{u}(x,0) = u_0(x), \quad \tilde{\phi}(x,0) = \phi_0(x).
\tag{3.3}
$$

We made the assumption

$$
P'(\rho) > 0,
$$

with $\rho > 0$, to ensure the strictly hyperbolicity of system (3.2). Defining $\tilde{v} := \tilde{\rho}\tilde{u}$, we can rewrite the system in the following form

$$
\begin{cases}
\partial_t\tilde{\rho} + \partial_x\tilde{v} = 0, \\[2mm]
\partial_t\tilde{v} + \partial_x(\frac{\tilde{v}^2}{\tilde{\rho}} + P(\tilde{\rho})) = -\alpha\tilde{v} + \mu\tilde{\rho}\partial_x\tilde{\phi}, \\[2mm]
\partial_t\tilde{\phi} = D\partial_{xx}\tilde{\phi} + a\tilde{\rho} - \frac{\tilde{\phi}}{\tau},
\end{cases}
\tag{3.4}
$$

which is equivalent for smooth solutions.

Our aim is to prove that, under suitable assumptions, the Cauchy problem associated to the hyperbolic-parabolic system admits a global smooth solution, for small and smooth initial data. In particular we consider solutions of the form $(\tilde{\rho}, \tilde{v}, \tilde{\phi}) = (\rho + \bar{\rho}, v, \phi + \bar{\phi})$, where $(\bar{\rho}, 0, \bar{\phi})$ is a constant stationary solution to the problem and (ρ, v, ϕ) is a perturbation. We assume that $\bar{\phi} = a\tau\bar{\rho}$, in order to ensure that the constant state $(\bar{\rho}, 0, \bar{\phi})$ is a solution to system (3.4).

Therefore, we can rewrite system (3.4) as follows in terms of the perturbations:

$$
\begin{cases}
\partial_t\rho + \partial_x v = 0, \\[2mm]
\partial_t v + \partial_x\left(\frac{v^2}{\rho+\bar{\rho}} + P(\rho+\bar{\rho})\right) = -\alpha v + \mu(\rho+\bar{\rho})\partial_x\phi, \\[2mm]
\partial_t\phi = D\partial_{xx}\phi + a\rho - \frac{\phi}{\tau}.
\end{cases}
\tag{3.5}
$$

Since the complete system (3.5) does not verify the dissipation condition in [86], to get our global existence result we consider the hyperbolic and the parabolic equations separately, in order to take advantage of their respective properties.

3.1.1 Strictly Entropy Dissipative Condition

In this section we focus our attention on the hyperbolic part of (3.5).

As we want to prove the global existence of solution by energy methods, we first prove some properties of the selected problem.

Then, let us consider

$$\begin{cases} \partial_t \rho + \partial_x v = 0, \\[2mm] \partial_t v + \partial_x \left(\frac{v^2}{\rho + \bar{\rho}} + P(\rho + \bar{\rho}) \right) = -\alpha v. \end{cases} \qquad (3.6)$$

In [73], Hanouzet and Natalini proposed a quite general framework of sufficient conditions which guarantees the global existence in time of smooth solutions to quasilinear hyperbolic systems. These are the entropy dissipative condition and the Shizuta Kawashima condition. In this section we are going to show that system (3.6) verifies both the conditions.

First of all, we want to prove that system (3.6) is endowed with an entropy function, that is a convex real function $\mathscr{E}$ such that there exists a related entropy-flux q satisfying the following condition

$$(f')^t \mathscr{E}' = q',$$

where f is the flux of system (3.6).

In order to ensure the existence of an entropy-flux function q, we need to prove that the previous condition is verified, which means that the differential form $(f')^t \mathscr{E}'$ is exact. This condition can be characterized by the property that the matrix $\nabla((f')^t \mathscr{E}')$ is symmetric.

Let us notice that $\nabla((f')^t \mathscr{E}') = (f')^t \mathscr{E}'' + f'' \mathscr{E}'$, therefore, in order to obtain the existence of an entropy-flux function q, it is sufficient to prove that

$$(f')^t \mathscr{E}'' \quad \text{is symmetric,}$$

or equivalently that $\mathscr{E}'' f'$ is symmetric.

Once we have proved the existence of an entropy function for system (3.6), an additional equation for the entropy evolution can be written. Indeed, fixing an equilibrium state $\hat{U}$ for system (3.6) (i.e. $g(\hat{U}) = 0$), we perform the scalar product of system (3.6) by $\mathscr{E}'(U) - \mathscr{E}'(\hat{U})$, to get the entropy identity

$$\partial_t (\mathscr{E}(U) - \mathscr{E}'(\hat{U}) \cdot U) + \partial_x (q(U) - \mathscr{E}'(\hat{U}) \cdot f(U)) = (\mathscr{E}'(U) - \mathscr{E}'(\hat{U})) \cdot (g(U) - g(\hat{U})).$$

From this equation, we deduce that the integral of $\mathscr{E}(U) - \mathscr{E}'(\hat{U}) \cdot U$ is decreasing if the term on the right-hand side is negative.

Denoted by γ the set of equilibrium states to the system (3.6), this decay property is encoded in the following definition (see [73]).

Definition 3.1.1. *The system* (3.6), *endowed by the entropy* $\mathscr{E}$, *is entropy dissipative if, for every* $\hat{U} \in \gamma$, *and for any U in a neighborhood of* $\hat{U}$, *the inequality*

$$(\mathscr{E}'(U) - \mathscr{E}'(\hat{U})) \cdot (g(U) - g(\hat{U})) \leq 0, \qquad (3.7)$$

is satisfied.

We know that property (3.7) is invariant under affine transformation. Then, by applying a simple change of variables, we can choose the entropy $\mathscr{E}$, such that, for a single equilibrium value $\hat{U} \in \gamma$, it is a strictly convex quadratic function. In our case, setting $\overline{U} = (\bar{\rho}, 0)$, we define a new function $\tilde{\mathscr{E}}$ that is still a dissipative entropy for system (3.6)

$$\tilde{\mathscr{E}}(U) = \mathscr{E}(U + \overline{U}) - \mathscr{E}(\overline{U}) - \mathscr{E}'(\overline{U}) \cdot U,$$

and moreover it is a quadratic function in $U = 0$.

Assuming that $\tilde{\mathscr{E}}$ is a strictly convex function, we can introduce the entropy variable (see [73])

$$W := \tilde{\mathscr{E}}'(U) = \mathscr{E}'(U + \overline{U}) - \mathscr{E}'(\overline{U}),$$

and the functions

$$
\begin{aligned}
\tilde{\mathscr{E}}^*(W) &:= W \cdot \Phi(W) - \tilde{\mathscr{E}}(\Phi(W)), \\
q^*(W) &:= W \cdot f(\Phi(W)) - q(\Phi(W)),
\end{aligned}
$$

where $\Phi := (\tilde{\mathscr{E}}')^{-1}$. Setting $A_0 = (\tilde{\mathscr{E}}^*)''(W)$, $A_1 = f'(\Phi(W))A_0$ and $\widetilde{G}(W) = g(\Phi(W))$. We can rewrite system (3.6) in the entropy variable as

$$A_0 \partial_t W + A_1 \partial_x W = \widetilde{G}(W). \tag{3.8}$$

Let us observe that A_0 is symmetric positive definite and A_1 is symmetric.
Now, we take $\mathscr{U}$ an open subset of $\mathbb{R}^2$ and set

$$
\begin{aligned}
\gamma &:= \left\{ U \in \mathscr{U} : g(U + \overline{U}) = 0 \right\}, \\
\Gamma &:= \tilde{\mathscr{E}}'(\gamma) = \left\{ W \in \tilde{\mathscr{E}}'(\mathscr{U}) : G(W) = 0 \right\}.
\end{aligned}
$$

Let us observe that, if $\overline{W} = (\overline{W}_1, \overline{W}_2) \in \Gamma$ and $W = (W_1, W_2)$ is any given point such that the segment $(W_1, sW_2 + (1-s)\overline{W}_2) \in \tilde{\mathscr{E}}'(\mathscr{U})$ for all $s \in [0, 1]$, then the point $W^* = (W_1, \overline{W}_2)$ is again in Γ. Therefore, we can write

$$Q(W) = \left(\int_0^1 (\partial_{W_2} Q)^t (W_1, sW_2 + (1-s)\overline{W}_2) ds \right) (W_2 - \overline{W}_2),$$

where $Q(W) = g_2(\Phi(W))$. In particular, from the dissipative condition, we deduce that there exists a real positive scalar function $B = B(W, \overline{W})$ such that, for every W in a suitable neighborhood of $\overline{W}$,

$$Q(W) = -B(W, \overline{W})(W_2 - \overline{W}_2).$$

Definition 3.1.2. *The system* (3.6)*, endowed with a strictly convex entropy, is strictly entropy dissipative if there exists a positive scalar function $B(W, \overline{W})$ such that*

$$Q(W) = -B(W, \overline{W})(W_2 - \overline{W}_2), \tag{3.9}$$

for every $W \in \tilde{\mathscr{E}}'(\mathscr{U})$ and $\overline{W} = (\overline{W}_1, \overline{W}_2) \in \Gamma$.

Now we want to prove that system (3.6) satisfies the latter condition. To this end, we consider the canonical entropy function

$$\mathscr{E} = \frac{1}{2} \frac{v^2}{\rho + \bar{\rho}} + (\rho + \bar{\rho}) \int_0^{\rho + \bar{\rho}} \frac{P(s)}{s^2} ds, \tag{3.10}$$

and the relative flux

$$q = \frac{1}{2} \frac{1}{(\rho + \bar{\rho})^2} v^3 + \frac{P(\rho + \bar{\rho})}{\rho + \bar{\rho}} v + v \int_0^{\rho + \bar{\rho}} \frac{P(s)}{s^2} ds.$$

Let us observe that this entropy is a strictly convex function. System (3.6), endowed with the entropy $\mathscr{E}$, satisfies the dissipative condition as

$$(\mathscr{E}'(U) - \mathscr{E}'(\hat{U})) \cdot (g(U) - g(\hat{U})) = -\alpha \frac{v^2}{\rho + \bar{\rho}} \leq 0.$$

Moreover, thanks to the strictly convexity of $\mathscr{E}$, we can rewrite the system (3.6) in the form (3.8) using the entropy variable $W = \mathscr{E}'(U)$. It is easy to show that in this case the scalar positive function B of condition (3.9) is given by $B = \alpha(\rho + \bar{\rho}) = \alpha \Phi_1(W, \overline{W}) > 0$. Therefore the system (3.8) is *strictly entropy dissipative*.

Let us finally observe that, in our case,

$$\gamma = \left\{ U \in \mathscr{U} : g(U + \overline{U}) = 0 \right\} = \left\{ U \in \mathscr{U} : U = (\rho, 0) \right\}, \tag{3.11}$$

therefore, thanks to the definition of $\tilde{\mathscr{E}}$, it can be easily verified that

$$\Gamma = \left\{ W \in \tilde{\mathscr{E}}'(\mathscr{U}) : G(W) = 0 \right\} = \left\{ W \in \tilde{\mathscr{E}}'(\mathscr{U}) : W_2 = 0 \right\}.$$

3.1.2   The Shizuta-Kawashima Condition

As observed before, the entropy dissipation condition is too weak to prevent the shock formation. In order to obtain global existence of smooth solutions to quasilinear hyperbolic system, Hanouzet and Natalini in [73] determinated a supplementary condition, the Shizuta-Kawashima condition, which guarantees these results.

This section is devoted to proving that system (3.8) satisfies the Shizuta-Kawashima condition [153], introduced in the previous chapter (Definition 2.1.1) for hyperbolic systems.

Let us recall that, in our case, as we have

$$f(U + \overline{U}) = \begin{pmatrix} v \\ \frac{v^2}{\rho + \bar{\rho}} + P(\rho + \bar{\rho}) \end{pmatrix}, \qquad g(U) = \begin{pmatrix} 0 \\ -\alpha v \end{pmatrix},$$

then

$$f'(U + \overline{U}) = \begin{pmatrix} 0 & 1 \\ -\frac{v^2}{(\rho + \bar{\rho})^2} + P'(\rho + \bar{\rho}) & 2\frac{v}{\rho + \bar{\rho}} \end{pmatrix}, \qquad g'(U) = \begin{pmatrix} 0 & 0 \\ 0 & -\alpha \end{pmatrix}.$$

Consequently, to ensure that system (3.8) satisfies the Shizuta-Kawashima condition, we need to prove that every eigenvector of $f'(\overline{U})$ is not in the null space of $g'(\overline{U})$, where $\overline{U} = (\bar{\rho}, 0)$ as indicated in (3.11).

Let us take $X \in \mathbb{R}^2 - \{0\}$ an eigenvector of $f'(\overline{U})$ and denote with $\lambda \neq 0$ the corresponding eigenvalue. This means that

$$\lambda X = f'(\overline{U})X \quad \Longleftrightarrow \quad \begin{pmatrix} \lambda X_1 \\ \lambda X_2 \end{pmatrix} = \begin{pmatrix} 0 & 1 \\ P'(2\bar{\rho}) & 0 \end{pmatrix} \begin{pmatrix} X_1 \\ X_2 \end{pmatrix}$$

$$\Longleftrightarrow \quad \begin{cases} \lambda X_1 = X_2, \\ \lambda X_2 = P'(2\bar{\rho})X_1. \end{cases}$$

Then, we have two possibilities:

(a) $\lambda = \sqrt{P'(2\bar{\rho})}$ and $X_2 = \sqrt{P'(2\bar{\rho})}X_1$;

(b) $\lambda = -\sqrt{P'(2\bar{\rho})}$ and $X_2 = -\sqrt{P'(2\bar{\rho})}X_1$.

Let us suppose for example that the case (*b*) is satisfied. It is possible to proceed in the same way in the other case. Now, we suppose that X is in the null space of $g'(\overline{U})$, which means that

$$g'(\overline{U})X = 0 \quad \Longleftrightarrow \quad \begin{pmatrix} 0 & 0 \\ 0 & -\alpha \end{pmatrix} \begin{pmatrix} X_1 \\ X_2 \end{pmatrix} = 0 \quad \Longleftrightarrow \quad -\alpha X_2 = 0.$$

So, if X is an eigenvector of $f'(\overline{U})$, X is not in the null space of $g'(\overline{U})$. This proves that system (3.8) satisfies the Shizuta-Kawashima condition.

In the case of strictly entropy dissipative system, Definition 2.1.1 is equivalent to:

(H1) for every $\lambda \in \mathbb{R}$ and every $X \in \mathbb{R}\backslash\{0\}$ the vector $(X,0)^t \in \mathbb{R}^2$ is not in the null space of $\lambda A_0(0) + A_1(0)$.

Then, the following lemma holds (see [73]).

Lemma 3.1.3. *Assume that system* (3.8) *is strictly entropy dissipative, then Condition (H1) is equivalent to:*
there exists a constant matrix $K \in \mathbb{R}^{2\times 2}$ such that

- *$KA_0(0)$ is skew-symmetric;*

- *the matrix*

$$\frac{1}{2}(KA_1(0) + (KA_1(0))^t) + \frac{1}{2}\begin{pmatrix} 0 & 0 \\ 0 & B(0) + B(0)^t \end{pmatrix}$$

  is positive definite.

3.2   The Global Existence of Smooth Solutions

In this section, by means of energy estimates, we aim at proving the global existence of smooth solutions to the complete hyperbolic-parabolic system

$$\begin{cases} \partial_t \rho + \partial_x v = 0, \\[2mm] \partial_t v + \partial_x\left(\frac{v^2}{\rho + \bar{\rho}} + P(\rho + \bar{\rho})\right) = -\alpha v + \mu(\rho + \bar{\rho})\partial_x \phi, \\[2mm] \partial_t \phi = D\partial_{xx}\phi + a\rho - \frac{\phi}{\tau}. \end{cases} \tag{3.12}$$

Let us recall that $\rho, u, \phi : \mathbb{R} \times \mathbb{R}^+ \to \mathbb{R}^+$, $v = \rho u$ and $P'(\rho) > 0$. Moreover, $\overline{U} = (\bar{\rho}, 0, \bar{\phi})$ is a constant stationary solution to the problem, with $\bar{\phi} = a\tau\bar{\rho}$.

3.2.1   Local Existence of Smooth Solutions

In order to prove the global existence of smooth solution with small initial data, a result of local existence is crucial for our proof. As we have shown in the previous sections, the hyperbolic part (3.6) of system (3.12) has a strictly convex entropy $\tilde{\mathscr{E}}$ and it satisfies the strictly entropy dissipative condition.

Now, let us write the first two equations of system (3.12) in the form:

$$\partial_t(U + \overline{U}) + \partial_x f(U + \overline{U}) = g(U + \overline{U}) + h(U + \overline{U}, \partial_x \phi), \tag{3.13}$$

where $U = (\rho, v)$, $g(U) = (0, -\alpha v)$, $f(U) = (v, \frac{v^2}{\rho} + P(\rho))$ and $h(U, \partial_x \phi) = (0, \mu\rho\partial_x\phi)$. Moreover we can introduce the entropy variable, $W = \tilde{\mathscr{E}}'(U)$, and rewrite the system (3.13) as

$$A_0\partial_t W + A_1\partial_x W = G(W) + H(W, \partial_x \phi). \tag{3.14}$$

Here, setting $\Phi(W) = (\tilde{\mathscr{E}}')^{-1}(W)$, we have

$$A_0(W) = (\Phi(W))', \qquad\qquad A_1(W) = f'(\Phi(W))A_0,$$
$$G(W) = g(\Phi(W)), \qquad\qquad H(W, \partial_x\phi) = h(\Phi(W), \partial_x\phi).$$

Then we can rewrite the complete system (3.12) as:

$$
\begin{cases}
A_0\partial_t W + A_1\partial_x W = G(W) + H(W, \partial_x\phi), \\[2mm]
\partial_t\phi = D\partial_{xx}\phi + a\Phi_1(W) - \dfrac{\phi}{\tau}.
\end{cases}
\tag{3.15}
$$

We can observe that (3.15) is a symmetric hyperbolic-parabolic system. This class of system has been studied by Kawashima in [86]. As a matter of fact he considered the initial value problem for systems of quasilinear partial differential equations in the form

$$
\begin{cases}
A_1^0(W,\phi)W_t + \displaystyle\sum_{j=1}^{n} A_{11}^j(W,\phi)W_{x_j} = f_1(W,\phi,D_x\phi), \\[4mm]
A_2^0(W,\phi)\phi_t - \displaystyle\sum_{j,k=1}^{n} B_2^{ij}(W,\phi)\phi_{x_i x_j} = f_2(W,\phi,D_x W,D_x\phi),
\end{cases}
\tag{3.16}
$$

where $t \geq 0$ and $x = (x_1,\ldots,x_n) \in \mathbb{R}^n$, $(n \geq 1)$. Here $W(x,t)$ and $\phi(x,t)$ are vectors with m' and m'' components, respectively, and the pair $(W,\phi)(x,t)$ takes its values in an open convex set $\mathcal{O}$ in $\mathbb{R}^m$ $(m = m' + m'' \geq 1)$. A_1^0 and $A_{11}^j \in \mathbb{R}^{m' \times m'}$ $(j = 1,\ldots,n)$ (resp. A_2^0 and $B_2^{jk} \in \mathbb{R}^{m'' \times m''}$ $(j,k = 1,\ldots,n))$. Functions f_1 and f_2 take values respectively in $\mathbb{R}^{m'}$ and $\mathbb{R}^{m''}$, and D_x denotes the derivatives $(\partial/\partial x)^\alpha$ with $|\alpha| = 1$.

The system (3.16) is complemented with the initial conditions

$$(W,\phi)(x,0) = (W_0,\phi_0)(x).\tag{3.17}$$

Kawashima assumed that system (3.16) is symmetric hyperbolic-parabolic in the following sense:

Condition 3.2.1. *The functions $A_1^0(W,\phi)$, $A_2^0(W,\phi)$, $A_{11}^j(W,\phi)$ $(j = 1,\ldots,n)$ and $B_2^{jk}(W,\phi)$ $(j,k = 1,\ldots,n)$ are sufficiently smooth in $(W,\phi) \in \mathcal{O}$ and such that:*

i) $A_1^0(W,\phi)$ *and* $A_2^0(W,\phi)$ *are real symmetric and positive definite for* $(W,\phi) \in \mathcal{O}$,

ii) $A_{11}^j(W,\phi)$ *is real symmetric for* $(W,\phi) \in \mathcal{O}$;

iii) $B_2^{jk}(W,\phi)$ *is real symmetric and satisfies* $B_2^{jk}(W,\phi) = B_2^{kj}(W,\phi)$ *for* $(W,\phi) \in \mathcal{O}$, *and*
   $\displaystyle\sum_{j,k=1}^{n} B_2^{ij}(W,\phi)\omega_j\omega_k$ *is symmetric positive definite for all* $(W,\phi) \in \mathcal{O}, \omega = (\omega_l,\ldots,\omega_n) \in S^{n-1}$.

Under these conditions $f_1(W,\phi,D_x\phi)$ and $f_2(W,\phi,D_x W,D_x\phi)$ can be regarded as lower order terms of the system. Denoted by $\eta \in \mathbb{R}^{nm'}$ and $\zeta \in \mathbb{R}^{nm''}$ the vectors corresponding to $D_x W$ and $D_x\phi$, the author assumed that

Condition 3.2.2. *The functions $f_1(W,\phi,\zeta)$ and $f_2(W,\phi,\eta,\zeta)$ are sufficiently smooth in $(W,\phi,\zeta) \in \mathcal{O} \times \mathbb{R}^{nm'}$ and $(W,\phi,\eta,\zeta) \in \mathcal{O} \times \mathbb{R}^{nm''}$, respectively, and satisfy $f_1(\overline{W},\overline{\phi},0) = f_2(\overline{W},\overline{\phi},0,0) = 0$ for some constant state $(\overline{W},\overline{\phi}) \in \mathcal{O}$.*

Fixed a constant d_1 so that $0 < d_1 < d_0 \equiv \text{dist}(\mathcal{O}_0,\partial\mathcal{O})$, let us denoted by $X_{T_1}^s$ the set of function $(W,\phi)(x,t)$ satisfying:

- $W - \overline{W} \in C([0,T), H^s(\mathbb{R}^n)), \partial_t W \in C([0,T)H^{s-1}(\mathbb{R}^n)),$

- $\phi - \overline{\phi} \in C([0,T)H^s(\mathbb{R}^n)) \cap L^2([0,T)H^{s+1}(\mathbb{R}^n)), \partial_t \phi \in C^0([0,T)H^{s-2}(\mathbb{R}^n)) \cap L^2(0,T;H^{s-1}(\mathbb{R}^n)),$

- $(W,\phi)(x,t) \in \mathscr{O}_1$ for any $(x,t) \in \mathbb{R}^n \times [0,T],$

- $\displaystyle \sup_{0 \le \tau \le t} \|(W - \overline{W}, \phi - \overline{\phi})(\tau)\|_{H^s}^2 + \int_0^t \|\phi - \overline{\phi}\|_{s+1}^2 \, d\tau \le M^2,$

- $\displaystyle \int_0^t \|\partial_t (W,\phi)(\tau)\|_{H^{s-1}}^2 \, d\tau \le M^1$ for $t \in [0,T].$

Existence and uniqueness of local in time solutions to the Cauchy problem are proved by the following theorem (Theorem 2.9 [86]).

Theorem 3.2.3. *Let Conditions 3.2.1 and 3.2.2 be assumed. Let $n \ge 1$ and $s \ge s_0 + 1$ ($s_0 \ge [n/2] + 1$) be integers. Suppose that the initial data satisfy $(W_0 - \overline{W}, \phi_0 - \overline{\phi}) \in H^s(\mathbb{R}^n)$ and $(W_0, \phi_0)(x) \in \mathscr{O}_0$ for any $x \in \mathbb{R}^n$, where $\mathscr{O}_0$ is a bounded open convex set in $\mathbb{R}^m$ satisfying $\overline{\mathscr{O}}_0 \subset \mathscr{O}$.*
Then there exists a positive constant T_1 ($\le T_0$), depending only on $\mathscr{O}_0$, d_1, and $\|W_0 - \overline{W}, \phi_0 - \overline{\phi}\|_{H^s}$ such that the initial value problem (3.16), (3.17) has a unique solution $(W,\phi) \in X_{T_1}^s(\mathscr{O}_1, M, M_1)$, where $\mathscr{O}_1, M$ and M_1 are determined as follows

$$\mathscr{O}_1 = d_1 - neighborhood\ of\ \mathscr{O}_0, \quad M = 2C_1(\mathscr{O}_1)\|W_0 - \overline{W}, \phi_0 - \overline{\phi}\|_s, \quad M_1 = 2C_3(\mathscr{O}_1, M)M.$$

In particular, the solution satisfies

$$W - \overline{W} \in C([0,T_1), H^s(\mathbb{R}^n)) \cap C^1([0,T_1), H^{s-1}(\mathbb{R}^n)),$$

$$\phi - \overline{\phi} \in C([0,T_1), H^s(\mathbb{R}^n)) \cap C^1([0,T_1), H^{s-2}(\mathbb{R}^n)) \cap L^2([0,T_1), H^{s+1}(\mathbb{R}^n)),$$

$$\sup_{0 \le \tau \le t} \|(W - \overline{W}, \phi - \overline{\phi})(\tau)\|_{H^s}^2 + \int_0^t \|(W - \overline{W})(\tau)\|_s^2 + \|(\phi - \overline{\phi})(\tau)\|_{s+1}^2 \, d\tau \le C_4^2 \|W_0 - \overline{W}, \phi_0 - \overline{\phi}\|_{H^s}^2$$
for $t \in [0,T_1],$

where $C_4 > 1$ is a constant depending only on $\mathscr{O}_0$, d_1 and $\|W_0 - \overline{W}, \phi_0 - \overline{\phi}\|_{H^s}$.

Coming back to our problem, we can observe that system (3.15) can be regarded as a coupled system of a symmetric hyperbolic system for W and a strongly parabolic equation for ϕ. Hence, thanks to this theorem, if the initial data (W_0, ϕ_0) are in $H^s(\mathbb{R})$, with $s \ge 2$, then there exists a local in time solution $(W,\phi) \in C([0,T_1), H^s(\mathbb{R}))$ to the Cauchy problem.
Let us consider now the variable $\psi = \partial_x \phi$. Deriving the parabolic equation with respect to the spatial variable we get the system

$$\begin{cases} A_0 \partial_t W + A_1 \partial_x W = G(W) + H(W,\psi), \\[2mm] \partial_t \psi = D\partial_{xx}\psi + a\partial_x \Phi_1(W) - \dfrac{\psi}{\tau}. \end{cases}$$

We can observe that, as this system verifies the conditions of Theorem 3.2.3, the local existence of its solutions follows. Considering system (3.15) and taking an initial datum $\phi_0 \in H^{s+1}$, then the parabolic equation admits the local existence in the space $C([0,T_1), H^{s+1}(\mathbb{R}))$.

Now we are going to prove the existence of global solution to system (3.15), by using the following theorem.

Theorem 3.2.4. *We consider the Cauchy problem associated to system* (3.15), *with small initial data* $W_0 \in H^2(\mathbb{R})$ *and* $\phi_0 \in H^2(\mathbb{R})$. *If* $\|W_0\|_{H^2(\mathbb{R})}$, $\|\phi_0\|_{H^2(\mathbb{R})}$ *and* $\bar{\rho}$ *are sufficiently small, then there exists a unique global solution* (W, ϕ) *to system* (3.15), *such that*

$$W \in C([0, \infty), H^2(\mathbb{R})), \quad \phi \in C([0, \infty), H^2(\mathbb{R})) \cap L^2([0, \infty), H^3(\mathbb{R}))$$

and, for each $T > 0$,

$$\|W(T)\|_{H^2}^2 + \int_0^T \|\partial_x W(\tau)\|_{H^1}^2 \, d\tau + \int_0^T \|W_2(\tau)\|_{H^2}^2 \leq C \|W_0\|_{H^2}^2,$$

$$\tag{3.18}$$

$$\|\phi(T)\|_{H^2}^2 + \int_0^T \|\partial_x \phi(\tau)\|_{H^2}^2 \, d\tau \leq C(\|W_0\|_{H^2}^2 + \|\phi_0\|_{H^2}^2),$$

where $C = C(\bar{\rho}, \|W_0\|_{H^2}, \|\phi_0\|_{H^2})$.

Energy Estimates for ϕ

Our aim is to prove this result by suitable energy estimates. Let us consider the local (in time) solution $(W, \phi) \in C([0, T], H^2(\mathbb{R})) \times C([0, T], H^2(\mathbb{R})) \cap L^2([0, T], H^3(\mathbb{R}))$.
First we focus on the parabolic equation providing energy estimates for the function ϕ.
We consider the parabolic equation

$$\partial_t \phi = D \partial_{xx} \phi + a\rho - \frac{\phi}{\tau}. \tag{3.19}$$

Deriving with respect to the spatial variable and multiplying by $\partial_x \phi$, we obtain

$$\partial_t \left(\frac{1}{2} (\partial_x \phi)^2 \right) = D \partial_{xxx} \phi \partial_x \phi + a \partial_x \rho \partial_x \phi - \frac{(\partial_x \phi)^2}{\tau}$$

$$= D \partial_x \left(\partial_{xx} \phi \partial_x \phi \right) - D (\partial_{xx} \phi)^2 + a \partial_x \rho \partial_x \phi - \frac{(\partial_x \phi)^2}{\tau}.$$

Then, integrating with respect to x and t, we get for every $\epsilon > 0$

$$\frac{1}{2} \int (\partial_x \phi)^2 \, dx + D \int_0^t \int (\partial_{xx} \phi)^2 \, ds \, dx \leq \frac{1}{2} \int (\partial_x \phi_0)^2 \, dx + \frac{a}{2\epsilon} \int_0^t \int (\partial_x \rho)^2 \, dx \, ds$$

$$+ \frac{a\epsilon}{2} \int_0^t \int (\partial_x \phi)^2 \, dx \, ds - \frac{1}{\tau} \int_0^t \int (\partial_x \phi)^2 \, dx \, ds,$$

that is

$$\frac{1}{2} \int (\partial_x \phi)^2 \, dx + D \int_0^t \int (\partial_{xx} \phi)^2 \, ds \, dx + \left(\frac{1}{\tau} - \frac{a\epsilon}{2} \right) \int_0^t \int (\partial_x \phi)^2 \, dx \, ds$$

$$\leq \frac{1}{2} \int (\partial_x \phi_0)^2 \, dx + \frac{a}{2\epsilon} \int_0^t \int (\partial_x \rho)^2 \, dx \, ds.$$

Here, we take ϵ such that $\epsilon < \frac{2}{a\tau}$.
In the same way, we can obtain

$$\frac{1}{2} \int (\partial_{xx} \phi)^2 \, dx + D \int_0^t \int (\partial_{xxx} \phi)^2 \, ds \, dx + \left(\frac{1}{\tau} - \frac{a\epsilon}{2} \right) \int_0^t \int (\partial_{xx} \phi)^2 \, dx \, ds$$

$$\leq \frac{1}{2} \int (\partial_{xx} \phi_0)^2 \, dx + \frac{a}{2\epsilon} \int_0^t \int (\partial_{xx} \rho)^2 \, dx \, ds.$$

Now, let us introduce the generic functional

$$N_l^2(t) := \sup_{0 \le s \le t} \|W(s)\|_{H^l}^2 + \int_0^t \|W_2(s)\|_{H^l}^2 \, ds + \int_0^t \|\partial_x W(s)\|_{H^{l-1}}^2, \quad \text{for } l = 1, 2.$$

We set also

$$N_0^2(t) := \sup_{0 \le s \le t} \|W(s)\|_{L^2}^2 + \int_0^t \|W_2(s)\|_{L^2}^2 \, ds.$$

Therefore we can rewrite the last two estimates for $\partial_x \phi$ and $\partial_{xx}\phi$, in the following way:

$$\|\partial_x \phi(t)\|_{L^2}^2 + c_1 \int_0^t \|\partial_{xx}\phi(s)\|_{L^2}^2 \, ds + c_2 \int_0^t \|\partial_x \phi(s)\|_{L^2}^2 \, dx \, ds \le \|\phi_0\|_{H^1}^2 + c_3 N_1^2(t), \tag{3.20}$$

$$\|\partial_{xx}\phi(t)\|_{L^2}^2 + \tilde{c}_1 \int_0^t \|\partial_{xxx}\phi(s)\|_{L^2}^2 \, ds + \tilde{c}_2 \int_0^t \|\partial_{xx}\phi(s)\|_{L^2}^2 \, ds \le \|\phi_0\|_{H^2}^2 + \tilde{c}_3 N_2^2(t). \tag{3.21}$$

Moreover, using these last estimates, we can control L^∞-norm of $\partial_x \phi$ too. Indeed, we have

$$\begin{aligned}
\sup_t \|\partial_x \phi\|_{L^\infty} &\le \sup_t \left(\int ((\partial_x \phi)^2 + (\partial_{xx}\phi)^2) \, dx \right)^{\frac{1}{2}} \\
&\le C \left(\|\phi_0\|_{H^1} + \|\phi_0\|_{H^2} + N_1(t) + N_2(t) \right) \\
&\le C \left(\|\phi_0\|_{H^2} + N_2(t) \right).
\end{aligned} \tag{3.22}$$

Zero Order Energy Estimate for W

Now, we want to estimate the L^2-norm of the function W. To this end, we multiply the system (3.13) by $\tilde{\mathscr{E}}'(U) = \mathscr{E}'(U + \overline{U}) - \mathscr{E}'(\overline{U})$, so we have

$$\partial_t \tilde{\mathscr{E}}(U) + \partial_x \tilde{Q}(U) = \tilde{\mathscr{E}}'(U) \cdot g(U + \overline{U}) + \tilde{\mathscr{E}}'(U) \cdot h(U + \overline{U}, \partial_x \phi),$$

where $\tilde{Q}(\cdot)$ is the entropy-flux associated to the function $\tilde{\mathscr{E}}$.

Let us observe that, thanks to definitions of the entropy $\tilde{\mathscr{E}}$ and variable $W = \tilde{\mathscr{E}}'(U)$, there exists a constant c_2 such that

$$\frac{1}{c_2} |W|^2 \le \tilde{\mathscr{E}}(U) \le c_2 |W|^2.$$

Moreover, as proved in Section 3.1.1, the system (3.13) satisfies the strictly entropy dissipative condition, therefore there exists a constant c_1 such that,

$$-(W \cdot \tilde{G}(W)) \ge c_1 |W_2|^2.$$

Let us integrate the previous system, with respect to space variable x, so we obtain:

$$\frac{d}{dt} \int \tilde{\mathscr{E}}(U) \, dx = \int \tilde{\mathscr{E}}'(U) \cdot g(U + \overline{U}) \, dx + \int \tilde{\mathscr{E}}'(U) \cdot h(U + \overline{U}, \partial_x \phi) \, dx,$$

which yields

$$\frac{1}{c_2} \frac{d}{dt} \int |W|^2 \, dx + c_1 \int |W_2|^2 \, dx \le \int \tilde{\mathscr{E}}'(U) \cdot h(U + \overline{U}, \partial_x \phi) \, dx.$$

Then, integrating respect to the temporal variable, we get

$$\frac{1}{c_2} \|W(t)\|_{L^2}^2 + \int_0^t c_1 \|W_2(s)\|_{L^2}^2 \, ds \le \frac{1}{c_2} \|W_0\|_{L^2}^2 + \int_0^t \int \tilde{\mathscr{E}}'(U + \overline{U}) \cdot h(U + \overline{U}, \partial_x \phi) \, dx \, ds.$$

Now, let us observe that, thanks to the definition of the function $h(U + \overline{U}, \partial_x \phi)$, the last integral can be estimated as follows

$$
\begin{aligned}
\int_0^t \int \tilde{\mathscr{E}}'(U) \cdot h(U + \overline{U}, \partial_x \phi) \, dx \, ds &= \int_0^t \int W_2 \mu(\rho + \bar{\rho}) \partial_x \phi \, dx \, ds \\
&\leq \int_0^t \mu \| W_2(s) \|_{L^2} \| \rho(s) \partial_x \phi(s) \|_{L^2} \, ds + \int_0^t \mu \bar{\rho} \| W_2(s) \|_{L^2} \| \partial_x \phi(s) \|_{L^2} \, ds \\
&\leq \int_0^t \mu \| W_2(s) \|_{L^2} \| \rho(s) \|_{L^\infty} \| \partial_x \phi(s) \|_{L^2} \, ds + \int_0^t \mu \bar{\rho} \| W_2(s) \|_{L^2} \| \partial_x \phi(s) \|_{L^2} \, ds \\
&\leq C \sup_{s \in (0,t)} \| \rho(s) \|_{L^\infty} \int_0^t \left(\| W_2(s) \|_{L^2}^2 + C \| \partial_x \phi(s) \|_{L^2}^2 \right) ds \\
&\quad + C \bar{\rho} \int_0^t \left(\| W_2(s) \|_{L^2}^2 + \| \partial_x \phi(s) \|_{L^2}^2 \right) ds.
\end{aligned}
$$

Then, thanks to the energy estimate (3.20) of ϕ, we obtain

$$
\int_0^t \int W_2 \mu(\rho + \bar{\rho}) \partial_x \phi \, dx \, ds \leq CN_1(t) \left[N_0^2(t) + \| \phi_0 \|_{H^1}^2 + N_1^2(t) \right] + C \bar{\rho} \left[N_0^2(t) + \| \phi_0 \|_{H^1}^2 + N_1^2(t) \right].
$$

In conclusion, the zero order estimate of function W is given by

$$
\| W(t) \|_{L^2} + \int_0^t \| W_2(s) \|_{L^2}^2 \, ds \leq N_0^2(0) + C(\| \phi_0 \|_{H^1}^2) N_1(t) + C(\bar{\rho}) N_1^2(t) + CN_1^3(t) + C(\bar{\rho}, \| \phi_0 \|_{H^1}^2).
$$

Let us observe that the positive constant $C(\bar{\rho}, \| \phi_0 \|_{H^1}^2)$ depends on the initial data and on the constant state and, when these data go to zero, it vanishes.

First Order Energy Estimate for W

Now we estimate the L^2-norm of the first derivative of the local solution W. To this end, we consider the system

$$
A_0 \partial_t W + A_1 \partial_x W = G(W) + H(W, \partial_x \phi). \tag{3.23}
$$

Deriving with respect to the spatial variable, we obtain

$$
\partial_x (A_0 \partial_t W) + \partial_x (A_1 \partial_x W) = \partial_x G(W) + \partial_x H(W, \partial_x \phi).
$$

Then, we take the inner product with $\partial_x W$, which yields

$$
\partial_x (A_0 \partial_t W) \cdot \partial_x W + \partial_x (A_1 \partial_x W) \cdot \partial_x W = \partial_x G(W) \cdot \partial_x W + \partial_x H(W, \partial_x \phi) \cdot \partial_x W.
$$

Thanks to the symmetry of matrices A_0 and A_1, we have

$$
\partial_x (A_0 \partial_t W) \cdot \partial_x W = \frac{1}{2} \partial_t ((A_0 \partial_x W) \cdot \partial_x W) - \frac{1}{2} (\partial_t A_0 \partial_x W) \cdot \partial_x W + (\partial_x A_0 \partial_t W) \cdot \partial_x W,
$$

$$
\partial_x (A_1 \partial_x W) \cdot \partial_x W = \frac{1}{2} \partial_x ((A_1 \partial_x W) \cdot \partial_x W) + \frac{1}{2} (\partial_x A_1 \partial_x W) \cdot \partial_x W.
$$

Therefore, substituting these relations in the previous system and integrating over $\mathbb{R}$, we get:

$$
\frac{1}{2} \frac{d}{dt} \int (A_0 \partial_x W) \cdot \partial_x W \, dx - \frac{1}{2} \int (\partial_t A_0 \partial_x W) \cdot \partial_x W \, dx + \int (\partial_x A_0 \partial_t W) \cdot \partial_x W \, dx
$$

$$
+ \frac{1}{2} \int (\partial_x A_1 \partial_x W) \cdot \partial_x W \, dx = \int \partial_x G(W) \cdot \partial_x W \, dx + \int \partial_x H(W, \partial_x \phi) \cdot \partial_x W \, dx.
$$

Let us observe that, thanks to the strictly entropy dissipative condition, there exists a positive scalar function B such that

$$\partial_x G(W) \cdot \partial_x W = \partial_x(-BW_2) \cdot \partial_x W_2 = -(\partial_x BW_2) \cdot \partial_x W_2 - (B\partial_x W_2) \cdot \partial_x W_2.$$

Substituting this equality in the last system, we obtain:

$$\frac{1}{2}\frac{d}{dt}\int (A_0 \partial_x W) \cdot \partial_x W dx \;+\; \int (B\partial_x W_2) \cdot \partial_x W_2 dx = \frac{1}{2}\int (\partial_t A_0 \partial_x W) \cdot \partial_x W dx$$
$$-\int (\partial_x A_0 \partial_t W) \cdot \partial_x W dx - \frac{1}{2}\int (\partial_x A_1 \partial_x W) \cdot \partial_x W dx \qquad (3.24)$$
$$-\int (\partial_x BW_2) \cdot \partial_x W_2 dx + \int \partial_x H(W, \partial_x\phi) \cdot \partial_x W dx.$$

Now, to estimate the right hand side of the previous inequality, we proceed along the lines of [73] and we rewrite the first equations of system (3.15) in the form

$$\partial_t W = -A\partial_x W - A_0^{-1}\begin{pmatrix} 0 \\ BW_2 \end{pmatrix} + A_0^{-1} H(W, \partial_x\phi),$$

where $A = A_0^{-1} A_1 = (f')^t(\Phi(W))$. Then

$$\partial_t A_0 = A_0' \partial_t W = -A_0'\left(A\partial_x W + A_0^{-1}\begin{pmatrix} 0 \\ BW_2 \end{pmatrix} - A_0^{-1} H(W, \partial_x\phi)\right).$$

We consider the following terms which will be useful in the estimate of (3.24).

$$
\begin{aligned}
I_1 \;:=\; & \frac{1}{2}[\partial_t A_0 \partial_x W + \partial_x A_1 \partial_x W] \cdot \partial_x W \\
=\; & \left\{\frac{1}{2}\left[A_1' \partial_x W - A_0'(A\partial_x W)\right] - \frac{1}{2} A_0'\left(A_0^{-1}\begin{pmatrix} 0 \\ BW_2 \end{pmatrix} - A_0^{-1} H(W, \partial_x\phi)\right)\right\}\partial_x W \cdot \partial_x W \\
=\; & \left\{\frac{1}{2}\left[(A_0' \partial_x W)A - A_0'(A\partial_x W) + A_0(A' \partial_x W)\right]\right. \\
& \left. - \frac{1}{2} A_0'\left(A_0^{-1}\begin{pmatrix} 0 \\ BW_2 \end{pmatrix} - A_0^{-1} H(W, \partial_x\phi)\right)\right\}\partial_x W \cdot \partial_x W \\
=\; & \left\{\frac{1}{2}\left[A_0(A' \partial_x W)\right] - \frac{1}{2} A_0'\left(A_0^{-1}\begin{pmatrix} 0 \\ BW_2 \end{pmatrix} - A_0^{-1} H(W, \partial_x\phi)\right)\right\}\partial_x W \cdot \partial_x W,
\end{aligned}
$$

and

$$
\begin{aligned}
I_2 \;:=\; & [\partial_x A_0 \partial_t W + \partial_x A_1 \partial_x W] \cdot \partial_x W \\
=\; & \left\{\left[(A_0 A)' \partial_x W - (A_0' \partial_x W)A\right]\partial_x W - (A_0' \partial_x W)\left(A_0^{-1}\begin{pmatrix} 0 \\ BW_2 \end{pmatrix} - A_0^{-1} H(W, \partial_x\phi)\right)\right\}\partial_x W \\
=\; & \left\{A_0(A' \partial_x W)\partial_x W - (A_0' \partial_x W)\left(A_0^{-1}\begin{pmatrix} 0 \\ BW_2 \end{pmatrix} - A_0^{-1} H(W, \partial_x\phi)\right)\right\} \cdot \partial_x W.
\end{aligned}
$$

Reporting $I_1 - I_2$ in (3.24) yields

$$\frac{1}{2}\frac{d}{dt}\int (A_0 \partial_x W) \cdot \partial_x W dx + \int (B\partial_x W_2) \cdot \partial_x W_2 dx = -\frac{1}{2}\int [A_0(A' \partial_x W)\partial_x W] \cdot \partial_x W dx$$

$$-\int \left\{ \frac{1}{2} A'_0 (A_0^{-1} \begin{pmatrix} 0 \\ BW_2 \end{pmatrix} \partial_x W \cdot \partial_x W + (B' \partial_x W) W_2 \cdot \partial_x W_2 \right\} dx$$

$$+\int (A'_0 \partial_x W) A_0^{-1} H(W, \partial_x \phi) \cdot \partial_x W dx + \frac{1}{2} \int (A'_0 A_0^{-1} H(W, \partial_x)) \partial_x W \cdot \partial_x W dx$$

$$+\int (A'_0 \partial_x W) A_0^{-1} \begin{pmatrix} 0 \\ BW_2 \end{pmatrix} \cdot \partial_x W dx + \int \partial_x H(W, \partial_x \phi) \cdot \partial_x W dx.$$

Let us observe that the first term on the right hand side is cubic in $\partial_x W$. It vanishes when the matrix $A_0(W) A'(W)$ is skew-symmetric. The other terms are quadratic namely they can be written in the form

$$\int \eta(W)(\partial_x W, \partial_x W) W_2.$$

Then, integrating with respect to time variable, we obtain

$$c_1 \int |\partial_x W(t)|^2 dx + c_2 \int_0^t\!\!\int |\partial_x W_2|^2 dx ds \quad \leq \quad \int |\partial_x W_0|^2 dx + C(\|\phi_0\|_{H^2}^2) N_2^3(t) + C(\|\phi_0\|_{H^2}^2, \bar\rho) N_1^3(t)$$

$$+ \quad \int_0^t\!\!\int \partial_x H(W, \partial_x \phi) \cdot \partial_x W dx ds. \tag{3.25}$$

Let us focus on the last integral. Thanks to the definition of the function H, we have $\partial_x H(W, \partial_x \phi) = [0, \mu \partial_{xx} \phi \rho + \mu \partial_x \rho \partial_x \phi + \mu \bar\rho \partial_{xx} \phi]^t$, therefore the last integrand is equal to

$$\partial_x H(W, \partial_x \phi) \cdot \partial_x W = \mu \partial_{xx} \phi \rho \partial_x W_2 + \mu \partial_x \rho \partial_x \phi \partial_x W_2 + \mu \bar\rho \partial_{xx} \phi \partial_x W_2.$$

Using the energy estimates (3.20), (3.21) for the function ϕ, yields

$$\int_0^t \int |\mu \partial_{xx} \phi \rho \partial_x W_2 + \mu \partial_x \rho \partial_x \phi \partial_x W_2 + \mu \bar\rho \partial_{xx} \phi \partial_x W_2| dx ds$$

$$\leq C \int_0^t \left(\|\partial_{xx} \phi(s)\|_{L^2} \|\partial_x W_2(s)\|_{L^2} \|\rho(s)\|_{L^\infty} + \|\partial_x \phi(s)\|_{L^2} \|\partial_x \rho(s)\|_{L^\infty} \|\partial_x W_2(s)\|_{L^2} ds \right.$$

$$+\mu \bar\rho \|\partial_{xx} \phi(s)\|_{L^2} \|\partial_x W_2(s)\|_{L^2} \big) ds$$

$$\leq C \sup_{s \in (0,t)} \|\rho(s)\|_{L^\infty} \int_0^t \left(\|\partial_x W_2(s)\|_{L^2}^2 + \|\partial_{xx} \phi(s)\|_{L^2}^2 \right) ds$$

$$+C \sup_{s \in (0,t)} \|\partial_x \rho(s)\|_{L^\infty} \int_0^t \left(\|\partial_x W_2(s)\|_{L^2}^2 + \|\partial_x \phi(s)\|_{L^2}^2 \right) ds$$

$$+C \mu \bar\rho \int_0^t \left(\|\partial_x W_2(s)\|_{L^2}^2 + \|\partial_{xx} \phi(s)\|_{L^2}^2 \right) ds$$

$$\leq C N_1(t) \left(N_1^2(t) + \|\phi_0\|_{H^1}^2 + N_1^2(t) \right) + C N_2(t) \left(N_1^2(t) + \|\phi_0\|_{H^1}^2 + N_1^2(t) \right)$$

$$+C \mu \bar\rho \left(N_1^2(t) + \|\phi_0\|_{H^1}^2 + N_1^2(t) \right).$$

Substituting this calculation in (3.25), we obtain the first order estimate:

$$\|\partial_x W(t)\|_{L^2}^2 + \int_0^t \|\partial_x W_2(s)\|_{L^2}^2 \quad \leq \quad N_1^2(0) + C(\|\phi_0\|_{H^1}^2) N_1(t) + C(\|\phi_0\|_{H^2}^2) N_2^3(t)$$

$$+ \quad C(\|\phi_0\|_{H^1}^2) N_2(t) + C(\bar\rho, \|\phi_0\|_{H^2}^2) N_1(t)^2 + C(\bar\rho, \|\phi_0\|_{H^1}^2),$$

that is

$$\|\partial_x W(t)\|_{L^2}^2 + \int_0^t \|\partial_x W_2(s)\|_{L^2}^2 ds \quad \leq \quad N_1^2(0) + C(\|\phi_0\|_{H^1}^2) N_2(t) + C(\bar\rho) N_1^2$$

$$+ \quad C N_2^3(t) + C(\bar\rho, \|\phi_0\|_{H^1}^2). \tag{3.26}$$

Second Order Energy Estimate for W

Now, we are interested in proving the validity of a second order estimate of W, in the L^2-norm. As done in the previous case, we perform the second space derivative of system (3.14) and take the inner product with $\partial_{xx}W$, which gives

$$\partial_{xx}(A_0\partial_t W)\cdot\partial_{xx}W + \partial_{xx}(A_1\partial_x W)\cdot\partial_{xx}W = \partial_{xx}G(W)\cdot\partial_{xx}W + \partial_{xx}H(W,\partial_x\phi)\cdot\partial_{xx}W.$$

Thanks to the symmetry of matrices A_0 and A_1, we deduce that

$$\partial_{xx}(A_0\partial_t W)\cdot\partial_{xx}W = \frac{1}{2}\partial_t\left((A_0\partial_{xx}W)\cdot\partial_{xx}W\right) - \frac{1}{2}(\partial_t A_0\partial_{xx}W)\cdot\partial_{xx}W$$
$$+ 2(\partial_x A_0\partial_{xt}W)\cdot\partial_{xx}W + (\partial_{xx}A_0\partial_t W)\cdot\partial_{xx}W,$$

$$\partial_{xx}(A_1\partial_x W)\cdot\partial_{xx}W = \frac{1}{2}\partial_x((A_1(W)\partial_{xx}W)\cdot\partial_{xx}W) + \frac{3}{2}(\partial_x A_1\partial_{xx}W)\cdot\partial_{xx}W$$
$$+ (\partial_{xx}A_1\partial_x W)\cdot\partial_{xx}W.$$

Moreover, as seen before, there exists a positive definite matrix B such that $G(W)\cdot W = -BW_2\cdot W_2$. Then, substituting these relations in the previous system and integrate it over $\mathbb{R}$, we obtain

$$\frac{1}{2}\frac{d}{dt}\int(A_0\partial_{xx}W)\cdot\partial_{xx}Wdx + \int(B\partial_{xx}W_2)\cdot\partial_{xx}W_2dx$$
$$= \int\left[\frac{1}{2}\partial_t A_0\partial_{xx}W - 2\partial_x A_0\partial_{xt}W - \partial_{xx}A_0\partial_t W\right]\cdot\partial_{xx}Wdx$$
$$- \int\left[\frac{3}{2}\partial_x A_1\partial_{xx}W + \partial_{xx}A_1\partial_x W\right]\cdot\partial_{xx}Wdx$$
$$- \int[2\partial_x B\partial_x W_2 + \partial_{xx}BW_2]\cdot\partial_{xx}W_2dx + \partial_{xx}H(W,\partial_x\phi)\cdot\partial_{xx}Wdx. \qquad (3.27)$$

To estimate the first terms on the right-hand side of the equation, we proceed along the lines of [73]. As previously, we are going to develop some terms which will be useful for estimate (3.27). By using again (3.23), we have

$$J_1 := (\partial_t A_0 + \partial_x A_1)\partial_{xx}W\cdot\partial_{xx}W$$
$$= \left[A_1'\partial_x W - A_0'A\partial_x W - A_0'A_0^{-1}\begin{pmatrix}0\\BW_2\end{pmatrix}\right]\partial_{xx}W\cdot\partial_{xx}W$$
$$= \left[A_0'\partial_x WA - A_0'A\partial_x W + A_0 A'\partial_x W - A_0'A_0^{-1}\begin{pmatrix}0\\BW_2\end{pmatrix} + A_0'A_0^{-1}H(W,\partial_x\phi)\right]\partial_{xx}W\cdot\partial_{xx}W.$$

By taking the x derivative of (3.23), we obtain also:

$$J_2 := (\partial_x A_0\partial_{xt}W + \partial_x A_1\partial_{xx}W)\cdot\partial_{xx}W$$
$$= -\left\{(A_0'\partial_x W)\left[(A'\partial_x W)\partial_x W + A\partial_{xx}W + \partial_x\left(A_0^{-1}\begin{pmatrix}0\\BW_2\end{pmatrix}\right)\right] - \partial_x(A_0^{-1}H(W,\phi))\right\}\cdot\partial_{xx}W$$
$$+ (\partial_x A_1\partial_{xx}W)\cdot\partial_{xx}W$$
$$= -\left[(A_0'\partial_x W)(A'\partial_x W)\partial_x W - A_0(A'\partial_x W)\partial_{xx}W + \partial_x(A_0'\partial_x W)\left(A_0^{-1}\begin{pmatrix}0\\BW_2\end{pmatrix}\right)\right]\cdot\partial_{xx}W$$
$$- (A_0'\partial_x W)\partial_x(A_0^{-1}H(W,\phi))\cdot\partial_{xx}W.$$

In a straightforward way we have also

$$J_3 := (\partial_{xx}A_0\partial_t W + \partial_{xx}A_1\partial_x W)\cdot\partial_{xx}W$$

$$
\begin{aligned}
= \quad & \left[2(A_0'\partial_x W)(A'\partial_x W)\partial_x W + A_0 A''(\partial_x W,\partial_x W)\partial_x W + A_0(A'\partial_{xx}W)\partial_x W\right]\cdot\partial_{xx}W \\
- \quad & \left[(A_0''(\partial_x W,\partial_x W) + A_0'\partial_{xx}W)A_0^{-1}\begin{pmatrix}0\\BW_2\end{pmatrix}\right]\cdot\partial_{xx}W \\
+ \quad & \left[(A_0''(\partial_x W\partial_x W) + A_0'\partial_{xx}W)A_0^{-1}H(W,\partial_x\phi)\right]\cdot\partial_{xx}W.
\end{aligned}
$$

Reporting $\frac{1}{2}J_1 - 2J_2 - J_3$ in (3.27) gets

$$
\begin{aligned}
\frac{1}{2}\frac{d}{dt}\int (A_0\partial_{xx}W)\cdot\partial_{xx}W\,dx + &\int (B\partial_{xx}W_2)\cdot\partial_{xx}W_2\,dx \\
= \; & \frac{1}{2}\int\left[A_0'\partial_x WA - A_0'(A\partial_x W)\right]\partial_{xx}W\cdot\partial_{xx}W\,dx \\
& - \int\left[A_0 A''(\partial_x W,\partial_x W)\partial_x W + A_0(A'\partial_{xx}W)\partial_x W + \frac{3}{2}A_0(A'\partial_x W)\partial_{xx}W\right]\cdot\partial_x W\,dx \\
& + \int\left[(A_0''(\partial_x W,\partial_x W) + A_0'\partial_{xx}W)A_0^{-1}\begin{pmatrix}0\\BW_2\end{pmatrix}\right]\cdot\partial_{xx}W\,dx \\
& - \int\left[\frac{1}{2}A_0'A_0^{-1}\begin{pmatrix}0\\BW_2\end{pmatrix}\partial_{xx}W - 2A_0'\partial_x W\partial_x\left(A_0^{-1}\begin{pmatrix}0\\BW_2\end{pmatrix}\right)\right]\partial_{xx}W\,dx \\
& + \frac{1}{2}\int[A_0'A_0^{-1}H(W,\partial_x\phi) - 2A_0'\partial_x W\partial_x A_0^{-1}H(W,\partial_x\phi)]\cdot\partial_x W\,dx \\
& + \int[A_0'\partial_{xx}WA_0^{-1}H(W,\partial_x\phi) - A_0''(\partial_x W,\partial_x W)]\cdot\partial_{xx}W\,dx \\
& - \int(2\partial_x B\partial_x W + \partial_{xx}BW_2)\cdot\partial_{xx}W_2 + \int\partial_{xx}H(W,\partial_x\phi)\cdot\partial_{xx}W\,dx.
\end{aligned}
$$

The right hand side of the previous inequality, with the exception of the last term, can be estimate following the technique used by Hanouzet and Natalini in [73].

Let us now focus our attention on the last integral of the previous inequality and we integrate with respect to time, i.e.

$$
\int_0^t\int \partial_{xx}H(W,\partial_x\phi)\cdot\partial_{xx}W\,dx\,ds,
$$

where $\partial_{xx}H(W) = [0, \mu(\partial_{xxx}\phi\rho + 2\phi_{xx}\partial_x\rho + \partial_x\phi\partial_{xx}\rho + \bar\rho\partial_{xxx}\phi)]^t$.

Proceeding along the line of the first order estimate, we get, using (3.20), (3.21),

$$
\begin{aligned}
\int_0^t\int \partial_{xx}H(W,\partial_x\phi)\cdot\partial_{xx}W\,dx\,ds &= \int_0^t\int \mu(\partial_{xxx}\phi\rho + 2\partial_{xx}\phi\partial_x\rho + \partial_x\phi\partial_{xx}\rho + \bar\rho\partial_{xxx}\phi)\partial_x W_2\,dx\,ds \\
&\leq C\sup\|\rho(s)\|_{L^\infty}\int_0^t\left(\|\partial_{xxx}\phi(s)\|_{L^2}^2 + \|\partial_{xx}W_2(s)\|_{L^2}^2\right)ds \\
&\quad + C\sup\|\partial_x\rho(s)\|_{L^\infty}\int_0^t\left(\|\partial_{xx}\phi(s)\|_{L^2}^2 + \|\partial_{xx}W_2(s)\|_{L^2}^2\right)ds \\
&\quad + C\sup\|\partial_x\phi(s)\|_{L^\infty}\int_0^t\left(\|\partial_{xx}\rho(s)\|_{L^2}^2 + \|\partial_{xx}W_2(s)\|_{L^2}^2\right)ds \\
&\quad + \mu\bar\rho\int_0^t\left(\|\partial_{xxx}\phi(s)\|_{L^2}^2 + \|\partial_{xx}W_2(s)\|_{L^2}^2\right)ds \\
&\leq CN_1(t)\left(\|\phi_0\|_{H^2}^2 + N_2^2(t)\right) + CN_2(t)\left(\|\phi_0\|_{H^1}^2 + N_2^2(t)\right) \\
&\quad + CN_2^2(t)\left(\|\phi_0\|_{H^2}^2 + N_2^2(t)\right) + C\bar\rho\left(\|\phi_0\|_{H^2}^2 + N_2^2(t)\right) \\
&\leq C(\|\phi_0\|_{H^2}^2)N_2(t) + CN_2^3(t) + C(\bar\rho,\|\phi_0\|_{H^2}^2)N_2^2(t) + C(\bar\rho,\|\phi_0\|_{H^2}^2).
\end{aligned}
$$

Substituting this inequality in (3.27) and following the proof in [73], we obtain the second order estimate:

$$\|\partial_{xx} W(t)\|_{L^2}^2 + \int_0^t \|\partial_{xx} W_2(s)\|_{L^2}^2 \, ds \le N_2^2(0) + C_2 N_2^3(t) + C(\|\phi_0\|_{H^2}^2) N_1(t) + C(\|\phi_0\|_{H^1}^2) N_2(t)$$
$$+ C(\|\phi_0\|_{H^2}) N_2^2(t) + C(\bar{\rho}, \|\phi_0\|_{H^2}^2) + C(\bar{\rho}) N_2^2(t),$$

that is

$$\|\partial_{xx} W(t)\|_{L^2}^2 + \int_0^t \|\partial_{xx} W_2(s)\|_{L^2}^2 \, ds \le N_2^2(0) + C(\|\phi_0\|_{H^2}^2) N_2(t) + C(\bar{\rho}, \|\phi_0\|_{H^2}^2) N_2^2(t)$$
$$+ C_2 N_2^3(t) + C(\bar{\rho}, \|\phi_0\|_{H^2}^2).$$

Let us observe that, even if in the previous inequality there is the third derivative of function ϕ, we have been able to estimate all the terms by the second order functional N_2 thanks to the energy estimates (3.20), (3.21).

3.2.2   Proof of the Global Existence Result

Now, we are finally able to prove the existence of a global smooth solution for system (3.12), that is the above stated Theorem 3.2.4.

Proof. Let us recall the definition of the functionals

$$N_l^2(t) := \sup_{0 \le s \le t} \|W(s)\|_{H^l}^2 + \int_0^t \|W_2(s)\|_{H^l}^2 \, ds + \int_0^t \|\partial_x W(s)\|_{H^{l-1}}^2 \, ds, \quad \text{for } l = 1, 2,$$

$$N_0^2(t) := \sup_{0 \le s \le t} \|W(s)\|_{L^2}^2 + \int_0^t \|W_2(s)\|_{L^2}^2 \, ds,$$

and the energy estimates, obtained in the previous sections:

$$\|W(t)\|_{L^2} + \int_0^t \|W_2(s)\|_{L^2}^2 \, ds \le N_0^2(0) + C(\|\phi_0\|_{H^1}^2) N_1(t) + C N_1^2(t) + C N_1^3(t) + C(\|\phi_0\|_{H^1}^2 \bar{\rho}), \quad (3.28)$$

$$\|\partial_x W(t)\|_{L^2}^2 + \int_0^t \|\partial_x W_2(s)\|_{L^2}^2 \, ds \le N_1^2(0) + C(\|\phi_0\|_{H^1}^2) N_2(t) + C(\bar{\rho}) N_1^2 + C N_2^3(t) + C(\bar{\rho}, \|\phi_0\|_{H^1}^2),$$
$$(3.29)$$

and

$$\|\partial_{xx} W(t)\|_{L^2}^2 + \int_0^t \|\partial_{xx} W_2(s)\|_{L^2}^2 \, ds \le N_2^2(0) + C(\|\phi_0\|_{H^2}^2) N_2(t) + C(\bar{\rho}, \|\phi_0\|_{H^2}^2) N_2^2(t) \qquad (3.30)$$
$$+ C_2(\|\phi_0\|_{H^2}) N_2^3(t) + C(\bar{\rho}, \|\phi_0\|_{H^2}^2).$$

Therefore, to obtain an estimate of the functional $N_l^2(t)$, we need to study also the term

$$\int_0^t \|\partial_x W(s)\|_{H^{l-1}}^2 \, ds, \quad \text{for } l = 1, 2.$$

It is here that we have to use the condition (SK). To this end, we rewrite system (3.14), as a linear hyperbolic system with a source term which depends on W and ϕ,

$$A_0(0)\partial_t W + A_1(0)\partial_x W = L(W, \partial_x W) + \tilde{H}(W, \partial_x \phi), \qquad (3.31)$$

where

$$L(W, \partial_x W) := \left[(A_1(0) - A_1(W)) - (A_0(0) - A_0(W)) A_0^{-1}(W) A_1(W) \right] \partial_x W$$
$$- \left[A_0(0) A_0^{-1}(W) \right] \begin{pmatrix} 0 \\ BW_2 \end{pmatrix},$$

$$\tilde{H}(W, \partial_x \phi) := \left[A_0(0) A_0^{-1}(W) \right] H(W, \partial_x \phi).$$

Let us recall that, in Section 3.1.2, we proved that system (3.14) (without the source term $H(W, \partial_x \phi)$) satisfies the condition (SK). As shown by Shizuta and Kawashima [153], and reported in Lemma 3.1.3 this means that there exists a constant matrix K such that

- $KA_0(0)$ is skew-symmetric;

- the matrix

$$\frac{1}{2} (KA_1(0) + (KA_1(0))^t) + \frac{1}{2} \begin{pmatrix} 0 & 0 \\ 0 & B(0) + B(0)^t \end{pmatrix}$$

  is positive definite.

Now, we apply the matrix K to our system and take the scalar product with $\partial_x W$. Then, integrating over $(0, t) \times \mathbb{R}$ yields

$$\int_0^t \int K [A_0(0) \partial_t W + A_1(0) \partial_x W] \cdot \partial_x W \, dx \, ds = \int_0^t \int K L(W, \partial_x W) \cdot \partial_x W \, dx \, ds$$
$$+ \int_0^t \int K \tilde{H}(W, \partial_x \phi) \cdot \partial_x W \, dx \, ds. \qquad (3.32)$$

First we have, by integrating by parts

$$\int_0^t \int K [A_0(0) \partial_t W] \cdot \partial_x W \, dx \, ds = - \int_0^t \int (KA_0(0) \partial_{tx} W) \cdot W \, dx \, ds$$
$$= - \int (KA_0(0) \partial_x W) \cdot W \, dx \Big|_0^t + \int_0^t \int (KA_0(0) \partial_x W) \cdot \partial_t W \, dx \, ds$$
$$= - \int (KA_0(0) \partial_x W) \cdot W \, dx \Big|_0^t - \int_0^t \int (KA_0(0) \partial_t W) \cdot \partial_x W \, dx \, ds,$$

thanks to the skew-symmetry of $KA_0(0)$. Then, there exists a positive constant C_1 such that

$$\int_0^t \int K [A_0(0) \partial_t W] \cdot \partial_x W \, dx \, ds = -\frac{1}{2} \int (KA_0(0) \partial_x W) \cdot W \, dx \mid_0^t, \qquad (3.33)$$
$$\geq -C_1 (\|W(t)\|_{H_1}^2 + \|W(0)\|_{H_1}^2).$$

Now we estimate the next term. We get

$$\int_0^t \int (KA_1(0) \partial_x W) \cdot \partial_x W \, dx \, ds = \frac{1}{2} \int_0^t \int \left[(KA_1(0) + (KA_1(0))^t) \partial_x W \right] \cdot \partial_x W \, dx \, ds$$
$$= \int_0^t \int \left[\left(\frac{1}{2} (KA_1(0) + (KA_1(0))^t) + \begin{pmatrix} 0 & 0 \\ 0 & S \end{pmatrix} \right) \partial_x W \right] \cdot \partial_x W \, dx \, ds$$
$$- \int_0^t \int (SW_2) \cdot \partial_x W_2 \, dx \, ds,$$

where S is the symmetric positive matrix $\frac{1}{2}(B(0) + B(0)^t)$, Then

$$\int_0^t \int (KA_1(0)\partial_x W) \cdot \partial_x W dx ds \geq C_2 \int_0^t \|\partial_x W\|_{L^2}^2 ds - C_3 \int_0^t \|W_2\|_{H^1}^2 ds,$$

for two positive constants C_2 and C_3. To estimate the right-hand side of (3.32), we consider the following relations

$$|KL(W, \partial_x W) \cdot \partial_x W| \leq C_1(\epsilon) \left(|W_2| + |W||\partial_x W|\right) |\partial_x W|, \tag{3.34}$$

$$\left|K\tilde{H}(W, \partial_x \phi) \cdot \partial_x W\right| \leq C_2(\epsilon) \left|H(W, \partial_x \phi)\right| |\partial_x W|. \tag{3.35}$$

Let us observe that

$$\int_0^t \int |W_2| |\partial_x W| \, dx ds \leq \nu \int_0^t \|\partial_x W(s)\|_{L^2}^2 \, ds + \frac{1}{4\nu} \int_0^t \|W_2(s)\|_{L^2}^2 \, ds,$$

where ν is an arbitrary small constant, and

$$\int_0^t \int |W| |\partial_x W|^2 \, dx ds \leq \|W(t)\|_{L^\infty} \int_0^t \|\partial_x W(s)\|_{L^2}^2 \, ds.$$

Hence, using (3.34) we obtain

$$
\begin{aligned}
\left|\int_0^t \int KL(W, \partial_x W) \cdot \partial_x W dx ds\right| \quad \leq \quad & \frac{1}{2} C_2 \int_0^t \|\partial_x W(s)\|_{L^2}^2 + C_4 \int_0^t \|W_2(s)\|_{L^2}^2 \, ds \\
& + \quad C_5 \|W(t)\|_{L^\infty} \int \|\partial_x W(s)\|_{L^2}^2 \, ds.
\end{aligned}
$$

Let us focus now on the last integral of the right-hand side of (3.32). First of all we recall that $H(W, \partial_x \phi) = (0, \mu\rho + \bar{\rho}\partial_x \phi)$, then starting from inequality (3.35) and taking into account the energy estimates for the function ϕ (see Section 3.2.1), we obtain:

$$
\begin{aligned}
\int_0^t \int \mu K\tilde{H}(W, \partial_x \phi) \cdot \partial_x W dx ds \quad \leq \quad & \mu \int_0^t C \|\partial_x W(s)\|_{L^2} \|\partial_x \phi(s)\|_{L^2} \|\rho(s)\|_{L^\infty} ds dx \\
& + \quad \mu \int_0^t C\bar{\rho} \|\partial_x W(s)\|_{L^2} \|\partial_x \phi(s)\|_{L^2} ds dx \\
& \leq \quad C \sup_{s \in (0,t)} \|\rho(s)\|_{L^\infty} \int_0^t \left(\|\partial_x W(s)\|_{L^2}^2 + \|\partial_x \phi(s)\|_{L^2}^2\right) ds \\
& + \quad C\bar{\rho} \int_0^t \left(\|\partial_x W(s)\|_{L^2}^2 + \|\partial_x \phi(s)\|_{L^2}^2\right) ds \\
& \leq \quad CN_1(t) \left(\|\phi_0\|_{H^1}^2 + N_1^2(t)\right) + C(\bar{\rho}) \left(\|\phi_0\|_{H^1}^2 + N_1^2(t)\right) \\
& \leq \quad C \left(\|\phi_0\|_{H^1}^2\right) N_1(t) + C(\bar{\rho}) N_1^2(t) + CN_1^3(t) + C\left(\bar{\rho}, \|\phi_0\|_{H^1}^2\right).
\end{aligned}
$$

Then, substituting these calculations in (3.32) and following again the proof in [HN], we get

$$\int_0^t \|\partial_x W(s)\|_{L^2}^2 ds \leq CN_1^2(0) + C(\|\phi_0\|_{H^1}^2) N_1(t) + C(\bar{\rho}) N_1^2(t) + CN_1^3(t) + C(\bar{\rho}, \|\phi_0\|_{H^1}^2). \tag{3.36}$$

Finally we need to estimate the term

$$\int_0^t \|W_{xx}(s)\|_{L^2} ds.$$

First we take the $x-$derivative of equation (3.31), and the scalar product with $\partial_{xx}W$

$$\int_0^t \int K\left[A_0(0)\partial_{tx}W + A_1(0)\partial_{xx}W\right]\cdot\partial_{xx}W dx ds = \int_0^t \int K\partial_x L\cdot\partial_{xx}W dx ds + \int_0^t \int K\partial_x\tilde{H}\cdot\partial_{xx}W dx ds.$$

By arguing as in the previous case, we easily obtain:

$$\int_0^t \|\partial_{xx}W(s)\|_{L^2}^2 ds \le CN_2^2(0) + C(\|\phi_0\|_{H^1}^2)N_2(t) + C(\bar{\rho})N_2^2(t) + C(\|\phi_0\|_{H^2}^2)N_2^3(t) + C(\bar{\rho}, \|\phi_0\|_{H^2}^2).$$

(3.37)

Now, let us sum up the inequalities (3.28), (3.29), (3.30), (3.36) and (3.37) to get

$$N_2^2(t) \quad \le \quad bN_2^2(0) + b_1 N_2(t) + b_2 N_2^2(t) + b_3 N_2^3(t) + b_4,$$

where the constants b_i depend on $\bar{\rho}$ and $\|\phi_0\|_{H^2}$, for $i = 1,\dots,4$.

Choosing small initial data and small constant state, that is C sufficient small, by using standard arguments we can prove the inequality (3.18). □

Remark 3.2.5. *Theorem 3.2.4 ensures that for $\phi_0 \in H^2(\mathbb{R})$ then there exists $\phi \in C([0,\infty), H^2(\mathbb{R}))$ solution to the parabolic equation of the system* (3.15). *Let us notice that it always possible to write this solution by the Duhamel formula*

$$\phi(x,t) = (e^{-\frac{t}{\tau}}\Gamma^p(t) * \phi_0)(x) + \int_0^t e^{-\frac{(t-s)}{\tau}}\Gamma^p(t-s) * a\rho(s) ds,$$

where

$$\Gamma^p(x,t) := \frac{e^{-\frac{x^2}{4Dt}}}{2\sqrt{\pi Dt}}.$$

As observed before, if we consider an initial datum $\phi_0 \in H^3(\mathbb{R})$, we get a local solution $\phi(t) \in C([0,T], H^3(\mathbb{R}))$ for $t \in (0,T)$. Moreover we have

$$\begin{aligned}
\|\phi(t)\|_{H^3} &= \|(e^{-\frac{t}{\tau}}\Gamma^p(t) * \phi_0)\|_{H^3} + \int_0^t \|e^{-\frac{(t-s)}{\tau}}\Gamma^p(t-s) * a\rho(s)\|_{H^3} ds \\
&\le e^{-\frac{t}{\tau}}\|\Gamma^p(t)\|_{L^1}\|\phi_0\|_{H^3} + \int_0^t e^{-\frac{(t-s)}{\tau}}\|\Gamma^p(t-s) * a\rho(s)\|_{H^3} ds \\
&\le e^{-\frac{t}{\tau}}C\|\phi_0\|_{H^3} + \int_0^t e^{-\frac{(t-s)}{\tau}}\|\Gamma^p(t-s) * a\rho(s)\|_{L^2} ds \\
&+ \int_0^t \sum_{|\alpha=3|} e^{-\frac{(t-s)}{\tau}}\|D_x^\alpha\Gamma^p(t-s) * a\rho(s)\|_{L^2} ds \\
&\le e^{-\frac{t}{\tau}}C\|\phi_0\|_{H^3} + \int_0^t Ce^{-\frac{(t-s)}{\tau}}\|a\rho(s)\|_{L^2} ds \\
&+ \int_0^t e^{-\frac{(t-s)}{\tau}}\|\partial_x\Gamma^p(t-s)\|_{L^1}\|a\rho(s)\|_{H^2} ds \\
&\le e^{-\frac{t}{\tau}}C\|\phi_0\|_{H^3} + \int_0^t e^{-\frac{(t-s)}{\tau}}(t-s)^{-\frac{1}{2}}\|a\rho(s)\|_{H^2} ds + \int_0^t Ce^{-\frac{(t-s)}{\tau}}\|a\rho(s)\|_{L^2} ds \\
&\le e^{-\frac{t}{\tau}}C\|\phi_0\|_{H^3} + C_1\int_0^t e^{-\frac{(t-s)}{\tau}}(t-s)^{-\frac{1}{2}} + C_1\int_0^t e^{-\frac{(t-s)}{\tau}} ds,
\end{aligned}$$

where $C_1 = \sup_{s\in(0,t)} \|\rho(s)\|_{H^2}$.
Which yields

$$\|\phi(t)\|_{H^3} \le C(e^{-\frac{t}{\tau}}\|\phi_0\|_{H^3} + C_1). \tag{3.38}$$

In conclusion, if the initial datum $\phi_0 \in H^3(\mathbb{R})$, even the global solution $\phi(t) \in C([0,\infty), H^3(\mathbb{R}))$.

Remark 3.2.6. *Let us observe that, considering initial data in $H^s(\mathbb{R}) \times H^{s+1}(\mathbb{R})$, Theorem 3.2.3 ensures the local existence of solution $(W, \phi)(t)$ in $C([0, T], H^s(\mathbb{R})) \times C([0, T], H^{s+1}(\mathbb{R})). Thanks to Theorem 3.2.4 we obtain the existence of global solution to this system in $C([0, T], H^2(\mathbb{R})) \times C([0, T], H^3(\mathbb{R}))$ when the initial data (W_0, ϕ_0) are in $H^2(\mathbb{R}) \times H^3(\mathbb{R})$.*
Then, following the approach of Majda (Theorem 2.2 in [107]), it is possible to prove the global existence of solutions in $C([0, \infty), H^s(\mathbb{R})) \times C([0, \infty), H^{s+1}(\mathbb{R}))$ taking initial data in $(W_0, \phi_0) \in H^s(\mathbb{R}) \times H^{s+1}(\mathbb{R})$.

3.3 Asymptotic Behavior

In this section we study the time decay properties of the global smooth solution to system (3.12), proceeding along the lines of [17].
By means of the decomposition of the Green function of the linearized problem, we aim to obtain the H^s and L^∞ decay estimates of solutions of the model.
To this end we rewrite system (3.12) in the Conservative-Dissipative form (Definition 2.1.3) as

$$\partial_t(U + \overline{U}) + \partial_x f(U + \overline{U}) = g(U) + h(U + \overline{U}, \partial_x \phi), \tag{3.39}$$

where

$$U = \begin{pmatrix} \rho \\ \frac{v}{\sqrt{P'(\bar{\rho})}} \end{pmatrix}, \quad \overline{U} = \begin{pmatrix} \bar{\rho} \\ 0 \end{pmatrix}, \quad f(U + \bar{U}) = \begin{pmatrix} \sqrt{P'(\bar{\rho})}\, v \\ \sqrt{P'(\bar{\rho})}\frac{v^2}{(\rho + \bar{\rho})} + \frac{P(\rho + \bar{\rho})}{\sqrt{P'(\bar{\rho})}} \end{pmatrix},$$

$$g(U) = \begin{pmatrix} 0 \\ -\alpha u \end{pmatrix}, \quad h(U + \overline{U}, \partial_x \phi) = \begin{pmatrix} 0 \\ \mu \frac{(\rho + \bar{\rho})}{\sqrt{P'(\bar{\rho})}} \partial_x \phi \end{pmatrix}.$$

Defined $\bar{f}(U) = f(U + \overline{U}) - f(\overline{U})$, and $\bar{\mu} = \frac{\mu}{\sqrt{P'(\bar{\rho})}}$ the system can be rewritten in the following way

$$\partial_t U + \bar{f}'(\overline{U}) \partial_x U = g(U) + \partial_x \left(\bar{f}'(\overline{U}) U - \bar{f}(U) \right) + h(U + \overline{U}, \partial_x \phi), \tag{3.40}$$

and its solution is given by

$$U(t) = \Gamma^h(t) * U_0 + \int_0^t \partial_x \Gamma^h(t - s) * \left[\bar{f}'(\overline{U}) U(s) - \bar{f}(U(s)) \right] ds + \int_0^t \Gamma^h(t - s) * h(U + \bar{U}, \partial_x \phi) ds, \tag{3.41}$$

where Γ^h denotes the Green function of the linearized system

$$\partial_t U + \bar{f}'(\overline{U}) \partial_x U = g(U).$$

We will use the estimates due to Bianchini, Hanouzet and Natalini [17], also reported in the previous chapter (Theorem 2.1.4). Let us recall the main estimates that will be useful to get our results.
For a linear dissipative system in the conservative-dissipative form

$$\partial_t w + \sum_{j=1}^n A_j \partial_{x_j} w = Bw, \tag{3.42}$$

it is possible to decompose the solution to the Cauchy problem as

$$w(t) = \Gamma^h(t) * w_0 = K(t) * w_0 + \mathcal{K}(t) * w_0,$$

for any function $w_0 \in L^1 \cap L^2(\mathbb{R}^n, \mathbb{R}^{n+1})$.

Moreover for any multi index β and for every $p \in [1, +\infty]$ the following estimates hold.

$K(t)$ estimates:

$$
\begin{aligned}
\|L_0 D^\beta K(t) * w_0\|_{L^p} &\leq C(|\beta|) \min\{1, t^{-\frac{m}{2}(1-\frac{1}{p})-\frac{|\beta|}{2}}\} \|L_0 w^0\|_{L^1} \\
&+ C(|\beta|) \min\{1, t^{-\frac{m}{2}(1-\frac{1}{p})-\frac{1}{2}-\frac{|\beta|}{2}}\} \|L_- w^0\|_{L^1},
\end{aligned}
$$

$$
\begin{aligned}
\|L_- D^\beta K(t) * w_0\|_{L^p} &\leq C(|\beta|) \min\{1, t^{-\frac{m}{2}(1-\frac{1}{p})-\frac{1}{2}-\frac{|\beta|}{2}}\} \|L_0 w^0\|_{L^1} \\
&+ C(|\beta|) \min\{1, t^{-\frac{m}{2}(1-\frac{1}{p})-1-\frac{|\beta|}{2}}\} \|L_- w^0\|_{L^1}.
\end{aligned}
$$

$\mathcal{K}(t)$ estimates:

$$
\|D^\beta \mathcal{K}(t) * w_0\|_{L^2} \leq C e^{-ct} \|D^\beta w_0\|_{L^2}.
$$

Remark 3.3.1. *As shown in [17], if we focus on the one-dimensional case, we have the following decomposition*

$$
\Gamma(x, t) = K(x, t) \chi \left\{ \underline{\lambda} t \leq x \leq \overline{\lambda} t, t \geq 1 \right\} + \mathcal{K}(x, t) + R(x, t) \chi \left\{ \underline{\lambda} t \leq x \leq \overline{\lambda} t \right\},
$$

where

$$
R(x, t) = \sum_j \frac{e^{-(x-\lambda_j^1)t^2/Ct}}{1+t}
\begin{bmatrix}
O(1) & O(1)(1+t)^{-1/2} \\
O(1)(1+t)^{-1/2} & O(1)(1+t)^{-1}
\end{bmatrix}.
$$

Moreover it is known that for the dissipative hyperbolic system

$$
\begin{cases}
\partial_t \rho + \partial_x v = 0, \\[2mm]
\partial_t v + \partial_x \rho = -\beta v,
\end{cases}
$$

that is the linearization of our quasilinear hyperbolic system, the diffusive part of the Green Kernel $K(x, t)$ can be decomposed as follows,

$$
K_{11}(x, t) = \Gamma^{\frac{1}{\beta}}(x, t), \quad K_{12}(x, t) = K_{21}(x, t) = \frac{1}{\beta} \partial_x \Gamma^{\frac{1}{\beta}}(x, t), \quad K_{22}(x, t) = \frac{1}{\beta^2} \partial_{xx} \Gamma^{\frac{1}{\beta}}(x, t),
$$

where $\Gamma^{\frac{1}{\beta}}$ is the Green Kernel of the heat equation. For more details see [17].

3.3.1 H^s Estimates of the Solution

This section is devoted to study the decay rates of solution to the system (3.39) in the H^s-norms. We define

$$
E_s := \max\left\{\|U_0\|_{L^1}, \|U_0\|_{H^s}\right\}, \quad D_s := \max\left\{\|\phi_0\|_{L^1}, \|\phi_0\|_{H^{s+1}}\right\},
$$

and the general functional

$$
M_w^\alpha := \sup_{0 \leq s \leq t} \left\{\max\{1, s^\alpha\} \|w(s)\|_{H^s}\right\}.
$$

Then, we shall prove the following theorem

Theorem 3.3.2. *Let $(U, \phi)(t)$ a global solution to problem* (3.12), *with initial conditions*

$$U(x, 0) = U_0(x), \quad \phi(x, 0) = \phi_0(x),$$

and regularity assumptions

$$U_0(x) \in H^{s+1}(\mathbb{R}) \cap L^1(\mathbb{R}), \quad \phi_0(x) \in H^{s+1}(\mathbb{R}) \cap L^1(\mathbb{R}), \ for \ s \geq 1.$$

Then the following decay estimate holds:

$$\|U(t)\|_{H^s} \leq C \min\{1, t^{-\frac{1}{4}}\}(E_{s+1} + D_{s+1}), \quad \|\phi(t)\|_{H^{s+1}} \leq C \min\{1, t^{-\frac{1}{4}}\}(E_{s+1} + D_{s+1}),$$

where the constant C depends on the constant state.

Proof. First we consider the parabolic equation

$$\partial_t \phi = D \partial_{xx} \phi + au - \frac{\phi}{\tau},$$

and using the Duhamel's formula, we can write the solution as

$$\phi(x, t) = (e^{-\frac{t}{\tau}} \Gamma^p(t) * \phi_0)(x) + \int_0^t e^{-\frac{(t-s)}{\tau}} \Gamma^p(t - s) * a\rho(s) \, ds, \qquad (3.43)$$

where

$$\Gamma^p(x, t) := \frac{e^{-\frac{x^2}{4Dt}}}{2\sqrt{\pi Dt}}.$$

Let us start with the H^{s+1} estimate:

$$
\begin{aligned}
\|\phi(t)\|_{H^{s+1}} &= \|(e^{-\frac{t}{\tau}} \Gamma^p(t) * \phi_0)\|_{H^{s+1}} + \int_0^t \|e^{-\frac{(t-s)}{\tau}} \Gamma^p(t - s) * a\rho(s)\|_{H^{s+1}} \, ds \\
&\leq e^{-\frac{t}{\tau}} \|\Gamma^p(t)\|_{L^1} \|\phi_0\|_{H^{s+1}} + \int_0^t e^{-\frac{(t-s)}{\tau}} \|\Gamma^p(t - s) * a\rho(s)\|_{H^{s+1}} \, ds \\
&\leq e^{-\frac{t}{\tau}} C \|\phi_0\|_{H^{s+1}} + \int_0^t e^{-\frac{(t-s)}{\tau}} \|\Gamma^p(t - s) * a\rho(s)\|_{L^2} \, ds \\
&\quad + \int_0^t e^{-\frac{(t-s)}{\tau}} \sum_{|\alpha=s+1|} \|D_x^\alpha \Gamma^p(t - s) * a\rho(s)\|_{L^2} \, ds \\
&\leq e^{-\frac{t}{\tau}} C \|\phi_0\|_{H^{s+1}} + \int_0^t C e^{-\frac{(t-s)}{\tau}} \|a\rho(s)\|_{L^2} \, ds \\
&\quad + \int_0^t e^{-\frac{(t-s)}{\tau}} \|\partial_x \Gamma^p(t - s)\|_{L^1} \|a\rho(s)\|_{H^s} \, ds \\
&\leq e^{-\frac{t}{\tau}} C \|\phi_0\|_{H^{s+1}} + \int_0^t C e^{-\frac{(t-s)}{\tau}} (t - s)^{-\frac{1}{2}} \|a\rho(s)\|_{H^s} \, ds + \int_0^t C e^{-\frac{(t-s)}{\tau}} \|a\rho(s)\|_{L^2} \, ds \\
&\leq e^{-\frac{t}{\tau}} C \|\phi_0\|_{H^{s+1}} + M_U^{\frac{1}{4}}(t) \int_0^t e^{-\frac{(t-s)}{\tau}} (t - s)^{-\frac{1}{2}} \min\{1, s^{-\frac{1}{4}}\} \, ds \\
&\quad + M_U^{\frac{1}{4}}(t) \int_0^t e^{-\frac{(t-s)}{\tau}} \min\{1, s^{-\frac{1}{4}}\} \, ds.
\end{aligned}
$$

So we obtain the following H^{s+1} estimate for ϕ

$$\|\phi(t)\|_{H^{s+1}} \leq C(e^{-\frac{t}{\tau}} \|\phi_0\|_{H^{s+1}} + \min\{1, |t - 1|^{-\frac{1}{4}}\} M_U^{\frac{1}{4}}(t) + \min\{1, t^{-\frac{1}{4}}\} M_U^{\frac{1}{4}}(t)),$$

which yields

$$M_{\phi_x}^{\frac{1}{4}}(t) \leq C(e^{-\frac{t}{\tau}}\max\{1, t^{\frac{1}{4}}\}\|\phi_0\|_{H^{s+1}} + M_U^{\frac{1}{4}}(t)). \tag{3.44}$$

Let us notice that from the previous inequality the decay rates if the function ϕ in H^{s+1} is the same rate of the function U in H^s. Moreover, proceeding in a similar way, it is possible to get the following estimate for the function ϕ in the space L^1:

$$\|\phi(t)\|_{L^1} \leq e^{-bt}\|\phi_0\|_{L^1} + c \sup_{s \in (0,t)} \|\rho(s)\|_{L^1}, \tag{3.45}$$

where, thanks to the conservation of the mass, $\sup_{s \in (0,t)} \|\rho(s)\|_{L^1} = \|\rho_0\|_{L^1}$.

Now we focus on the estimate of function U. We can easily observe that

$$\bar{f}(U) - \bar{f}'(\overline{U})U = \overbrace{\overline{f(\overline{U})}}^{=0} + U^2 r(U),$$

where $r: \mathbb{R} \to \mathbb{R}$ is a suitable smooth function. Therefore, using (3.41) and the definition of E_s, we obtain

$$\|U(t)\|_{H^s} \leq C\min\{1, t^{-\frac{1}{4}}\}\|U_0\|_{L^1} + Ce^{-ct}\|U_0\|_{H^s} + C\int_0^t \min\{1, (t-s)^{-\frac{3}{4}}\}\|U^2(s)r(U)(s)\|_{L^1}ds$$

$$+ C\int_0^t e^{-c(t-s)}\|\partial_x(U^2(s)r(U))(s)\|_{H^s}ds + \int_0^t \|\Gamma^h(t-s) * h(U + \overline{U}, \partial_x\phi)(s)\|_{H^s}ds$$

$$\leq C\min\{1, t^{-\frac{1}{4}}\}E_s + C\int_0^t \min\{1, (t-s)^{-\frac{3}{4}}\}\|U^2(s)r(U)(s)\|_{L^1}ds$$

$$+ C\int_0^t e^{-c(t-s)}\|\partial_x(U^2(s)r(U))(s)\|_{H^s}ds + \int_0^t \|\Gamma^h(t-s) * h(U + \overline{U}, \partial_x\phi)(s)\|_{H^s}ds. \tag{3.46}$$

At this stage we want to estimate the right hand side of this inequality.

Let us start studying the first integral in (3.46), as follows

$$\int_0^t \min\{1, (t-s)^{-\frac{3}{4}}\}\|U^2(s)r(U)(s)\|_{L^1}ds \leq \int_0^t \min\{1, (t-s)^{-\frac{3}{4}}\}\|U^2(s)\|_{L^2}\|r(U)(s)\|_{L^2}ds$$

$$\leq \int_0^t \min\{1, (t-s)^{-\frac{3}{4}}\}\|U(s)\|_{L^2}^2\|r(U)(s)\|_{L^\infty(|U|\leq\delta_0)}ds$$

$$\leq \left(CM_U^{\frac{1}{4}}(t)\right)^2 \int_0^t \min\{1, (t-s)^{-\frac{3}{4}}\}\min\{1, s^{-\frac{1}{2}}\}ds.$$

Then from Lemma 2.4.1, we deduce

$$\int_0^t \min\{1, (t-s)^{-\frac{3}{4}}\}C\|U^2(s)r(U)\|_{L^1}ds \leq C\int_0^t \min\{1, (t-s)^{-\frac{3}{4}}\}\min\{1, s^{-\frac{1}{2}}\}\left(M_U^{\frac{1}{4}}(t)\right)^2$$

$$\leq C_1\min\{1, t^{-\frac{1}{4}}\}\left(M_U^{\frac{1}{4}}(t)\right)^2. \tag{3.47}$$

In order to estimate the following term in (3.46) we recall an useful lemma.

Lemma 3.3.3. *Fixed $s > \frac{m}{2}$, $\beta \in \mathbb{N}^m$, and let $u \in H^{s'}(\mathbb{R}^{m'})$ verify inequality*

$$|u(x, t)| \leq \delta_0,$$

where $\delta_0 > 0$ and $s' \geq s + |\beta|$. Then, we have

$$\|D^\beta(u^2 r(u))\|_{H^s} \leq C(\delta_0, \|u\|_{H^s}, \|r\|_{C^{s+|\beta|}(|u|\leq\delta_0)})\|u\|_{L^\infty}\|D^\beta u\|_{H^s}.$$

Thanks to this lemma we deduce that

$$\left\|\partial_x(U^2 r(U))\right\|_{H^s} \leq C(\delta_0, \|u\|_{H^s}, \|r\|_{C^{s+|\beta|}(|u|\leq\delta_0)}) \|U\|_{L^\infty} \|\partial_x U\|_{H^s} \leq C \|U\|_{L^\infty} \|U\|_{H^{s+1}}$$

$$\leq C \|U\|_{H^s} \|U\|_{H^{s+1}}, \tag{3.48}$$

then we have

$$\int_0^t e^{-c(t-s)} \left\|\partial_x(U^2 r(U))(s)\right\|_{H^s} ds \leq C \int_0^t e^{-c(t-s)} \|U(s)\|_{L^\infty} \|U(s)\|_{H^{s+1}} ds$$

$$\leq C \int_0^t e^{-c(t-s)} \|U(s)\|_{H^s} \|U(s)\|_{H^{s+1}} ds$$

$$\leq C M_U^{\frac{1}{4}}(t) E_{s+1} \int_0^t e^{-c(t-s)} \min\{1, s^{-\frac{1}{4}}\} ds$$

$$\leq C \min\{1, t^{-\frac{1}{4}}\} M_U^{\frac{1}{4}}(t) E_{s+1}. \tag{3.49}$$

In the last inequalities, we have used Lemma 2.4.1 and the estimate of Theorem 3.2.4 to controll the norm in H^s.

Remark 3.3.4. *In the previous chapter we have shown the global existence of solutions and their decay rates simultaneously by estimate of the L^∞ and H^s-norms of the functions.*
Let us notice that the presence of the term $\partial_x(U^2 r(U))$ precludes the direct use of the decay estimates. As a matter of fact, due to the presence of this term, it is not possible to close our estimate, because starting from in H^s, we get terms in H^{s+1}.

Finally we estimate the last integral of (3.46)

$$\int_0^t \|\Gamma^h(t-s) * h(U+\overline{U},\partial_x\phi)(s)\|_{H^s} ds \leq \int_0^t \|\mathcal{K}(t-s) * h(U+\overline{U},\partial_x\phi)(s)\|_{H^s} ds$$

$$+ \int_0^t \|K(t-s) * h(U+\overline{U},\partial_x\phi)(s)\|_{H^s} ds.$$

For the first term, we have:

$$\int_0^t \|\mathcal{K}(t-s) * h(U+\overline{U},\partial_x\phi)(s)\|_{H^s} ds \leq \int_0^t ce^{-c(t-s)} \|h(U+\overline{U},\partial_x\phi)(s)\|_{H^s} ds$$

$$\leq \int_0^t ce^{-c(t-s)} \|\partial_x\phi(s)\|_{H^s}(\bar\rho + \|\rho(s)\|_{H^s}) ds$$

$$\leq \bar\rho M_{\phi_x}^{\frac{1}{4}}(t) \int_0^t ce^{-c(t-s)} \min\{1, s^{-\frac{1}{4}}\} ds$$

$$+ M_{\phi_x}^{\frac{1}{4}}(t) M_U^{\frac{1}{4}}(t) \int_0^t ce^{-c(t-s)} \min\{1, s^{-\frac{1}{2}}\} ds$$

$$\leq c_1 \min\{1, t^{-\frac{1}{4}}\} \bar\rho M_{\phi_x}^{\frac{1}{4}}(t) + c_1 \min\{1, t^{-\frac{1}{2}}\} M_{\phi_x}^{\frac{1}{4}}(t) M_U^{\frac{1}{4}}(t). \tag{3.50}$$

In order to complete our estimate, we need to study the contribution of the hyperbolic Green function diffusive part.

$$\int_0^t \|K(t-s) * h(U+\overline{U},\partial_x\phi)(s)\|_{H^s} ds = \int_0^t \|K_{12}(t-s) * \bar\mu(\rho(s)+\bar\rho)\partial_x\phi(s)\|_{H^s} ds$$

$$+ \int_0^t \|K_{22}(t-s) * \mu(\rho(s)+\bar\rho)\partial_x\phi(s)\|_{H^s} ds$$

$$\leq \int_0^t C\|K_{12}(t-s) * \mu(\rho(s)+\bar\rho)\partial_x\phi(s)\|_{H^s} ds$$

$$\leq \int_0^t C\|\partial_x K_{12}(t-s)*\mu\bar{\rho}\phi(s)\|_{H^s} + \|K_{12}(t-s)*\mu\rho\partial_x\phi\|_{H^s}\,ds$$

$$\leq \bar{\mu}\int_0^t \min\{1,(t-s)^{-\frac{5}{4}}\}\bar{\rho}\|\phi(s)\|_{L^1}\,ds$$

$$+\bar{\mu}\int_0^t \min\{1,(t-s)^{-\frac{3}{4}}\}\min\{1,s^{-\frac{1}{2}}\}\,ds\,M_{\phi_x}^{\frac{1}{4}}(t)M_U^{\frac{1}{4}}(t). \qquad (3.51)$$

Since in our study we do not differentiate the decays of conservative and the dissipative variables, in the previous inequalities we have estimated the decay of K_{22} with the same decay rate of K_{12}, even if it decays faster.

Thanks to (3.45) we deduce that

$$\bar{\mu}\int_0^t \min\{1,(t-s)^{-\frac{5}{4}}\}\bar{\rho}\|\phi(s)\|_{L^1}\,ds \leq \bar{\mu}\int_0^t \min\{1,(t-s)^{-\frac{5}{4}}\}(e^{-bs}\|\phi_0\|_{L^1}+c\|\rho_0\|_{L^1})\,ds \qquad (3.52)$$

$$\leq \bar{\mu}\min\{1,t^{-\frac{5}{4}}\}\bar{\rho}\|\phi_0\|_{L^1}+c\|\rho_0\|_{L^1}\bar{\rho}t^{-\frac{1}{4}}.$$

The second integral of (3.51) can be estimated as

$$\int_0^t \|K_{12}(t-s)*\bar{\mu}\rho\partial_x\phi\|_{H^s}\,ds \leq C\min\{1,t^{-\frac{1}{4}}\}M_{\phi_x}^{\frac{1}{4}}(t)M_U^{\frac{1}{4}}(t). \qquad (3.53)$$

In conclusion, substituting (3.47), (3.49), (3.50), (3.52), (3.53) in (3.46), it results

$$\|U(t)\|_{H^s} \leq \tilde{C}\Bigg(\min\{1,t^{-\frac{1}{4}}\}E_s + \min\{1,t^{-\frac{1}{4}}\}M_U^{\frac{1}{4}}E_{s+1} + \min\{1,t^{-\frac{1}{4}}\}(M_U^{\frac{1}{4}}(t))^2$$

$$+\min\{1,t^{-\frac{1}{4}}\}\bar{\rho}M_{\phi_x}^{\frac{1}{4}}(t) + \min\{1,t^{-\frac{1}{2}}\}M_{\phi_x}^{\frac{1}{4}}(t)M_U^{\frac{1}{4}}(t)$$

$$+\min\{1,t^{-\frac{1}{4}}\}M_{\phi_x}^{\frac{1}{4}}(t)M_U^{\frac{1}{4}}(t) + \bar{\mu}\min\{1,t^{-\frac{5}{4}}\}\bar{\rho}\|\phi_0\|_{L^1} + \|\rho_0\|_{L^1}\bar{\rho}t^{-\frac{1}{4}}\Bigg).$$

Multiplying this relation by $\max\{1,t^{\frac{1}{4}}\}$ we get

$$M_U^{\frac{1}{4}}(t) \leq C\Bigg(E_s + M_U^{\frac{1}{4}}(t)E_{s+1} + (M_U^{\frac{1}{4}}(t))^2 + \bar{\rho}(M_{\phi_x}^{\frac{1}{4}}(t)+t^{-1}\bar{\rho}\|\phi_0\|_{L^1}+\|\rho_0\|_{L^1})$$

$$+\left(1+\min\{1,t^{-\frac{1}{4}}\}\right)M_{\phi_x}^{\frac{1}{4}}(t)M_U^{\frac{1}{4}}(t)\Bigg).$$

Now, we substitute inequality (3.44) in the previous one, obtaining

$$M_U^{\frac{1}{4}}(t) \leq C\Bigg(E_s + M_U^{\frac{1}{4}}(t)E_{s+1} + (M_U^{\frac{1}{4}}(t))^2 + \bar{\rho}\max\{1,t^{\frac{1}{4}}\}e^{-t/\tau}\|\phi_0\|_{H^{s+1}}$$

$$+\bar{\rho}M_U^{\frac{1}{4}}(t) + \min\{1,t^{-1}\}\bar{\rho}\left\|\phi_0\right\|_{L^1} + \bar{\rho}\|\rho\|_{L^1} + e^{-t/\tau}\|\phi_0\|_{H^{s+1}}M_U^{\frac{1}{4}}(t)$$

$$+\max\{1,t^{\frac{1}{4}}\}e^{-t/\tau}\|\phi_0\|_{H^{s+1}}M_U^{\frac{1}{4}}(t) + (M_U^{\frac{1}{4}}(t))^2 + \min\{1,t^{-\frac{1}{4}}\}(M_U^{\frac{1}{4}}(t))^2\Bigg).$$

Then, for $t > \delta > 0$, we get

$$M_U^{\frac{1}{4}}(t) \leq C_s + C_1 M_U^{\frac{1}{4}}(t) + C_2(M_U^{\frac{1}{4}}(t))^2, \qquad (3.54)$$

where $C_s = C_s(E_s, D_{s+1}, \bar{\rho})$ and $C_1 = C_1(E_{s+1}, D_{s+1}, \bar{\rho})$.

From this inequality we deduce that, if the initial data and the perturbation $\bar{\rho}$ are sufficiently small, then we have

$$M_U^{\frac{1}{4}}(t) \leq CC_s,$$

that yields

$$\|U(t)\|_{H^s} \le C \min\{1, t^{-\frac{1}{4}}\} C_s,$$

and the same for the solution ϕ

$$\|\phi(t)\|_{H^{s+1}} \le C \min\{1, t^{-\frac{1}{4}}\} C_s.$$

$\square$

3.3.2 L^∞ Estimates of the Solution

In this section our aim to estimate the L^∞-norm of solutions to the system (3.39). As done before, we define the functional

$$N_w^\alpha(t) := \sup_{0 \le s \le t} \left\{ \max\{1, s^\alpha\} \|w(s)\|_{L^\infty} \right\},,$$

and set

$$E_s := \max\left\{ \|U_0\|_{L^1}, \|U_0\|_{H^s} \right\}, \quad D_s := \max\left\{ \|\phi_0\|_{L^1}, \|\phi_0\|_{H^s} \right\}.$$

Our aim is to prove the following theorem

Theorem 3.3.5. *Let $(U, \phi)(t)$ a global solution to system* (3.12)*, with initial conditions*

$$U(x, 0) = U_0(x), \quad \phi(x, 0) = \phi_0(x),$$

and regularity assumptions

$$U_0(x) \in H^2(\mathbb{R}) \cap L^1(\mathbb{R}), \quad \phi_0(x) \in H^2(\mathbb{R}) \cap L^1(\mathbb{R}), \ for \ s \ge 1.$$

Then the following decay estimate holds:

$$\|U(t)\|_{L^\infty} \le C \min\{1, t^{-\frac{1}{2}}\}(E_2 + D_2), \quad \|\phi(t)\|_{L^\infty} \le C \min\{1, t^{-\frac{1}{2}}\}(E_2 + D_2),$$

where the constant C depends on the constant state.

Proof. Proceeding as done before we obtain L^∞ estimates for ϕ and $\partial_x \phi$. First of all we show that

$$
\begin{aligned}
\|\phi(t)\|_{L^\infty} &= \|(e^{-\frac{t}{\tau}} \Gamma^p(t) * \phi_0)\|_{L^\infty} + \int_0^t \|e^{-\frac{(t-s)}{\tau}} \Gamma^p(t-s) * a\rho(s)\|_{L^\infty} ds \\
&\le e^{-\frac{t}{\tau}} \|\Gamma^p(t)\|_{L^1} \|\phi_0\|_{L^\infty} + \int_0^t e^{-\frac{(t-s)}{\tau}} \|\Gamma^p(t-s) * a\rho(s)\|_{L^\infty} ds \\
&\le e^{-\frac{t}{\tau}} C \|\phi_0\|_{L^\infty} + \int_0^t e^{-\frac{(t-s)}{\tau}} \|\Gamma^p(t-s)\|_{L^1} \|a\rho(s)\|_{L^\infty} ds \\
&\le e^{-\frac{t}{\tau}} C \|\phi_0\|_{L^\infty} + \int_0^t e^{-\frac{(t-s)}{\tau}} C \|a\rho(s)\|_{L^\infty} ds \\
&\le e^{-\frac{t}{\tau}} C \|\phi_0\|_{L^\infty} + N_U^{\frac{1}{2}}(t) \int_0^t e^{-\frac{(t-s)}{\tau}} C \min\{1, s^{-\frac{1}{2}}\} ds,
\end{aligned}
$$

which yields

$$\|\phi(t)\|_{L^\infty} \le C \left(e^{-\frac{t}{\tau}} \|\phi_0\|_{L^\infty} + \min\{1, t^{-\frac{1}{2}}\} N_U^{\frac{1}{2}}(t) \right). \tag{3.55}$$

In a similar way, we get

$$\|\partial_x \phi(t)\|_{L^\infty} \leq C \left(e^{-\frac{t}{\tau}} \|\partial_x \phi_0\|_{L^\infty} + \min\{1, |t-1|^{-\frac{1}{2}}\} N_U^{\frac{1}{2}}(t) \right). \tag{3.56}$$

Now let us consider the solution of our system written in the form (3.40), so its solution is given by

$$U(t) = \Gamma^h(t) * U_0 + \int_0^t \partial_x \Gamma^h(t-s) * \left[f'(\overline{U}) U(s) - f(U(s)) \right] ds + \int_0^t \Gamma^h(t-s) * h(U + \overline{U}, \partial_x \phi)(s) ds.$$

Let us estimate the L^∞-norm of U in the following way

$$\begin{aligned}
\|U(t)\|_{L^\infty} \leq & \|\Gamma^h(t) * U_0\|_{L^\infty} + \int_0^t \left\| \partial_x \Gamma^h(t-s) * \left[f'(\overline{U}) U(s) - f(U(s)) \right] \right\|_{L^\infty} ds \\
& + \int_0^t \|\Gamma^h(t-s) * h(U + \overline{U}, \partial_x \phi)(s)\|_{L^\infty} ds \\
\leq & \|\Gamma^h(t) * U_0\|_{L^\infty} + \int_0^t \|\partial_x \Gamma^h(t-s) * (U^2 r(U)(s))\|_{L^\infty} ds \\
& + \int_0^t \|\Gamma^h(t-s) * h(\phi, U + \bar{U})(s)\|_{L^\infty} ds \\
\leq & C \min\{1, t^{-\frac{1}{2}}\} \|U_0\|_{L^1} + C e^{-ct} \|U_0\|_{H^1} + \int_0^t \|\mathcal{K}(t-s) * U^2 r(U)(s)\|_{L^\infty} ds \\
& + \int_0^t \left\| K(t-s) * \partial_x(U^2 r(U))(s) \right\|_{L^\infty} ds + \int_0^t \|\Gamma^h(t-s) * h(U + \overline{U}, \partial_x \phi)(s)\|_{L^\infty} ds. \tag{3.57}
\end{aligned}$$

As observed before, in the one dimensional case it is possible to decompose the Green function as

$$\Gamma(x, t) = K(x, t) \chi \left\{ \underline{\lambda} t \leq x \leq \overline{\lambda} t, t \geq 1 \right\} + \mathcal{K}(x, t) + R(x, t) \chi \left\{ \underline{\lambda} t \leq x \leq \overline{\lambda} t \right\},$$

then the remainder $R(x, t)$ and the diffusive part $K(x, t)$ in (3.57) can be estimated as

$$\begin{aligned}
\int_0^t (\|\partial_x K\|_{L^2} + \|\partial_x R\|_{L^2}) \left\| U^2 r(U)(s) \right\|_{L^2} ds \leq & \int_0^t \min\{1, (t-s)^{-\frac{3}{4}}\} \left\| U^2 r(U)(s) \right\|_{L^2} ds \\
\leq & \int_0^t \min\{1, (t-s)^{-\frac{3}{4}}\} \|r(U)(s)\|_{L^2} \left\| U^2(s) \right\|_{L^\infty} ds \\
\leq & \int_0^t \min\{1, (t-s)^{-\frac{3}{4}}\} \|r(U)\|_{L^2(|U(s)| \leq \delta_0)} \|U(s)\|_{L^\infty} \|U(s)\|_{H^s} ds \\
\leq & c \min\{1, t^{-\frac{1}{2}}\} N_U^{\frac{1}{2}}(t) M_U^{\frac{1}{4}}(t).
\end{aligned}$$

While the term $\mathcal{K}(x, t)$ is estimated as

$$\begin{aligned}
\int_0^t \left\| \mathcal{K}(t-s) * \partial_x(U^2 r(U)) \right\|_{L^\infty} ds \leq & \int_0^t e^{-c(t-s)} \left\| \partial_x(U^2 r(U)(s)) \right\|_{H^1} ds \\
\leq & \int_0^t e^{-c(t-s)} C \|U(s)\|_{L^\infty} \|U(s)\|_{H^2} ds \\
\leq & N_U^{\frac{1}{2}}(t) E_2 \int_0^t e^{-c(t-s)} \min\{1, s^{-\frac{1}{2}}\} ds, \\
\leq & C \min\{1, t^{-\frac{1}{2}}\} N_U^{\frac{1}{2}}(t) E_2,
\end{aligned}$$

where we have used the estimate (3.48).

Finally we estimate the last term in (3.57). Proceeding in a similar way it can be decomposed as

$$\int_0^t \|\Gamma^h(t-s) * h(U + \overline{U}, \partial_x \phi)(s)\|_{L^\infty} ds \leq \int_0^t \|K(t-s) * h(U + \overline{U}, \partial_x \phi)(s)\|_{L^\infty} ds$$

$$+ \int_0^t \|\mathcal{K}(t-s) * h(U+\overline{U}, \partial_x \phi)(s)\|_{L^\infty} ds$$

$$+ \int_0^t \|R(t-s) * h(U+\overline{U}, \partial_x \phi)(s)\|_{L^\infty} ds.$$

Let us start from the first integral on the right hand side.

$$
\begin{aligned}
\int_0^t \|\mathcal{K}(t-s) * h(U+\overline{U}, \partial_x \phi)\|_{L^\infty} ds &\leq \int_0^t c e^{-c(t-s)} \|h(U+\overline{U}, \partial_x \phi)(s)\|_{L^\infty} ds \\
&\leq \int_0^t c e^{-c(t-s)} \left(\bar{\rho} \|\partial_x \phi(s)\|_{L^\infty} + \|\rho(s)\partial_x \phi(s)\|_{L^\infty} \right) ds \\
&\leq \int_0^t c e^{-c(t-s)} \left(\bar{\rho} \|\partial_x \phi(s)\|_{L^\infty} + \|\rho(s)\|_{L^\infty} \|\partial_x \phi(s)\|_{L^\infty} \right) ds \\
&\leq \int_0^t c e^{-c(t-s)} \min\{1, s^{-\frac{1}{2}}\} ds \bar{\rho} N_{\phi_x}^{\frac{1}{2}}(t) \\
&\quad + \int_0^t c e^{-c(t-s)} \min\{1, s^{-1}\} ds N_{\phi_x}^{\frac{1}{2}}(t) N_U^{\frac{1}{2}}(t) \\
&\leq c_1 \min\{1, t^{-\frac{1}{2}}\} \bar{\rho} N_{\phi_x}^{\alpha_2}(t) + c_1 \min\{1, t^{-1}\} N_{\phi_x}^{\frac{1}{2}}(t) N_U^{\frac{1}{2}}(t), \quad (3.58)
\end{aligned}
$$

thanks to Lemma 2.4.1.

Now need to estimate the contributions of the hyperbolic Green function dissipative and remainder part

$$
\int_0^t \|(K(t-s)+R(t-s)) * h(U+\overline{U}, \partial_x \phi)(s)\|_{L^\infty} ds = \int_0^t \|(K(t-s)+R(t-s)) * (\bar{\rho}+\rho)\partial_x \phi(s)\|_{L^\infty} ds
$$

$$
\leq \int_0^t \|(K(t-s)+R(t-s)) * \rho(s)\phi_x(s)\|_{L^\infty} ds + \int_0^t \|\partial_x(K(t-s)+R(t-s)) * \bar{\rho}\phi(s)\|_{L^\infty} ds.
$$

For the first integral we have

$$
\begin{aligned}
\int_0^t \|(K(t-s)+R(t-s)) * \rho(s)\phi_x(s)\|_{L^\infty} ds &\leq \int_0^t \min\{1, (t-s)^{-\frac{3}{4}}\} \|\rho(s)\phi_x(s)\|_{L^2} ds \\
&\leq N_U^{\frac{1}{2}}(t) M_{\phi_x}^{\frac{1}{4}}(t) \int_0^t \min\{1, (t-s)^{-\frac{3}{4}}\} \min\{1, s^{-\frac{3}{4}}\} ds \\
&\leq \min\{1, t^{-\frac{1}{2}}\} N_U^{\frac{1}{2}}(t) M_{\phi_x}^{\frac{1}{4}}(t).
\end{aligned}
$$

While for the second one we get

$$
\begin{aligned}
\int_0^t \|\partial_x(K(t-s)+R(t-s)) * \bar{\rho}\phi(s)\|_{L^\infty} ds &\leq \int_0^t \min\{1, (t-s)^{-\frac{3}{2}}\} \bar{\rho} \|\phi(s)\|_{L^1} ds \\
&\leq \int_0^t \min\{1, (t-s)^{-\frac{3}{2}}\} \bar{\rho} e^{-bs} ds \\
&\quad + \int_0^t \min\{1, (t-s)^{-\frac{3}{2}}\} \bar{\rho} \|\rho_0\|_{L^1} ds \\
&\leq \min\{1, t^{-\frac{3}{2}}\} \bar{\rho} + t^{-\frac{1}{2}} \bar{\rho} \|\rho_0\|_{L^1}.
\end{aligned}
$$

In conclusion we obtain that

$$
\begin{aligned}
\|U(t)\|_{L^\infty} \leq C \Big(&\min\{1, t^{-\frac{1}{2}}\} \|U_0\|_{L^1} + e^{-ct} \|U_0\|_{H^1} + \min\{1, t^{-\frac{1}{2}}\} N_U^{\frac{1}{2}}(t)) M_U^{\frac{1}{4}}(t) \\
&+ \min\{1, t^{-\frac{1}{2}}\} N_U^{\alpha_2}(t) E_2 + \min\{1, t^{-\frac{1}{2}}\} \bar{\rho} N_{\phi_x}^{\frac{1}{2}}(t) + \min\{1, t^{-1}\} N_{\phi_x}^{\frac{1}{2}}(t) N_U^{\frac{1}{2}}(t)
\end{aligned}
$$

$$+ \min\{1, t^{-\frac{3}{4}}\} N_{\phi_x}^{\frac{1}{2}}(t) M_U^{\frac{1}{4}}(t) + \bar{\mu}(\min\{1, t^{-\frac{3}{2}}\}\bar{\rho} + t^{-\frac{1}{2}}\bar{\rho}\|\rho\|_{L^1})\bigg). \tag{3.59}$$

Let us recall that $M_U^{\frac{1}{4}} \le cC_1$ and $M_{\phi_x}^{\frac{1}{4}} \le cC_2$. Then, substituting inequalities (3.55) and (3.56) in (3.59), we obtain

$$\|U(t)\|_{L^\infty} \le C\bigg(\min\{1, t^{-\frac{1}{2}}\}\|U_0\|_{L^1} + e^{-ct}\|U_0\|_{H^1} + \min\{1, t^{-1}\}(N_U^{\frac{1}{2}}(t))^2$$

$$+ \min\{1, t^{-\frac{1}{2}}\}N_U^{\frac{1}{2}}(t)E_2 + \min\{1, t^{-\frac{1}{2}}\}\bar{\rho}(E_1 + D_2)$$

$$+ \min\{1, t^{-\frac{3}{4}}\}(E_1 + D_2)N_U^{\frac{1}{2}}(t) + \min\{1, t^{-\frac{3}{4}}\}(D_2 + N_U^{\frac{1}{2}}(t))E_1$$

$$+ \bar{\mu}(\min\{1, t^{-\frac{3}{2}}\}\bar{\rho} + t^{-\frac{1}{2}}\bar{\rho}\|\rho\|_{L^1})\bigg).$$

Multiplying the previous relation by $\max\{1, t^{\frac{1}{2}}\}$, we get

$$N_U^{\frac{1}{2}}(t) \le C\left[B_1 + N_U^{\frac{1}{2}}(t)C_1 + (N_U^{\frac{1}{2}}(t))^2 C_2\right],$$

where $B_1 = B_1(D_2, \bar{\rho}, E_1)$ and $C_i = C_i(D_i, \bar{\rho}, E_i)$.

In conclusion, if initial data and the constant state are sufficiently small, for the L^∞ norm of the function U we obtain the following estimate

$$\|U(t)\|_{L^\infty} \le C\min\{1, t^{-\frac{1}{2}}\}C_{s+1}.$$

This means that the decay rate of the function U, and of course of the function ϕ, in L^∞-norm is $O(t^{-\frac{1}{2}})$ also in the case of perturbation of non-null constant state.

$\square$

Chapter 4

Numerical Approximations and Simulations

In this chapter we focus our attention on the numerical approximation of two hyperbolic-parabolic models which arise to describe chemotactical movements. In Chapters 2 and 3 we proved theorems of global existence of smooth solutions for these systems. Since our results hold only for small regular initial data, we are motivated to use numerical simulations as a tool to investigate the evolution of solutions also for larger data.

One goal would be to know whether hyperbolic-parabolic systems have the same behavior as parabolic-elliptic systems, that is to say global existence for small initial data and blow up of solutions for large initial data, in dimensions greater than 2 [135], or the parabolic-parabolic systems that, in two-dimensional case, have a critical mass threshold below which global existence is ensured [26]. It has also to be noticed that the previous analytical results about global existence of solutions were obtained on the whole space, whereas numerical simulations will be performed on a bounded domain.

The chapter is organized as follows: at the beginning we give an introduction to finite difference schemes, defining fundamental concepts like consistency, convergence, stability and monotonicity. Then we will present some finite difference schemes for hyperbolic conservation laws.

A section is dedicated to the relaxation method, which is used in our simulations, and asymptotic high order methods. We briefly present also some classical schemes for parabolic equations.

The third and the fourth parts of the chapter are devoted to the numerical simulations in the two dimensional case of the hyperbolic-parabolic models for chemotaxis and vasculogenesis studied previously from the analytical point of view.

4.1 An Introduction to Finite Difference Schemes

In this section we shall present some numerical backgrounds for finite difference schemes. The main reference is [157] from which most of the contents are taken.

We start defining a grid of points in the (x, t) plane. Let h and k be positive numbers called space step and time step ; then the grid will be given by the points $(x_m, t_n) = (mh, nk)$ for arbitrary integers n and m. We are interested in grids with small values of h and k. For a function v defined on the grid we write v_m^n for the value of v at the grid point (x_m, t_n). We also use the notation u_m^n, for $u(x_m, t_n)$, when u is defined for continuously varying (x, t).

The basic idea of finite difference schemes is to replace derivatives by finite differences. This can

be done in many ways. As two examples we may have:

$$
\begin{aligned}
\frac{\partial u}{\partial t}(x_m, t_n) &\approx \frac{u(x_m, t_n + k) - u(x_m, t_n)}{k} \\
&\approx \frac{u(x_m, t_n + k) - u(x_m, t_n - k)}{2k}.
\end{aligned}
$$

These are valid approximations, as seen from the formulas

$$
\begin{aligned}
\frac{\partial u}{\partial t}(t, x) &= \lim_{\varepsilon \to 0} \frac{u(x, t + \varepsilon) - u(x, t)}{\varepsilon} \\
&= \lim_{\varepsilon \to 0} \frac{u(x, t + \varepsilon) - u(x, t - \varepsilon)}{2\varepsilon},
\end{aligned}
$$

relating the derivative of u to some values of u. Similar formulas approximate derivatives with respect to x.

The method for deriving these schemes is very simple and this is one of the significant features of the general method of finite differences. Moreover the finite difference method is known for the great variety of schemes that can be used to approximate a given partial differential equation. However, the analysis of these schemes to determine if they are accurate approximations of the differential equation requires some powerful mathematical tools.

4.1.1   Convergence and Consistency

The most basic property that a scheme must have in order to be used is that its solutions approximate the solution of the corresponding partial differential equation and that the approximation improves as the time and space steps, h and k, tend to zero. We call such a scheme a *convergent* scheme. We consider linear partial differential equations of the form

$$
P(\partial_x, \partial_t) u = f(x, t), \tag{4.1}
$$

which are of first order in the derivative with respect to t. We also assume for such equations, or systems of equations, that the specification of initial data, $u(x, 0)$, completely determines a unique solution. The real variable x ranges over the whole real line or an interval. Examples of equations that are first order in time are the transport equation

$$
\partial_t u + a \partial_x u = 0, \tag{4.2}
$$

where a is a constant, and the heat equation

$$
\partial_t u - b \partial_{xx} u = 0, \tag{4.3}
$$

where $b > 0$ is a constant.

Definition 4.1.1. *A one-step finite difference scheme approximating a partial differential equation is a convergent scheme if, for any solution to the partial differential equation, $u(x, t)$, and solutions to the finite difference scheme, v_m^n, such that v_m^0 converges to $u_0(x)$ as mh converges to x, then v_m^n converges to $u(x, t)$ as (mh, nk) converges to (x, t) with h, k converging to 0.*

This definition is not complete until we clarify the nature of the convergence. Let Ω be a real interval and J_Ω the set of values with index m such that $mh \in \Omega$. The discretization values $v = \{v_m^n\}$ at time t_n will be defined by

$$
v^n := \{v_m^n : m \in J_\Omega\}.
$$

The two most common discrete norm used to estimate the convergence error are the $l^{\infty}-$ norm

$$\|v_n\|_{\infty,h} = \max\{|v_m^n|, m \in J_\Omega\},$$

and the l^2- norm

$$\|v_n\|_{2,h} = \left\{ \sum_{m \in J_\Omega} h|v_m^n|^2 \right\}^{\frac{1}{2}}.$$

We will say that a scheme is convergent in norm $\|\cdot\|_{\cdot,h}$ if

$$\|v_n - u_n\|_{\cdot,h} \to 0$$

as $h, k \to 0$, $nk \to t \in (0, T)$ for all initial data u_0 such that the corresponding initial value problem is well-posed in the chosen norm $\|\cdot\|_{\cdot,h}$.

Proving that a given scheme is convergent is not easy in general, if attempted in a direct manner. However, there are two related concepts that are easy to check: *consistency* and *stability*. First, we define consistency (for linear partial differential equations).

Definition 4.1.2. *Given a partial differential equation, $Pu = f$, and a finite difference scheme, $P_{k,h}v = f$, we say that the finite difference scheme is consistent with the partial differential equation if for any smooth function $\phi(x, t)$:*

$$P\phi - P_{k,h}\phi \to 0 \quad \text{as } k, h \to 0, \tag{4.4}$$

the convergence being pointwise convergence at each point (x, t).

Consistency implies that the solution of the partial differential equation, if it is smooth, is an approximate solution of the finite difference scheme. Similarly, convergence means that a solution of the finite difference scheme approximates a solution to the partial differential equation. It is natural to consider whether consistency is sufficient for a scheme to be convergent.

Consistency is certainly necessary for convergence, but as the following example shows, a scheme may be consistent but not convergent.

Remark 4.1.3. *Consider the partial differential equation $\partial_t u + \partial_x u = 0$ with the following forward-time forward-space scheme:*

$$\frac{v_m^{n+1} - v_m^n}{k} + \frac{v_{m+1}^n - v_m^n}{h} = 0.$$

The scheme may be rewritten as

$$
\begin{aligned}
v_m^{n+1} &= v_m^n - \frac{k}{h}\left(v_{m+1}^n - v_m^n\right) \\
&= (1 + \lambda)v_m^n - \lambda v_{m+1}^n,
\end{aligned}
\tag{4.5}
$$

where we have set $\lambda = \dfrac{k}{h}$. This scheme is consistent, as a matter of fact:

$$
\begin{aligned}
P\phi &= \partial_t\phi + \partial_x\phi, \\
P_{k,h}\phi &= \frac{\phi_m^{n+1} - \phi_m^n}{k} + \frac{\phi_{m+1}^n - \phi_m^n}{h}.
\end{aligned}
$$

Using the Taylor series of the function ϕ in t and x about (x_m, t_n), we have that

$$\phi_m^{n+1} = \phi_m^n + k\partial_t\phi + \frac{1}{2}k^2\partial_{tt}\phi + O(k^3),$$

$$\phi_{m+1}^n \quad = \quad \phi_m^n + h\partial_x \phi + \frac{1}{2}h^2 \partial_{xx} \phi + O(h^3)$$

where the derivatives on the right-hand side are all evaluated at (x_m, t_n), and so

$$P_{k,h}\phi = \partial_t \phi + \partial_x \phi + \frac{1}{2}k\partial_{tt}\phi + \frac{1}{2}h\partial_{xx}\phi + O(k^2) + O(h^2).$$

Thus

$$P\phi - P_{k,h}\phi = -\frac{1}{2}k\partial_{tt}\phi - \frac{1}{2}h\partial_{xx}\phi + O(k^2) + O(h^2) \to 0, \quad as\ (h,k) \to 0.$$

As initial condition for the differential equation we take:

$$u_0(x) = \begin{cases} 1 & if -1 \le x \le 0. \\ 0 & elsewhere. \end{cases}$$

The solution of the partial differential equation is a shift of u_0 to the right by t. In particular, for t greater than 0, there are positive values of x for which $u(x,t)$ is nonzero. For the difference scheme take the initial datum:

$$v_m^0 = \begin{cases} 1 & if -1 \le mh \le 0. \\ 0 & elsewhere. \end{cases}$$

As equation (4.5) *shows, the solution of the difference scheme at (x_m, t_n) depends only on $x_{m'}$ for $m' > m$ at previous times. Thus we conclude that v_m^n, is always 0 for points x_m to the right of 0, that is,*

$$v_m^n = 0 \quad for\ m > 0, n \ge 0.$$

Therefore, v_m^n cannot converge to $u(x,t)$, since for positive t and x, the function u is not identically zero, yet v_m^n is zero.

4.1.2   Stability

The previous remark shows that a scheme must satisfy other conditions besides consistency before we can conclude that it is convergent. The important property that is required is *stability*. To introduce this concept we note that, if a scheme is convergent, as v_m^n converges to $u(x,t)$, then certainly v_m^n is bounded in some sense. This is the essence of stability. The following definition of stability is for the homogeneous initial value problem, that is, one in which the right-hand-side function f is 0.

Before giving the definition of stability we need to define the stability region. For many schemes there are restrictions on the way that h and k should be chosen so that the scheme is stable, and therefore useful in computation. A stability region is any bounded nonempty region of the first quadrant of $\mathbb{R}^2$ that has the origin as an accumulation point. That is, a stability region must contain a sequence (k_ν, h_ν) that converges to the origin as ν tends to infinity. A common example is a region of the form $\{(k,h) : 0 < k \le ch \le C\}$ for some positive constants c and C.

Definition 4.1.4. *A finite difference scheme $P_{k,h}v = 0$ for a first-order equation is stable in the norm $\|\cdot\|_{\cdot,h}$ in a stability region Λ, if for all $T > 0$ there is a constant C_T such that, for all v^0,*

$$\|v^n\|_{\cdot,h} \le C_T \|v^0\|_{\cdot,h}$$

for $0 \le nk \le T$, $(k,h) \in \Lambda$.

The importance of the concepts of consistency and stability can be seen in the Lax-Richtmyer equivalence theorem, which is the fundamental theorem in the theory of finite difference schemes for initial value problems.

Theorem 4.1.5 (The Lax-Richtmyer Equivalence Theorem). *A consistent finite difference scheme for a partial differential equation for which the initial value problem is well-posed is convergent if and only if it is stable.*

The proof of this theorem can be found in [157]. As underlined in [157], the Lax-Richtmyer equivalence theorem is a very useful theorem, since it provides a simple characterization of convergent schemes.

Determining whether a scheme is convergent or nonconvergent can be difficult if we attempt to verify Definition 4.1.1 in a rather direct way. However, the determination of the consistency of a scheme is quite simple, and determining the stability of a scheme is also quite easy. Thus the more difficult result of convergence is replaced by the equivalent and easily verifiable conditions of consistency and stability. It is also significant that the determination of the consistency and stability of schemes involves essentially algebraic manipulations.

This discussion of Theorem 4.1.5 has focused on the half part of the theorem that states that consistency and stability imply convergence. The theorem is useful in the other direction also. It states that we should not consider any unstable schemes, since none of these will be convergent. Thus the class of reasonable schemes is precisely delimited by those that are consistent and stable. The usefulness of the Lax-Richtmyer theorem arises both from the ease of verifying consistency and stability and from the precise relationship established between these concepts and the concept of convergence.

Let us consider now the class of three points schemes, i.e. schemes with the following form:

$$v_m^{n+1} = \alpha v_{m+1}^n + \beta v_m^n + \gamma v_{m-1}^n, \tag{4.6}$$

where α, β and γ are constants to fix. We have a first result of stability in l^2−norm.

Proposition 4.1.6. *Let us consider an explicit scheme as* (4.6) *for the transport equation* (4.2)*. A sufficient condition for the stability in the l^2-norm is that the following inequality yields:*

$$|\alpha| + |\beta| + |\gamma| \leq 1.$$

Proof. For sake of simplicity we assume that our interval is the real line, i.e. $\Omega = \mathbb{R}$. Then we have:

$$
\begin{aligned}
\sum_{m=\infty}^{\infty} |v_m^{n+1}|^2 &= \sum_{m=\infty}^{\infty} |\alpha v_{m+1}^n + \beta v_m^n + \gamma v_{m-1}^n|^2 \\
&\leq \sum_{m=\infty}^{\infty} |\alpha|^2 |v_{m+1}^n|^2 + |\beta|^2 |v_m^n|^2 + |\gamma|^2 |v_{m-1}^n|^2 \\
&+ 2|\alpha||\beta||v_{m+1}^n||v_m^n| + 2|\beta||\gamma||v_m^n||v_{m-1}^n| + 2|\alpha||\gamma||v_{m+1}^n||v_{m-1}^n| \\
&\leq (|\alpha|^2 + 2|\alpha||\beta| + |\beta|^2 + 2|\beta||\gamma| + |\gamma|^2 + 2|\alpha||\gamma|) \sum_{m=\infty}^{\infty} |v_m^n|^2 \\
&= (|\alpha| + |\beta| + |\gamma|)^2 \sum_{m=\infty}^{\infty} |v_m^n|^2,
\end{aligned}
$$

where we used the relation $2xy \leq x^2 + y^2$. This completes the proof. □

Scheme	(α, β, γ)	q	Convergence
Upwind ($a < 0$)	$(-\lambda a, (1 + \lambda a), 0)$	$-\lambda a$	$-1 \leq \lambda a \leq 0$
Upwind ($a > 0$)	$(0, (1 - \lambda a), \lambda a)$	λa	$0 \leq \lambda a \leq 1$
Forward-central	$(-\lambda a/2, 1, \lambda a/2)$	0	never
Lax-Friedrichs	$((1 - \lambda a)/2, 0, (1 + \lambda a)/2)$	1	$|\lambda a| \leq 1$
Lax-Wendroff	$((-\lambda a + \lambda^2 a^2)/2, 1 - \lambda^2 a^2, (\lambda a + \lambda^2 a^2)/2)$	$(\lambda a)^2$	$|\lambda a| \leq 1$

Table 4.1: Three-points explicit finite difference schemes for scalar transport equation.

To ensure the consistency with equation (4.2) we have the following proposition.

Proposition 4.1.7. *Let the ratio $\dfrac{k}{h}$ be equal to a fixed constant $\lambda > 0$. Then a three-points explicit finite difference scheme* (4.6) *is consistent with equation* (4.2), *if and only if $\alpha + \beta + \gamma = 1$ and $\gamma - \alpha = \lambda a$.*

Proof. Thanks to Taylor series we have:

$$
\begin{aligned}
u_m^{n+1} &= u_m^n + k\partial_t u + \frac{1}{2}k^2 \partial_{tt} u + O(k^3), \\
u_{m\pm1}^n &= u_m^n \pm h\partial_x u + \frac{1}{2}h^2 \partial_{xx} u \pm \frac{1}{6}h^3 \partial_{xxx} u + O(h^4).
\end{aligned}
$$

Then we get

$$
\begin{aligned}
&\frac{1}{k}\left[u_m^{n+1} - (\alpha u_{m+1}^n + \beta u_m^n + \gamma u_{m-1}^n)\right] \\
&= \frac{1 - \alpha - \beta - \gamma}{k}u_m^n + \partial_t u + (\gamma - \alpha)\lambda^{-1}\partial_x u + \frac{1}{2}k(\partial_{tt} u - \lambda^{-2}(\alpha + \gamma)\partial_{xx} u) + O(k^2).
\end{aligned}
$$

This completes the proof. $\qquad\square$

To conclude this part, we briefly point out that the class of linear explicit schemes consistent for problem (4.2), forms a family depending on a parameter. If we set

$$
q = \alpha + \gamma,
$$

we can rewrite these schemes in the "viscous" form:

$$
v_m^{n+1} = v_m^n - \frac{a\lambda}{2}(v_{m+1}^n - v_{m-1}^n) + \frac{q}{2}(v_{m+1}^n - 2v_m^n + v_{m-1}^n). \tag{4.7}
$$

The q parameter is linked to the numerical viscosity of the scheme, as the scheme is formally consistent at the second order with the viscous equation:

$$
\partial_t u + a\partial_x u = \frac{1}{2}\lambda h\left(\frac{q}{\lambda^2} - a^2\right)\partial_{xx} u.
$$

In Table 4.1 we show possible coefficients choices for three-points explicit finite difference schemes for scalar transport equations.

Theorem 4.1.8 (The Courant-Friedrichs-Lewy Condition). *For an explicit scheme for the hyperbolic equation* (4.2) *of the form $v_m^{n+1} = \alpha v_{m+1}^n + \beta v_m^n + \gamma v_{m-1}^n$ with $k/h = \lambda$ held constant, a necessary condition for stability is the **Courant-Friedrichs-Lewy (CFL) condition**,*

$$
|a\lambda| < 1.
$$

For systems of equations for which v is a vector and α, β and γ are matrices, we must have $|\theta_i \lambda| < 1$ for all eigenvalues θ_i of the matrix A.

Proof. First consider the case of a single equation. If $a\lambda > 1$, then by considering the point $(x, t) = (0, 1)$ we see that the solution to the partial differential equation depends on the values of $u_0(x)$ at $x = -a$. But the finite difference scheme gives that v_0^n depends on v_m^0 only for $|m| < n$, by the form of the scheme. Since $h = \lambda^{-1}k$, we have $|m|h < \lambda^{-1}kn = \lambda^{-1}$, since $nk = 1$. So v_0^n depends on x only for $|x| < \lambda^{-1} < |a|$. Thus v_0^n cannot converge to $u(0, 1)$ as $h \to 0$.

For the case of a system of equations, we have that $u(x, 1)$ depends on $u_0(x)$ for x in the interval $[-a, a]$, where a is the maximum magnitude of the characteristic speeds θ_i. If $|\theta_i \lambda| > 1$ for some characteristic speed θ_i, then we can take initial data that are zero in $[-\lambda^{-1}, \lambda^{-1}]$ but not zero near θ_i. Then $u(x, 1)$ will not be zero, in general, and yet v_0^n with $nk = 1$ will be zero. Thus v^n cannot converge to $u(\cdot, 1)$, and the theorem is proved. $\qquad\square$

4.1.3 l^∞-Stability and Monotonicity

A useful way to get $l^\infty -$ stable approximations, is to construct schemes which verify the monotone comparison property, i.e if v_m^0 and $\tilde{v}_m^0$ are two approximations of the initial datum such that for all $m > 0$, $v_m^0 \le \tilde{v}_m^0$, then $v_m^n \le \tilde{v}_m^n$ for all $m, n > 0$.

Definition 4.1.9. *A one-step scheme of the form*

$$v_m^{n+1} = \sum_j c_{j,n} v_j^n, \tag{4.8}$$

is monotone if $c_{j,n} \ge 0$ for all j, n.

Let us observe that, thanks to this definition, monotone schemes are l^∞-stable.

Theorem 4.1.10. *Let be given a monotone scheme of the form* (4.8) *and let define*

$$v_{min} := \min\{v_m^0\}, \quad v_{max} := \max\{v_m^0\},$$

then, for all n, m

$$v_{min} \le v_m^n \le v_{max}.$$

Then, Theorem 4.1.5 allows us to state that all consistent and monotone schemes of the form (4.8), are convergent.

It is possible to characterize monotone schemes between the consistent schemes of the form (4.6) ; for that purpose, we will use the viscous form (4.7) of the scheme.

Proposition 4.1.11. *A three-points explicit scheme consistent with equation* (4.2)*, in the viscous form* (4.7) *is monotone if and only if*

$$\lambda|a| \le q \le 1.$$

Proof. Le us observe that

$$\alpha = \frac{1}{2}(q - a\lambda), \quad \beta = 1 - q, \quad \gamma = \frac{1}{2}(q + a\lambda).$$

$\qquad\square$

Unfortunately, the class of monotone schemes is too limited to hold more accurate approximations. Indeed a monotone scheme is at most of first order accurate.

Then, it is useful to analyze the class of l^2-stable schemes, which will turn out to be less restricted.

4.1.4   The Von Neumann Stability Analysis

In this section we develop the basic properties of Fourier analysis in the discrete case as an important tool for analyzing finite difference schemes and their solutions.

We will use Fourier analysis on the grid of integers $\mathbb{Z}$ or $h\mathbb{Z}$, which is defined by $h\mathbb{Z} = \{hm : m \in \mathbb{Z}\}$. Since the spacing between the grid points is h, we define the transform by

$$\hat{v}(\xi) = \frac{1}{\sqrt{2\pi}} \sum_{m=-\infty}^{\infty} e^{-imh\xi} v_m h, \tag{4.9}$$

for $\xi \in [-\pi/h, \pi/h]$, and then the inversion formula is

$$v_m = \frac{1}{\sqrt{2\pi}} \int_{-\pi/h}^{\pi/h} e^{imh\xi} \hat{v}(\xi) \, d\xi. \tag{4.10}$$

For the discrete transform, the Parseval's relation also holds, then we have equality for the l^2-norm of v and the the l^2-norm of $\hat{v}$,

$$\|\hat{v}\|_h^2 = \int_{-\pi/h}^{\pi/h} |\hat{v}(\xi)|^2 \, d\xi = \sum_{m=-\infty}^{\infty} |v_m|^2 h = \|v\|_h^2. \tag{4.11}$$

Parseval's relation will be used extensively in the study of stability. It allows us to replace the stability estimates by the equivalent inequality

$$\|\hat{v}^n\|_h \leq C_T^* \|\hat{v}_0\|_h,$$

for the transform of the grid function. In the next section we study the stability of schemes by examining the effect of the scheme on the transform of the solution. It should also be pointed out that there is no relation equivalent to Parseval's relation in the case of $l^\infty-$ norm. Because there is no such relation, the Lax-Richtmyer theorem is more difficult to use in the maximum norm.

We now apply Fourier analysis to the initial value problem for the transport equation

$$\partial_t u + a \partial_x u = 0. \tag{4.12}$$

We begin by transforming only in the spatial variable. We obtain for $\hat{u}(\omega, t)$ the equation

$$\partial_t \hat{u} = -ia\omega \hat{u},$$

which is an ordinary differential equation in t. This equation is easily solved and, using the initial datum, the solution is

$$\hat{u}(\omega, t) = e^{-ia\omega t} \hat{u}_0(\omega).$$

We now show that the initial value problem for (4.12) is well-posed. By the use of Parseval's relation and this last relationship, we obtain, using $|e^{-ia\omega t}| = 1$,

$$\int_{-\infty}^{\infty} |u(x, t)|^2 \, dx = \int_{-\infty}^{\infty} |\hat{u}(\omega, t)|^2 \, d\omega = \int_{-\infty}^{\infty} |e^{-ia\omega t} \hat{u}_0(\omega)|^2 \, d\omega = \int_{-\infty}^{\infty} |\hat{u}_0(\omega)|^2 \, d\omega = \int_{-\infty}^{\infty} |u_0(x)|^2 \, dx.$$

An important application of Fourier analysis is the von Neumann analysis of stability of finite difference schemes. With the use of Fourier analysis we can give necessary and sufficient conditions for the stability of finite difference schemes. We illustrate the method by considering a particular example and then discussing the method in general. Through the use of the Fourier transform the

determination of the stability of a scheme is reduced to relatively simple algebraic considerations. We begin by studying the forward-time backward-space scheme

$$\frac{v_m^{n+1} - v_m^n}{k} + a \frac{v_m^n - v_{m-1}^n}{h} = 0,$$

which can be rewritten as

$$v_m^{n+1} = (1 - a\lambda) v_m^n + a\lambda v_{m-1}^n, \tag{4.13}$$

where $\lambda = k/h$. Using the Fourier inversion formula for v^n, we have

$$v_m^n = \frac{1}{\sqrt{2\pi}} \int_{-\pi/h}^{\pi/h} e^{imh\xi} \hat{v}^n(\xi) d\xi,$$

and substituting this in (4.13) for v_m^n and v_{m-1}^n, we obtain

$$v_m^{n+1} = \frac{1}{\sqrt{2\pi}} \int_{-\pi/h}^{\pi/h} e^{imh\xi} \left[(1 - a\lambda) + a\lambda e^{-ih\xi} \right] \hat{v}^n(\xi) d\xi.$$

Comparing this formula with the Fourier inversion formula for v^{n+1},

$$v_m^{n+1} = \frac{1}{\sqrt{2\pi}} \int_{-\pi/h}^{\pi/h} e^{imh\xi} \hat{v}^{n+1}(\xi) d\xi.$$

and using the fact that the Fourier transform is unique, we deduce that the integrand is the same as the one in the inversion formula. We then have that

$$\hat{v}^{n+1}(\xi) = \left[(1 - a\lambda) + a\lambda e^{-ih\xi} \right] \hat{v}^n(\xi) = g(h\xi) \hat{v}^n(\xi), \tag{4.14}$$

where

$$g(h\xi) = (1 - a\lambda) + a\lambda e^{-ih\xi}.$$

The formula (4.14) shows that advancing the solution of the scheme by one time step is equivalent to multiplying the Fourier transform of the solution by the amplification factor $g(h\xi)$. From (4.14) we obtain the important formula

$$\hat{v}^n(\xi) = g(h\xi)^n \hat{v}^0(\xi). \tag{4.15}$$

By means of the Fourier transform every one-step scheme can be put in the form (4.15), and this provides a standard method for studying the wide variety of schemes. All the information about a scheme is contained in its amplification factor, and we show how to extract important information from it. In particular, the stability and accuracy of schemes is easy to determine from the amplification factor. We now use formula (4.15) to study the stability of scheme (4.13). By Parseval's relation,

$$h \sum_{m=-\infty}^{\infty} |v_m^n|^2 = \int_{-\pi/h}^{\pi/h} |\hat{v}^n(\xi)|^2 d\xi = \int_{-\pi/h}^{\pi/h} |g(h\xi)|^{2n} |\hat{v}^0(\xi)|^2 d\xi.$$

Thus we see that the stability inequality will hold, with $J = 0$, if $|g(h\xi)|^{2n}$ is suitably bounded. We now evaluate $|g(h\xi)|$. Setting $\theta = h\xi$, we have

$$g(\theta) = (1 - a\lambda) + a\lambda e^{-i\theta} = (1 - a\lambda) + a\lambda \cos\theta - i a\lambda \sin\theta.$$

To evaluate $|g(\theta)|^2$ we add the squares of the real and imaginary parts. We also make use of the half-angle formulas for the sine and cosine functions. These are

$$1 - \cos\varphi = 2\sin^2 \frac{1}{2}\varphi \quad \sin\varphi = 2\sin\frac{1}{2}\varphi\cos\frac{1}{2}\varphi.$$

We then have:

$$
\begin{aligned}
|g(\theta)|^2 &= (1 - a\lambda + a\lambda\cos\theta)^2 + a^2\lambda^2\sin^2\theta \\
&= (1 - 2a\lambda\sin^2\tfrac{1}{2}\theta)^2 + 4a^2\lambda^2\sin^2\tfrac{1}{2}\theta\cos^2\tfrac{1}{2}\theta \\
&= 1 - 4a\lambda\sin^2\tfrac{1}{2}\theta + 4a^2\lambda^2\sin^4\tfrac{1}{2}\theta + 4a^2\lambda^2\sin^2\tfrac{1}{2}\theta\cos^2\tfrac{1}{2}\theta \\
&= 1 - 4a\lambda(1 - a\lambda)\sin^2\tfrac{1}{2}\theta.
\end{aligned}
$$

We see from this last expression that $|g(\theta)|$ is bounded by 1 if $0 < a\lambda < 1$; thus

$$
h\sum_{m=-\infty}^{\infty}|v_m^n|^2 \le \int_{-\pi/h}^{\pi/h}|\hat{v}^0(\xi)|^2\,d\xi = h\sum_{m=-\infty}^{\infty}|v_m^0|^2,
$$

and the scheme is stable by Definition 4.1.4.

The exact condition for stability of constant coefficient one-step schemes is given in the next theorem. In general the amplification factor g will also depend on h and k.

Theorem 4.1.12. *A one-step finite difference scheme (with constant coefficients) is stable in a stability region Λ if and only if there is a constant K (independent of θ, k, and h) such that*

$$
|g(\theta, k, h)| \le 1 + Kk \tag{4.16}
$$

with $(k, h) \in \Lambda$. If $g(\theta, k, h)$ is independent of h and k, the stability condition (4.16) can be replaced by the restricted stability condition

$$
|g(\theta)| \le 1.
$$

The result of this theorem is proved in [157]. This theorem shows that to determine the stability of a finite difference scheme we need to consider only the amplification factor $g(h\xi)$. This analysis is usually called von Neumann analysis.

In the previous sections we classified schemes only on the basis of whether or not they are convergent, considering via the Lax-Richtmyer equivalence theorem, stability and consistency. But, two convergent schemes may differ considerably in how their solution approximates the solution of differential equations. Let us introduce the order of accuracy of a scheme (for a linear partial differential equation).

Definition 4.1.13. *A scheme $P_{h,k}v = 0$ that is consistent with the differential equation $Pu = 0$ is accurate of order p in time and order q in space if for any smooth function $\phi(x, t)$*

$$
P\phi - P_{h,k}\phi = O(k^p) + O(h^q).
$$

We will say that this scheme is accurate of order (p, q).

The quantity $P\phi - P_{h,k}\phi = O(k^p) + O(h^q)$ is called the *truncation error* of the scheme. Let us notice that, even if the schemes introduced in the previous sections refer to linear equations, they can be generalize to nonlinear hyperbolic equations.

4.1.5   Example of 3-Points Difference Schemes for Hyperbolic Conservation Laws

In this section, following [68] we present two of the most usual $3-$points difference schemes for hyperbolic conservation laws. We will use these schemes in the next section for our numerical simulations.

Let us consider the following Cauchy problem

$$\begin{cases} \partial_t u + \partial_x f(u) = 0 & x \in \mathbb{R}, t > 0, \\ \\ u(x,0) = u_0(x) \end{cases} \tag{4.17}$$

where f is a C^2 real valued function, $u_0 \in L^\infty(\mathbb{R})$, and we set $a(u) = f'(u)$. Let us consider the $(2l+1)-$points explicit difference scheme of the form:

$$v_m^{n+1} = H(v_{m-l}^n, \ldots, v_{m+l}^n), \quad \forall \, n \geq 0, m \in \mathbb{Z}, \tag{4.18}$$

where $H : \mathbb{R}^{2l+1} \to \mathbb{R}$, is a continuous function.

Definition 4.1.14. *The difference scheme* (4.18) *can be put in the conservative form if there exists a continuous function $g : \mathbb{R}^{2l} \to R$ such that*

$$H(v_{-l}, \ldots, v_l) = v_0 - \lambda\{g(v_{-l+1}, \ldots, v_l) - g(v_{-l}, \ldots, v_{l-1})\}. \tag{4.19}$$

The function g is called *numerical flux.* Then the scheme (4.18) becomes:

$$v_m^{n+1} = v_m^n - \lambda\{g(v_{m-l+1}^n, \ldots, v_{m+l}^n) - g(v_{m-l}^n, \ldots, v_{m+l-1}^n)\}.$$

Let us set for simplicity

$$g_{m+1/2}^n = g(v_{m-l+1}^n, \ldots, v_{m+l}^n), \quad g_{m-1/2}^n = g(v_{m-l}^n, \ldots, v_{m+l-1}^n).$$

1. **Lax-Friedrichs Scheme**

$$v_m^{n+1} = \frac{(v_{m+1}^n + v_{m-1}^n)}{2} - \lambda \frac{(f(v_{m+1}^n) - f(v_{m-1}^n))}{2}. \tag{4.20}$$

It can be put in the conservative form with the following numerical flux

$$g^{LF}(u,v) = \frac{(f(u) + f(v))}{2} - \frac{(v-u)}{2\lambda},$$

and it is l^2-stable and first order accurate.

2. **The Upwind Scheme**
We have already introduced this scheme in the previous section in the case of transport equation. The scheme has a natural extension in the nonlinear case when the function f is monotone:

$$v_m^{n+1} = \begin{cases} v_m^n - \lambda\{f(v_m^n) - f(v_{m-1}^n)\} & \text{if } f' > 0 \\ \\ v_m^n - \lambda\{f(v_{m+1}^n) - f(v_m^n)\} & \text{if } f' < 0. \end{cases} \tag{4.21}$$

This scheme is consistent with equation (4.17), l^2-stable and first order accurate monotone. In the general case where f is not monotone, a scheme that provides suitable extensions of the upwind scheme is the Engquist-Osher scheme. More details on three points different schemes can be found in [68].

4.1.6   High Order Schemes

Given a sequence $v = \{v_m\}_{m \in \mathbb{Z}}$, let us introduce the following norm

$$TV(v) = \sum_{m \in \mathbb{Z}} |v_{m+1} - v_m|.$$

Definition 4.1.15. *A finite difference scheme is said to be total variation diminishing (TVD) if*

$$TV(v^{n+1}) \leq TV(v^n), \quad \forall\, n \geq 0.$$

A 3− points TVD conservative difference scheme is at most first order accurate, but it is possible to construct second order TVD schemes thanks to different techniques.

The first one, proposed by Sweby and Davis, is the Flux Limiters method. It is based on the idea to convert a 3−points first order accurate TVD scheme into a 5−points second order accurate TVD scheme. In the Flux Limiters approach, the numerical flux is corrected, and this correction to the underlying 3− points scheme is limited to ensure that the limiting scheme is TVD.

Another technique is the Van Leer's scheme, that is to say a second order extension of the Godunov's method, using piecewise linear instead of piecewise constant approximation of the solution. It relies on the integral form of the conservation law and involves the exact or approximate solution of local Riemann problems, adding a procedure of slope-limiting to preserve monotonicity. Piecewise Parabolic Method (PPM) and Essentially Non Oscillatory (ENO) schemes are higher order Godunov-type schemes. For much details about high order schemes see for instance [68].

4.1.7   Finite Difference Schemes for Parabolic Equations

In this section we present finite difference schemes for parabolic equations. The definitions of convergence, consistency, stability, and accuracy of finite difference schemes given in previous sections were given in a sufficient general way so that they also apply to schemes for parabolic equations.

1. **The standard Explicit Scheme**

   $$v_m^{n+1} = v_m^n + \frac{bk}{h^2}(v_{m-1}^n - 2v_m^n + v_{m+1}^n). \tag{4.22}$$

   Let $\mu = k/h^2$. The parameter μ plays a role for parabolic equations similar to the role of λ for hyperbolic equations. The scheme (4.22) is easily seen to be first-order accurate in time and second-order in space. The stability analysis is similar to what we did for hyperbolic equations, i.e., replace v_m^n by $g^n e^{im\theta}$. So this scheme is stable under the CFL condition $b\mu \leq \frac{1}{2}$.

2. **The standard Implicit Scheme**

   $$v_m^{n+1} = v_m^n + \frac{bk}{h^2}(v_{m-1}^{n+1} - 2v_m^{n+1} + v_{m+1}^{n+1}). \tag{4.23}$$

   This scheme is unconditionally stable. By a Taylor expansion it is also easy to check that also this scheme is accurate of order $(1,2)$, first order in time and second order in space. It is then useful to introduce other schemes to have higher accuracy.

3. **The θ-Method and the Crank-Nicolson Scheme**
   A natural generalization of the two previous schemes is the following

   $$v_m^{n+1} = v_m^n + \frac{bk}{h^2}\left[\theta(v_{m-1}^{n+1} - 2v_m^{n+1} + v_{m+1}^{n+1}) + (1-\theta)(v_{m-1}^n - 2v_m^n + v_{m+1}^n)\right], \tag{4.24}$$

where $0 \le \theta \le 1$. It is clear that for $\theta = 0$ we get the explicit scheme (4.22), while for $\theta = 1$ we get the implicit one (4.23). Let $\theta \ne 0$, by the von Neumann analysis we obtain

$$g = \frac{1 - 4b(1-\theta)\mu\sin^2\frac{\chi}{2}}{1 + 4b\theta\mu\sin^2\frac{\chi}{2}},$$

since $\mu > 0$ then $g \le 1$. Thus we have instability for $g < -1$, i.e. if

$$4(1-2\theta)\mu\sin^2\frac{\chi}{2} > 2.$$

Therefore, for $0 \le \theta < \frac{1}{2}$ the method is l^2-stable if and only if

$$\mu \le \frac{1}{2}(1-2\theta)^{-1},$$

while, for $1/2 \le \theta \le 1$ the method is l^2-stable for all μ.

For this scheme the truncation error is given by

$$
\begin{aligned}
T_m^{n+\frac{1}{2}} & = (\partial_t u - b\partial_{xx} u) + \left[\left(\frac{1}{2} - \theta\right) bk\partial_{xx}\partial_t u - \frac{b}{12}h^2\partial_x^4 u\right] + \left[\frac{1}{24}k^3\partial_t^3 u - \frac{b}{8}k^2\partial_{xx}\partial_{tt}\right] + \\
& + \left[\frac{1}{12}\left(\frac{1}{2} - \theta\right)bkh^2\partial_x^4\partial_t u - \frac{2b}{6!}h^4\partial_x^6 u\right].
\end{aligned}
$$

The scheme is then accurate of order $(1,2)$ for all $\theta \ne 1/2$. For $\theta = 1/2$ the scheme is accurate of order $(2,2)$ and it is called the Crank-Nicolson scheme. Let us notice that the Crank-Nicolson scheme is unconditionally stable.

4.2 Advanced Methods for Hyperbolic Systems

4.2.1 Relaxation Schemes

In this section we present a class of numerical schemes based on a discrete kinetic approximation for multidimensional hyperbolic systems of conservation laws proposed by Aregba-Driollet and Natalini in [13].

We will use this class of schemes in the following to approximate solutions to two dimensional hyperbolic, and hyperbolic-parabolic systems studied analytically in Chapters 2 and 3.

We consider a weak solution $u : \mathbb{R}^d \times [0, T] \to \mathcal{U}$, with $\mathcal{U}$ a convex subset of $\mathbb{R}^k$ to the Cauchy problem

$$\partial_t u + \sum_{j=1}^{d} \partial_{x_j} A_j(u) = 0, \tag{4.25}$$

$$u(x,0) = u_0(x), \tag{4.26}$$

where the system is hyperbolic (symmetrizable) and the flux functions A_j are locally Lipschitz continuous on $\mathbb{R}^k$ with values in $\mathcal{U}$. First we introduce the BGK discrete approximation and outline the general setting of own framework.

Let us consider also a non-empty family E of convex smooth entropies for (4.25). We assume that E is separable, that is to say it contains a countable set which is dense in a suitable topology. In particular, E can be just a single convex entropy.

We approximate problem (4.25), (4.26) by a sequence of semilinear systems

$$\partial_t f^\epsilon + \sum_{j=1}^d \Lambda_j \partial_{x_j} f^\epsilon = \frac{1}{\epsilon}(M(\sum_{i=1}^l f_i^\epsilon) - f^\epsilon) \tag{4.27}$$

with Cauchy data

$$f^\epsilon(x,0) = f_0^\epsilon(x). \tag{4.28}$$

Here ϵ is a positive number, Λ_j are real diagonal $l \times l$ matrices, $f_i = (f_i^1, \ldots, f_i^k)$ for $i = 1, \ldots, l$, and M is a Lipschitz continuous function defined on $\mathbb{R}^k$ with values in $\mathbb{R}^l$. Then we have

$$\partial_t f_i^\epsilon + \sum_{j=1}^d \Lambda_j^{i,i} \partial_{x_j} f_i^\epsilon = \frac{1}{\epsilon}(M_i(\sum_{i=1}^l f_i^\epsilon) - f_i^\epsilon), \, i = 1, \ldots l. \tag{4.29}$$

Then we set $u^\epsilon := \sum_{i=1}^l f_i^\epsilon$.

Moreover we suppose that the following relations are satisfied for all $u \in \Omega$, for some fixed rectangle $\Omega \subset \mathbb{R}^k$:

$$\begin{cases} \sum_{i=1}^l M_i(u) = u, \\ \\ \sum_{i=1}^l \Lambda_j M_i(u) = A_j(u), \quad j = 1, \ldots, d. \end{cases} \tag{4.30}$$

It is easy to see that, if f^ϵ converges in some strong topology to a limit f and, if $\sum_{i=1}^l f_{i0}^\epsilon$ converges to u_0, then $\sum_{i=1}^l f_i$ is a solution of problem (4.25), (4.26).

In fact system (4.27) is just a BGK approximation for (4.25); see [29] and references therein.

The interaction term on the right-hand side is given by the difference between a nonlinear function, which describes the equilibria of the system, in our case $M(\sum_{i=1}^l f_i)$, and the unknown f. Now, we consider a family of convex sets $\mathscr{D}_i \subset \mathbb{R}^k$ and assume that it is invariant under the action of the kinetic equation (4.29). Indeed, if we assume that

$$\forall u \in \mathscr{U}: \quad M_i(u) \in \mathscr{D}_i, \tag{4.31}$$

then we have

$$\forall t \geq 0, \forall x \in \mathbb{R}^d: \quad f_i(x,t) \in \mathscr{D}_i$$

as soon as it is true at t = 0. In the following, we will assume that convex sets $\mathscr{D}_i$ are chosen, and in particular we will take $\mathscr{D}_i := \{M_i(u) : u \in \mathscr{U}\}$.

Definition 4.2.1. *A kinetic entropy for the system* (4.29) *is a convex function* $H(f) = \sum_{i=1}^l H_i(f)$, *with* $H_i : \mathscr{D}_i \to \mathbb{R}$ *such that*

(H1) *for each* $u \in \mathscr{U}$

$$H(M(u)) = \eta(u),$$

where $\eta \in E$, *the family of convex smooth entropies.*

(H2) *for each $f = (f_1, \ldots, f_l)$, with $f_i \in \mathscr{D}_i$, let $u_f := \sum\limits_{i=1}^{l} f_i \in \mathscr{U}$*

$$H(M(u_f)) \leq H(f).$$

Let us notice that for any $\eta \in E$, there exists a kinetic entropy H for system (4.29). Under conditions (H1) and (H2), it is easy to obtain an entropy inequality for the function H.

Now we characterize the existence of a kinetic entropy H that satisfies (H1) and (H2).

We assume that M_i are given functions satisfying the consistency conditions (4.30) and $\mathscr{D}_i$ are convex sets such that the condition (4.31) holds. We define the vector space of Maxwellians:

$$\mathscr{M}^\epsilon = \left\{ M : \mathscr{U} \to \mathbb{R}^l \,|\, \forall \eta \in E, \forall i : (M_i')^t \eta'' \text{ is symmetric everywhere in } \mathscr{U} \right\}, \tag{4.32}$$

and the convex cone of nondecreasing Maxwellians

$$\mathscr{M}_+^\epsilon = \left\{ M \in \mathscr{M}^\epsilon \,|\, \forall \eta \in E, \forall i : (M_i')^t \eta'' \geq 0 \text{ everywhere in } \mathscr{U} \right\}. \tag{4.33}$$

Moreover, we introduce the function

$$\widetilde{H}(u) = \sum_{i=1}^{l} \widetilde{H}_i(u) \tag{4.34}$$

where $\widetilde{H}_i(u) := H_i(M_i(u))$. So the condition (H_1) can be written in the form

$$\widetilde{H}(u) = \eta(u) \quad u \in \mathscr{U}.$$

Now, we report a characterization of kinetic entropy H, which has been proved by Bouchut in [21, 22].

Theorem 4.2.2. *Let us assume that $\mathscr{U}$ is an open subset of $\mathbb{R}^k$, and that $M \in C^1(\mathscr{U})$. We also assume that*

(i) *for η in a dense subset of E, $\eta'' > 0$ and $\nabla_u \eta(\mathscr{U})$ is convex;*

(ii) *for each $i = 1, \ldots, l$ M_i is a C^1 diffeomorphism from U onto the convex open set $\mathscr{D}_i = \{M_i(u) : u \in \mathscr{U}\}$.*

Then, the existence of convex functions $(H)_{\eta \in E}$ satisfying (H1)-(H2) and such that the $\widetilde{H}$ defined in (4.34) is $C^1(\mathscr{U})$, is equivalent to

$$M \in \mathscr{M}_+^E.$$

Moreover, if this is true, we have

$$\forall u \in \mathscr{U}, \forall i : \quad \nabla_u \widetilde{H}_i = (M_i')^t \nabla_u \eta.$$

The general result of Bouchut [21, 22] ensure that, if the Maxwellian functions satisfy a "nondecreasing" condition, a BGK model is endowed with a kinetic entropy, namely entropy for the semilinear approximating system, which reduces to a given entropy of the limit system, as the relaxation parameter tends to zero.

Let us notice that the "nondecreasing" condition on the Maxwellians has a key role in the study of discrete kinetic approximations, and it is important to have a characterization of the space of this kind of functions. Here we report a characterization of the stability condition presented in [21].

Proposition 4.2.3. *Consider an open set $\mathcal{U} \subset \mathbb{R}^k$. Assume that E contains at least a strictly convex entropy η_0 and $M \in \mathcal{M}^\epsilon$ belongs to $C^1(\mathcal{U})$. Then, for all $u \in \mathcal{U}$ and $i \in 1,\ldots,l$ the Jacobian matrix M_i' is diagonalizable (and thus has only real eigenvalues). Moreover, $M \in \mathcal{M}_+^\epsilon$ if and only if*

$$\forall u \in \mathcal{U}^+, \forall i \in 1,\ldots,l \quad \sigma(M_i') \subset [0,+\infty[, \tag{4.35}$$

where σ denotes the spectrum.

A proof of the proposition can be found in [21].

Let us now present a numerical scheme for the relaxing problem (4.27)-(4.28) in order to obtain a numerical approximation of (4.17), in the relaxed limit $\epsilon = 0$.

The numerical schemes presented in [13] are constructed by splitting (4.27) into a homogeneous linear part and an ordinary differential system, which is exactly solved thanks to the particular structure of the source term.

In the scalar case this construction allows to preserve the monotonicity properties of (4.28) and to prove convergence results.

The approximation framework generalizes to systems the construction presented in [119] for the scalar case, and shares most of the advantages of the relaxation approximation as proposed in [85] (see also [118, 12]): simple formulation even for general multidimensional systems of conservation laws and easy numerical implementation, hyperbolicity, regular approximating solutions.

Actually the main advantage, especially in the multidimensional case, of both the approximations, seems to be the possibility of avoiding the resolution of local Riemann problems in the design of numerical schemes as done in Godunov scheme. Moreover this framework presents some special properties:

- the scalar and the system cases are treated in the same way at the numerical level;

- all the approximating problems are in diagonal form, which is very likely for numerical and theoretical purposes;

- we can easily change the number and the geometry of the velocities involved in our construction to improve the accuracy of the method.

Even if these algorithms are not optimal, they illustrate how to construct an efficient and simple approximation even for very complicated systems. And this property could be useful in the numerical investigation of systems like those arising in chemotaxis and vasculogenesis modeling.

First we report the technique adopted by Aregba-Driollet and Natalini, [13] to solve numerically (4.27)-(4.28). The space time domain $\mathbb{R}^d \times [0,T]$ is discretized by a square grid

$$\mathbb{R}^d = \bigcup_{\alpha \in \mathbb{Z}^d} I_\alpha, \quad [0,T] = \bigcup_{0 \le n \le N-1} [t_n, t_{n+1}].$$

Set $\alpha = (\alpha_j)_{1 \le j \le d}$ and let e_j be the canonical j^{th} vector in $\mathbb{R}^d$. Let us now denote by $f_\alpha^{\epsilon,n}$ the approximation of f at the point $x_\alpha \in \mathbb{R}^d$ and at time t_n.

System (4.27) is split into a linear diagonal hyperbolic part and an ordinary differential system. For a given $f^{\epsilon,n}$, the function $f^{\epsilon,n+\frac{1}{2}}$ is an approximate solution at time t_{n+1} of the problem

$$\begin{cases} \partial_t f + \sum_{j=1}^d \Lambda_j \partial_{x_j} f = 0, \\ f(t_n) = f^{\epsilon,n}. \end{cases} \tag{4.36}$$

As the system is diagonal, it is possible to consider each equation separately. We suppose that the scheme can be put in conservative form:

$$f_\alpha^{\epsilon,n+\frac{1}{2}} = f_\alpha^{\epsilon,n} - \frac{k}{h}\sum_{j=1}^{d}\Lambda_j(\Phi_{\alpha+\frac{1}{2}e_j}^{\epsilon,n} - \Phi_{\alpha-\frac{1}{2}e_j}^{\epsilon,n}) \tag{4.37}$$

where

$$\Phi_{\alpha+\frac{1}{2}e_j}^{\epsilon,n} = \begin{pmatrix} \Psi_{1,j}(f_{\alpha-k_1+e_j,1}^{\epsilon,n},\ldots,f_{\alpha+k_1,1}^{\epsilon,n}) \\ \cdot \\ \cdot \\ \cdot \\ \Psi_{l,j}(f_{\alpha-k_l+e_j,l}^{\epsilon,n},\ldots,f_{\alpha+k_l,l}^{\epsilon,n}) \end{pmatrix}.$$

Here $k_i \in \mathbb{Z}^d$ and $\Psi_{i,j}(g,\ldots,g) = g$, for $i = 1,\ldots,l$.

To take into account the contribution of the singular perturbation term on the right-hand side, the following ordinary differential system is solved on $[t_n, t_{n+1}]$

$$F' = \frac{1}{\epsilon}(M(\sum_{i=1}^{l} F_i) - F) \tag{4.38}$$

with the initial data

$$F(t_n) = f_\alpha^{\epsilon,n+\frac{1}{2}},$$

for all $\alpha \in \mathbb{Z}^d$. Using (4.30) we obtain

$$\sum_{i=1}^{l} F_i' = 0,$$

so that the solution of (4.38) with data $F(t_n) = G$ at t_n can be explicitly obtained as

$$S(t, t_n, G) = M(\sum_{i=1}^{l} G_i) + \exp\left(-\frac{t-t_n}{\epsilon}\right)[G - M(\sum_{i=1}^{l} G_i)].$$

Hence

$$f_\alpha^{\epsilon,n+1} = M(u_\alpha^{\epsilon,n+\frac{1}{2}}) + \exp\left(-\frac{\Delta t_n}{\epsilon}\right)[f_\alpha^{\epsilon,n+\frac{1}{2}} - M(u_\alpha^{\epsilon,n+\frac{1}{2}})],$$

where u is defined by

$$u = \sum_{i=1}^{l} f_i.$$

Note that

$$u_\alpha^{\epsilon,n+1} = u_\alpha^{\epsilon,n+\frac{1}{2}}.$$

This way a wide family of numerical schemes for the semilinear system (4.27), which differ by the choice of the homogeneous scheme (HS) has been constructed. In the following, the numerical scheme described will be referred to as discrete kinetic scheme (DKS).

When $\epsilon \to 0$ in DKS, we obtain the relaxed limit of the scheme:

$$\begin{cases} f^{n,\alpha} &= M(u^{n,\alpha}), \\\\ f^{n+\frac{1}{2},\alpha} &= H(k)f^{n,\alpha}, \\\\ u^{n+1,\alpha} &= \sum_{i=1}^{l} f_i^{n+\frac{1}{2},\alpha}, \end{cases} \tag{4.39}$$

In [12] it is shown a rigorous convergence result for DKS and the associated relaxed scheme for the scalar conservation law obtaining the convergence towards the unique solution of (4.27) - (4.28) when ϵ is fixed. Moreover the authors showed the behavior of the numerical schemes as the parameter ϵ tends to zero.

The resulting numerical scheme is TVD and converges to a weak solution of (4.25) -(4.26). Moreover, if HS is monotone, the limit scheme is also monotone and converging to the unique entropy solution of (4.25) -(4.26).

4.2.2   Asymptotic High Order Schemes

It is often difficult to find an effective numerical approximation to hyperbolic equations with a source term, due to problems like stiffness of the source term, instability of the solutions, incorrect approximation of stationary solutions.

Many families of schemes were introduced to face these problems: well balanced, Runge-Kutta IMEX, upwinding source, and asymptotic preserving. One of the main ideas is to plug the knowledge of the analytical behavior of the solutions into the scheme, to guarantee a better approximation, at least around some relevant asymptotic states of the problem. This is not always easy, also due to the problem of obtaining a fine "qualitative analysis" of the solutions, in particular for nonlinear problems.

Following [143, 24, 120] we introduce some schemes which are increasingly accurate for large times, with respect to the asymptotic behavior of solutions. This property of accuracy is required in order to get better results for large time simulations when computing perturbations of non constant stable states. Given a family of stable asymptotic states for a given evolutionary problem, we say that a numerical scheme is Asymptotic High Order, in the following we simply write AHO, if it is high-order accurate, with respect to the local truncation error, when restricted to every element of this family.

A similar approach has been first introduced by Roe [143] for hyperbolic conservation laws with source term. The author proposed the upwinding of the source term, giving a first example of a first order monotone scheme, which is second order on all steady states.

In [73] and [17], a quite complete theory of global existence and of the asymptotic behavior of smooth solutions for this type of systems was developed, actually in a nonlinear and fully multi-dimensional framework.

As seen in the previous chapters this theory needs for an extra assumption, the so-called Shizuta-Kawashima condition [153], which guarantees for a sufficient coupling between the source and the advection terms. Roughly speaking, under these assumptions, it is possible to prove that for every perturbation of a given stationary solution to problem, the corresponding solution decays in the L^p-norm to its unperturbed state as $O(t^{-\frac{1}{2}(1-\frac{1}{p})})$ for $p \in [1, \infty]$. Here we present some results of [24, 11] on this type of scheme. Following [11] here we show that, for 2×2 dissipative hyperbolic systems, it is possible to introduce AHO schemes which are compatible with the behavior predicted by the qualitative analysis, respectively for the long-time asymptotic and in the Chapman-Enskog regimes.

The main idea is to modify standard upwinding schemes to keep into account the long-time behavior of the solutions. Here we will show the description of these schemes which are AHO respectively around the perturbation of general steady states and in the diffusion limit. In [11] some numerical tests presented, showed the better performance of these schemes with respect to the usual pointwise approximation of the source term, and even with the classical upwinding of the source pro-

posed by Roe in 1986 [143]. In particular, numerical tests showed that the L^∞ global error of main diffusive adapted AHO2p-scheme decays as $O(1/t)$, in agreement with the decay given, for a given fixed space step, against the decay as $O(1/\sqrt{t})$ of the other schemes.

Now we outline briefly the core ideas which shape AHO schemes for general hyperbolic systems. Let u be a solution to the general 2×2 linear hyperbolic system

$$\partial_t u + A \partial_x u = Bu, \tag{4.40}$$

where

$$A = \begin{pmatrix} a & b \\ b & c \end{pmatrix}, \quad B = -\begin{pmatrix} 0 & 0 \\ 0 & d \end{pmatrix}. \tag{4.41}$$

Let

$$u^{n+1} = H(u^n) \tag{4.42}$$

be a numerical scheme consistent with system (4.40) and T^h its local truncation error. Usually, the local truncation error is only of first order for a smooth solution to (4.40), which is

$$T^h(u) = O(h + k).$$

We also consider generic stationary solutions $\hat{u}$ to the same problem, namely such that

$$A \partial_x \hat{u} = B \hat{u}.$$

We can diagonalize the matrix A:

$$A = R \Lambda R^{-1}$$

where $\Lambda = \text{diag}(\lambda_1, \lambda_2)$ and $R = (r^{(1)}, r^{(2)})$ is the column matrix of the right eigenvectors, i.e. $A r^{(i)} = \lambda_i r^{(i)}$. Introducing the notation

$$w = R^{-1} u$$

problem (4.40) becomes

$$\begin{cases} \partial_t w + \Lambda \partial_x w = \tilde{B} w, \\ \\ w(x, 0) = w_0(x) = R^{-1} u_0(x), \end{cases} \tag{4.43}$$

we denote by $\tilde{B} = R^{-1} B R$. We will present the method for problem (4.43).

We denote by h the uniform mesh-length and by $x_l = lh$ the spatial grid points for all $l \in \mathbb{Z}$. The time levels t_n, with $t_0 = 0$, are also spaced uniformly with mesh-length $k = t_{n+1} - t_n$ for $n \in \mathbb{N}$. We denote by δ the CFL ratio $\delta = k/h$, which is taken constant.

The initial data w_0 is supposed to be smooth and is approximated by its node values. The approximate solution $w^{n,l} = (w_1^{n,l}, w_2^{n,l})^t$ is given by

$$\frac{w^{n+1,l} - w^{n,l}}{k} + \frac{\Lambda}{2h}(w^{n,l+1} - w^{n,l-1}) - \frac{Q}{2h}(w^{n,l+1} - 2w^{n,l} + w^{n,l-1}) \tag{4.44}$$
$$= \tilde{\mathscr{B}}_{-1} w^{n,l-1} + \tilde{\mathscr{B}}_0 w^{n,l} + \tilde{\mathscr{B}}_1 w^{n,l+1}, \quad l \in \mathbb{Z}, n \in \mathbb{N}$$
$$w^{0,l} = w^0(x_l), \quad l \in \mathbb{Z},$$

where $Q = \text{diag}(q_1, q_2)$ is the diagonal matrix of the artificial diffusion terms $q_i \geq 0$ ($i \in \{1, 2\}$), and $\tilde{\mathscr{B}}_{-1} = (\tilde{\beta}_{ij}^{-1})_{i,j=1,2}$, $\tilde{\mathscr{B}}_0 = (\tilde{\beta}_{ij}^0)_{i,j=1,2}$ and $\tilde{\mathscr{B}}_1 = (\tilde{\beta}_{ij}^1)_{i,j=1,2}$ are 2×2 constant matrices that define the

source approximation. Those matrices may depend on h.

The scheme (4.44) can be seen as a linear function

$$w^{n+1} = H(w^n). \tag{4.45}$$

More precisely we have

$$w_i^{n+1,l} = H_i(w^{n,l-1}, w^{n,l}, w^{n,l+1}), \quad i \in \{1,2\}, \quad l \in \mathbb{Z}.$$

Moreover we assume that the scheme satisfies the following property:

- Consistency.
  The scheme (4.44) is consistent with problem (4.43), i.e

$$\tilde{\mathscr{B}}_{-1} + \tilde{\mathscr{B}}_0 + \tilde{\mathscr{B}}_1 = \tilde{B} + h\tilde{C}, \tag{4.46}$$

  where $\tilde{C} = (\tilde{c}_{ij})_{i,j=1,2}$ is a 2×2 constant matrix not depending on h and k.

In [11], Aregba Driollet et al. showed that, under an additional monotonicity assumption the scheme (4.44) converges in $L^\infty([0, T], L^1(\mathbb{R}) \cap L^\infty(\mathbb{R}))$ towards the solution of the Cauchy problem (4.43).

Moreover in [11] the discretization of the source term, defined by coefficients $\tilde{\mathscr{B}}_{-1,0,1}$, is studied to present some schemes which are increasingly accurate for large times, with respect to the asymptotic behavior of solutions. This property of accuracy is required in order to get better results for large time simulations when computing perturbations of non constant stable states.

We say that the scheme (4.42) is (locally) Asymptotic High Order of order p, which will be denoted by (AHO)p, for system (4.40), if the scheme is of order p on every stationary solution $\hat{u}$, i.e.

$$T^h(\hat{u}) = O(h^p).$$

Now we present two AHO schemes of different order, presented in [11].

1. **Pointwise approximation of the source term (AHO1-UP).**
   Fixing, for the differential terms, the upwind approximation $Q = \text{diag}(|\lambda_1|, |\lambda_2|)$, the basic scheme gives a first-order approximation even on the stationary solution:

$$\tilde{\mathscr{B}}_{up}^{-1} = \begin{pmatrix} 0 & 0 \\ 0 & 0 \end{pmatrix}, \tilde{\mathscr{B}}_{up}^{0} = \begin{pmatrix} \tilde{b}_{11} & \tilde{b}_{12} \\ \tilde{b}_{21} & \tilde{b}_{22} \end{pmatrix}, \tilde{\mathscr{B}}_{up}^{1} = \begin{pmatrix} 0 & 0 \\ 0 & 0 \end{pmatrix},$$

   where $\tilde{B} = R^{-1}BR$. If we choose the matrix of the diagonalization of the system (4.40) as

$$R = \frac{d}{\lambda_2 - \lambda_1} \begin{pmatrix} 1 & 1 \\ -\dfrac{(a-\lambda_1)}{b} & -\dfrac{(\lambda_2 - a)}{b} \end{pmatrix},$$

   the corresponding source term is given by

$$\tilde{B} = \frac{d}{\lambda_2 - \lambda_1} \begin{pmatrix} -(a-\lambda_1) & (\lambda_2 - a) \\ (a-\lambda_1) & -(\lambda_2 - a) \end{pmatrix}. \tag{4.47}$$

2. **Upwinding of the source term (AHO2-ROE).**

   An improvement of the previous example is given by a second order upwinding scheme:

$$\tilde{\mathscr{B}}^{-1}_{roe} = \frac{1}{2} \begin{pmatrix} H(\lambda_1)\tilde{b}_{11} & H(\lambda_1)\tilde{b}_{12} \\ H(\lambda_2)\tilde{b}_{21} & H(\lambda_2)\tilde{b}_{21} \end{pmatrix}, \tilde{\mathscr{B}}^{0}_{roe} = \frac{1}{2} \begin{pmatrix} \tilde{b}_{11} & \tilde{b}_{12} \\ \tilde{b}_{21} & \tilde{b}_{21} \end{pmatrix}, \tag{4.48}$$

$$\tilde{\mathscr{B}}^{1}_{roe} = \frac{1}{2} \begin{pmatrix} (1-H(\lambda_1))\tilde{b}_{11} & (1-H(\lambda_1))\tilde{b}_{12} \\ (1-H(\lambda_2))\tilde{b}_{21} & (1-H(\lambda_2))\tilde{b}_{21} \end{pmatrix},$$

where $H(\cdot)$ is the Heaviside function and where, as above, $Q = \mathrm{diag}(|\lambda_1|,|\lambda_2|)$, and $\tilde{B}$ is defined as in (4.47).

4.3   Numerical Simulations: Semilinear Case

This section is devoted to the numerical simulations of the solutions to the semilinear hyperbolic-parabolic system studied in the previous chapter,

$$\begin{cases} \partial_t u + \nabla \cdot v = 0, \\\\ \partial_t v + \gamma^2 \nabla u = -b(\phi, \nabla\phi)v + h(\phi, \nabla\phi, u), \\\\ \partial_t \phi = \Delta\phi + f(u, \phi). \end{cases} \tag{4.49}$$

We consider the two dimensional case with $u, \phi : \mathbb{R}^2 \times \mathbb{R}^+ \to \mathbb{R}$ and $v : \mathbb{R}^2 \times \mathbb{R}^+ \to \mathbb{R}^2$. We start our numerical study by considering only the hyperbolic part of the system without any source term, i.e. the wave equation. Subsequently we study the wave equation with damping and finally, we present the results obtained for the complete hyperbolic-parabolic system (4.49).

4.3.1   Wave Equation

Let us start our study considering the following system

$$\begin{cases} \partial_t u + \nabla \cdot v = 0, \\\\ \partial_t v + \gamma^2 \nabla u = 0, \end{cases} \tag{4.50}$$

with initial data

$$u(x,0) = u_0(x), \quad v(x,0) = v_0(x). \tag{4.51}$$

We can observe that this system is equivalent to the wave equation

$$\partial_t^2 u - \gamma^2 \Delta u = 0.$$

Our aim is to solve numerically equations (4.50) on a bounded domain $\Omega \subset \mathbb{R}^2$ with homogeneous Neumann boundary conditions for the function u :

$$\nabla u \cdot n|_{\partial\Omega} = 0, \tag{4.52}$$

and zero boundary condition for the normal component of v

$$v \cdot n|_{\partial\Omega} = 0. \tag{4.53}$$

Let us take $\Omega = [0, L] \times [0, L]$ and let us denote by h the space step. We consider the discretization points $x_\alpha = (\alpha_1 h, \alpha_2 h), 0 \le \alpha_i \le N + 1$. We denote the time step by k and the approximation of a function f at time $t_n = nk$ by f^n.

For each time step, we solve the hyperbolic equations using a relaxation method [13]. We choose this method for our simulations, instead of Lax Friedrichs, Godunow or Upwind, because these are quite dissipative.

As a matter of fact in Figure 4.4 it is possible to observe how the Relaxation scheme approximates better the solution than the Lax Friedrichs one.

Moreover our system even if linear, is not diagonalizable so it is not possible to use the Upwind scheme. The advantage of our relaxation method is the approximation of the equations by a diagonal system, easy to solve. Relaxation is also a convenient setting to extend the schemes to higher orders.

Now we explain our scheme in more details. Let us denote $w = (u, v^1, v^2)$ and rewrite (4.50) as

$$\partial_t w + \partial_{x_1} A_1(w) + \partial_{x_2} A_2(w) = 0,$$

with

$$A_1(w) = \begin{pmatrix} 0 & 1 & 0 \\ \gamma^2 & 0 & 0 \\ 0 & 0 & 0 \end{pmatrix} w, \quad A_2(w) = \begin{pmatrix} 0 & 0 & 1 \\ 0 & 0 & 0 \\ \gamma^2 & 0 & 0 \end{pmatrix} w.$$

We consider a simple 5-velocities relaxation scheme. Let us choose the five velocities as

$$\lambda_1 = \lambda(1, 0), \ \lambda_2 = \lambda(0, 1), \ \lambda_3 = \lambda(-1, 0), \ \lambda_4 = \lambda(0, -1), \ \lambda_5 = (0, 0), \tag{4.54}$$

for some $\lambda > 0$. Now we introduce the corresponding Maxwellians $M_i(w) \in \mathbb{R}^3, i = 1, \dots, 5$, of the form

$$M_i(w) = a_i w + b_{i1} A_1(w) + b_{i2} A_2(w), \tag{4.55}$$

for some constants a_i, b_{i1} and b_{i2} to be chosen.

The conditions of consistency of the Maxwellians are

$$\sum_{i=1}^{5} M_i(w) = w, \qquad \sum_{i=1}^{5} \lambda_{i,j} M_i(w) = A_j(w), \quad j = 1, 2. \tag{4.56}$$

Then, a possible choice of the coefficients a_i and b_{ij} is the following

$$a_1 = \cdots = a_4 = a, \ a_5 = 1 - 4a;$$

$$b_{11} = b_{22} = -b_{31} = -b_{42} = \frac{1}{2\lambda}, \ b_{ij} = 0 \text{ otherwise.}$$

It is easy to see that these coefficients satisfy conditions (4.56).

Let us now denote by $w^{n,\alpha}$ the approximation of w at the point $x_\alpha \in \mathbb{R}^2$ and at time t_n. We set the discretization of Maxwellians (4.55) as

$$f_i^{n,\alpha} = M_i(w^{n,\alpha}), \quad \text{for } i = 1, \cdots, 5. \tag{4.57}$$

We evolve each of the functions f_i, $1 \le i \le 5$, in time by following the velocity λ_i:

$$\begin{aligned}
f_i^{n+1/2,\alpha} = f_i^{n,\alpha} &- \mu \sum_{j=1}^{2} \lambda_{ij} (f_i^{n,\alpha_j+1} - f_i^{n,\alpha_j-1}) \\
&+ \mu \sum_{j=1}^{2} |\lambda_{ij}| (f_i^{n,\alpha_j+1} - 2 f_i^{n,\alpha} + f_i^{n,\alpha_j-1}),
\end{aligned} \tag{4.58}$$

where $\mu = \dfrac{k}{2h}$ and $\alpha_j + 1$ is a shift of the j-th component of the index α. We can observe that thanks to the choice of the velocities (4.54) the scheme for one component f_i becomes a one-dimensional scheme. Finally, we just end by setting

$$w^{n+1} = \sum_{i=1}^{5} f_i^{n+1/2}.$$

Here, following the results of Bouchut [21] (Proposition 4.2.3), we set the velocity $\lambda = \gamma$ and the time and space steps will have to satisfy the stability condition $\gamma \dfrac{k}{h} \leq 1$.

Now we explain how to impose the boundary conditions.

Let us consider our domain $\Omega = [0, L] \times [0, L]$ and the normal vectors n_i, for $i = 1, \dots, 4$, as indicated in Figure 4.1.
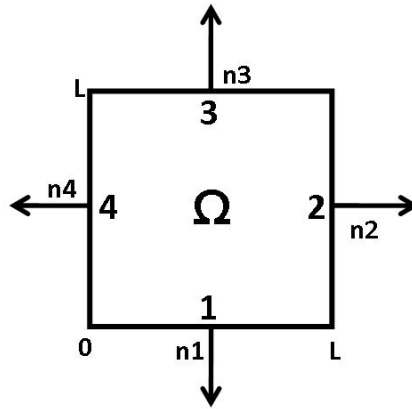
Figure 4.1: Domain $\Omega = [0, L] \times [0, L]$.

First we consider the edge 1. Since the normal vector $n_1 = (0, -1)$, by the boundary conditions (4.52)-(4.53) it follows that

$$\nabla u \cdot n_1 = -\partial_{x_2} u = 0, \qquad v \cdot n_1 = -v_2 = 0, \qquad \partial_{x_2} v_1 = 0. \tag{4.59}$$

The boundary condition for v_1 is obtained directly from the equations (4.50). Proceeding in a similar way for the edge 2, where $n_2 = (1, 0)$, we get

$$\nabla u \cdot n_2 = \partial_{x_1} u = 0, \qquad v \cdot n_2 = v_1 = 0, \qquad \partial_{x_1} v_2 = 0. \tag{4.60}$$

Regarding the conditions on edges 3 and 4, they are equivalent to the conditions (4.59) and conditions (4.60) respectively.

Using the above scheme, we have solved numerically system (4.50) with boundary conditions (4.52), (4.53) on a square domain $\Omega = [0, 1] \times [0, 1]$.

As initial data, we have chosen

$$u_0(x) = u_0(x_1, x_2) = \cos(2\pi x_1)\cos(2\pi x_2), \quad v_0(x) = 0,$$

and we have set $\gamma^2 = 1$. In Figure 4.2 we show numerical solutions of system (4.50) at different times. We can observe that the behavior of the approximate solution respects the oscillatory nature of the phenomenon, while the Lax Friedrichs scheme is more dissipative as shown in Figure 4.3.
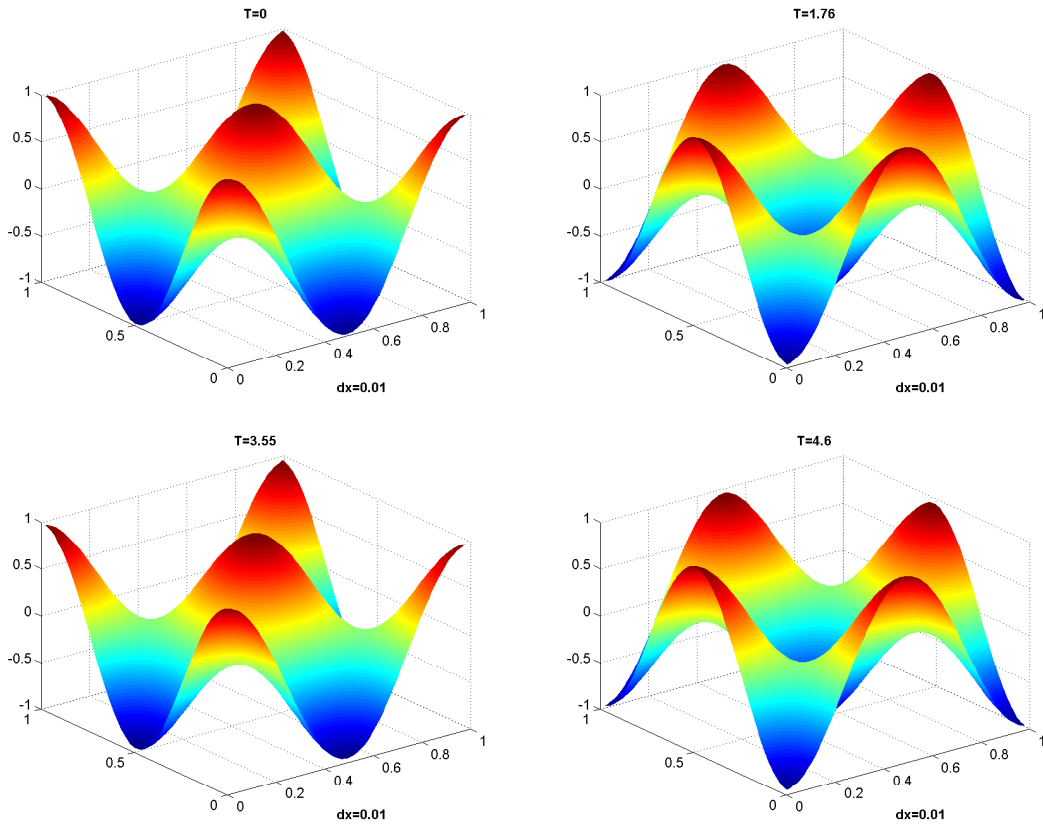
Figure 4.2: Numerical solution of system (4.50) with initial condition $u_0(x) = \cos(2\pi x_1)\cos(2\pi x_2)$, $v_0(x) = 0$, on a square domain $[0, 1] \times [0, 1]$ at different times $T = 0, 1.76, 3.55$ and 4.6. The numerical approximations are obtained by the Relaxation scheme.
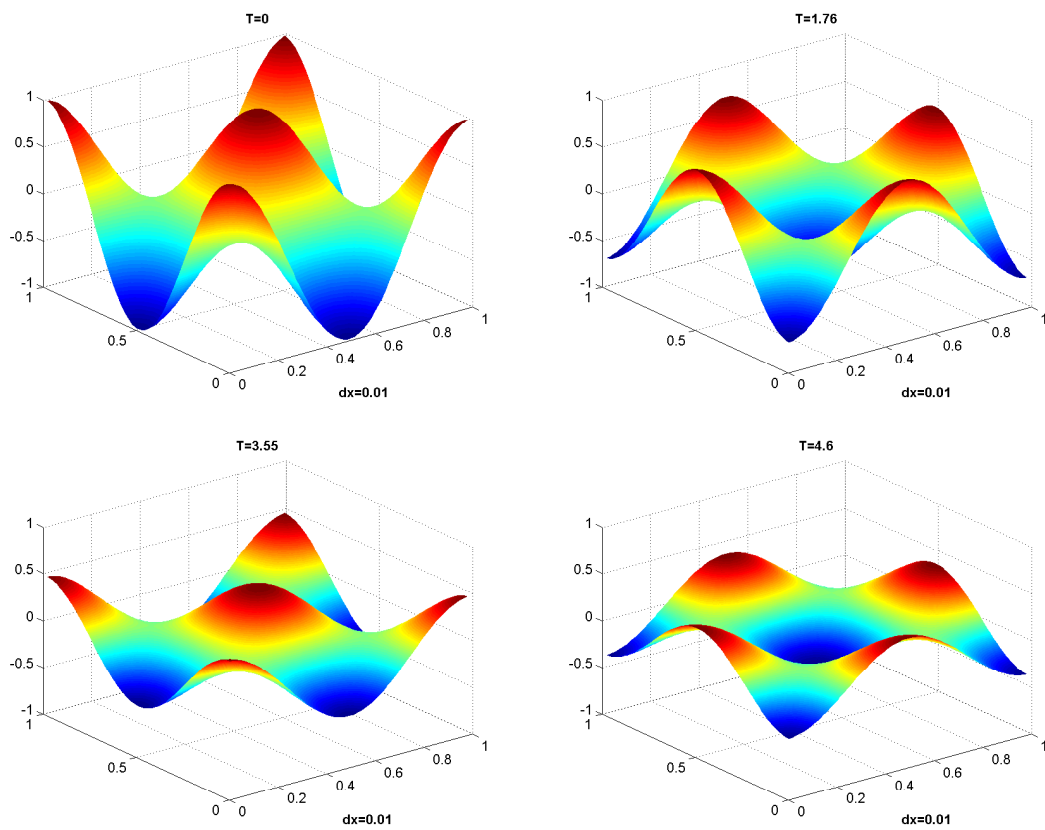
Figure 4.3: Numerical solution of system (4.50) with initial condition $u_0(x) = \cos(2\pi x_1)\cos(2\pi x_2)$, $v_0(x) = 0$ on a square domain $[0,1] \times [0,1]$ at different times $T = 0$, 1.76, 3.55 and 4.6. The numerical approximations are obtained by the Lax Friedrichs scheme.

Since the solution to this Cauchy problem is known, it is possible to compare the approximate solution to the real one

$$u(x,t) = \cos(\sqrt{2}2\pi t) u_0(x).$$

In Figure 4.4 we can notice that the dissipation of the Relaxation scheme is smaller than the dissipation of the Lax Friedrichs scheme.
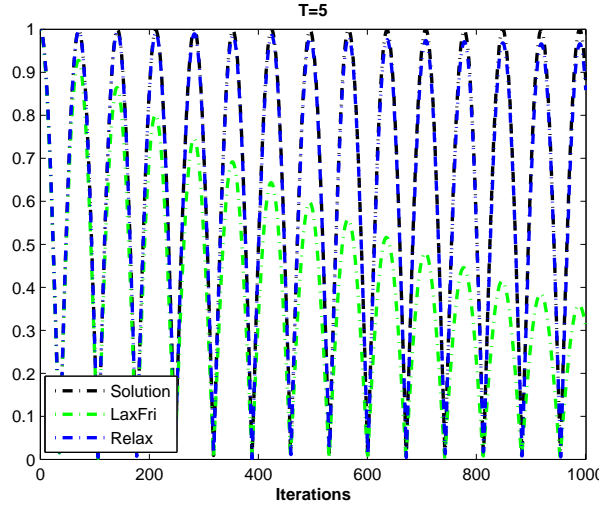
Figure 4.4: Comparison between the maximal values of the solution and of the approximated solutions to system (4.50) with Lax Friedrichs scheme and the Relaxation one until time $T = 5$. The initial conditions are $u_0(x) = \cos(2\pi x_1)\cos(2\pi x_2)$, $v_0(x) = 0$ and the domain is the square $[0,1] \times [0,1]$.

4.3.2   Wave Equation with Damping

Let us consider now the following system

$$\begin{cases} \partial_t u + \nabla \cdot v = 0, \\ \\ \partial_t v + \gamma^2 \nabla u = \gamma^2 \nabla \bar{u}_0 - v, \end{cases} \tag{4.61}$$

supplemented with initial data

$$u(x,0) = u_0(x), \quad v(x,0) = v_0(x). \tag{4.62}$$

System (4.61) is equivalent to the wave equation with damping, where we add a source term $\gamma^2 \nabla \bar{u}_0$,

$$\partial_t^2 u - \gamma^2 \Delta(u - \bar{u}_0) + \partial_t u = 0.$$

Due to the presence of a source term in (4.61), it is not easy to find an effective numerical approximation of the solution. We have solved numerically this problem by two methods, the first is the Relaxation method presented in the previous section, and the second one is the Relaxation joint with an AHO method for the source term.

We have solved system (4.61) with boundary conditions (4.52), (4.53) on a square domain $\Omega = [0,1] \times [0,1]$.

As initial data, we have chosen:

$$u_0(x) = u_0(x_1, x_2) = \cos(2\pi x_1)\cos(2\pi x_2) + \bar{u}_0,$$

$$v_0^1(x) = v_0^1(x_1, x_2) = \frac{4\pi}{(4\omega^2 - 1)}\gamma^2 \sin(2\pi x_1)\cos(2\pi x_2), \tag{4.63}$$

$$v_0^2(x) = v_0^2(x_1, x_2) = \frac{4\pi}{(4\omega^2 - 1)}\gamma^2 \cos(2\pi x_1)\sin(2\pi x_2),$$

where $\gamma^2 = 1$, and $\omega = \frac{\sqrt{4\gamma^2 8\pi^2 - 1}}{2}$. Here the source term $\bar{u}_0$ is taken equal to

$$\bar{u}_0(x) = \exp\left[-\frac{(x - \frac{1}{2})^2 + (y - \frac{1}{2})^2}{0.001}\right].$$

Then, the explicit solution of problem (4.61)-(4.63), is

$$u(x, t) = u(x_1, x_2, t) = \exp(-\frac{1}{2}t)\cos(\omega t)\cos(2\pi x_1)\cos(2\pi x_2) + \bar{u}_0(x_1, x_2). \tag{4.64}$$

First we have solved the Cauchy problem (4.61)-(4.63) using the Relaxation method presented in the previous section (4.58), adding the source term

$$F(w, \bar{w}) = \begin{pmatrix} 0 \\ \gamma^2 \partial_{x_1} \bar{u}_0 - v^1 \\ \gamma^2 \partial_{x_2} \bar{u}_0 - v^2 \end{pmatrix}.$$

Then we have obtained

$$w^{n+1} = \sum_{i=1}^{5} f_i^{n+1/2} + kF(w^n, \bar{w}).$$

Subsequently, in order to find a better approximation of the source term, we have used a generalization of the AHO2-Roe scheme (4.48). Then, starting from (4.58), we evolve each of the functions f_i, $1 \le i \le 5$, in time by following the velocity λ_i and we add the source term as:

$$f_i^{n+1/2,\alpha} = f_i^{n,\alpha} - \mu \sum_{j=1}^{2} \lambda_{ij}(f_i^{n,\alpha_j+1} - f_i^{n,\alpha_j-1}) + \mu \sum_{j=1}^{2} |\lambda_{ij}|(f_i^{n,\alpha_j+1} - 2f_i^{n,\alpha} + f_i^{n,\alpha_j-1})$$

$$+ \underbrace{k\nu_i \sum_{j=1}^{2}(\tilde{\beta}_{ij}^{-1} F^{n,\alpha_j-1} + \tilde{\beta}_{ij}^0 F^{n,\alpha} + \tilde{\beta}_{ij}^1 F^{n,\alpha_j+1})}_{G_i},$$

where $\sum_{i=1}^{5} \nu_i = 1$. The source terms G_i are respectively:

$$\lambda_1 = \lambda(1, 0), \quad G_1 = k\nu \frac{F^{n,\alpha_1-1} + F^{n,\alpha_1}}{2},$$

$$\lambda_2 = \lambda(0, 1), \quad G_2 = k\nu \frac{F^{n,\alpha_2-1} + F^{n,\alpha_2}}{2},$$

$$\lambda_3 = -\lambda(1, 0), \quad G_3 = k\nu \frac{F^{n,\alpha_1+1} + F^{n,\alpha_1}}{2}, \tag{4.65}$$

$$\lambda_4 = -\lambda(0, 1), \quad G_4 = k\nu \frac{F^{n,\alpha_2+1} + F^{n,\alpha_2}}{2},$$

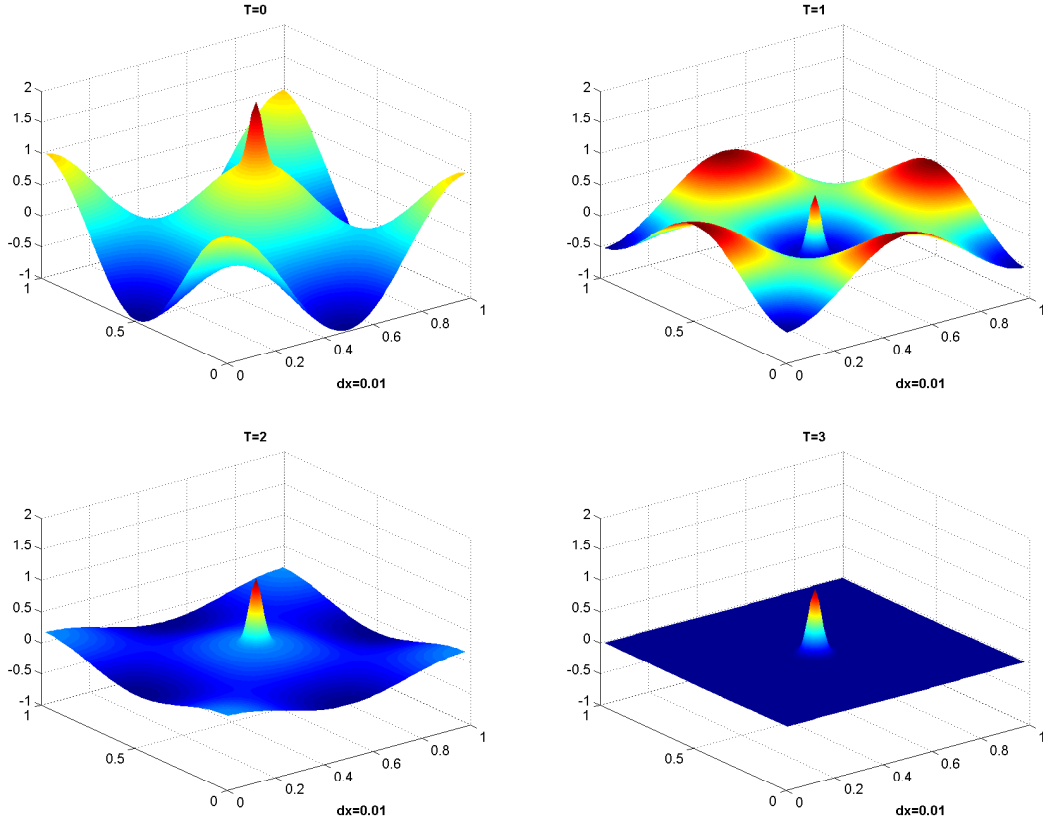$$\lambda_5 = \lambda(0, 0), \quad G_5 = k(1 - 4\nu)F^{n,\alpha},$$

Figure 4.5: Numerical solution of system (4.61) with initial condition $u_0(x) = \cos(2\pi x_1)\cos(2\pi x_2) + \bar{u}_0(x)$ on a square domain $[0,1] \times [0,1]$ at different times $T = 0, 1, 2$ and 3. The numerical approximations are obtained by the Relaxation scheme joint with AHO2 scheme for the source term.
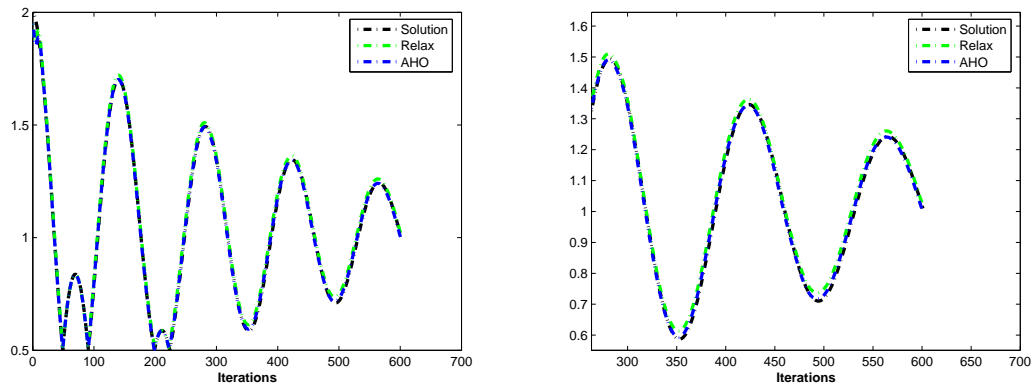

Figure 4.6: Comparison between the maximal values of solution of (4.61) and the approximations by Relaxation method and Relaxation + AHO until time $T = 3$. Initial condition is $u_0(x) = u_0(x_1, x_2) = \cos(2\pi x_1)\cos(2\pi x_2) + \bar{u}_0$ and the domain is the square $[0,1] \times [0,1]$.

T	Relaxation	Relaxation+AHO
5	0.0142	0.0097
10	0.0203	0.0056
20	0.0216	0.0044
50	0.0217	0.0044

Table 4.2: Relative error in l^∞ norm for the solution to system (4.61) approximated by Relaxation and Relaxation+AHO with $h = 0.01$ at different times T.

T	Relaxation	Relaxation+AHO
5	0.0564	0.0549
10	0.024	0.0185
20	0.0177	0.0087
50	0.0177	0.0087

Table 4.3: Relative error in l^2 norm for the solution to system (4.61) approximated by Relaxation and Relaxation+AHO with $h = 0.01$ at different times T.

where we fix $v = 0.1$.

We can observe in Figure 4.6 that this method approximates better the solution of the problem than the method with an explicit form of the source term.

Let us define the error in l^∞ norm and the relative error in l^∞ norm respectively as

$$E_\infty^{T,h} = \| u^h - u^{ex} \|_\infty = \max |u_{i,j}^{h,n} - u_{i,j}^{ex,n}|, \qquad En_\infty^{T,h} = \frac{E_\infty^{T,h}}{\| u^{ex} \|_\infty}$$

and the error in l^2 norm and the relative error in l^2 norm as:

$$E_2^{T,h} = \| u^h - u^{ex} \|_2 = (\sum |u_{i,j}^{h,n} - u_{i,j}^{ex,n}|^2)^{\frac{1}{2}}, \qquad En_2^{T,h} = \frac{E_2^{T,h}}{\| u^{ex} \|_2}$$

for $h \to 0$ and $T \to \infty$.

Observing in Tables 4.2 and 4.3 the values obtained with these two methods, we can note that we get better results using the AHO method for the source term.

4.3.3   A Semilinear Hyperbolic-Parabolic Model of Chemotaxis

Now we study, from the numerical point of view, the complete hyperbolic-parabolic system

$$\begin{cases} \partial_t u + \nabla \cdot v = 0, \\ \\ \partial_t v + \gamma^2 \nabla u = -b(\phi, \nabla\phi) v + h(\phi, \nabla\phi, u), \\ \\ \partial_t \phi = \Delta\phi + f(u, \phi), \end{cases} \qquad (4.66)$$

which was studied analytically in Chapter 2. In [51] Hillen and Dolak proposed a model to describe the slime molds behavior, where a supplementary logistic term is introduced to avoid blow up.

Actually the slime mold Dictyostelium discoideum has a particular mechanism: upon starvation, the amoebae form tissue-like aggregates. This process is controlled by chemotaxis: the cells move upward gradients of the messenger molecule cAMP produced by the cells. However the chemotactic sensitivity may saturate and possibly vanishes for high values of the population density. The non-dimensional system introduced in [51] is:

$$\begin{cases} \partial_t u + \nabla \cdot v = 0, \\[2mm] \tau \partial_t v + \gamma^2 \nabla u = -v + u(1-u)\nabla\phi, \\[2mm] \partial_t \phi = D\Delta\phi + \alpha u - \phi, \end{cases} \tag{4.67}$$

where u, v, and ϕ are used for the particle density, the particle flux, and the signal concentration respectively. The non-dimensional system depends only on D, τ, γ and α.

We can observe that the theorem of global existence of smooth solutions introduced in Chapter 2 holds also for system (4.66).

Let us explain now how we solve numerically problem (4.67) on a bounded domain $\Omega \subset \mathbb{R}^2$ with homogeneous Neumann boundary conditions for the chemical concentration ϕ and the population density u:

$$\nabla\phi \cdot n|_{\partial\Omega} = 0, \quad \nabla u \cdot n|_{\partial\Omega} = 0, \tag{4.68}$$

and zero boundary condition for the normal component of v

$$v \cdot n|_{\partial\Omega} = 0. \tag{4.69}$$

Let us take $\Omega = [0, L] \times [0, L]$ and let us denote by h the space step. We consider the discretization points $x_\alpha = (\alpha_1 h, \alpha_2 h), 0 \leq \alpha_i \leq N+1$. We denote the time step by k and the approximation of a function f at time $t_n = nk$ by f^n.

For each time step, we solve first the hyperbolic equations using Relaxation scheme, presented in the previous section, obtaining $w^{n+1} = (u^{n+1}, v_1^{n+1}, v_2^{n+1})$.

Then, we solve the parabolic equation for the chemical ϕ using a classical Crank-Nicolson method for the time discretization and a Finite Difference Method for the space discretization [157]. Let us denote by M the $N \times N$ classical second order Finite Difference matrix for the laplacian using second order derivatives for the computation of boundary values.

The third equation of (4.67) is therefore discretized as

$$\frac{\phi^{n+1} - \phi^n}{k} = \frac{D}{2}M(\phi^{n+1} + \phi^n) + \frac{\alpha}{2}(u^{n+1} + u^n) - \frac{1}{2}(\phi^{n+1} + \phi^n),$$

which leads to the following linear system:

$$\left((1+\frac{k}{2})I - \frac{k}{2}DM\right)\phi^{n+1} = \left((1-\frac{k}{2})I + \frac{k}{2}DM\right)\phi^n + \frac{\alpha}{2}(u^{n+1} + u^n). \tag{4.70}$$

Using the above scheme, we have solved numerically system (4.67) with boundary conditions (4.68), (4.69) on a square domain $\Omega = [0, 20] \times [0, 20]$.

In our simulations the initial conditions are homogeneous distributions of the cell density with random fluctuations of 1%. Moreover the flux v and the chemical concentration ϕ are initially zero. In Figures 4.7 and 4.8 we show the evolution of the population density with different initial conditions for different times. We notice that due to initial irregularities of the cell density, there is a pattern formation. The aggregations continue to grow, until the saturation $u = 1$ is reached locally.
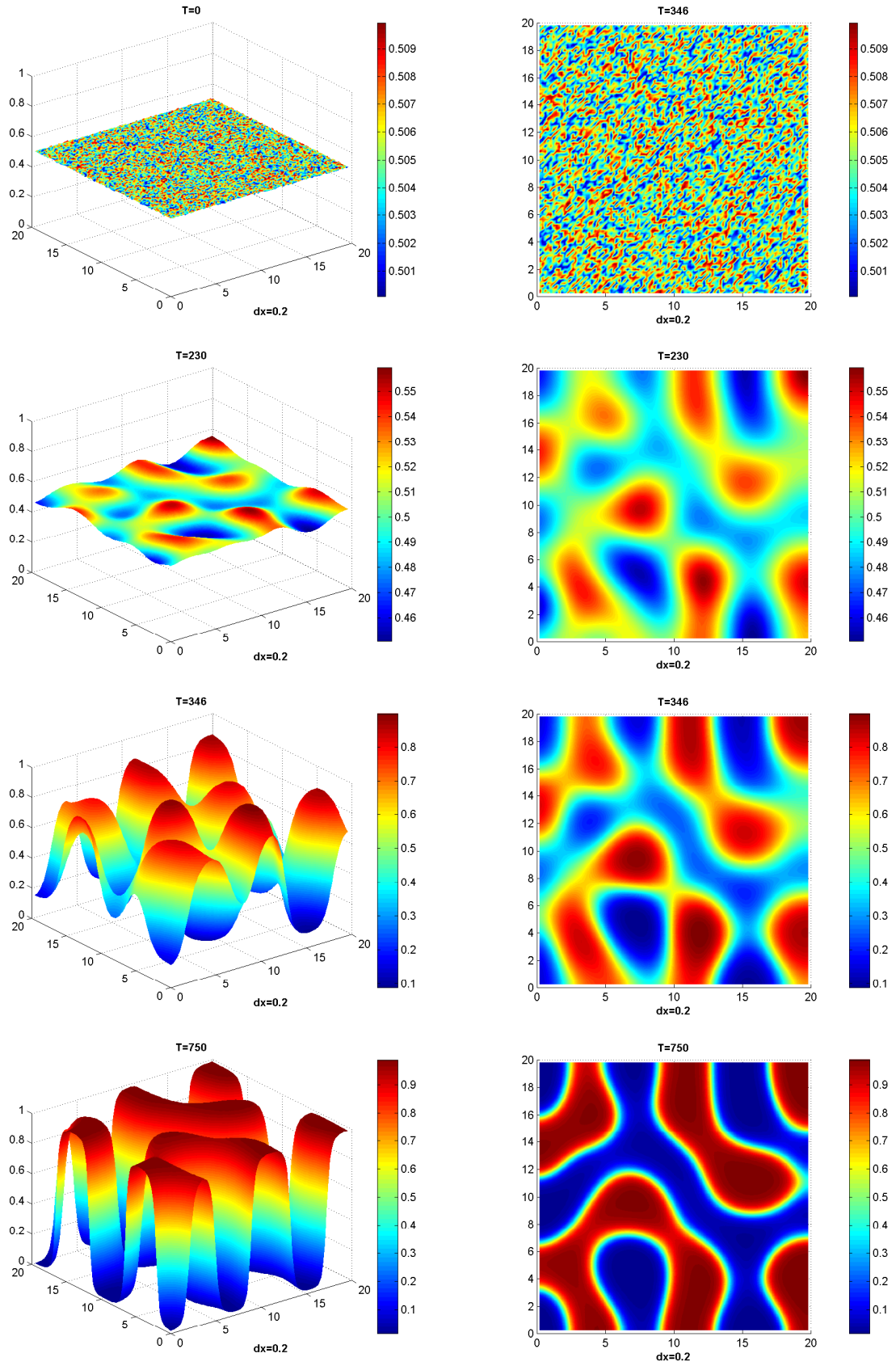
Figure 4.7: Numerical solution of the model (4.67) with initial condition $u_0(x) \in [0.5, 0.51]$ on a square domain $[0, 20] \times [0, 20]$ at different times $T = 0, 230, 346$ and 750. Parameter values: $D = 0.03$, $\tau = 1$, $\alpha = 0.5$, $\gamma = 1$.
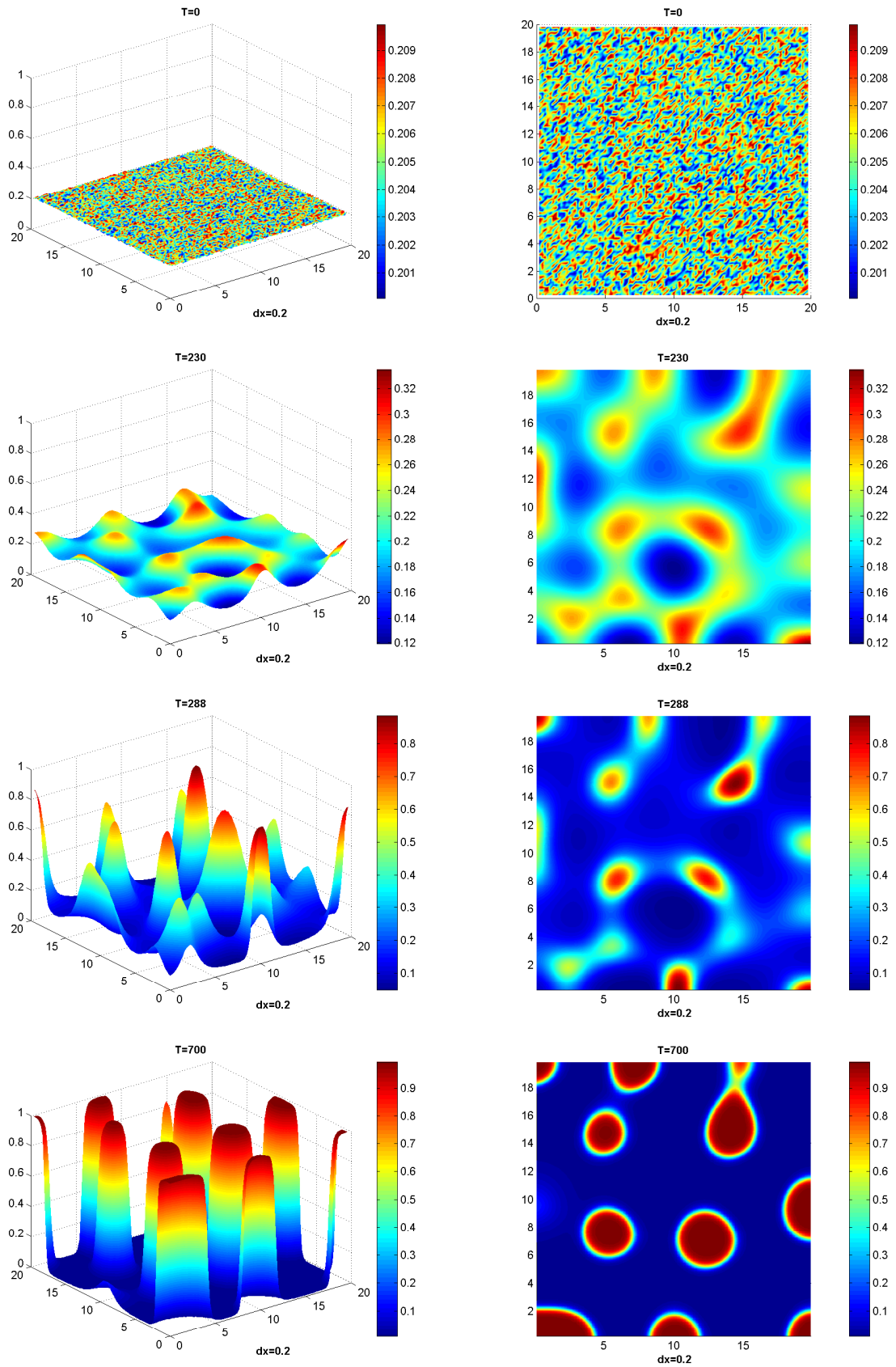
Figure 4.8: Numerical solution of the model (4.67) with initial condition $u_0(x) \in [0.2, 0.21]$ on a square domain $[0, 20] \times [0, 20]$ at different times $T = 0, 230, 288$ and 700. Parameter values: $D = 0.03$, $\tau = 1$, $\alpha = 0.8$, $\gamma = 1$.

Finally, we have solved numerically the following system in the two dimensional case

$$\begin{cases} \partial_t u + \nabla \cdot v = 0, \\[2mm] \tau \partial_t v + \gamma^2 \nabla u = -v + u \nabla \phi, \\[2mm] \partial_t \phi = \Delta \phi + \alpha u - \phi. \end{cases} \tag{4.71}$$

In Chaper 2 we have presented some global existence results to the Cauchy problem for small initial data, but nothing is known for the moment for large initial data, bounded domains and blow-up phenomena, and in particular, the ability of this model to capture aggregation phenomena. This result would be of high importance for the liability of the hyperbolic models we consider.

In order to have some ideas on the behaviors of the solution, we have performed some numerical tests with different initial data.

In Figure 4.9 we show numerical solutions of system (4.71) with different initial conditions. We can observe that with small initial data, like a perturbation of the zero state or perturbation of small constant state for the population density, we obtain global existence of solution, while if we consider large initial data the blow up of solution occurs.

These are only preliminary results, but it could be extremely interesting to investigate the asymptotic behavior of solutions to this system in general, to find out if they exist globally in time or explode in finite time. Another hypothesis is that both of these situations occur with a critical threshold as for the parabolic model.

4.4 Numerical Simulations: Quasilinear Case

In this section we show numerical simulations of the solutions to the hyperbolic-parabolic system

$$\begin{cases} \partial_t \rho + \nabla \cdot (\rho u) = 0, \\[2mm] \partial_t (\rho u) + \nabla \cdot (\rho u \otimes u) + \nabla P(\rho) = -\alpha \rho u + \mu \rho \nabla \phi, \\[2mm] \partial_t \phi = D \Delta \phi + a \rho - \frac{\phi}{\tau}. \end{cases} \tag{4.72}$$

As in the previous section, we start our numerical approximation by studying a simplified version of (4.72), i.e. the Isentropic Euler Equations, and subsequently we will approximate solutions to the complete system.

4.4.1 Isentropic Euler Equations

Euler equations of compressible fluid dynamics have been the subject of intensive research in the last decades thanks to the variety of their applications, e.g. aircrafts, ships, weather predictions. The main numerical problem with these equations, and with quasilinear conservation laws in general, is that solution naturally develops discontinuities and in particular shock waves.

We consider the system

$$\begin{cases} \partial_t \rho + \nabla \cdot (\rho u) = 0, \\[2mm] \partial_t (\rho u) + \nabla \cdot (\rho u \otimes u) + \nabla P(\rho) = 0, \end{cases} \tag{4.73}$$
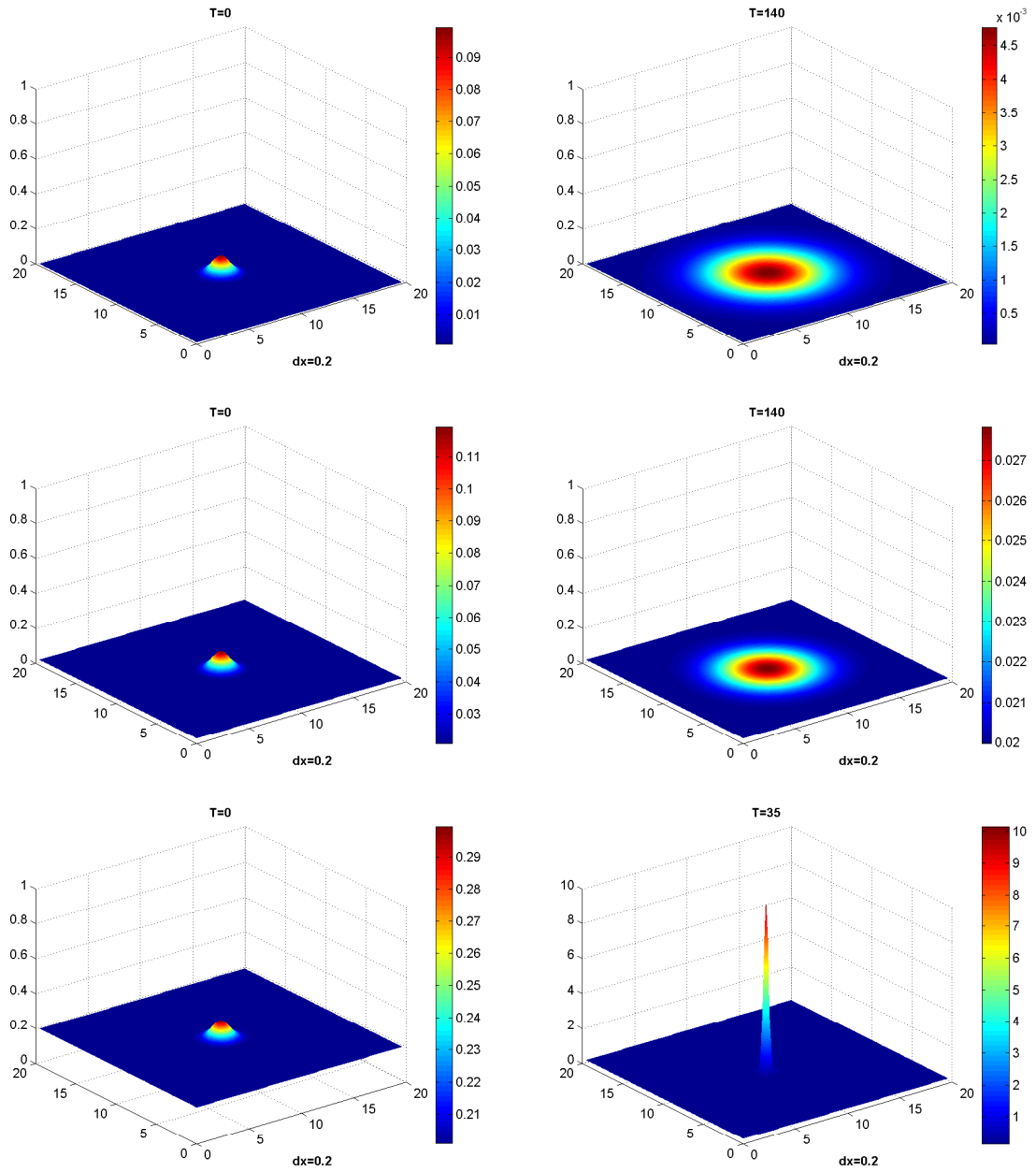
Figure 4.9: Numerical simulations of the population density in (4.71) with three different initial conditions u_0 on a square domain $[0.20] \times [0.20]$. On the left, we have the initial conditions and on the right the final approximated solutions. In the first case we have a compact support perturbation of zero state and the solution at time $T = 140$. In the middle the initial condition, which is a compact support perturbation of the constant state equal to 0.02, and the solution at time $T = 140$ are displayed. In the final case the initial condition is a compact support perturbation of the constant state equal to 0.2 and the solution is calculated until time $T = 35$. In this case we can observe that blow up occurs.

with initial data

$$\rho(x,0) = \rho_0(x), \quad u(x,0) = u_0(x), \tag{4.74}$$

where $\rho : \mathbb{R}^2 \times \mathbb{R}^+ \to \mathbb{R}$ and $u : \mathbb{R}^2 \times \mathbb{R}^+ \to \mathbb{R}^2$. Here we set the function $P(\rho) = \rho^\gamma$, with $\gamma = 5/3$.

Our aim is to solve numerically equation (4.73) on a bounded domain $\Omega \subset \mathbb{R}^2$ with homogeneous Neumann boundary conditions for variable ρ

$$\nabla \rho \cdot n|_{\partial\Omega} = 0, \tag{4.75}$$

and zero boundary condition for the normal component of u

$$u \cdot n|_{\partial\Omega} = 0. \tag{4.76}$$

Let us take $\Omega = [0, L] \times [0, L]$ and let us denote by h the space step. We consider the discretization points $x_\alpha = (\alpha_1 h, \alpha_2 h)$, $0 \le \alpha_i \le N+1$. We denote the time step by k and the approximation of a function f at time $t_n = nk$ by f^n.

For each time step, we solve the hyperbolic equations using a relaxation method [13]. Let us denote $w = (\rho, \rho u^1, \rho u^2)$ and rewrite (4.73) as

$$\partial_t w + \partial_{x_1} A_1(w) + \partial_{x_2} A_2(w) = 0,$$

with

$$A_1(w) = \begin{pmatrix} \rho u_1 \\ \rho u_1^2 + P(\rho) \\ \rho u_1 u_2 \end{pmatrix}, \quad A_2(w) = \begin{pmatrix} \rho u_2 \\ \rho u_1 u_2 \\ \rho u_2^2 + P(\rho) \end{pmatrix}.$$

We use the 5-velocities relaxation scheme proposed in the previous section. Following the results of Bouchut [21] (Proposition 4.2.3), we set the velocity $\lambda = \max\{|\theta_{ij}|\}$, where θ_{ij} are the eigenvalues of the Jacobian of the fluxes; the time and space steps will have to satisfy the stability condition $\lambda \dfrac{k}{h} \le 1$.

Using the above scheme, we have solved numerically system (4.73) with boundary condition (4.75), (4.76) on a square domain $\Omega = [0, 1] \times [0, 1]$.

As initial data we have taken

$$\rho_0(x) = 1 + 0.1 \exp\left[-\frac{(x-0.5)^2}{0.001}\right], \quad u_0^1(x) = 0, \quad u_0^2(x) = 0.$$

In Figure 4.10 we show numerical solutions to this Cauchy problem at different times. As observed before, in Isentropic Euler equations shock waves can develop. We can notice in Figure 4.11, where a discontinuous initial datum has been considered, that the relaxation scheme used for our simulations is able to catch the discontinuities even if it is a first order scheme.

4.4.2 A Quasilinear Hyperbolic-Parabolic Model of Vasculogenesis

Following [66, 150, 137], we performed numerical simulations on the non-dimensional system

$$\begin{cases} \partial_t \rho + \nabla \cdot (\rho u) = 0, \\\\ \partial_t(\rho u) + \nabla \cdot (\rho u \otimes u) + \nabla P(\rho) = -\alpha \rho u + \mu \rho \nabla \phi, \\\\ \xi \partial_t \phi = \Delta \phi + a(\rho) - \xi \phi, \end{cases} \tag{4.77}$$
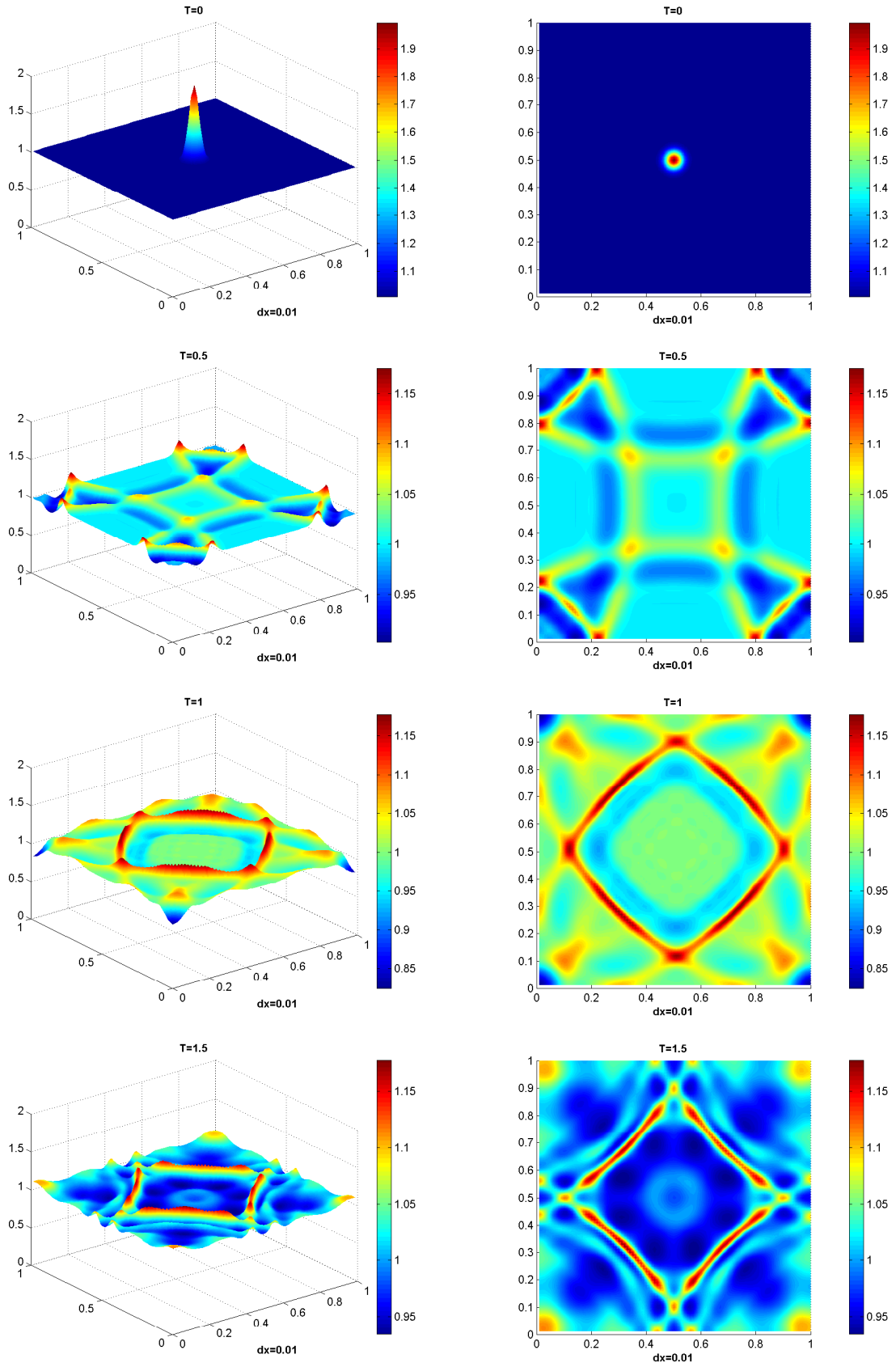
Figure 4.10: Numerical solution of the system (4.73) with initial conditions $\rho_0(x) = 1 + 0.1 *$ $\exp\left[-\frac{(x-0.5)^2}{0.001}\right]$, $u_0(x) = 0$ on a square domain $[0,1] \times [0,1]$ at different times $T = 0, 0.5, 1$ and 1.5.
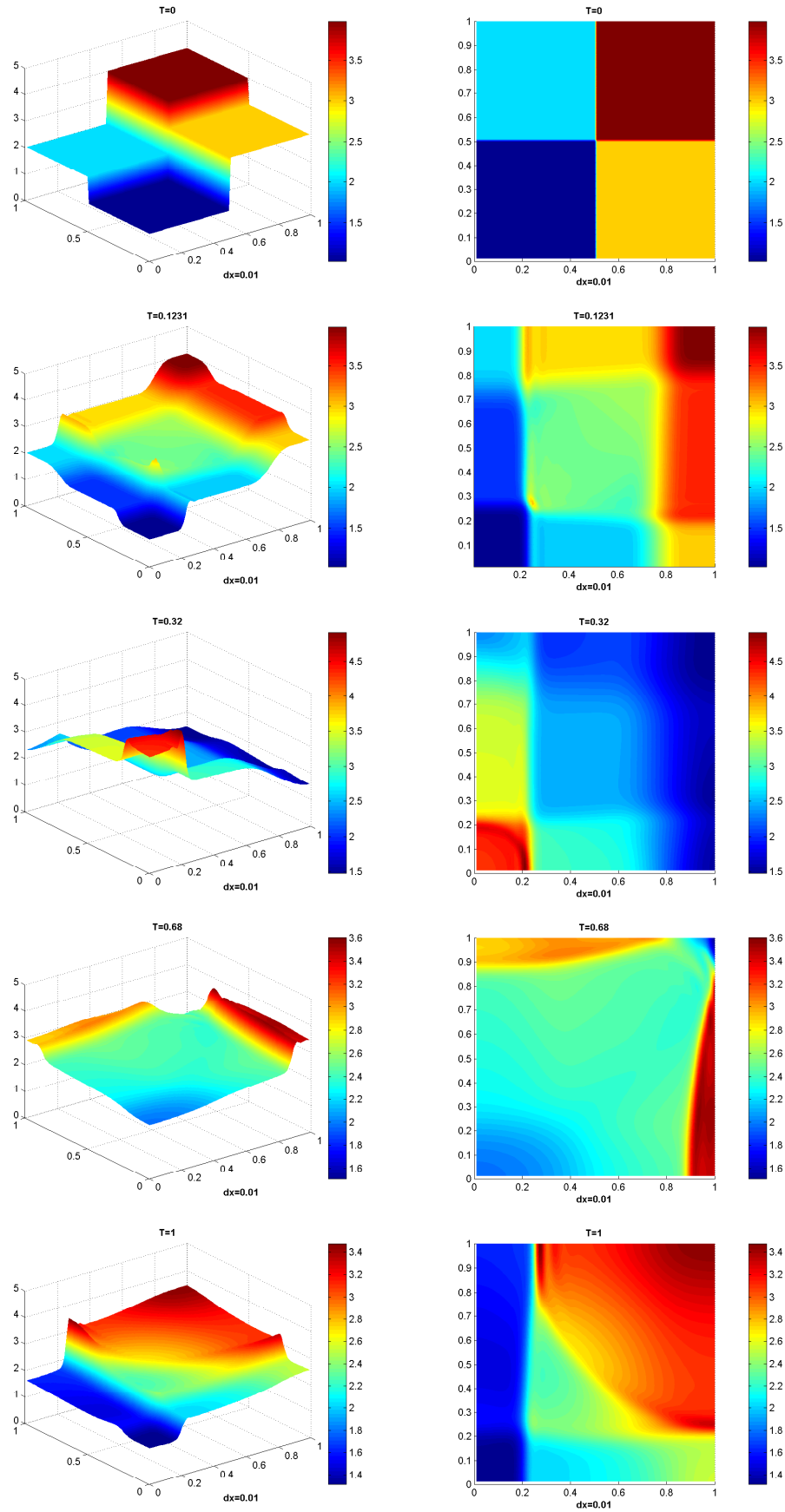
Figure 4.11: Numerical solution of system (4.73) with $\rho_0(x)$ discontinuous initial datum and $u_0(x) = 0$, on a square domain $[0, 1] \times [0, 1]$ at different times $T = 0, 0.12, 0.32, 0.68$ and 1 .

Parameter	Value
ϵ	10^{-8}
α	0 or 0.2
μ	0.02
a	30
b	0.2
ξ	100
σ	0.015

Table 4.4: Non-dimensional values of parameters adopted in simulation.

where $\rho, \phi : \mathbb{R}^2 \times \mathbb{R}^+ \to \mathbb{R}$, and $u : \mathbb{R}^2 \times \mathbb{R}^+ \to \mathbb{R}^2$. Here $P(\rho) = \epsilon \rho$ and $a(\rho) = \frac{a\rho}{1+b\rho^2}$.

This model was introduced by Gamba et al. [150, 66] to study the development of vascular network formation. As reported in Chapter 1, their basic assumption is that the persistence and chemotaxis are key features, determining the size of the structure. They assume that the mechanical interaction of the cells with the matrigel can be neglected for describing the behavior of the system along the first hours.

We can notice that, with reference to the quasilinear hyperbolic-parabolic system (4.72) studied in Chapter 3, we have introduced, following [164], the function $a(\rho)$ for the production rate of the chemoattractant factor.

Numerical simulations have been performed using a set of non-dimensional parameters proposed by [164] and reported in Table 4.4.

A finite difference Relaxation scheme with source term in explicit has been adopted for the hyperbolic part of the system, and a simple implicit scheme has been used for the equation of the chemical substance.

Periodic boundary conditions have been prescribed for all the state variables. The initial condition on the cellular density corresponds to a set of M gaussian bumps whose amplitude is assumed to be of the order of the non-dimensional average cell radius σ, centered randomly in x_j, $j = 1, \ldots, M$ with a uniform distribution over the square,

$$\rho(x,0) \quad = \quad \frac{0.01}{2\pi\sigma^2} \sum_{j=1}^{M} \exp\left(-\frac{|x - \mathbf{x}_j|^2}{2\sigma^2}\right) \tag{4.78}$$

$$u(x,0) \quad = \quad 0, \tag{4.79}$$

$$\phi(x,0) \quad = \quad 0. \tag{4.80}$$

We can observe in Figures 4.13 and 4.15 how the initial density of cells influences the structure of the network. Indeed by varying the initial cells number we switch from a phase with several disconnected structures to a phase with a single connected structure.

Moreover we can notice how the presence of the dissipative term, $-\alpha\rho u$, affects the evolution of the network. This term physically represents a friction term between endothelial cells and the substratum. Thus when the coefficient $\alpha \neq 0$ we have a more stable structure of the networks as shown by Figures 4.14 and 4.15.

As done in the previous section for the semilinear case, we perform some simulations on the quasilinear hyperbolic-parabolic system studied analytically in Chapter 3. We have proved a global
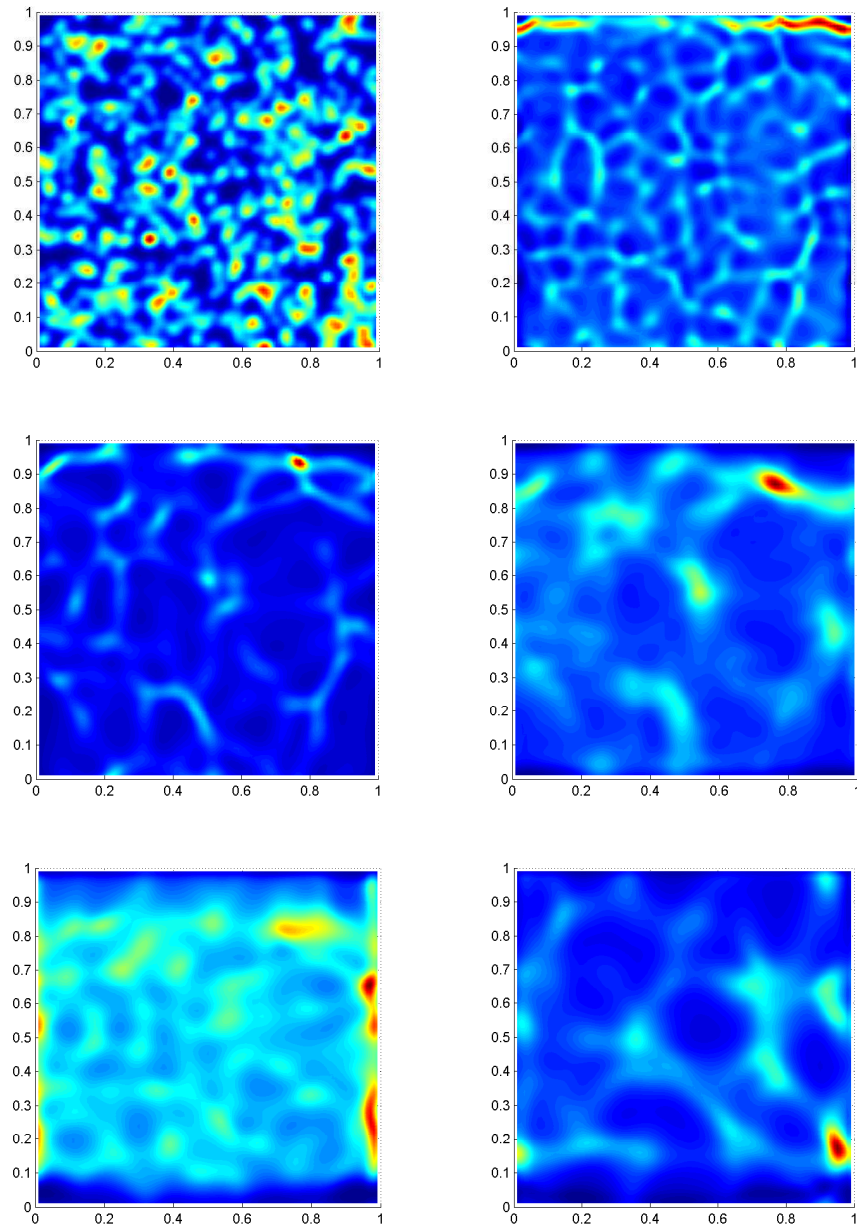
Figure 4.12: Simulation of the initial development of vascular network model (4.77) with initial data (4.78) and $M = 800$ until the numerical time $T = 1100$. Here we take the coefficient $\alpha = 0$. The other parameters values are indicated in Table 4.4.

Figure 4.13: Dependence of the specific network structure on the initial condition. Here we have three different values of $M = 100$, 800 and 4000. Here we take the coefficient $\alpha = 0$. The other parameters values are indicated in Table 4.4.

Figure 4.14: Simulation of the initial development of vascular network model (4.77) with initial data (4.78) and $M = 800$ until the numerical time $T = 400$. Here we take the coefficient $\alpha = 0.2$. The other parameters values are indicated in Table 4.4.
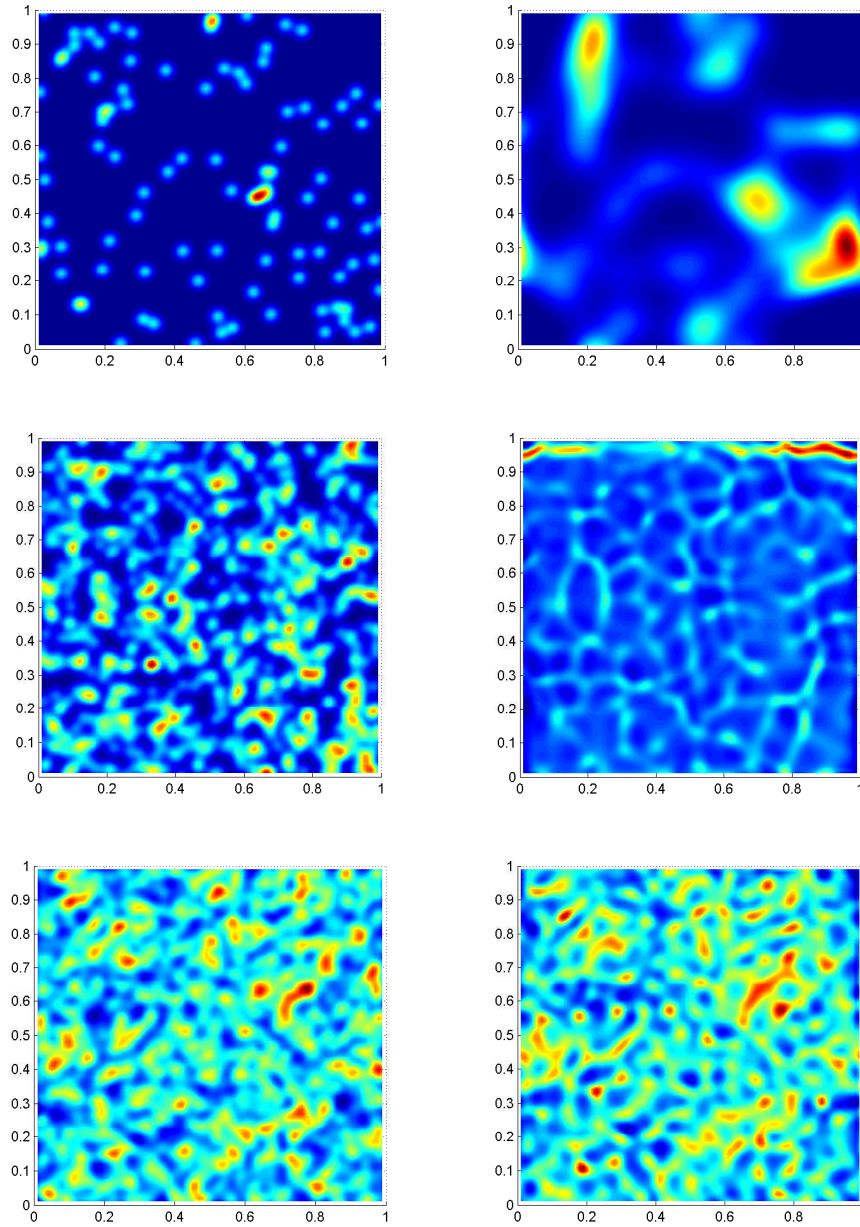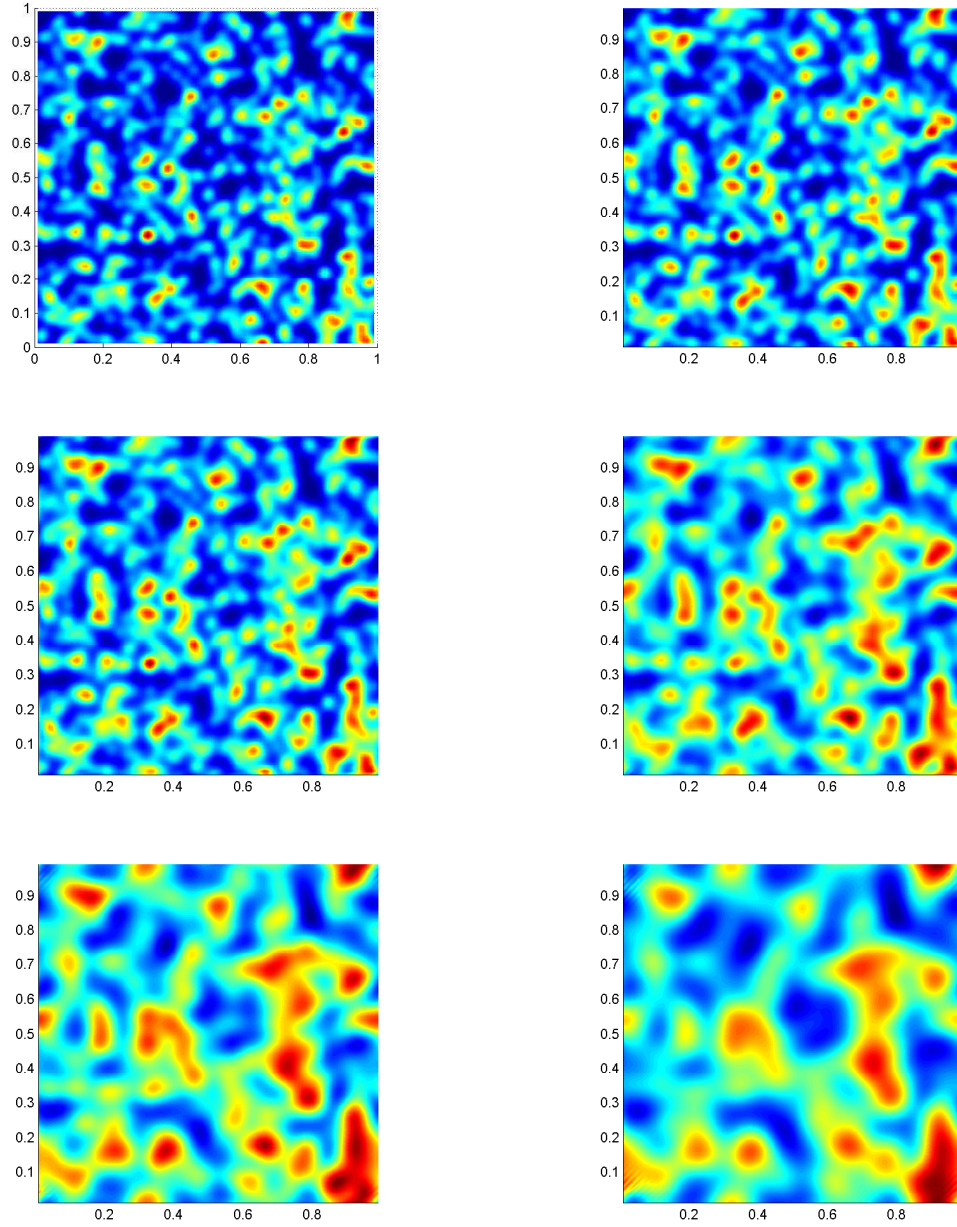
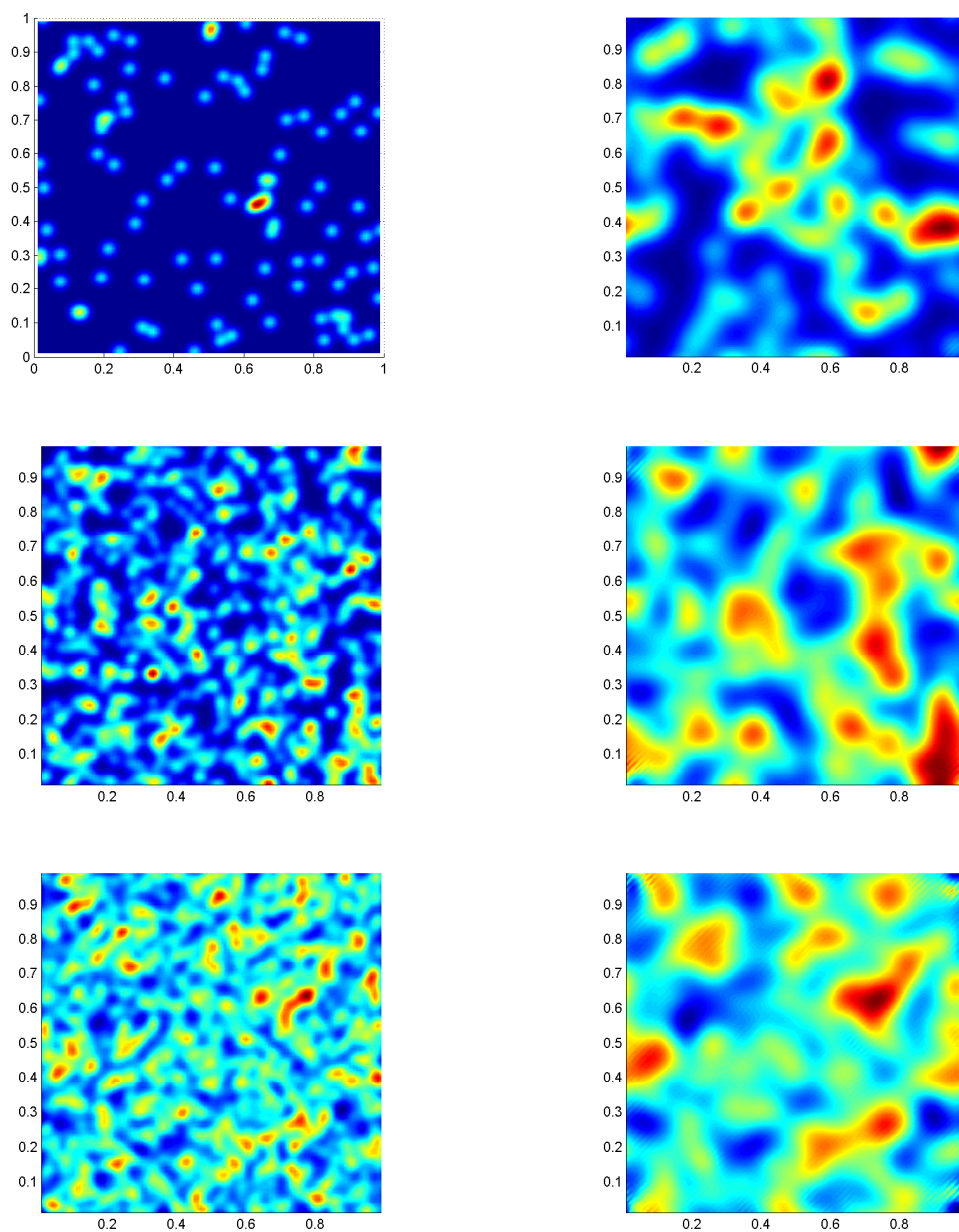Figure 4.15: Dependence of the specific network structure on the initial condition. Here we have three different values of $M = 100$, 800 and 4000. We take the coefficient $\alpha = 0.2$. The other parameters values are indicated in Table 4.4.

existence result for small and smooth solutions, but nothing is known for the moment for large initial data, or blow-up phenomena. Our aim is to investigate the possible behavior of solutions to the following system,

$$
\begin{cases}
\partial_t \rho + \nabla \cdot (\rho u) = 0, \\[2mm]
\partial_t (\rho u) + \nabla \cdot (\rho u \otimes u) + \nabla(\rho^\gamma) = -\rho u + \rho \nabla \phi, \\[2mm]
\partial_t \phi = D\Delta \phi + \rho - \phi,
\end{cases}
\tag{4.81}
$$

with different initial conditions. We solve numerically system (4.81) on a bounded domain $\Omega \subset \mathbb{R}^2$ with homogeneous Neumann boundary conditions for variable ρ and ϕ:

$$
\nabla \rho \cdot n|_{\partial \Omega} = 0, \quad \nabla \phi \cdot n|_{\partial \Omega} = 0
\tag{4.82}
$$

and zero boundary condition for the normal component of u

$$
u \cdot n|_{\partial \Omega} = 0.
\tag{4.83}
$$

The numerical scheme adopted is the relaxation scheme presented in the previous section (4.58) adding the source term

$$
F(w, \bar{w}) = \begin{pmatrix} 0 \\ \rho \partial_{x_1} \phi - u_1 \\ \rho \partial_{x_2} \phi - u_2 \end{pmatrix}.
$$

Then we obtained

$$
w^{n+1} = \sum_{i=1}^{5} f_i^{n+1/2} + kF(w^n, \bar{w}).
$$

On the other hand we solve the parabolic equation in (4.81) using a Crank Nicolson method for time discretization, and a Finite difference method for the space discretization, as done for the semilinear case in the previous section.

We can observe in Figure 4.16 that with small initial data, like a perturbation of the zero state or a perturbation of a small constant state for the population density, we obtain global existence of solution, while if we consider large initial data the blow up of solution occurs.

It could be interesting to study this aspect from an analytical perspective, and compare these results with the ones yet proved for the parabolic Patlak-Keller-Segel system.
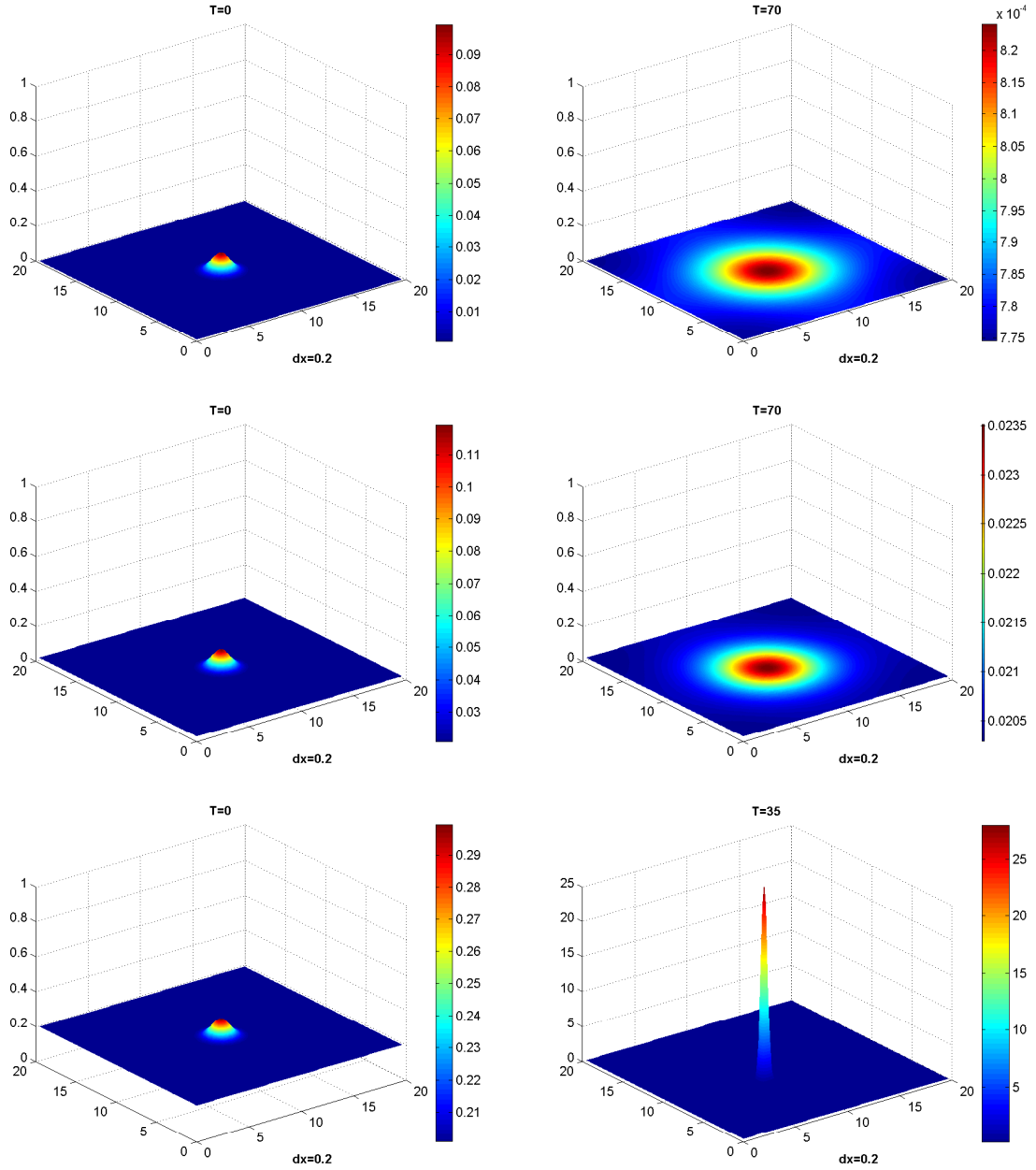
Figure 4.16: Numerical simulations of the population density in (4.81) with three different initial conditions u_0 on a square domain $[0, 20] \times [0, 20]$. On the left, we have the initial conditions and on the right the final approximated solutions. In the first case we have a compact support perturbation of 0 and the solution at time $T = 70$. In the middle the initial condition, which is a compact support perturbation of the constant state equal to 0.02, and the solution at time $T = 79$ are displayed. In the final case the initial condition is a compact support perturbation of the constant state equal to 0.2 and the solution at time $T = 35$ are displayed. In this case we can observe that blow up occurs.

Chapter 5

A Model of Inflammation during Ischemic Stroke

In this chapter we propose a model to describe the inflammatory process which occurs during ischemic stroke [47]. Our purpose is to obtain *in silico* experiments (i.e. simulations on a computer) to study and discuss the influence of the inflammation during stroke and to propose some possible therapeutic approaches.

The chapter is organized as follows: first, an introduction to some basic concepts about the biological phenomenon is given. Then, a detailed derivation of the model and the numerical scheme used are presented. Finally, the studies of the model robustness and sensitivity are showed and some numerical results on the time and space evolution of the process are presented and discussed.

5.1 Biological Backgrounds

Strokes are the second worldwide death cause and the sixth source of handicap in the world [112, 113]. They consist in a rapid developing loss of brain functions due to a disturbance in the cerebral blood flow. This can be due to ischemia (80% of stroke), when the lack of blood supply is caused by thrombosis or embolism, or due to hemorrhage. During a stroke, the affected area of the brain is unable to function, leading to trouble moving, walking, seeing, speaking or understanding. It is a medical emergency and can cause permanent neurological damage, complications, and death.

We focus our study on one of the pathophysiological mechanisms involved in ischemic stroke, the inflammatory process [45, 83]. In a general setting, inflammation is a complex biological response of vascular tissues to harmful stimuli such as pathogens, damaged cells or irritants. During ischemic stroke, inflammation is triggered to eliminate the dead cells but can also lead to the death of some other cells.

Ischemic stroke begins with the decrease of the cerebral blood flow which can drop below 10 % of the normal blood flow. Cells around the occluded vessel begin to die and create what we call the infarcted core. Around this infarcted core, we can find the penumbra which is an area of moderate ischemia and which is able to recover thanks to reperfusion or therapeutic intervention. In these two ischemic areas, cells can die either through necrosis or through apoptosis. Necrosis occurs mainly in the infarcted core and occurs very early after the stroke onset. It leads to the rupture of cell membrane, the disintegration of intracellular organelles and the release of intracellular contents in the extracellular space. As a consequence, necrotic cells "pollute" the environment and damage the surrounding cells. On the contrary, apoptosis appears later (from 30 minutes up to 2

or 3 days after the stroke onset) and apoptotic death is much slower than necrosis as shown in Ru-palla et al. [146]. Moreover, apoptosis occurs mainly in the penumbra and is not deleterious for the neighboring cells. We can also notice that, as indicated in [10] by Ankarcrona et al., apoptosis can lead to the inflammatory process, even if it was observed that inflammatory process is mainly induced by necrotic cells in the infarcted core. So, inflammation contribute to cell death by necrosis [98] and apoptosis [145, 131].

During an ischemic stroke, the first phase of the inflammatory process consists in the activation of microglia. Microglia are the resident immune cells aimed at protecting brain cells. In ischemic conditions, microglia get activated: their shapes change, which increases their abilities to phagocytosis and production of cytokines and chemokines. Cytokines are proteins that trigger the accumulation of adhesion molecules on the vascular endothelium leading to the entrance of leukocytes (i.e immune cells circulating in the blood) into brain tissue. Among cytokines, chemokines induce chemotaxis in nearby responsive cells to attract leukocytes from the blood. Moreover, activated microglial cells are able to phagocytize necrotic and apoptotic cells as showed by Vilhardt in [169] and by Schilling et al. in [147]. But, during phagocytosis, microglia produce and release free radicals such as nitric oxide (NO) which is deleterious for the surrounding cells. Thus, microglia have both deleterious roles through the production of toxic substances and beneficial ones through the prevention of damage extension by phagocytosis and the production of trophic molecules and anti-inflammatory cytokines that can mediate neuroprotection and tissue repair [156].

The second phase of the inflammatory process consists in the infiltration of leukocytes in brain tissue. The leukocytes involved in this process are neutrophils and monocytes. The latter are called macrophages once they leave the blood to enter the tissue. Neutrophils infiltrate the tissue about 12 hours after the stroke onset and produce lots of deleterious substances (that are useful to slow down an infection for example but that are totally counterproductive in an ischemic stroke). Moreover, they are able to phagocytize small quantities of dead bodies and produce free radicals like NO [67]. Macrophages infiltrate the tissue later, about 24 hours after the stroke onset. Like microglia, they produce cytokines, chemokines and free radicals and they are able to phagocytize necrotic and apoptotic cells. These leukocytes enter cerebral tissue through their interactions with the adhesion molecules located on endothelium. These cells have a beneficial role by cleaning the infarcted core and allowing the tissue cicatrization but they can also increase the ischemic damage by producing free radicals and pro-inflammatory cytokines as presented by Hallenbeck and Dutka in [72]. So, as microglia, these cells have both beneficial and deleterious effects during the inflammatory process. The two phases of inflammation influence both in a positive and a negative way the survival of neurons and glial cells. In this study, we are interested in understanding which influence dominates, depending on the situation. Our final aim is to understand if and how it is possible to control the positive and negative aspects of this biological process, which could be helpful for the development of new therapeutic strategies in ischemic stroke.

5.2 Previous Models

In the literature, there are several models of systemic inflammation. For example, the models proposed by Ibragimov et al. [84], Kumar et al. [95], Lauffenburger and Kennedy [102] and Reynolds et al. [139] describe the behavior only of blood cells. Instead Ladeby et al. in [96] and Lai and Todd [97] consider also glial cells. Adrian and Marshall in [2], Eldestein-Keshet and Spiros in [54], Gray

and Brookmeyer in [69], Mentis et al. in [109] and Ridall et al. in [140] describe models for neurode-generative diseases. These works are focused on the behavior of cell components at subcellular level of a single cell type. In our model, we considered the cell level and we modeled the behaviors of several types of cells (microglia, leukocytes, neurons and astrocytes). As a starting point, we considered the cell model proposed recently by T. Lekelov-Boissard et al. [33]. They proposed an ODEs model and took into account the two phases of inflammation: activation of microglia and infiltration of blood leukocytes. In their model, they studied the dynamics of the densities of cells dead by necrosis and apoptosis, and of living cells. Moreover they considered the proportion of activated and inactivated resident microglia and the proportion of neutrophils and macrophages in the tissue. They also introduced the release of pro-inflammatory molecules (like cytokines, chemokines and free radicals) by microglia and leukocytes and their phagocytic abilities. But this model is "phenomenological" and does not consider the space dimension. Using the methods proposed in [33], we introduced in the model the space dimension. More precisely, we introduced the diffusion and the chemotaxis of proteins and leukocytes.

5.3 The Mathematical Model

5.3.1 The Equations

In our model, we considered a macroscopic level with a cell population scale. Thus, we used ordinary and partial differential equations to describe inflammation. The model reproduces the inflammatory process during the first 72 hours of the stroke. Every function depends on the time t and on the space x. Figure 5.1 represents the mechanisms included in our model.
The functions of the model are:

H density of healthy brain cells in relation to the usual total number of brain cells,

N density of necrotic cells in relation to the usual total number of brain cells,

A_s density of cells that have started the apoptosis process in relation to the usual total number of brain cells,

A_e density of cells that have ended the apoptosis process in relation to the usual total number of brain cells,

M_i density of inactivated microglia in relation to the usual total amount of microglia,

M_a density of activated microglia in relation to the usual total amount of microglia,

L_m density of macrophages in relation to the maximal number of macrophages that can occupy a point of the space,

L_n density of neutrophils in relation to the maximal number of neutrophils that can occupy a point of the space,

$[cy]$ concentration of pro-inflammatory cytokines,

$[ch]$ concentration of chemokines,

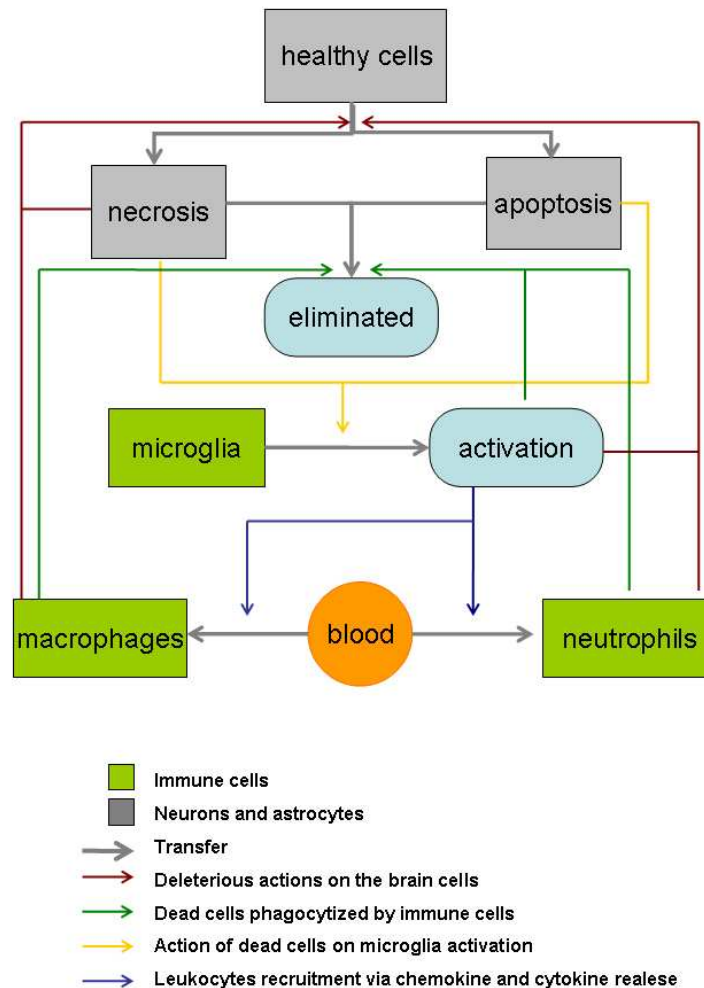$\mathcal{M}_{adh}$ density of adhesion molecules.

Figure 5.1: Connections between the different cells. 1) When an ischemic stroke occurs, neurons and glial cells die by necrosis or apoptosis. 2) These dead cells trigger the activation of the resident microglia and, due to the toxic substances in the environment, also to the death of other cells. 3) Activated microglia are able to phagocytize dead cells but they also produce cytokines (triggering the accumulation of adhesion molecules) and chemokines (attracting leukocytes). 4) Then, macrophages and neutrophils infiltrate brain tissue. These cells are able to phagocytize but they also produce toxic substances which are deleterious for healthy cells.

Neurons and Astrocytes

Neurons and glial cells such as astrocytes are resident brain cells which can be damaged during an ischemic stroke. We considered four different states for these cells: healthy cells, two types of dying cells (through apoptosis or through necrosis) and dead cells that have been eliminated from the tissue by phagocytosis. Cell death can occur either by necrosis or by apoptosis. These two different mechanisms have different roles, time scales and consequences in the inflammatory process. Thus, we modeled them separately. Moreover, to distinguish the early reversible phase of the apoptotic cascade from the late irreversible phase, we used two variables A_s and A_e for apoptotic cells. The cells beginning their apoptotic cascade are denoted A_s and those ending their apoptotic cascade are denoted A_e.

The biological facts we wanted to reproduce are the following ones:

- cells are mainly damaged by cytokines and other substances produced by neutrophils and by the deleterious substances released by the surrounding necrotic cells (we neglected the diffusion of the two last substances).

- When damage is important, cells die. Some of them die through necrosis and the other through apoptosis.

- Apoptosis is not instantaneous and needs a delay t_A.

- Microglial cells, macrophages and neutrophils phagocyte dead cells and eliminate them of the tissue.

Finally, since neurons and astrocytes do not have any mobility, we proposed the following laws:

$$\partial_t N = p_N \mathscr{D} H - \mathscr{E} N, \tag{5.1}$$

$$\partial_t A_s = p_A \mathscr{D} H - p_A \mathscr{D}(. - t_A) H(. - t_A), \tag{5.2}$$

$$\partial_t A_e = p_A \mathscr{D}(. - t_A) H(. - t_A) - \mathscr{E} A_e, \tag{5.3}$$

$$\partial_t H = -\mathscr{D} H, \tag{5.4}$$

with $\mathscr{D}$ the dying cells density, $\mathscr{E}$ the density of cells which are phagocytizing, equal to:

$$\mathscr{D} = \left[(p_{N,[cy]}[cy] + p_{N,L_n} L_n (N + A_e) + p_{N,N} N) - \mathscr{D}_0 \right]^+, \tag{5.5}$$

$$\mathscr{E} = e_{N,M_a} M_a + e_{N,L_m} L_m + e_{N,L_n} L_n + e_{N,M_i} M_i., \tag{5.6}$$

In equations (5.1) and (5.2), p_N and p_A represent respectively the proportion of cells dying through necrosis or through apoptosis. Hence $p_N + p_A = 1$.

Microglia

The microglial behavior is not very clear in spite of many experimental studies on these cells. In this model, we considered the following mechanisms:

- apoptotic and/or necrotic cells in the tissue trigger the activation of microglia.

- In absence of any stimulus, microglia get progressively inactivated.

- During stroke, inactivated microglial cells multiply by mitosis. This process takes a long time (about 24 hours).

Also these cells do not have mobility, so their densities verify the following ODEs:

$$\partial_t M_a = (c_A A_e + c_N N) M_i - \frac{M_a}{T_{M,1}}, \tag{5.7}$$

$$\partial_t M_i = -(c_A A_e + c_N N) M_i + \frac{M_a}{T_{M,1}} + c_{M_i} M_i (1 - M_i) \mathbf{1}_{t > T_{M,2}}. \tag{5.8}$$

$\mathbf{1}_{t > T_{M,2}}$ is a characteristic function hence is equal to 1 if $t > T_{M,2}$ and equal to 0 otherwise.

Leukocytes

The immune blood cells are called leukocytes. They circulate in the non occluded vessels and enter the ischemic tissue from these vessels. So, in our model, we assume that there is no infiltration of these cells through the obstructed vessel. There are two cell species involved in this inflammation process: macrophages (L_m) and neutrophils (L_n). The biological assumptions are the following ones:

- leukocytes are recruited in blood vessels by chemical signals.

- They can enter brain tissue only through adhesion molecules.

- The crossing of the blood-brain barrier takes about 12 hours for leukocytes and 24 hours for macrophages.

- Once in the cerebral tissue, leukocytes are attracted by chemokines (by chemotaxis).

- In absence of any stimulus, leukocytes progressively leave the tissue.

We proposed the following equations:

$$\partial_t L_m - \overbrace{D_{L_m} \Delta L_m}^{\text{diffusion}} = \overbrace{-\mu_m \nabla \cdot (L_m (1 - L_m) \nabla [ch])}^{\text{chemotaxis}} + \overbrace{c_{L_m} \mathscr{B}(. - T_{L_{min}}) \tilde{H}(L_M)}^{\text{carrying by blood}} - \overbrace{\frac{L_m}{T_{L_m}}}^{\text{natural decay}} \tag{5.9}$$

$$\partial_t L_n - D_{L_n} \Delta L_n = -\mu_n \nabla \cdot (L_n (1 - L_n) \nabla [ch]) + c_{L_n} \mathscr{B}(. - T_{L_{nin}}) \tilde{H}(L_M) - \frac{L_n}{T_{L_n}} \tag{5.10}$$

where $\mathscr{B}$ quantify the permeability of the blood vessel (in a healthy brain, the blood-brain barrier prevents the access to the brain) and $\tilde{H}(x)$ a regularization of the Heaviside function to model a saturation effect:

$$\mathscr{B} = \mathscr{M}_{adh}$$
$$\tilde{H}(x) = \frac{1 - \tanh R(0.75 - x)}{2},$$

where R=1000.
Since the number of leukocytes in a point of brain is limited, we introduced a saturation in the chemotaxis term.

Chemical species

Let us denote by $[cy]$ and $[ch]$ the cytokine and the chemokine concentrations. In our model, we considered that cytokines were pro-inflammatory and their production, as for chemokines, was proportional to the number of macrophages and activated microglia. Moreover, these substances are progressively absorbed/degraded by the tissue.

Since these chemical species diffuse in the tissue, we proposed the following equations:

$$\partial_t[cy] - \overbrace{D_{cy}\Delta[cy]}^{\text{diffusion}} = \overbrace{\left(p_{M_a,cy}M_a + p_{L_m,cy}L_m\right)(N + A_e)}^{\text{production by immune cells}} - \overbrace{e_{cy}[cy]}^{\text{natural decay}} , \tag{5.11}$$

$$\partial_t[ch] - D_{ch}\Delta[ch] = \left(p_{M_a,ch}M_a + p_{L_m,ch}L_m\right)(N + A_e) - e_{ch}[ch]. \tag{5.12}$$

The parameters $p_{x,cy}$, $x = M_a$ or L_m, are production rates. Since we only considered pro-inflammatory cytokines in this model, it was necessary to transform these parameters into functions of time and cytokine concentration:

$$p_{x,cy} = p_{x,cy,0}\frac{1 - [cy]}{1 + t/t_0}.$$

With this assumption, we considered that the anti-inflammatory cytokines were less secreted than the pro-inflammatory ones at the beginning of the inflammatory process, but that they were more secreted at the end of the process. This limits the effect of pro-inflammatory cytokines if they are too numerous.

Let us denote by $\mathcal{M}_{adh}$ the density of adhesion molecules. From experimental data we know that cytokines trigger a production of adhesion molecules on the vessel endothelium. Moreover, without any cytokine, adhesion molecules progressively disappear. Since these cells remain fixed in the blood vessel, their density follows an ordinary differential equation:

$$\partial_t\mathcal{M}_{adh} = \left[p_{\mathcal{M}_{adh},[cy]}\overbrace{(1 - \mathcal{M}_{adh})}^{\text{saturation}}[cy] - e_{\mathcal{M}_{adh}}\mathcal{M}_{adh}\right]\overbrace{\mathbf{1}_{\text{blood vessels}}}^{\text{localisation}}. \tag{5.13}$$

We finally obtained a close system of 13 equations. There are 7 ordinary differential equations to model fixed species :

$$\partial_t N = p_N\mathcal{D}H - \mathcal{E}N,$$

$$\partial_t A_s = p_A\mathcal{D}H - p_A\mathcal{D}(. - t_A)H(. - t_A),$$

$$\partial_t A_e = p_A\mathcal{D}(. - t_A)H(. - t_A) - \mathcal{E}A_e,$$

$$\partial_t H = -\mathcal{D}H,$$

$$\partial_t M_a = (c_A A_e + c_N N)M_i - \frac{M_a}{T_{M,1}},$$

$$\partial_t M_i = -(c_A A_e + c_N N)M_i + \frac{M_a}{T_{M,1}} + c_{M_i}M_i(1 - M_i)\mathbf{1}_{t > T_{M,2}},$$

$$\partial_t\mathcal{M}_{adh} = \left[p_{\mathcal{M}_{adh},[cy]}(1 - \mathcal{M}_{adh})[cy] - e_{\mathcal{M}_{adh}}\mathcal{M}_{adh}\right]\mathbf{1}_{\text{blood vessels}}.$$

And there are 4 reaction-diffusion equations to describe mobile species:

$$\partial_t L_m - D_{L_m}\Delta L_m = -\mu_{L_m}\nabla\cdot(L_m(1 - L_m)\nabla[ch]) + c_{L_m}\mathcal{M}_{adh}(. - T_{L_{min}})\tilde{H}(L_M) - \frac{L_m}{T_{L_m}},$$

$$\partial_t L_n - D_{L_n}\Delta L_n = -\mu_{L_n}\nabla\cdot(L_n(1 - L_n)\nabla[ch]) + c_{L_n}\mathcal{M}_{adh}(. - T_{L_{nin}})\tilde{H}(L_M) - \frac{L_n}{T_{L_n}},$$

$$\partial_t[cy] - D_{cy}\Delta[cy] = p_{cy}(M_a + L_m)(N + A_e) - e_{cy}[cy],$$
$$\partial_t[ch] - D_{ch}\Delta[ch] = p_{ch}(M_a + L_m)(N + A_e) - e_{ch}[ch].$$

33 parameters appear in our system. In the next section, we discuss how to determine the values of these parameters.

5.3.2 Numerical Approximation

There are three kinds of equations to solve: ordinary differential equation, basic reaction-diffusion and reaction-diffusion equations with a chemotaxis term. Thus we had to implement three different solvers: one for the diffusion terms, one for the reaction terms, and one for chemotaxis parts. For all these equations we used Strang splitting. For instance, for a reaction-diffusion equation $\partial_t f - K\Delta f = P$ we proceeded as follows:

1. we solve $\partial_t f = P$ for a half time step,

2. then we solve $\partial_t f = K\Delta f$ for a complete time step,

3. and finally we solve $\partial_t f = P$ for a half time step.

We used a finite volume discretization. It is classical for diffusion equations [57]: by integrating the diffusion term and using Stokes formula, we obtain an exact space discretization, and thus we easily transform the diffusion equation in a linear problem. Since the diffusion coefficient is constant, there is no discretization difficulties to ensure flux continuity.

Being the diffusion matrix constant, we preferred to solve the associated linear problem by the inversion of the matrix by a LU method rather than an iterative method. By this way we only had to compute the inverse once for each diffusion equation to solve it at each time step.

The exponential reaction term $\partial_t f = \alpha f$ in the equations, was solved by recognizing, after multiplication by $exp(t\alpha)$ the exact time derivate of $f exp(t\alpha)$. This other source term was computed by using a simple Euler scheme.

The chemotaxis term was separated into a reaction term and a transport term:

$$\begin{aligned}\partial_t f &= -\mu\nabla\cdot(f(1-f)\nabla[ch])\\ &= -(\mu(1-f)\nabla[ch])\cdot\nabla f - (-(\mu\nabla\cdot((1-f)\nabla[ch]))f).\end{aligned} \tag{5.14}$$

As usual, we used Strang splitting. Thus to solve equations (5.9) and (5.10), we had to solve:

1. the reaction term for a half time step,

2. the diffusion part for a half time step,

3. the advection term for a complete time step,

4. the reaction term for a half time step,

5. the diffusion part for a half time step.

Solving two times the diffusion part was not too expensive because we only had to multiply by the inverse matrix, that is constant depending only on the diffusion coefficient and we had already computed it in the initialization algorithm.

The advection part was solved by using an upwind scheme.

5.3.3 Parameter Adjustement

One of the main problems in modeling and simulating the inflammatory process is that few parameter values are known. Some of these parameters have no biological or chemical or physical reality. Other have been measured during *in vitro* or *in vivo* experiments but, as the data come from various species, cells and experimental conditions, they cannot be mixed and used in a single model.

At first, we listed the parameters which could be determined by experimental data. The number of the other parameters had to be reduced to be able to perform a simulation: too many parameters can not be determined by inverse problem and the model would have too many freedom degrees. As a consequence, many sets of parameters would be able to reproduce the same behaviors. For this reason we could not attempt to fit them by inverse problem method. Moreover, our model would not stay pertinent anymore: since the space of mathematical solution of our differential system would be too high, we would not be able to distinguish "biological" solution to unreasonable solution. We explain - and justify - in 5.3.3 the assumptions done to reduce the number of unknown parameters.

Since there were still unknown parameters after these simplifications, we fitted them by reproducing some behaviors which had been observed in *in vitro* or *in vivo* experiments. We have determined some "rules" about the behaviors of the different components involved in the biological phenomenon based on [67, 19, 3]. We chose the values of our parameters in order that the model could respect these rules.

Parameter values determined on biological bases

In this model, some values of the parameters are well known.

- Experimental studies have shown that there is a duplication of microglial store about 24 hours after the stroke onset, and this increase of microglial amount lasts several days [27]. It is not possible to know exactly when this increase begins, just after the stroke onset or just before 24 hours. So we assumed that the increase of microglial cells began about 18 hours after the stroke onset ($T_{M,2} = 18h$) with a rapid growth in the first hours.

- Garcia et al. in [67] observed that, in experiments performed on rats that underwent permanent ischemia, neutrophils infiltrate the tissue after 12 hours. Macrophages infiltrate the tissue later, after 24 hours. So, in our model, we assumed the following delay times: $T_{L_{nin}} = 12$ h and $T_{L_{min}} = 24$ h.

- *in vitro* studies of leukocytes have shown that macrophages can remain in brain tissue for 4 to 5 days while neutrophils remain only few hours in brain tissue [147, 67]. Hence we fixed $T_{L_m} = 90$ h and $T_{L_n} = 3$ h.

Parameter values arbitrarily determined

Activated microglia and macrophages have been observed to have the same behaviors and the same features in brain tissue, which make them difficult to distinguish. So we assumed that their abilities of phagocytosis were the same ($e_{N,L_m} = e_{N,M_a}$) and that their production rates of chemokines

- respectively cytokines - were also the same ($p_{M_a,cy,0} = p_{L_m,cy,0}$ and $p_{M_a,cy} = p_{L_m,ch}$). Neutrophils and inactivated microglial cells have also phagocytic activities but these activities are lower than those of macrophages and activated microglia. For simplicity, we assumed that $e_{N,L_n} = e_{N,M_i}$. Thus we obtained:

$$\mathscr{E} = e_{N,1}(M_a + L_m) + e_{N,2}(L_n + M_i).$$

Moreover we fixed arbitrary that

$$e_{N,2} = \frac{e_{N,1}}{4}.$$

The threshold of cell resistance to toxicity $\mathscr{D}_0$ was also fixed arbitrary. This threshold is compulsory so that the resting state is stable but the quantification of damage is arbitrary. Thus we fixed $\mathscr{D}_0 = 0.02$. Moreover, we assumed that the diffusion coefficients of macrophages and neutrophils were the same ($D_{L_m} = D_{L_n}$), that the diffusion coefficients of chemokines and cytokines were the same ($D_{ch} = D_{cy}$), that the activations of microglia by necrotic or apoptotic cells were the same ($c_A = c_N$) and finally that half the cells died through necrosis ($p_N = p_A = 0.5$).

Determination of the other parameter values

With the simplifications established above, there are still 19 parameter values to determine. We fixed the values of these parameters in order to check the following biological assertions:

- the number of microglial cells doubles in 24 hours [27].

- The concentration of cytokines reaches its peak after 12 hours [170]. Cytokines and chemokines are degradated and gradually eliminated.

- The density of neutrophils decreases after 48 hours [67].

- The density of macrophages does not decrease in the first 72h [67].

- The cytokine concentration reaches its peak in 12h [171].

In the following, the set of assertions listed above will be called the basis of rules. The parameter values that meet this basis of rules are listed together to the others values in Table 5.1. This set of parameter values is called reference set in the following sections.

5.4 Numerical Simulations

### 5.4.1 Simulation of Inflammation during an Ischemic Stroke

We present here *in silico* experiments that represent an inflammatory process which occurs during 72 hours of a typical ischemic stroke. The infarcted core after 30 minutes of ischemia is a disc of radius 5.5mm composed only of necrotic cells. In our simulations we used the reference set of parameter values. Figure 5.2 presents the numerical results obtained with a simulation over 72 hours. As required by the determination of parameter values, these results reproduce the basis of rules of Section 5.3.3.

In Figure 5.2(a), we can notice different behaviors related to the death process. As a matter of fact, there is a constant decrease of necrotic cells while, for apoptotic cells, there is first a growth and then a slower decrease due to the different elimination times of phagocytosis.

Figure 5.2(c) shows the dynamics of activated microglia and of all the microglial cells (activated and

| Parameter		Value in ref. set
t_A	duration of apoptotic process	12
$T_{M,1}$	characteristic time of microglia deactivation	60
$T_{M,2}$	characteristic time of microglia duplication	18
$T_{L_{min}}$	characteristic time of macrophages recruitment	24
$T_{L_{nin}}$	characteristic time of neutrophils recruitment	12
T_{L_m}	characteristic time of macrophages degradation	90
T_{L_n}	characteristic time of neutrophils degradation	3
$\mathscr{D}_0$	threshold of cells resistance to toxicity	0.02
p_N	proportion of cells dead by necrosis	0.5
$e_{N,2}$	elimination by neutrophils and inactivated microglia	0.0125
c_N	microglia activation by necrotic cells	0.06
D_{L_n}	neutrophils diffusion coefficient	1.5
D_{cy}	cytokines diffusion coefficient	0.2
$p_{N,[cy]}$	cytokines toxicity	0.1
p_{N,L_n}	neutrophils toxicity	0.4
$p_{N,N}$	necrotic cells toxicity	0.05
$e_{N,1}$	elimination by macrophages and activated microglia	0.05
c_A	microglia activation by apoptotic cells	0.06
c_{M_i}	mitosis rate of microglia	0.38
$p_{\mathscr{M}_{adh},[cy]}$	adhesion molecules recruitment by cytokines	5
$e_{\mathscr{M}_{adh}}$	elimination rates of adhesion molecules	0.1
t_0	charac. time of balance between pro/contra infla. cytokines	72/6
$p_{cy,0}$	cytokines production rate	10
e_{cy}	cytokines elimination rate	0.1
p_{ch}	chemokines production rate	4.5
e_{ch}	chemokines elimination rate	0.18
c_{L_m}	macrophages recruitment rate	24
c_{L_n}	neutrophils recruitment rate	28
μ_m	macrophages chemotaxis coefficient	0.15
μ_n	neutrophils chemotaxis coefficient	0.3
D_{L_m}	macrophages diffusion coefficient	1.5
D_{ch}	chemokines diffusion coefficient	0.2

Table 5.1: Reference set of parameter values: at the beginning there are the values determinated on biological bases, then values arbitrary determinated and, at the end, values determinated in accordance to the basis of rules.
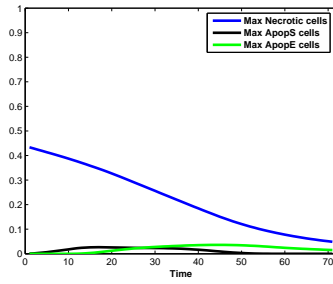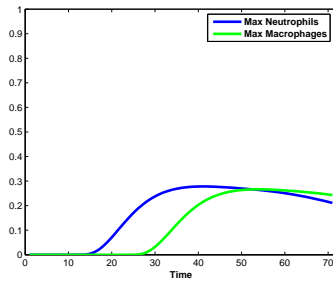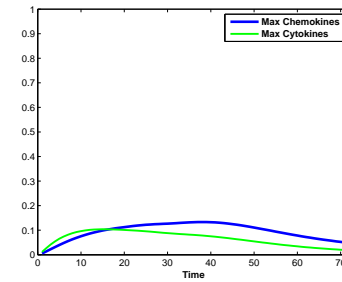
(a) Necrosis and apoptosis.
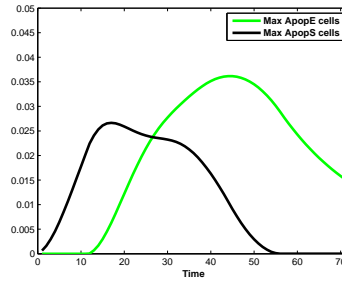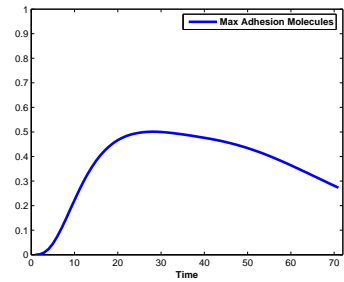

(b) Apoptosis (bigger scale).
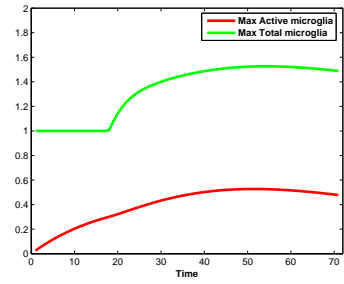
(c) Activated microglia and total microglial cells.

(d) Macrophages and neutrophils.

(e) Cytokines and chemokines

(f) Adhesion molecules

Figure 5.2: Time evolution of the maximum over space variable of various functions of the model.

inactivated). We can notice a progressive activation of these resident immune cells that lasts for the whole time of simulation. On the contrary, we can observe a brutal increase of activated microglia due to its duplication.

In Figure 5.2(d), we can observe a similar behavior of macrophages and neutrophils with a delay due to different times of entrance into the tissue. We can also notice that, at the end of the simulation, when the dead bodies have been eliminated, leukocytes begin to decrease in brain tissue.

Figure 5.2(e) shows that the dynamics of the maximal concentration of cytokines is quite different from the dynamics of the maximal concentration of chemokines. We can see that the concentration of cytokines rapidly increases and slowly decreases whereas the concentration of chemokines slowly increases and decreases.

Figure 5.2(f) describes a rapid increase of adhesion molecules during the first 20 hours of the stroke. Then, we observe a stable level in the following 30 hours and, at the end of the process, we can see a slow decrease of this density.

5.4.2   Robustness and Sensitivity of Parameters

Our model includes many parameters and their values were chosen following a basis of rules as indicated in 5.3.3. We determined a reference set of parameter values and, before exploring the parameter space, we studied the influence of these parameters on the model. Thus we studied the robustness and the sensitivity of the model to these parameter values.

Robustness

In this part we wanted to check if the model with different values of parameters would still meet the basis of rules established in Section 5.3.3. Hence we changed the value of one parameter keeping all the other parameter values unchanged. Then we solved the equations and checked if the basis of rules was still met. Results are summed up in Table 5.2.
We can sort the parameters in three classes:

- the parameters that have little influence on the model results (T_{L_n}, T_{L_m}, $T_{L_{min}}$, $T_{L_{nin}}$, c_A, c_N, t_A, $T_{M,1}$, $T_{M,2}$, t_0, D_{ch}, D_{cy}, $p_{\mathcal{M}_{adh},cy}$, C_{M_i}, p_{ch}),

- the parameters that have a moderate influence on the model results (e_{ch}, c_{L_m}, c_{L_n}, μ_m, D_{L_n}, D_{L_m}, D_0, $p_{cy,0}$, e_{ch}, $p_{N,cy}$, p_{N,L_n}, $p_{N,N}$),

- The parameters that have a strong influence on the model results (μ_n, $e_{N,1}$, $e_{N,2}$, $e_{\mathcal{M}_{add}}$.).

We can notice that, even if we highly change the values of some parameters (e_{ch}, c_{L_m}, c_{L_n}, μ_m, D_{L_n} and D_{L_m}), we obtain quite stable results. Therefore they affect mainly the related cells but do not influence the whole process. On the contrary, the interval range found for the neutrophils chemotaxis coefficient μ_n is $[0.03; 0.75]$ and its bigger modification brings to significant changes in the simulated results. Concerning parameters related to time, such as T_{L_n}, T_{L_m}, $T_{L_{min}}$ and $T_{L_{nin}}$, we can note that changes in their values lead to negligible consequences in the simulated process.

Sensitivity

In this section, we studied the sensitivity of the model results to the parameter values. It is important to check this point before using the model for *in silico* experiments in order to be aware of the limitations due to parameter values used in the simulations. The sensitivity study can also give information for the further exploration of the parameter space.
To study the sensitivity, we considered six outputs of the model: the final dead area, the final density of macrophages, neutrophils, inactivated and activated microglia, cytokines, chemokines and adhesion molecules.
And we proceeded as follows: if $s(p_1, p_2, \cdots, p_n)$ is one of the chosen outputs obtained with the parameter values $\{p_1, p_2, \cdots, p_n\}$, the sensitivity of this output for example to the parameter p_1 is given by:

$$S = \left(\frac{s(p_1 + \varepsilon, p_2, \cdots, p_n) - s(p_1, p_2 \cdots, p_n)}{s(p_1, p_2 \cdots, p_n)} \right) / \left(\frac{\varepsilon}{p_1} \right).$$

In our study, we considered a change ε equal to $\varepsilon = 5\%$ of the parameter.
The sensitivity of the size of the final dead area is small (equal to 4.10^{-4}) for all the parameters except for the diffusion coefficient of the neutrophils D_{L_n} where the sensitivity is null. Similarly, the sensitivity of the final total density of inactivated microglia is null for all the parameters. The results concerning the sensitivities of the other output functions are presented in Table 5.3. We made other simulations with a smaller change ($\varepsilon = 0.5\%$ of the value of parameter) but the sensitivity results were similar.
Most parameters appear to have small influences on the main outputs of the model. As a consequence, we can introduce some small variations on the parameter values without changing the simulation results. But few parameters (D_0, $p_{N,[cy]}$, $p_{N,N}$, $e_{N,1}$, $e_{N,2}$, p_N, c_N, $T_{M,1}$, $p_{\mathcal{M}_{adh},[cy]}$, $e_{\mathcal{M}_{adh}}$, t_0, e_{cy}, $p_{cy,0}$) have a strong influence on the model outputs.

Parameter	Value in the reference set	Range of values where the rules are met
t_A	12	$\pm 50\%$
$T_{M,1}$	60	$\pm 50\%$
$T_{M,2}$	18	$[-90\%; +250\%]$
$T_{L_{min}}$	24	$[-95\%; +50\%]$
$T_{L_{nin}}$	12	$[-90\%; +300\%]$
T_{L_m}	90	$[-97\%; +100\%]$
T_{L_n}	3	$[-66\%; +3000\%]$
$\mathscr{D}_0$	0.02	$[-20\%; +13\%]$
p_N	0.5	$\pm 10\%$
$e_{N,2}$	0.0125	$[-10\%; +20\%]$
c_N	0.06	$\pm 50\%$
D_{L_n}	1.5	$[-50\%; +3000\%]$
D_{cy}	0.2	$[-50\%; +600\%]$
$p_{N,[cy]}$	0.1	$[-50\%; +30\%]$
p_{N,L_n}	0.4	$[-50\%; +25\%]$
$p_{N,N}$	0.05	$[-20\%; +120\%]$
$e_{N,1}$	0.05	$[-15\%; +25\%]$
c_A	0.06	$\pm 66\%$
c_{M_i}	0.38	$[-95\%; +200\%]$
$p_{\mathscr{M}_{adh},[cy]}$	5	$[-50\%; +100\%]$
$e_{\mathscr{M}_{adh}}$	0.1	$[-50\%; +650\%]$
t_0	72/6	$[-50\%; +150\%]$
$p_{cy,0}$	10	$\pm 50\%$
e_{cy}	0.1	$[-90\%; +400\%]$
p_{ch}	4.5	$[-78\%; +100\%]$
e_{ch}	0.18	$[-94\%; +200\%]$
c_{L_m}	24	$[-84\%; +150\%]$
c_{L_n}	28	$[-92\%; +115\%]$
μ_m	0.15	$[-80\%; +33\%]$
μ_n	0.3	$[-90\%; +150\%]$
D_{L_m}	1.5	$[-84\%; +3000\%]$
D_{ch}	0.2	$[-50\%; +2500\%]$

Table 5.2: Robustness study. Range of values for each parameter where the model still meets the basis of rules described in 5.3.3. Biologically fixed parameters at first, arbitrary fixed at second and the others parameter at the end.

Parameter	Num. of L_m	Num. of L_n	Num. of M_a	Mass of $[cy]$	Mass of $[ch]$	Mass of $\mathcal{M}_{adh}$
Ref. values	1.4707	1.0184	0.1514	0.0978	0.1876	0.0272
t_A	0	0	0	0	0	0
$T_{M,1}$	+	+	+ +	+	+	+
$T_{M,2}$	0	0	0	0	0	0
$T_{L_{min}}$	0	0	0	0	0	0
$T_{L_{nin}}$	0	+	0	+	+	0
T_{L_m}	0	0	0	0	0	0
T_{L_n}	0	+	0	0	0	0
$\mathscr{D}_0$	+ +	+ +	+	+ + +	+ + +	+ +
p_N	+ + +	+ + +	+ + +	+ + +	+ + +	+ + +
$e_{N,2}$	+	+ +	+ +	+ + +	+ + +	+ +
c_N	+ +	+ +	+ +	+	+	+
D_{L_n}	0	0	0	0	0	0
D_{cy}	+	+ +	+	0	+	0
$p_{N,[cy]}$	+	+	+	+ +	+ +	+ +
p_{N,L_n}	0	0	0	+	+	0
$p_{N,N}$	+ +	+ +	+	+ + +	+ + +	+ +
$e_{N,1}$	+	+ +	+	+ + +	+ + +	+ +
c_A	0	0	0	0	0	0
c_{M_i}	0	0	0	0	0	0
$p_{\mathcal{M}_{adh},[cy]}$	+ +	+ +	0	+	+	+ +
$e_{\mathcal{M}_{adh}}$	+ +	+ +	0	+	+	+ + +
t_0	+ +	+ + +	0	+ + +	+ +	+ +
$p_{cy,0}$	+ +	+ + +	+	+ + +	+ +	+ + +
e_{cy}	+ +	+ +	0	+ +	+	+ +
p_{ch}	0	0	0	0	+ + +	0
e_{ch}	0	0	0	0	+ +	0
c_{L_m}	+ + +	0	0	+	+	+
c_{L_n}	0	+ + +	0	+	+	0
μ_m	0	0	0	0	0	0
μ_n	0	0	0	0	0	0
D_{L_m}	+ + +	0	0	0	0	0
D_{ch}	0	0	0	+	+	+

Table 5.3: Sensitivity study with $\varepsilon = 5\%$ of the parameter value in the reference set. In each row, you find a symbol which indicates the value of S (with respect to each parameter) regarding the output written on the first line. Here "0" indicates that a parameter influences not at all the corresponding output variable, " + " that it influences a little, " + +" that it influences moderatly and finally " + + +" indicates that the paramenter influences strongly the corresponding output. The thresholds chosen are the following $0 \leq 0 < 0.1$, $0.1 \leq + < 0.4$, $0.4 \leq + + < 0.9$ and $+ + + \geq 0.9$.

We can also notice that the proportion of cells dying by necrosis and apoptosis (represented by parameters p_N) is very significant in the model, because a little change of its value leads to important changes in the final quantities of leukocytes, microglia, cytokines, chemokines and adhesion molecules.

Concerning the final number of macrophages, we can observe that this quantity is sensible to several parameters such as $p_{\mathcal{M}_{adh},[cy]}$ the production rate of adhesion molecules, $e_{\mathcal{M}_{adh}}$ the natural decay of adhesion molecules, $p_{cy,0}$ the production rate of cytokines by macrophages and microglia, c_{L_m} a measure of the quantity of macrophages that filter into the tissue and D_{L_m} the diffusion coefficient of these leukocytes. The final density of neutrophils has a similar response. It is sensitive to small changes in parameters related to adhesion molecules, and of course to the parameter c_{L_n} which quantifies the neutrophils that infilter the tissue. It is interesting to notice that a small variation of the diffusion coefficient D_{L_n} does not really influence them. Concerning activated microglia, we can note that they react also to small changes in the values of c_N, their activation rate by necrotic cells, and of $T_{M,1}$, the characteristic time of microglia deactivation. For proteins, cytokines and chemokines, we notice similar behaviors. As a matter of fact, they react to small changes of the following parameters: $\mathcal{D}_0$, a threshold of damage of living cells, $p_{N,N}$ that estimates the effects of necrotic cells on dead cells elimination, and $e_{N,1}$, $e_{N,2}$ that are the elimination rates of dead cells by phagocytosis respectively of macrophages, activated microglia and inactivated microglia and neutrophils. These proteins are also affected by changes in their production rates, $t_0, p_{cy,0}, p_{ch}$, and natural decay e_{cy}, e_{ch}.

Finally, we can note that the density of adhesion molecules is mainly sensitive to changes in their production rate, $p_{\mathcal{M}_{adh},[cy]}$, and natural decay, $e_{\mathcal{M}_{adh}}$, and in addition to small changes in parameters related to cytokines t_0, $p_{cy,0}$ and e_{cy}.

5.4.3 Influence of the Size of the Initial Infarct

We then used this model to carry out *in silico* experiments in order to explore the beneficial and/or deleterious effects of inflammation during stroke depending on the size of the initial infarct.
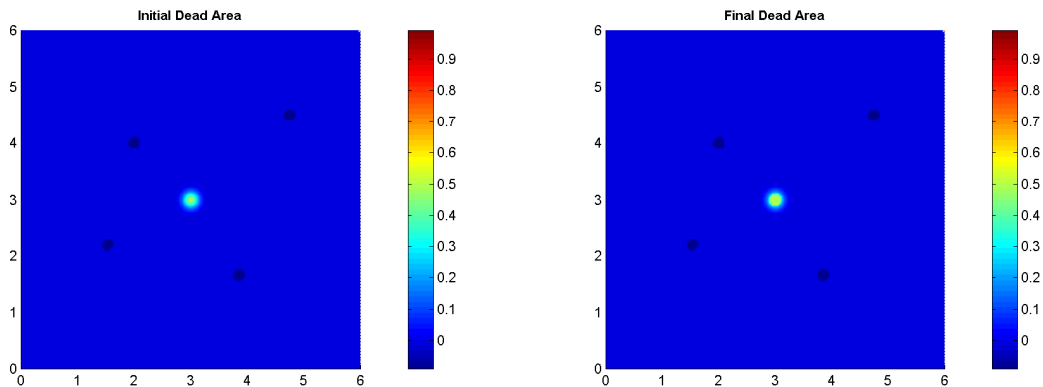

Figure 5.3: Initial and final dead areas obtained with an initial small size of the infarct.

Figures 5.3, 5.4 and 5.5 show the influence of initial dimension of the infarct in the development of the inflammatory process. We can observe that the aggravation due to inflammation is not a linear function of the initial size of the stroke. Therefore even if we had considered an initial infarct twice
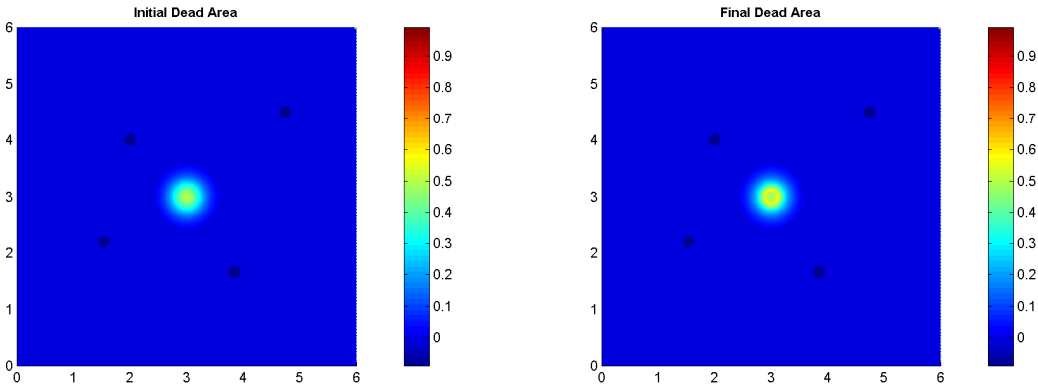
Figure 5.4: Initial and final dead areas obtained with an initial medium size of the infarct.
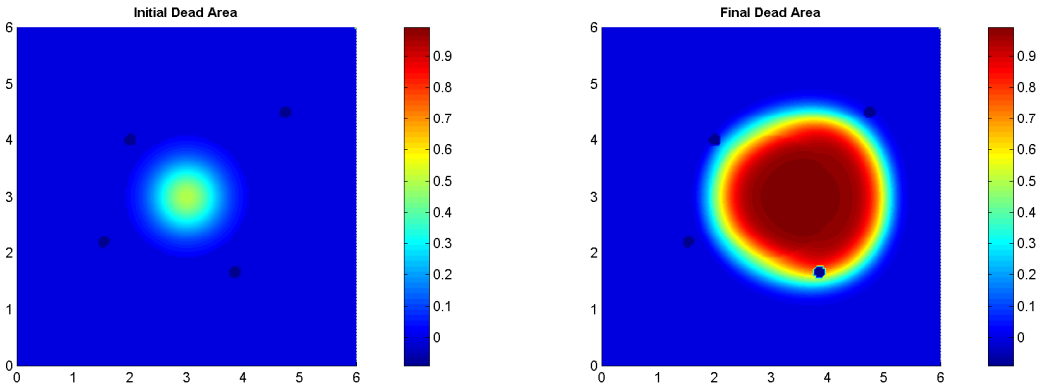

Figure 5.5: Initial and final dead areas obtained with an initial large size of the infarct.

smaller (or twice bigger) than the standard stroke used in the previous simulations, the final size of the dead area would not have been twice smaller (or twice bigger) than the final area previously obtained. We can note that for small and medium initial data there is not an increase of the dead area, but, in the case of big size of the infarct, Figure 5.5, we have a significant increment of 235%. In this case the initial dead area is 3.5911, while the final dead area is 12.0504, which correspond to 335% of the initial area.

5.5   Discussion

In this study, we built a model based on a set of ordinary and partial differential equations to represent the biological phenomena involved in the inflammatory process during an ischemic stroke. In our model, we considered different types of cells and of chemical substances. Therefore we represented the behavior of healthy, necrotic and apoptotic cells, and of immune cells like microglia, neutrophils, macrophages. Moreover we have included the cytokines, chemokines and adhesion molecules. The most important feature of the model is its spatial dimension, which allows to reproduce some mechanisms such as the diffusion of proteins and the recruitment of leukocytes by chemotaxis.

The model includes many parameters and one of the main problems was to determine the values of these parameters. We fixed these values with different methods (as explain in 5.3.3). Some parameters were determinated by fitting the results of the model to real data coming from experiments on rats that underwent permanent ischemia [67], other parameters thanks to biological knowledge and the remaining parameters in order not to disturb the system. It was possible to find a set of parameter values that allows the model to respect the rules detailed in Section 5.3.3. Thus, with this reference set of parameter values, we could obtain realistic simulations of the biological phenomenon. However a further study of the parameter space should be made to check if the qualitative behavior of the model is completely determined by those rules or if we have to complete them.

In the robustness study, Section 5.4.2, we mainly obtained narrow ranges of parameter values, which guarantees a quite stable behavior of the whole system. Another significant aspect underlined by the robustness study is the main role of chemotaxis. As a matter of fact, alterations of chemotaxis coefficients, especially the neutrophil ones, highly affect the behavior of the whole process, leading to a system that does not meet the basis of rules any more.

In the sensitivity study, Section 5.4.2, we observed that no parameter influenced the final total amount of inactivated microglia. It may be explained by the fact that the mitosis rate of microglia (c_{M_i}) is too high compared to the other terms of equation (5.8). As a consequence, whatever the parameter values, the final amount of inactivated microglia is always at its maximum value ($M_i = 1$). This behavior could be modified with the introduction of some decay for inactivated microglia. In this sensitivity study, we also noticed a quite stable behavior of adhesion molecules. If we exclude the parameters directly related to this variable, significant changes in the other parameters do not affect the behavior of these molecules in blood vessels. This sensitivity study is a first step in the exploration of the parameter space. Now with this first set of parameters we are able to manage the system in order to investigate the balance between positive and negative aspects of each components in inflammation.

After determining and studying this reference set of parameter values, we used it in the model in order to perform *in silico* experiments in different conditions. We studied how the size of the initial infarct could influence the development of the inflammatory process (see Section 5.4.3). The simu-

lation results show that the aggravation due to inflammation is not linearly correlated to the infarct size, which is an interesting result. These results suggest that blocking inflammation would be more interesting for severe ischemic stroke whereas the benefit of inflammation could be stronger than the aggravation in small infarct. In this latter case, anti-inflammatory drugs could aggravating the cell damage instead of bring to beneficial effects. This point needs to be confirmed by further experiments.

We can also use this model to simulate different therapeutic strategies. Currently, the only therapeutic approach used in the Stroke Units in hospitals is thrombolysis which is aimed at reopening the obstructed vessel. We could simulate a reperfusion (i.e. a reopening of the obstructed vessel) in our model by including the role of blood flow and of ATP on each mechanism involved in the inflammatory process. Since thrombolysis can only be given to about 5 percents of stroke patients, other therapeutic strategies have been developed for about twenty years. They are called neuroprotective strategies and are aimed at blocking the biological process leading to cell death. Anti-inflammatory drugs belong to these neuroprotective approaches. The anti-inflammatory molecules already tested block either the first phase (i.e. activation of microglia) or the second phase of inflammation (i.e. infiltration of leukocytes). With our model, we can simulate different anti-inflammatory treatments acting on various targets (microglia, adhesion molecules, cytokines, neutrophils) and we can compare the effects of these treatments. Moreover, since we distinguished in the model the apoptotic cells at the beginning (reversible phase) of the apoptotic cascade and those at the end (irreversible phase) of the apoptotic cascade, we can also simulate the effects of anti-apoptotic drugs and study their roles on the ischemic damage.

The model can thus already be used to carry out *in silico* experiments that could contribute to a better understanding of the mechanisms involved in the inflammatory process (their influences and their connections) and of the effects of various therapeutic strategies. However, this model can also be prolonged and refined. First of all, it could be interesting to introduce in the model the rupture of the blood-brain barrier which occurs during a stroke and increases the infiltration of leukocytes in brain tissue. This could be done by adding a function that would increase membrane permeability when the density of adhesion molecules would increase (which is currently the case in the model) and when the blood-brain barrier would disrupt. Moreover, it could be interesting to add in the model a specific function describing the dynamics of endogenous anti-inflammatory cytokines. This dynamics is currently taken into account in the global function representing cytokines but it could be modeled in more details. This work is under development. Besides, we could also model in more details the deleterious effects of the free radicals (such as NO) that are produced by microglia and leukocytes and that can also be therapeutic targets. Finally, it could also be relevant to study the phenomenon in different geometrical conditions, for example with other distributions of vessels. Moreover, since the infarct size influences the effects of the inflammatory process, it could be interesting to perform simulations of realistic brain infarcts on a whole brain section (by adding no-flux conditions on its boundaries). To perform these simulations on brain sections, we should take into account brain geometry, brain heterogeneity (white matter / grey matter) and brain anisotropy. These features are important to study more precisely the propagation of the inflammatory process. This could also be the first step of a 3D study of the inflammatory process in ischemic stroke.

Chapter 6

A Fluid Dynamics Model of the Growth of Phototrophic Biofilms

In this chapter, a system of nonlinear hyperbolic partial differential equations is derived to model the formation of biofilms [39, 38]. In contrast with most of the existing models, our equations have a finite speed of propagation, without using artificial free boundary conditions. In addition, we are able to deal in a natural and effective way with regions where one of the phases is vanishing.

The plan of the chapter is the following. Firstly, an introduction to some basic concepts about the biological phenomenon is given; then, in Section 6.3, we present a detailed derivation of our fluid dynamics model, paying special attention to modeling the influence of the light on the growth of the biofilms. An adapted numerical scheme is described in details in Section 6.4. Finally, in the last section, we present some numerical tests, with the aim of illustrating the power of our approach and also the influence of the various parameters. Our tests are performed in one, two, and three space dimensions, for a domain with no flux conditions. We study the influence of light on the system and we detect how the estimate of the sound velocity of the medium affects the final output and in particular the speed of the front (it should be noted that this is not an easy task from the experimental point of view).

We are interested in particular in the formation and evolution in several space dimensions of cyanobacteria biofilms, with special attention to their development on the stone surfaces of ancient monuments, as for instance fountains walls, i.e. on stone substrates and under a water layer.

Here, our model refers essentially to the class of Chroococcales, in particular Gleocapsa, which is a genus of photoautotrophic bacteria and is a prokaryote. The cells secrete individual gelatinous sheaths which can often be seen as sheaths around recently divided cells within outer sheaths. Notice that, even if our focus is on phototropic species, like cyanobacteria, it is clear that most of the framework we are going to deal with in this thesis can be extended to other species and mixed colonies.

Our first goal is to introduce a model which keeps the physical finite speed of propagation of the fronts. Starting from the ideas of the mixture theory [138, 14, 137], we write some balance equations which contain the main assumptions coming from biophysical considerations (mass and momentum conservation, influence of nutrients and light, ...). The inertial terms in the momentum equations guarantees the hyperbolicity of the system and the finite speed of propagation. Actually, in most of the models coming from the mixture theory approach, as for instance [137, 58], these terms are neglected, in order to simplify the analysis and the numerical approximation. In fact, diffusive terms stabilize the fluid and prevent possible breakdowns or other instabilities. Nevertheless, this

simplification introduces a non-physical infinite speed of propagation in the problem, and makes it difficult to study effectively the evolution of interfaces between the solid (biofilm) and the liquid (water) phases. A possible solution is to use moving fronts techniques, see [4, 137], which however introduce other analytical and numerical difficulties and require a further approximation in the model. We prefer to keep the inertial terms and to solve the full hyperbolic problem using some robust and Riemann Solver-free scheme like relaxation schemes [13]. However, there are two important differences with respect to a usual hyperbolic system. First, since we are dealing with a multiphase fluid, it is difficult to deal with regions where one of the phases may vanish. This is usually solved by neglecting these regions, for instance by selecting special initial conditions. In a biofilm these choice is not possible, since it is important to model also the region where there is only the biofilm or the liquid. It turns out that this problem of vanishing phases can be solved by approximating source terms just by using an Implicit-Explicit scheme (see Section 6.4 for more details).

The other problem arises from the fact that our model is supplemented with a constraint term due to the mass conservation, which implies that the average hydrodynamic velocity of the mixture is divergence free. This constraint is needed to compute the hydrostatic pressure. To enforce the divergence free constraint, we used a fractional step approach similar to the Chorin-Temam projection scheme [36, 161] for the Navier-Stokes equations, with a very accurate reconstruction of the pressure term.

6.1   Biological Backgrounds

A biofilm is a complex gel-like aggregation of microorganisms like bacteria, cyanobacteria, algae, protozoa and fungi, embedded in an extracellular matrix of polymeric substances, called EPS. Even if a biofilm contains water, it is mainly in a solid phase. Biofilms can develop on surfaces which are in permanent contact with water, i.e. on a solid/liquid interfaces, but the growth of microorganisms also occurs on different types of interfaces such as air/solid, liquid/liquid or air/liquid.

Biofilms are not simply passive assemblages of cells that are stuck to surfaces, but they are structurally and dynamically complex biological systems. Their development is often characterized as a multistage process. First, some free-floating bacteria approach the surface and within a few minutes they get attached. Then, during a phase of colonization, bacteria loose flagella and produce EPS. During the growth phase, bacteria build a 3D structure, influenced by a variety of environmental factors. In the end, a part of the biofilm may detach itself in order to colonize other parts of the surface [63].

Biofilms are present in different contexts. Some biofilms are useful, providing valuable services to human society or to the functioning of natural ecosystems. Other biofilms are harmful, causing serious health and economic problems. For example, in the subsurface bacteria normally grow as biofilms on the soil matrix and can help to remove contaminants from the soil or ground waters. On the other hand, their propensity for attachment causes problems in many situations, such as in industrial pipelines, ship hulls, nuclear power stations, space stations, air conditioning systems, water distribution systems.

Since biofilms play a significant role in many natural and engineered systems, understanding the mechanisms of biofilm formation, growth, and removal could be the key in promoting good biofilms and contrasting bad ones. Since many of the physiological characteristics of biofilm formation (like localized clusters of bacteria adhering to a substratum and resistance to antibiotic therapy) are sim-

ilar in the natural environment and in an animal host, the knowledge of biofilm formation from environmental studies helped to characterize biofilms growing on medical devices and biofilm infections [71].

6.1.1 Infectious Diseases

Hospitals are susceptible to colonization by microorganisms growing in biofilms as well. In many cases, harmful biofilms cannot be prevented and they develop even under adverse conditions (extreme pH values or temperatures up to 95 C), so removing them is often difficult in technological systems without a direct access to the exposed surfaces.

Biofilms associated with medical devices were first noted in the early 1980s when electron microscopy revealed bacteria deposited on the surface of indwelling devices, such as intravenous catheters and cardiac pacemakers [63].

Biofilm formation as a protective mechanism could have profound implications for the host, because the microorganisms that are growing in these matrix-enclosed aggregates are more resistant to antibiotics and host defences. Intravenous catheters, prosthetic heart valves, joint prostheses, peritoneal dialysis catheters, cardiac pacemakers, cerebrospinal fluid shunts and endotracheal tubes save millions of lives, but they all have an intrinsic risk of surface-associated infections. The microorganisms that are most frequently associated with medical devices are the staphylococci (particularly S. epidermidis and S. aureus), followed by P. aeruginosa and other environmental bacteria that infect a host who is compromised by invasive medical intervention .

Biofilm formation on medical implants has even led to the characterization of a new infectious disease called chronic polymer-associated infection. The most noticeable characteristic of the adherent staphylococci colonizing medical implants is the copious amount of EPS that encases and protects cells from host defences and antibiotic treatment.

Biofilm infections within the human body, characterized by adherent bacteria on tissue, might also include host cells and molecules as part of a surface-associated infection such as bacterial endocarditis. Moreover, biofilms are a major problem also in dental hygiene (caries, gingivitis, periodontitis) and persistent and chronic infections (otitis media, cystic fibrosis, diabetic foot ulcers).

6.1.2 Biodeterioration

Since active biofilms can be found in any place where there are microorganisms and humidity, a biofilm can develop also on external walls of buildings [43]. The microbiota on building stones represent a complex ecosystem which develops in various ways, depending on environmental conditions and the physicochemical properties of the material.

There is an increasing experimental evidence about the essential role of biological agents in the deterioration of stone; it is clear that many physical, chemical, and biological factors combine their effects in affecting the material. The colonization of external surfaces of buildings, monuments and archeological sites by microorganisms causes an unaesthetically appearance of staining of the stone surfaces and the production of extracellular polymeric substances (EPS), which cause mechanical stresses onto the mineral structure inside the pore system. This can lead to the alteration of pore size and distribution, together with changes in moisture circulation patterns and temperature response. Microorganisms may also alter the water permeability of the minerals by the deposition of surfactants. Moreover, it has been shown that the early presence of biofilms on exposed stone surfaces accelerates the accumulation of atmospheric pollutants [130], [163]. So this mi-

crobial contamination acts as a precursor of the formation of detrimental crusts on rock surfaces caused by acidolytic and oxidoreductive (bio-) erosion of the mineral structure.

Organisms present on stone monuments can include photolithoautotrophs, such as algae, cyanobacteria, mosses, and higher plants. Chemolithoautotrophic bacteria are also present; they can release acids such as nitrous acid, nitric acid, or sulfuric acid, that change the local pH. Chemoorganotrophic bacteria and fungi, instead, may release chelating organic compounds or weaken the mineral lattice by the oxidation of metal cations.

The microbial colonization of stones starts with phototrophic organisms which build up a visible biofilm of enriched organic biomass on the stone surface. The growth and metabolic activity of these algae, cyanobacteria, and lichens, as well as mosses and higher plants, is regulated by parameters such as light and moisture [144]. Phototrophic microorganisms may grow on the stone surface (epilithic phototrophs) or may penetrate some millimeters into the rock pore system (endolithic phototrophs). These epilithic and endolithic organisms can potentially contribute to the breakdown of rock crystalline structures such as sandstone, granite, gneiss, limestone, dolomite, amphibolite, basalt, dolerite, bricks, or even glazes.

As a lots of investigations have stressed the importance of phototrophs in the physical and chemical deterioration of stones, we focused our attention on a particular class of phototrophs: the *cyanobateria.*

Cyanobacteria, also known as blue-green algae, blue-green bacteria or Cyanophyta, are a phylum of bacteria that obtain their energy through photosynthesis. Their name comes from the color of the bacteria. They colonize a wide variety of terrestrial habitats, including rocks, hot and cold desert crusts, as well as modern and ancient buildings.

Cyanobacteria include unicellular and colonial species. Colonies may form filaments, sheets or even hollow balls. Each individual cell of a cyanobacterium typically has a thick, gelatinous cell wall. Cyanobacteria have an elaborate and highly organized system of internal membranes which allows photosynthesis.

The role of cyanobacteria in the deterioration of surfaces of historical buildings has been the subject of several recent studies. These bacteria are generally adapted to resist adverse conditions because of their thick outer envelopes and the presence of protective pigments. Since they are phototrophs and require no more than light, water, and mineral ions to grow, these microorganisms, along with algae, readily colonize the external surfaces of ancient monuments and develop a biofilm, which, in turn, alters the appearance of the building and serves as a substrate for the growth of other deteriogens. Both these microorganisms and cyanobacteria can cause aesthetic, chemical, and physical decay.

6.2 Previous Models

For a so huge topic, it is not surprising to find that there exist many mathematical models. At the beginning, mathematical modeling of biofilm was mainly focused on predicting growth balance, sometimes with practical applications in mind, as in [34, 110, 173, 174]. These are generally 1-D models with reaction-diffusion equations for nutrient and other substrates, sometimes with a moving boundary. The first multidimensional models were discrete and based on cellular automata. For example, models proposed by the Delft's team [172] are mainly multidimensional, multispecies and multisubstrates spatially discrete models, which have been solved by individual-

based approach or cellular automata. They are quite exhaustive from the biological point of view, at least qualitatively, but not fully satisfactory, because of the difficulties to simulate large colonies of millions of individuals with discrete approach, and to give a precise description of the behavior of the solutions.

At the same time, fully continuum models have been considered. The recent review by Klapper and Dockery [91], focus mainly on this kind of models, following the idea of treating the biofilm as a viscoelastic material that expands in response to growth-induced pressure. Among them, an important class of models was proposed by Alpkvist and Klapper [4], and it is based on a multidimensional and multispecies description, where biofilms are divided into biomass and liquid. Since all these models are based on diffusion equations, they experience an unrealistic movement of the fronts, since in priciple bacteria can move infinitely fast. Moreover, due to diffusivity, it is also difficult to obtain sharp interfaces and finger-like structures which characterize biofilms, which are usually recovered by supplementing the model with artificial interfaces which are solved by moving fronts techniques. Another model has been proposed more recently by Zang, Cogan, and Wang [179]. They consider two phases: the polymer network and the solvent, and analyze numerically the case of detachment under different initial conditions. This model does not consider the different biological components and it is unable to describe the evolution of specific bacteria.

Another continuous model, including more biological details, was proposed by Anguine, King and Ward [9]. It concerns the biofilm produced by the *Pseudomonas aeruginosa*, a bacterium that causes serious infections. It is multispecies PDEs model and four different phases are considered: live cells, dead cells, EPS, and liquid. The influence of nutrients is also taken into account, as well as quorum sensing, one of the various signaling mechanism of cells, and also some different medical treatments, like antibiotics and antiQS drugs. Transport equations are introduced to model the four phases and advection-diffusion equations for nutrients, antibiotics and antiQS. A common velocity for bacteria, dead bacteria and EPS is assumed, while a different velocity is taken for the liquid. To close the system, the no-void condition is assumed together with a supplementary relation between the liquid and EPS, namely: a local increment of EPS causes a local increment of liquid. Thanks to these assumptions, no equation for velocities is needed. For this reason, the model works only in one space dimension.

6.3   The Fluid Dynamics Model

To describe the complex structure of biofilms, we have chosen to consider four different components, see [9]: Live cyanobacteria (B), Dead cyanobacteria (D), EPS (E), and Liquid (L). We denote the concentration of biomass by $C_\phi = \rho_\phi \phi$, where ρ_ϕ is the mass density of a phase in $[g/cm^3]$ and $\phi = B, D, E, L$ is the volume fraction of the phases. We assume that the biomasses are incompressible and Newtonian, so that ρ_B, ρ_D, ρ_L and ρ_E are positive constants. We also assume that the phases have all the same constant density.

We have reduced the composition of biofilm, which is usually composed by many different types of organisms, to one single species of cyanobacteria (for example Chroococcales, which have a sort of Eps sheats). Our four components can be considered like a mixture. It is possible to describe a mixture as "mixed-state or condition, co-existence of different ingredients or of different groups that mutually diffuse through each other" [138]. When one of the components is preponderant and the other are essentially insignificant, the body is usually assumed to be of the predominant single component. In our case, however, we will consider the four different components which equally

describe the growth of biofilms. This approach has been yet used by Preziosi et al. to model the formation of vascular tumors [137, 8].

6.3.1 Mass Balance Equations

Since the EPS encompasses the cells for this class of cyanobacteria, we can make the hypothesis that live cells, dead cells, and EPS have the same transport velocity, called $\mathbf{v_S}$. We denote instead by $\mathbf{v_L}$ the velocity of liquid, and by Γ_ϕ, with ($\phi = B, D, E, L$), the mass exchange rates. Consequently, the equations expressing the mass balance are:

$$\partial_t B + \nabla \cdot (B\mathbf{v_S}) = \Gamma_B, \tag{6.1a}$$

$$\partial_t D + \nabla \cdot (D\mathbf{v_S}) = \Gamma_D, \tag{6.1b}$$

$$\partial_t E + \nabla \cdot (E\mathbf{v_S}) = \Gamma_E, \tag{6.1c}$$

$$\partial_t L + \nabla \cdot (L\mathbf{v_L}) = \Gamma_L. \tag{6.1d}$$

We assume the following volume constraint:

$$B + D + E + L = 1, \tag{6.2}$$

that is to say the mixture is saturated. This means that the liquid fills all interstices of the mixture, so that no empty space is left.

From the mixture theory, we know that in addition to the balance of mass of each component, we also have the total conservation of mass of the mixture, that is to say:

$$\Gamma_B + \Gamma_D + \Gamma_E + \Gamma_L = 0. \tag{6.3}$$

This states that the mixture is closed, i.e. there is no net production of mass for the whole mixture.

6.3.2 Biomass Growth Rates

Now let us precise and comment the form of the mass production terms. We assume that

$$\Gamma_B \quad = \quad k_B B L - k_D B, \tag{6.4}$$

$$\Gamma_D \quad = \quad \alpha k_D B - k_N D, \tag{6.5}$$

$$\Gamma_E \quad = \quad k_E B f(L) - \varepsilon E. \tag{6.6}$$

The term Γ_B, the mass exchange rate for the active bacterial cells, is the difference between a birth term with rate k_B and a death term with rate k_D; the birth of new cells at a point highly depends on the quantity of liquid available in the neighborhood of the point, that is why the birth term is a product between the volume ratio B of active cells and the volume ratio L of liquid.

Now, the death term in the expression of Γ_B gives rise to a creation term in the mass exchange rate for dead cells Γ_D, however with a proportional coefficient α, since a part of the active cells becomes liquid when the cell dies. In Γ_D, we also find a natural decay of dead cells with a constant decay rate k_N.

The EPS is produced by active cells in presence of liquid and therefore the production term will be of the form $k_E f(L)B$, where k_E is the growth rate and $f(L)$ is a non-dimensional function of the liquid fraction with $0 \leq f(L) \leq 1$. There is also a natural decay of EPS with rate ε.

In the end, we choose the mass exchange rate of liquid Γ_L in order to enforce condition (6.3), that is to say

$$\Gamma_L = B\big((1-\alpha)k_D - k_B L - k_E f(L)\big) + k_N D + \varepsilon E. \tag{6.7}$$

All the coefficients k_B, k_D, k_E and k_N may depend on temperature, light intensity and concentration of nutrients.

Here, we want to estimate the growth rates of involved components (B, E, D), which are influenced by several environmental conditions such as temperature and light. Also, we would establish the optimal values for these parameters. Indeed, light is a fundamental variable in the life of some types of cyanobacteria (photoautotrophic cyanobacteria), allowing these organisms to photosynthesize inorganic compounds. Because photosynthesis responds quantitatively to changes in light, environmental variation in its quantity and quality potentially accounts for much of the variation in the physiology and population growth of cyanobacteria. In the same way, there exists a range of temperature, as well as a range of nutrient concentrations, necessary to the survival of cyanobacteria.

Light and temperature directly influence the specific growth rates and can reduce them when optimal values are not reached [55, 162]. To estimate the growth coefficient of cyanobacteria, we write the coefficient k_B as

$$k_B = k_{B0} \cdot g(I, T),$$

where k_{B0} is the optimal growth rate, and $g(T, I) \in [0, 1]$ is an efficiency factor given as a function of temperature and light.

Many authors have already formulated the effect of light upon algae growth with empirical mathematical functions, see [162]. In many models, the effects of the light and of the temperature are assumed independent, and the resultant growth is taken as the product of two limiting factors, namely $g_1(T) \cdot g_2(I)$. However, this choice highly overestimates limitations. In absence of appropriated experiments, we assume here that

$$g(T, I) = max(g_1(T), g_2(I)).$$

Here we assume that the death rate of cyanobacteria k_D, which is also the production rate of dead cells D, is independent of T and I, as well as EPS growth rate k_E [121] and decay rate for dead cells k_N, that is to say

$$k_D = k_D(I, T) \approx k_{D0} \tag{6.8}$$

$$k_E = k_E(I, T) \approx k_{E0} \tag{6.9}$$

$$k_N = k_N(T) \approx k_{N0} \tag{6.10}$$

where k_{D0}, k_{E0} and k_{N0} are the optimal rates. Numerical values of these optimal rates and other useful coefficients are given at Table 6.1.

It would be interesting to consider also a variable growth rate for all these coefficients, since they clearly also depend on the environmental conditions. However, we keep the model as simple as possible, as far as experimental evidences is missing.

Light Dependence

To describe the light influence on the biofilm growth, we indicate by I_0 the light intensity on the upper surface of water, and by $I(x, y, t)$ the intensity in the water. We assume that the light intensity

is attenuated following the law of photon absorption in the matter. Thus, we assume that $I(x, y, t)$ is constant in x for every fixed y (vertical coordinate) and t. Then, assuming $y \in [0, H]$ we have:

$$\frac{I(y, t)}{I_0(t)} = e^{-\int_0^y \mu(s)\,ds}, \tag{6.11}$$

where the absorption coefficient μ depends on the matter and on the frequency of radiation and $s = H - y$. By experimental observations, it has been estimated that $\mu \approx 0.9\ m^{-1}$ if the water is turbid, and $\mu \approx 0.2\ m^{-1}$ if the water is clear.

We still need to find the form of the correction factor and we assume that

$$\mu = \mu_0 \left(1 + h_\mu (B + E + D)\right), \tag{6.12}$$

where μ_0 is the absorption coefficient when the water is clear, and h_μ is a coefficient in the biomasses.

Finally, following [162], [55] and references therein, we assume that the specific growth rate as function of irradiation $I(x, y, t)$ is given by

$$g_2(I) = 2 w_2 \left(1 + \beta_2\right) \frac{\hat{I}}{\hat{I}^2 + 2\beta_2 \hat{I} + 1}, \tag{6.13}$$

where $\hat{I} = I / I_0$, w_2 is the maximum specific growth rate and β_2 is a shape coefficient.

Temperature Dependence

We assume that cyanobacteria have an optimal growth rate where the temperature is maximal and that the growth rate diminishes where the temperature is far from this optimal value. Following [162], we choose the specific growth rate as a function of temperature T, that is to say:

$$g_1(T) = 2 w_1 \left(1 + \beta_1\right) \frac{\theta}{\theta^2 + 2\beta_1 \theta + 1}, \tag{6.14}$$

where

$$\theta = \frac{T - T_{min}}{T_{opt} - T_{min}}. \tag{6.15}$$

Here w_1 corresponds to the maximum growth rate, β_1 is a shape parameter, and T_{min} is the minimal temperature for the model.

It can be easily added to the model a nutrient for cyanobacteria, using a classical diffusive equation.

6.3.3 Force Balance Equations

Adding the four equations of system (6.1) and using equations (6.2) and (6.3) yields:

$$\nabla \cdot ((1 - L)\mathbf{v_S} + L\mathbf{v_L}) = 0, \tag{6.16}$$

which means that the divergence of the average hydrodynamic velocity is equal to zero. It can be seen as an average incompressibility.

Next, let us write the equations for the force balance. We denote by $\tilde{\mathbf{T}}_\phi$ the partial stress tensor relative to the component ϕ, and by $\tilde{\mathbf{m}}_\phi$ the respective interaction force. So we can write the equation of force balance for the component ϕ ($\phi = B, D, E, L$) as follows:

$$\partial_t (\phi \mathbf{v}_\phi) + \nabla \cdot (\phi \mathbf{v}_\phi \otimes \mathbf{v}_\phi) = \nabla \cdot \tilde{\mathbf{T}}_\phi + \tilde{\mathbf{m}}_\phi + \Gamma_\phi \mathbf{v}_\phi. \tag{6.17}$$

The total conservation of momentum yields:

$$\sum_{\phi} (\tilde{\mathbf{m}}_{\phi} + \Gamma_{\phi} \mathbf{v}_{\phi}) = 0. \tag{6.18}$$

This equation means that the net momentum supply to the mixture due to all the components is equal to zero. As a matter of fact, if the mixture is closed, it is possible to prove that the sum of interaction forces and momentum transfers due to mass exchanges is null.

If a saturation condition like (6.2) is assumed, equations for the partial stress tensor and interaction forces are characterized by the presence of a Lagrange multiplier classically identified with the interstitial pressure of the liquid. So, from the theory of mixtures [138], it is possible to decompose the interaction forces as $\tilde{\mathbf{m}}_{\phi} = P \nabla \phi + \mathbf{m}_{\phi}$, where P is the hydrostatic pressure, a scalar common to all the phases, and $\mathbf{m}_{\phi}$ is the force exerted by the phase ϕ on the other phases. It is also possible to decompose the partial stress tensor as $\tilde{\mathbf{T}}_{\phi} = -\phi P I + \phi \mathbf{T}_{\phi}$, where $\mathbf{T}_{\phi}$ is the excess stress tensor. Hence, equation (6.17) can be rewritten as:

$$\partial_t (\phi \mathbf{v}_{\phi}) + \nabla \cdot (\phi \mathbf{v}_{\phi} \otimes \mathbf{v}_{\phi}) = \mathbf{m}_{\phi} - \phi \nabla P + \nabla \cdot (\phi \mathbf{T}_{\phi}) + \Gamma_{\phi} \mathbf{v}_{\phi}. \tag{6.19}$$

Now, let us sum equations (6.19) for $\phi = B, D, E$ altogether. First, using equations (6.2), (6.3) and (6.18), we find

$$\sum_{\phi \neq L} \mathbf{m}_{\phi} + \Gamma_{\phi} \mathbf{v}_{\phi} = -\mathbf{m}_L - \Gamma_L \mathbf{v_L}$$

and therefore, using (6.2) once again, we obtain:

$$\partial_t ((1-L)\mathbf{v_S}) + \nabla \cdot ((1-L)\mathbf{v_S} \otimes \mathbf{v_S}) = -(1-L)\nabla P + \nabla \cdot (\sum_{\phi \neq L} \phi \mathbf{T}_{\phi}) - \mathbf{m}_L - \Gamma_L \mathbf{v_L}. \tag{6.20}$$

For the liquid phase we have:

$$\partial_t (L\mathbf{v_L}) + \nabla \cdot (L\mathbf{v_L} \otimes \mathbf{v_L}) = -L\nabla P + \nabla \cdot (L\mathbf{T}_L) + \mathbf{m}_L + \Gamma_L \mathbf{v_L}. \tag{6.21}$$

Now we make some assumptions on the form of the excess stress tensors, namely

$$\sum_{\phi \neq L} \phi \mathbf{T}_{\phi} = \Sigma \mathbf{I} \quad \text{and} \quad \mathbf{T}_L = 0, \tag{6.22}$$

where Σ is a monotone decreasing scalar function depending on the volume ratios $B + D + E = 1 - L$. A first approximation, useful for numerical tests, is a linear form of the stress function as

$$\Sigma = -\gamma (1 - L). \tag{6.23}$$

Here negative values of Σ indicate compression. Let us notice that this choice of the stress function is similar to the isothermal case of the isentropic gas equations.

We are assuming that the excess stress tensor is only present in the solid component, so in the liquid there is only the hydrostatic pressure; this means that if in the liquid there is no bacteria nor EPS, then the liquid is at rest. This type of assumption is usually adopted in the theory of deformable porous media, where the excess stress tensor $\mathbf{T}_L$ is neglected in order to get Darcy like laws.

We also assume that the interaction forces for the liquid follow the Darcy law: this is obtained taking $\mathbf{m}_L$ proportional to the difference between the relative velocities of fluid and of component, namely:

$$\mathbf{m}_L = -M(\mathbf{v_L} - \mathbf{v_S}), \tag{6.24}$$

where M is an experimental constant.

The assumptions are made following the works by Preziosi [8, 14], where the theory of mixture is used to model tumour growth.

Thanks to these assumptions, we can rewrite the equations for the velocities so that using (6.1), (6.16) we can obtain a closed system of equations

$$
\begin{cases}
\partial_t B + \nabla \cdot (B\mathbf{v_S}) = B\,(Lk_B(I,T,N) - k_D(I,T,N)), \\[2ex]
\partial_t D + \nabla \cdot (D\mathbf{v_S}) = \alpha Bk_D(I,T,N) - Dk_N(T), \\[2ex]
\partial_t E + \nabla \cdot (E\mathbf{v_S}) = BLk_E(I,T,N) - \epsilon E, \\[2ex]
\partial_t L + \nabla \cdot (L\mathbf{v_L}) = B((1-\alpha)\,k_D(I,T,N) - Lk_B(I,T,N) - Lk_E(I,T,N)) + Dk_N(T) + \epsilon E, \\[2ex]
\partial_t((1-L)\mathbf{v_S}) + \nabla \cdot ((1-L)\mathbf{v_S} \otimes \mathbf{v_S}) + (1-L)\nabla P = \nabla\Sigma + (M - \Gamma_L)\mathbf{v_L} - M\mathbf{v_S}, \\[2ex]
\partial_t(L\mathbf{v_L}) + \nabla \cdot (L\mathbf{v_L} \otimes \mathbf{v_L}) + L\nabla P = -(M - \Gamma_L)\mathbf{v_L} + M\mathbf{v_S}, \\[2ex]
\nabla \cdot ((1-L)\mathbf{v_S} + L\,\mathbf{v_L}) = 0
\end{cases}
\qquad (6.25)
$$

Let us observe that in this model the inertial terms are not neglected.

To complete the system, we have to find the values of the coefficients of the source terms and of the Darcy constant M.

We impose Neumann boundary conditions for the volume ratios:

$$
\nabla B \cdot n|_{\partial\Omega} = \nabla E \cdot n|_{\partial\Omega} = \nabla D \cdot n|_{\partial\Omega} = 0,
\qquad (6.26)
$$

and no-flux boundary conditions for the velocities:

$$
\mathbf{v_S} \cdot n|_{\partial\Omega} = \mathbf{v_L} \cdot n|_{\partial\Omega} = 0.
\qquad (6.27)
$$

In the following sections, we present first the numerical scheme we use and the numerical difficulties we had to face to solve numerically this complex system of equations. We then present some numerical simulations first in the one-dimensional case, and then in the two and three-dimensional cases, to prove the efficiency of our model to reproduce a front propagation for the production of EPS, and also to investigate the behavior of our model.

6.4   The Numerical Scheme

Let us explain now how to solve the complete system (6.25) by a Finite Difference method in space and an explicit-implicit method in time in the two-dimensional case. The same procedure can be easily adapted also to the three dimensional case.

Let us consider a square $\Omega = [0; L] \times [0; L]$ and denote by δx the space step. We consider the discretization points $x_\alpha = (\alpha_1 \delta x, \alpha_2 \delta x)$, $0 \le \alpha_i \le N + 1$. We denote the time step by δt and the discretization times will be given by $t_n = n\delta t$, $n \in \mathbb{N}$.

Let us denote by Y the volume ratio of one of the solid phase, i.e. $Y = B, D$ or E; its approximation at point $x_\alpha \in \Omega$ and at time t_n will be denoted by $Y^{n,\alpha}$. We also consider the time discretization vector Y^n, which components are the N^2 terms $Y^{n,\alpha}$, $1 \le \alpha_i \le N$.

6.4.1 Spatial Discretization

We use a relaxation scheme for the spatial discretization of the transport part [13], and, as a first approach, an explicit Euler scheme for the time discretization. Using a relaxation method, we approximate the equations by a diagonal system, easy to solve and easy to complement eventually with flux limiters. Relaxation is also a convenient setting to extend the scheme to higher orders. Let us explain this method with more details.

Let us consider a two-dimensional hyperbolic problem of d equations in a generic form:

$$\partial_t \mathbf{W} + \partial_{x_1} A_1(\mathbf{W}) + \partial_{x_2} A_2(\mathbf{W}) = \mathbf{F}(\mathbf{W}),$$

where $\mathbf{W} \in \mathbb{R}^d$, for a finite $d \in \mathbb{N}$.

We consider a simple 5-velocities relaxation scheme following [13]. Let us choose the five velocities as

$$\lambda_1 = \lambda(1,0), \ \lambda_2 = \lambda(0,1), \ \lambda_3 = \lambda(-1,0), \ \lambda_4 = \lambda(0,-1), \ \lambda_5 = (0,0), \tag{6.28}$$

for some $\lambda > 0$.

Now we introduce the corresponding Maxwellians $M_i(\mathbf{W}) \in \mathbb{R}^d$, $i = 1, \dots, 5$, of the form

$$M_i(\mathbf{W}) = a_i \mathbf{W} + b_{i1} A_1(\mathbf{W}) + b_{i2} A_2(\mathbf{W}), \tag{6.29}$$

for some constants a_i, b_{i1} and b_{i2} to be chosen.

The conditions of consistency of the Maxwellians are

$$\sum_{i=1}^{5} M_i(\mathbf{W}) = \mathbf{W}, \qquad \sum_{i=1}^{5} \lambda_{i,j} M_i(\mathbf{W}) = A_j(\mathbf{W}), \quad j = 1, 2. \tag{6.30}$$

Then, a possible choice for the coefficients a_i and b_{ij} is the following

$$a_1 = \cdots = a_4 = a, \ a_5 = 1 - 4a;$$

$$b_{11} = b_{22} = -b_{31} = -b_{42} = \frac{1}{2\lambda}, \ b_{ij} = 0 \text{ otherwise.}$$

It is easy to see that these coefficients satisfy conditions (6.30). Let us now denote by $\mathbf{W}^{n,\alpha}$ the approximation of $\mathbf{W}$ at point $x_\alpha \in \Omega \subset \mathbb{R}^2$ and time t_n. We set the discretization of Maxwellians (6.29) as

$$f_i^{n,\alpha} = M_i(\mathbf{W}^{n,\alpha}), \text{ for } i = 1, \cdots, 5. \tag{6.31}$$

We evolve each of the functions f_i, $1 \le i \le 5$, in time by following the velocity λ_i :

$$f_i^{n+1/2,\alpha} = f_i^{n,\alpha} - \mu \sum_{j=1}^{2} \lambda_{ij} (f_i^{n,\alpha_j+1} - f_i^{n,\alpha_j-1})$$

$$+ \mu \sum_{j=1}^{2} |\lambda_{ij}| (f_i^{n,\alpha_j+1} - 2f_i^{n,\alpha} + f_i^{n,\alpha_j-1}),$$

where $\mu = \dfrac{\delta t}{2\delta x}$ and $\alpha_j + 1$ is a shift of the j-th component of the index α. Let us remark that, in our case, thanks to the choice of velocities (6.28), the scheme for one component f_i becomes a one-dimensional scheme. Finally, we just end by setting

$$\mathbf{W}^{n+1,\alpha} = \sum_{i=1}^{5} f_i^{n+1/2,\alpha} + \delta t \, \mathbf{F}(\mathbf{W}^{n,\alpha}).$$

Here, following the results of Bouchut [21, 22] on the stability condition for BGK approximation, we set the velocity $\lambda = \max |\theta_i|$, where $\theta_i \in \sigma(A_i)$ are the eigenvalues of the jacobian matrices of the fluxes and the time and space steps will have to satisfy the stability condition $\lambda \dfrac{\delta t}{\delta x} \leq 1$.

In our case the hyperbolic system (6.25) can be written as

$$\partial_t \mathbf{W} + \partial_{x_1} A_1(\mathbf{W}) + \partial_{x_2} A_2(\mathbf{W}) = \mathbf{F}(\mathbf{W}, \nabla P), \tag{6.32}$$

where:

$$\mathbf{W} = \begin{pmatrix} B \\ D \\ E \\ (1-L)\mathbf{v_{S}}_1 \\ (1-L)\mathbf{v_{S}}_2 \\ L\mathbf{v_{L}}_1 \\ L\mathbf{v_{L}}_2 \end{pmatrix} \tag{6.33}$$

$$A_1(\mathbf{W}) = \begin{pmatrix} B\mathbf{v_{S}}_1 \\ D\mathbf{v_{S}}_1 \\ E\mathbf{v_{S}}_1 \\ (1-L)\mathbf{v_{S}}_1^2 + \gamma(1-L) \\ (1-L)\mathbf{v_{S}}_1\mathbf{v_{S}}_2 \\ L\mathbf{v_{L}}_1^2 \\ L\mathbf{v_{L}}_1\mathbf{v_{L}}_2 \end{pmatrix}, \quad A_2(\mathbf{W}) = \begin{pmatrix} B\mathbf{v_{S}}_2 \\ D\mathbf{v_{S}}_2 \\ E\mathbf{v_{S}}_2 \\ (1-L)\mathbf{v_{S}}_1\mathbf{v_{S}}_2 \\ (1-L)\mathbf{v_{S}}_2^2 + \gamma(1-L) \\ L\mathbf{v_{L}}_1\mathbf{v_{L}}_2 \\ L\mathbf{v_{L}}_2^2 \end{pmatrix}, \tag{6.34}$$

$$\mathbf{F}(\mathbf{W}, \nabla P) = \begin{pmatrix} B(k_B L - k_D) \\ \alpha k_D B - k_N D \\ k_E B f(L) - \epsilon E \\ -(1-L)\partial_x P + (M - \Gamma_L)\mathbf{v_{L}}_1 - M\mathbf{v_{S}}_1 \\ -(1-L)\partial_y P + (M - \Gamma_L)\mathbf{v_{L}}_2 - M\mathbf{v_{S}}_2 \\ -L\partial_x P - (M - \Gamma_L)\mathbf{v_{L}}_1 + M\mathbf{v_{S}}_1 \\ -L\partial_y P - (M - \Gamma_L)\mathbf{v_{L}}_2 + M\mathbf{v_{S}}_2 \end{pmatrix}. \tag{6.35}$$

Here, we used the obvious notations $\mathbf{v_L} = (\mathbf{v_{L}}_1, \mathbf{v_{L}}_2)^T$ and $\mathbf{v_S} = (\mathbf{v_{S}}_1, \mathbf{v_{S}}_2)^T$. Let us observe that the relevant eigenvalues θ_i of the jacobian matrices of the fluxes are $\{2\mathbf{v_{L}}_1, \mathbf{v_{S}}_1 - \sqrt{\gamma}, \mathbf{v_{S}}_1 + \sqrt{\gamma}, 2\mathbf{v_{L}}_2, \mathbf{v_{S}}_2 - \sqrt{\gamma}, \mathbf{v_{S}}_2 + \sqrt{\gamma}\}$, so the coefficient γ assumes an important role in the numerical resolution of the system. As a matter of fact we use a variable time step which satisfies the CFL condition.

As for boundary conditions, we use Neumann boundary conditions (6.26) for the generic component Y and no-flux boundary conditions (6.27) for the velocities $\mathbf{v_S}, \mathbf{v_L}$.

We notice that L is computed using relation (6.2).

Two remarks have to be done regarding the scheme mentioned in previous subsection. The first one is that we did not mention how to compute the pressure P appearing in the source term $\mathbf{F}$. One solution would be to find an equation for P. Summing the two force balance equations in (6.25) and using equation (6.16), we find the elliptic equation satisfied by P, namely

$$-\Delta P = \nabla \cdot (\nabla \cdot ((1-L)\mathbf{v_S} \otimes \mathbf{v_S} + L\mathbf{v_L} \otimes \mathbf{v_L})) - \Delta\Sigma.$$

However, the solution of this equation is not unique and it is known that it is not an efficient way to compute the pressure. We will rather use a projection method as the one proposed by Chorin [36] and Temam [161] to solve Navier-Stokes equation, as explained in details in the following subsection.

6.4.2   Time Discretization

The vanishing phases problem

A problem comes from the vanishing phases. Indeed, using a discretization like the one of previous subsection, we compute $(1 - L^{n+1})\mathbf{v_S}^{n+1}$ and $L^{n+1}\mathbf{v_L}^{n+1}$, whereas we need $\mathbf{v_S}^{n+1}$ and $\mathbf{v_L}^{n+1}$ in order to compute the sixth and seventh components of $\mathbf{F}$ in (6.33). However we cannot calculate $\mathbf{v_S}^{n+1}$ if L^{n+1} is equal to 1, or $\mathbf{v_L}^{n+1}$ if L^{n+1} is equal to zero. Furthermore, we cannot take the data to avoid vanishing phases, like in gas dynamic, because those phases are physically relevant in our case corresponding respectively for pure liquid or pure biofilm. We will therefore use an explicit-implicit time discretization for the velocities in order to compute directly $\mathbf{v_S}^{n+1}$ and $\mathbf{v_L}^{n+1}$.
We can notice that these issues concern only the discretization of the force balance equations in (6.25) and not the discretization of mass balance equations (6.1).
Let us consider therefore only the equations of velocities in (6.25). Using an explicit Euler scheme in time and omitting to detail the space discretization, we obtain :

$$(1 - L^{n+1}\mathbf{v_S}^{n+1}) = G_1^n - \delta t \, ((1 - L)\nabla P)^n + \delta t (M - \Gamma_L^n)\mathbf{v_L}^n - M\mathbf{v_S}^n,$$
$$L^{n+1}\mathbf{v_L}^{n+1} = G_2^n - \delta t (M - \Gamma_L^n)\mathbf{v_L}^n - M\mathbf{v_S}^n,$$

where

$$G_1^n = (1 - L^n)\mathbf{v_S}^n - \delta t \, (\nabla \cdot (1 - L)\mathbf{v_S} \otimes \mathbf{v_S}))^n + \delta t \, (\nabla\Sigma)^n,$$
$$G_2^n = L^n\mathbf{v_L}^n - \delta t \, (\nabla \cdot (L\mathbf{v_L} \otimes \mathbf{v_L}) + L\nabla P)^n.$$

However, it is not possible to compute $\mathbf{v_S}^{n+1}$ if $L^{n+1} = 1$, nor $\mathbf{v_L}^{n+1}$ if $L^{n+1} = 0$.
Here, we propose to overcome this problem by using an implicit approximation for the reaction terms of the equations of velocities, which can be written as:

$$\begin{cases} (1 - L^{n+1})\mathbf{v_S}^{n+1} = G_1^n - \delta t \, ((1 - L)\nabla P)^n + \delta t (M - \Gamma_L^{n+1})\mathbf{v_L}^{n+1} - M\mathbf{v_S}^{n+1}, \\ L^{n+1}\mathbf{v_L}^{n+1} = G_2^n - \delta t (M - \Gamma_L^{n+1})\mathbf{v_L}^{n+1} - M\mathbf{v_S}^{n+1}. \end{cases} \tag{6.36}$$

In this way we obtain values of the velocities even in the particular cases when one of the phases, liquid or solid, vanishes. To compute the terms G_1^n and G_2^n we adopt the same relaxation scheme used to solve the equations for B, D, E.
Solving system (6.36) is possible under the condition

$$(1 - L^{n+1,j})L^{n+1,j} + \delta t (M + (L^{n+1,j} - 1)\Gamma_L^{n+1,j}) \neq 0,$$

that is to say δt small enough.

The pressure problem

Projection method was introduced by Chorin [36] and Temam [161] to solve equations for incompressible fluids, like Navier-Stokes equations

$$u_t + \nabla p = -(u \cdot \nabla) u + \nu \nabla^2 u,$$
$$\nabla \cdot u = 0. \tag{6.37}$$

This method is based on the observation that the left-hand side of the first equation of (6.37) is the Hodge decomposition of the right-hand side, namely the sum of a gradient term and of a divergence-free term. Its strategy is mainly focused on some approximation of the momentum equation to determinate, in a prediction step, a previsional velocity and then, in a correction step, to solve an elliptic equation that enforces the divergence constraint and determines the pressure. Let us now explain our scheme in two different steps, a prediction one and a correction one.

- **Step 1**

  At the beginning we use a relaxation scheme to solve system (6.32) and the scheme can be written as follows:
  $$\mathbf{W}^{n+1} = \mathbf{W}^n - \delta t \left(\nabla \cdot (A(\mathbf{W}))\right)^n + \delta t \, \mathbf{F}^n_{ex} + \delta t \, \mathbf{F}^*_{im}$$

  where the source term $\mathbf{F}$ of (6.35) is considered without pressure and split into two terms: an explicit term $\mathbf{F}_{ex}$, corresponding to the mass balance equations and an implicit term $\mathbf{F}_{im}$, corresponding to the force balance equations, more precisely:

  $$\mathbf{F}^n_{ex} = \begin{pmatrix} B^n(k_B L^n - k_D) \\ \alpha k_D B^n - k_N D^n \\ k_E B^n f(L^n) - \epsilon E^n \\ 0 \\ 0 \\ 0 \\ 0 \end{pmatrix}, \mathbf{F}^*_{im} = \begin{pmatrix} 0 \\ 0 \\ 0 \\ (M - \Gamma_L^{n+1})\mathbf{v_{L}}_1^* - M\mathbf{v_{S}}_1^* \\ (M - \Gamma_L^{n+1})\mathbf{v_{L}}_2^* - M\mathbf{v_{S}}_2^* \\ -(M - \Gamma_L^{n+1})\mathbf{v_{L}}_1^* + M\mathbf{v_{S}}_1^* \\ -(M - \Gamma_L^{n+1})\mathbf{v_{L}}_2^* + M\mathbf{v_{S}}_2^* \end{pmatrix}.$$

  We solve easily the first three equations, the ones referred to the solid component B, D and E. So we can approximate the values of these components at time t_{n+1}. Then, thanks to the condition (6.2), it is possible to compute an approximation L^{n+1} of the liquid volume ratio at time t_{n+1} as:
  $$L^{n+1} = 1 - (B^{n+1} + D^{n+1} + E^{n+1}).$$

  Then, we calculate the values of $\mathbf{v_S}^*$ e $\mathbf{v_L}^*$ implicitly without any pressure solving system (6.36).

- **Step 2**

  Then we pass to the second phase of the projection method for the hydrostatic pressure. We set the Hodge decomposition of the average predicted velocity as

  $$(1 - L)\mathbf{v_S}^* + L\mathbf{v_L}^* = (1 - L)\mathbf{v_S}^{n+1} + L\mathbf{v_L}^{n+1} + \delta t \nabla P, \tag{6.38}$$

  using the discretized version of average incompressibility (6.16)

  $$\nabla \cdot \left((1 - L)\mathbf{v_S}^{n+1} + L\mathbf{v_L}^{n+1}\right) = 0. \tag{6.39}$$

  Taking the divergence of equation (6.38) and using equation (6.39), we obtain the following equation for the pressure P:

  $$\delta t \Delta P^{n+1} = \nabla \cdot \left((1 - L^{n+1})\mathbf{v_S}^* + L^{n+1}\mathbf{v_L}^*\right),$$
  $$\nabla P^{n+1} \cdot n = 0.$$

Param.	Value	Indications
k_{B0}	$8 \cdot 10^{-6}$ [$1/sec$]	Cyanob. growth rate
k_{D0}	$2 \cdot 10^{-7}$ [$1/sec$]	D growth rate
k_{E0}	$12 \cdot 10^{-6}$ [$1/sec$]	EPS growth rate
ϵ	$1 \cdot 10^{-7}$ [$1/sec$]	EPS death rate
k_{N0}	$1 \cdot 10^{-6}$ [$1/sec$]	D consumption rate
γ	$2.5 - 10 \cdot 10^{-16}$ $\left[cm^2/sec^2\right]$	tensor coefficient
α	0.25 [$dimensionless$]	fraction dead cells
M	10^{-8} [$1/sec$]	tensor coefficient
I_{opt}	0.01 $\left[\mu mol \cdot cm^{-2} sec^{-1}\right]$	optimal light intensity
I_0	0.01 $\left[\mu mol \cdot cm^{-2} sec^{-1}\right]$	average incident light
T_{opt}	25 [^oC]	optimal temperature
T_0	25 [^oC]	average temperature
$w_1 = w_2$	1 [$dimensionless$]	constants light-temperature
$\beta_1 = \beta_2$	0.1 [$dimensionless$]	constants light-temperature
μ_0	0.002 $\left[cm^{-1}\right]$	clear water coeff.
μ_h	6 [$dimensionless$]	biomasses coeff.

Table 6.1: Parameters (dimensional) list

Since this problem does not possess a unique solution, we write the system satisfied by ∇P, which is the quantity we need to conclude. Namely, we solve:

$$\delta t \Delta \nabla P^{n+1} = \nabla \nabla \cdot \left((1 - L^{n+1})\mathbf{v_S}^* + L^{n+1}\mathbf{v_L}^*\right),$$
$$\nabla P^{n+1} \cdot n = 0.$$

And, as a final step, we update velocities as :

$$\mathbf{v_S}^{n+1} = \mathbf{v_S}^* - \delta t \nabla P^{n+1},$$
$$\mathbf{v_L}^{n+1} = \mathbf{v_L}^* - \delta t \nabla P^{n+1}.$$

6.5   Numerical Simulations

6.5.1   Parameters Estimations

In this section we discuss the values of parameters chosen in our simulations. Some information can be found in the book [172], where a maximum specific biofilm growth rate is assumed to be $5.88 \, d^{-1}$, where d = day and $d^{-1} = \frac{1}{\text{day}}$, while in [162] the biofilm growth of the two models presented varying between $1 - 2 \, d^{-1}$. For this reason we choose $k_{B0} = 1 \, d^{-1}$. Following [172], we find that the decay rate coefficient is about 5% of the growth coefficient, thus we choose $k_D \approx 0.01 - 0.05 k_{B0}$. The estimate of the EPS growth rate depends on the specie of biofilm and the environmental conditions, see for example [121, 50, 105]. Thus in absence of specific experiments, and considering that we chose to follow the behavior of chrococcales cyanobacteria, we assume that the order of magnitude of EPS growth is comparable with cyanobacteria growth.
We did not find an experimental estimation for the parameter γ in current literature, for this reason we assessed the value of $\sqrt{\gamma}$ as a sort of upper limit of bacteria velocity; which is estimated to be

around $\frac{10^{-4}}{3600} \frac{cm}{sec}$, so

$$\sqrt{\gamma} = \frac{10^{-4}}{3600} \frac{cm}{sec} \approx 2.7 \cdot 10^{-8} \frac{cm}{sec},$$

therefore we fix $\gamma = 5 \cdot 10^{-16} \left[\frac{cm^2}{sec^2} \right]$.

6.5.2   Simulations

In this section we focus our attention on simulations in several space dimensions. The main parameter to estimate is γ, and, for this reason, it is appropriate studying the biofilm evolution as function of γ. Thus, simulations take into account several value of γ to reproduce the biofilm growth in several dimensions, in particular we have realized simulations in one and two dimensions, and, finally, a simulation with constant coefficients in three dimensions.

The one-dimensional case

In the one-dimensional case, we simulate the evolution of cyanobacteria, EPS, dead cells and liquid. In this case, the single variable space accounts for the height, that is to say we consider an homogeneous planar biofilm where volume fractions of the phases and velocities are independent of length and width and only depends on height.

We give the evolution of the biofilm after 60 days, see Figure 6.1. Our domain is the interval $L = [0, 1]$ (cm) and we take spatial step h equal to $0.001 \, cm$. We consider as initial data Heaviside functions for cyanobacteria and EPS: $B_0 = 0.2 \cdot \chi_{[0,0.007]}$, $E_0 = 0.008 \cdot \chi_{[0,0.007]}$. The other variables are initially equal to zero.

Simulations are done with three different values of γ: $\gamma_1 = 10^{-16} \, (cm^2/sec^2)$, $\gamma_2 = 5 \cdot 10^{-16} (cm^2/sec^2)$ and $\gamma_3 = 10^{-15} \, (cm^2/sec^2)$ (respectively on the top, in the middle and on the bottom of Figure 6.1) and with two different values of k_B : $k_B = k_{B0}$ and $k_B = k_B(T, I)$ (respectively, on the left and on the right side of Figure 6.1). Here, we can notice how the parameter γ influences the diffusion of the biomass, that is to say the process is accelerated with bigger values of γ. Also, with the biggest value $\gamma = 10^{-15} \, (cm^2/sec^2)$, the front propagation reaches the highest height (≈ 0.3), while the heights reached with the values $\gamma = 10^{-16} \, (cm^2/sec^2)$ and $\gamma = 5 \cdot 10^{-16} \, (cm^2/sec^2)$ are respectively ≈ 0.1, 0.2. Let us notice that computing the height of the biofilm is particularly simple in the 1D case, since the sum $B + D + E$ is null for space variable x large enough.

Furthermore, we can observe the differences in the cyanobacteria growth using a constant coefficient $k_B = k_{B0}$ or using a coefficient $k_B = k_B(T, I)$ which depends on temperature and light. Since k_{B0} is the optimal growth rate of cyanobacteria, the cyanobacteria growth is higher in the constant case whereas the growths of EPS and liquid are greater in the case $k_B = k_B(I, T)$.

The two-dimensional case

In this section, we simulate the biofilm growth in two-dimension space case during 30 days. We used parameters listed in Table 6.1. As first step we want to study the light response of the model.

Influence of Light

We take for B as an initial condition the sum of 3 gaussian functions, centered respectively in 0.35, 0.5 and 0.7 (cm) with a total fraction of volume for the cyanobateria $BT_0 = 1.0762 \cdot 10^{-5}$. We choose an optimal light intensity $I_{opt} = 0.01 \, (\mu mol \, cm^{-2} sec^{-1})$ in equation (6.13) and we change the incident light intensity I_0 defined at equation (6.11). Let us consider different cases listed below:
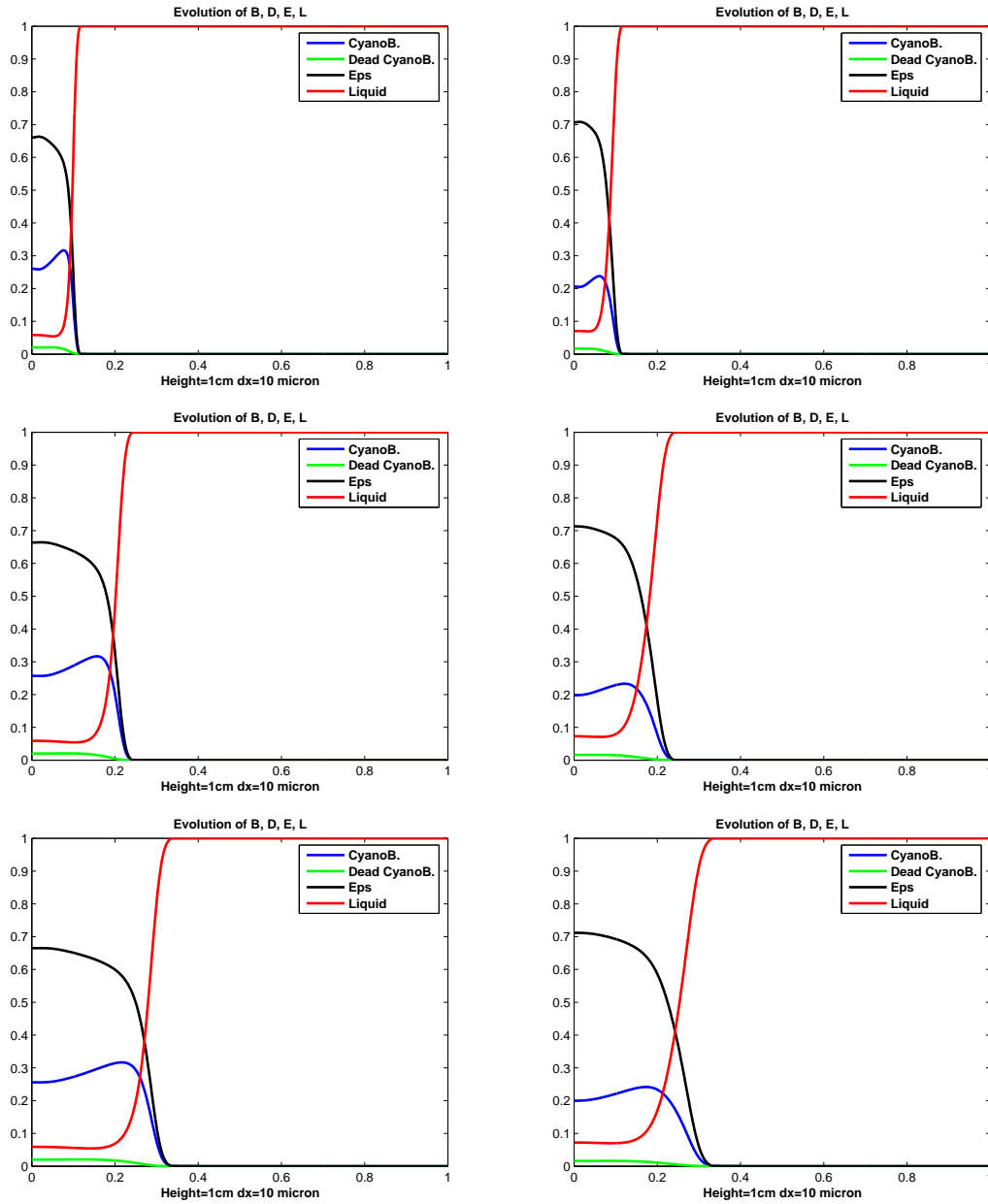
Figure 6.1: Volume fractions of the biofilm components as functions of height x after 60 days. We use three different values of the parameter γ, $\gamma_1 = 10^{-16}$ (cm^2/sec^2) (on the top), $\gamma_2 = 5 \cdot 10^{-16}$ (cm^2/sec^2) (in the middle), $\gamma_3 = 10^{-15}$ (cm^2/sec^2) (on the bottom). On the left, we display the results for an optimal constant rate $k_B = k_{B0}$, while, on the right, we show the results for a variable rate depending on light and temperature. Our domain is the interval $L = [0,1]$ (cm) and the spatial step h is equal to $0.001 cm$. We consider as initial data Heaviside functions for cyanobacteria and EPS: $B_0 = 0.2 \cdot \chi_{[0,0.007]}$, $E_0 = 0.008 \cdot \chi_{[0,0.007]}$. The variable D is initially equal to zero.
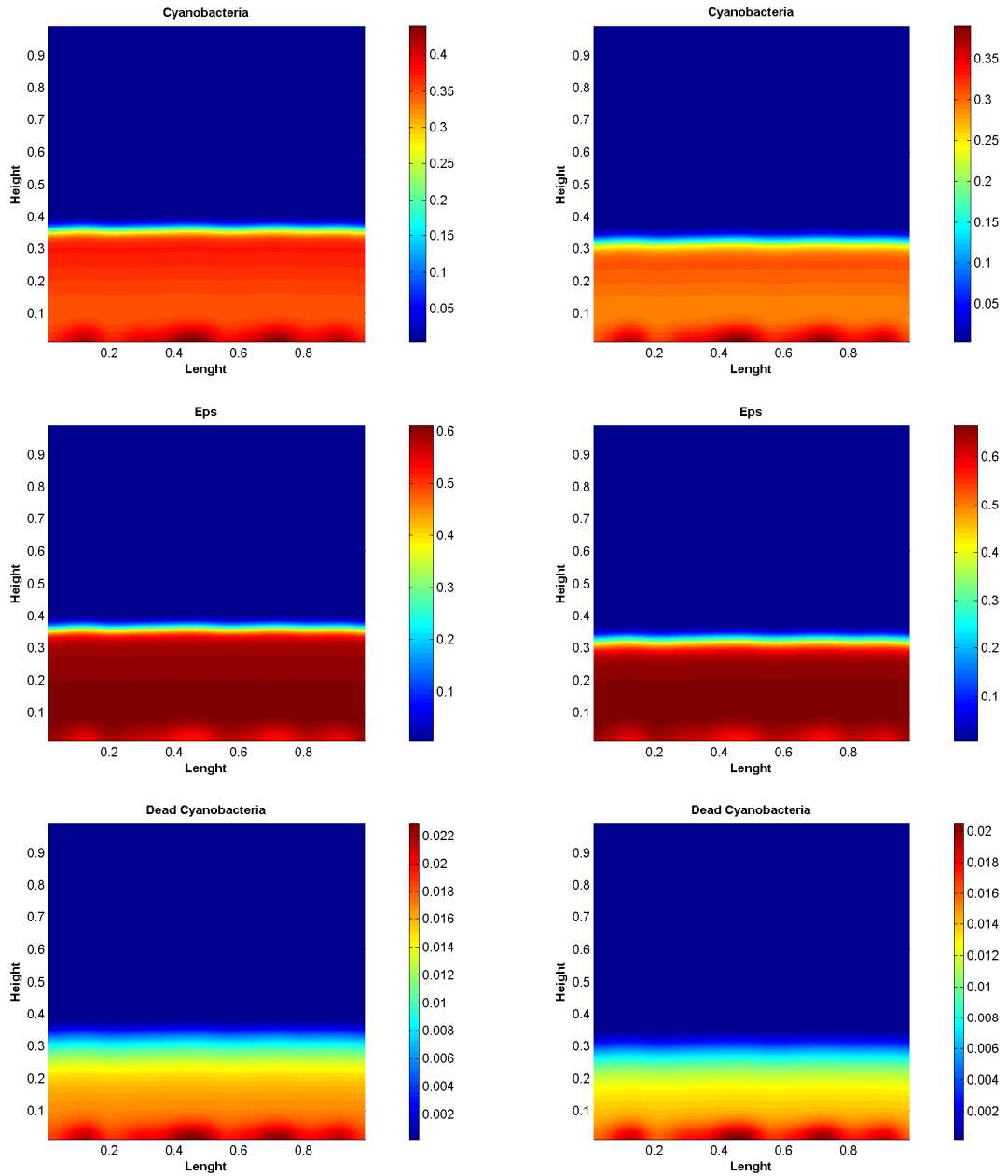
Figure 6.2: Numerical simulation of the biofilm after 45 days with optimal rate (on the left) and variable rate (on the right). Our numerical domain is the square $\Omega = [0,1] \times [0,1]$ (cm^2) and the spatial steps h_x, h_y, h_z are equal to $0.01\,cm$. We consider as initial data Heaviside functions for cyanobacteria while the other variables are equal to zero.

1. Case $k_B = k_{B0}$, and $g = 1$; we find a total fraction of volume of cyanobacteria $BT = 0.0029$, i.e. the volume growth is about 269.5 times.

2. Case $k_B = k_{B0} \cdot g_I$, with amplitude of daily light oscillations of 90%; we choose $I_{opt} = 0.01$, $I_0 = 0.01$ ($\mu mol cm^{-2} sec^{-1}$). We find a total fraction of volume of cyanobacteria $BT = 0.0019$, i.e. the volume growth is about 177 times.

3. Case $k_B = k_{B0} \cdot g_I$; we choose $I_{opt} = 0.01$, $I_0 = 0.003$. We find a total fraction of volume of cyanobacteria $BT = 0.0014$, i.e. the volume growth is about 130.6 times.

4. Case $k_B = k_{B0} \cdot g_I$; we choose $I_{opt} = 0.01$, $I_0 = 0.001$, ten times lower. We obtain a total fraction of volume of cyanobacteria $BT = 2.4481 \cdot 10^{-4}$, i.e. the volume growth is about 22.75 times.
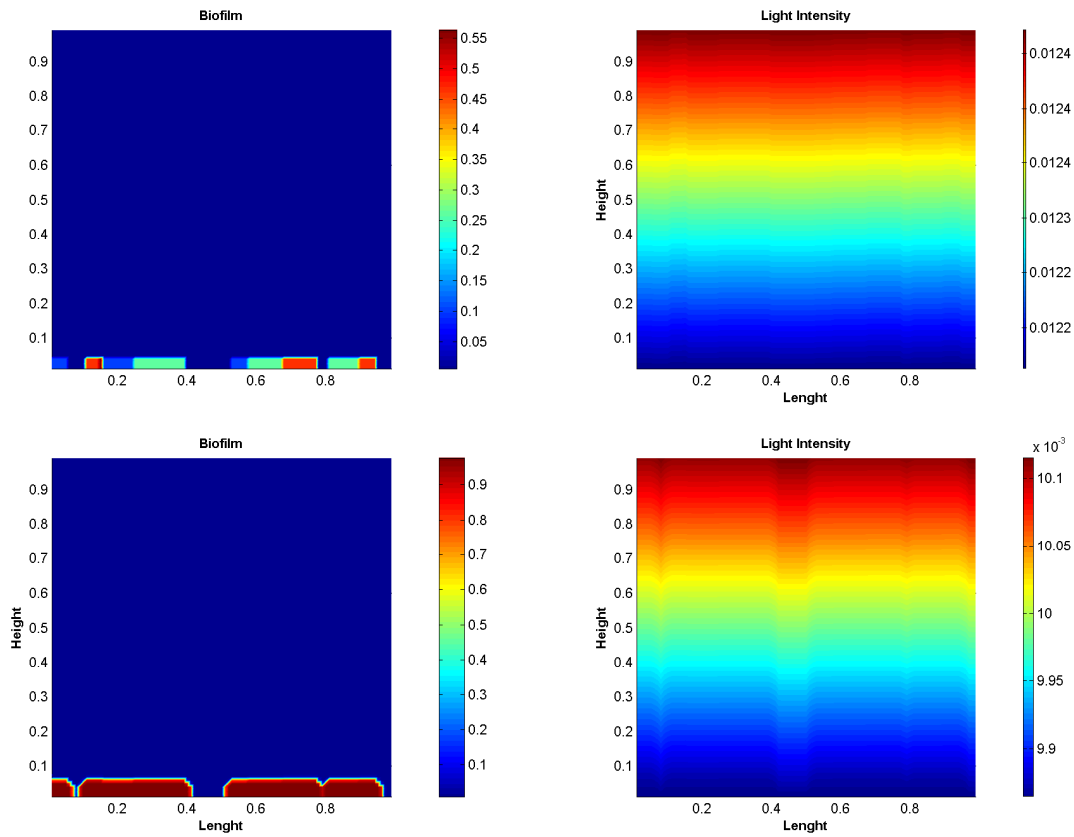

Figure 6.3: Numerical simulation of the biofilm after 30 days with variable rate. Our numerical domain is the square $\Omega = [0,1] \times [0,1]$ (cm^2) and the spatial steps h_x, h_y, h_z are equal to $0.01cm$. We consider as initial data Heaviside functions for cyanobacteria while the other variables are equal to zero. On the left of the figure we have the biofilm growth and on the right is presented the variation of light intensity

Influence of γ

The parameter γ also has a great influence on the solution. Here, we compare solutions with several values of γ (maintaining constant all other parameters), and with total initial fraction of volume of cyanobacteria equal to $1.0762 \cdot 10^{-5}$, distributed as the sum of the same three gaussian functions as before.

1. For $\gamma = 1 \cdot 10^{-16}$ (cm^2/sec^2), we obtain a final total fraction of volume for B equal to 0.0027, which correponds to a mass growth of 250. A plot of the volume fraction of cyanobacteria after 30 days is displayed at Figure 6.4.
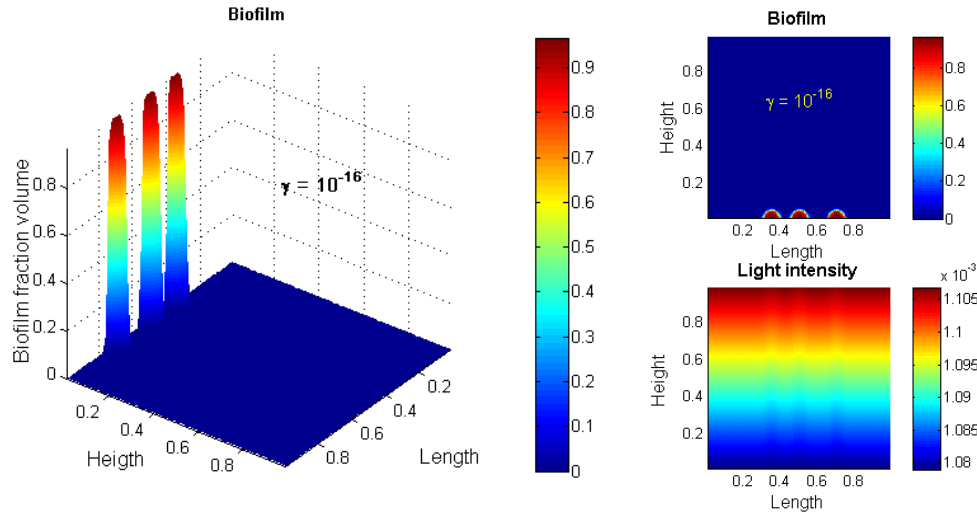
2. For $\gamma = 1 \cdot 10^{-15}$ (cm^2/sec^2), we obtain a final total fraction of volume for B equal to 0.012, which correponds to a mass growth of 1115. A plot of the volume fraction of cyanobacteria after 30 days is displayed at Figure 6.5.

Figure 6.4: Case I. Biofilm evolution after 30 days, with coefficient $\gamma = 10^{-16}(cm^2/sec^2)$, and initial condition for B given by the sum of three gaussian functions centered in 0.35, 0.5 and 0.7, (cm). On the left, we display the fraction volume of cyanobacteria as a function of length and height. On the upper right, we present the level curves of the function B as a function of length and height and on the lower right, we show the level curves of the light intensity variation. The light intensity is in $\mu mol\, cm^{-2} sec^{-1}$.

We can observe that the light intensity propagation in the biofilm phase is attenuated by the biofilm mass itself, as expected by the model assumptions. It will be possible to calibrate this attenuation with appropriated experiments of cyanobacteria growth, measuring the number of photons emitted and the photons which pass through the biofilm with a light sensor under the biofilm itself. Now, adding an intermediate simulation with $\gamma = 5 \cdot 10^{-15}$ (cm^2/sec^2), to the previous two (illustrated in Figures 6.4 and 6.5), we have observed a total biofilm mass increasing (from initial value), which is function of γ values; the mass growth, in these three cases, is presented in Figure 6.6.

Front velocity

Now, let us describe the biofilm front velocity behavior as a function of γ, using as initial condition a single gaussian function centered in 0.5. To do so, we have to define what is the biofilm front. Let us consider the ratio between the biofilm volume fraction (that is to say the sum of B, D and E) and the maximum of this volume fraction at the same time. We can define two regions, the first one composed of the points where the value of this ratio is less than 1% and the second one composed of the points where the value of this ratio is more than 1%. The biofilm front will be the boundary between these two regions. Considering different values for γ, we can observe the behavior of the
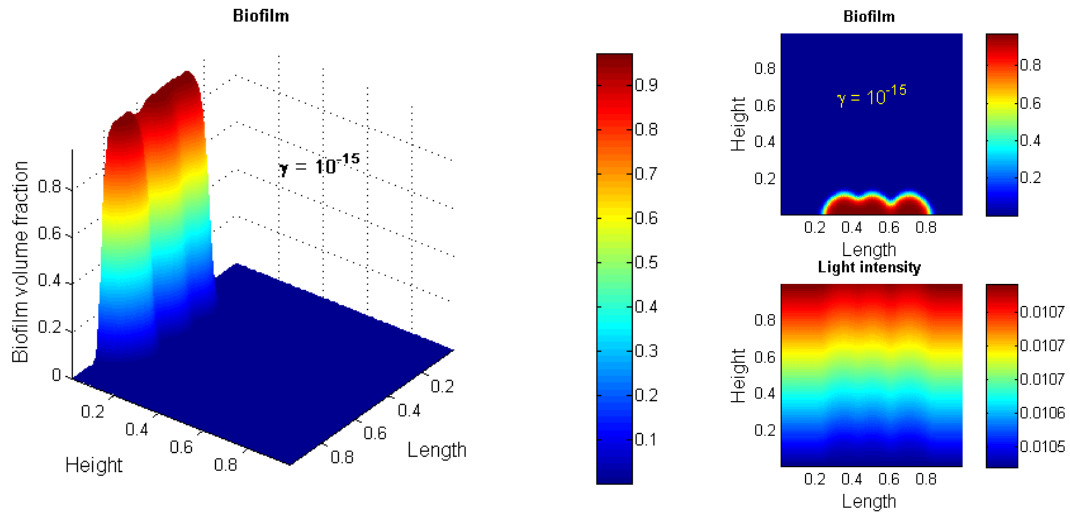
Figure 6.5: Case II. Biofilm evolution, with coefficient $\gamma = 10^{-15}$, (cm^2/sec^2) and initial condition for B given by the sum of three gaussian functions centered in 0.35, 0.5 and 0.7, (cm). On the left, we display the fraction volume of cyanobacteria as a function of length and height. On the upper right, we present the level curves of the function B as a function of length and height and on the lower right, we show the level curves of the light intensity variation. The light intensity is in $\mu mol\, cm^{-2} sec^{-1}$.
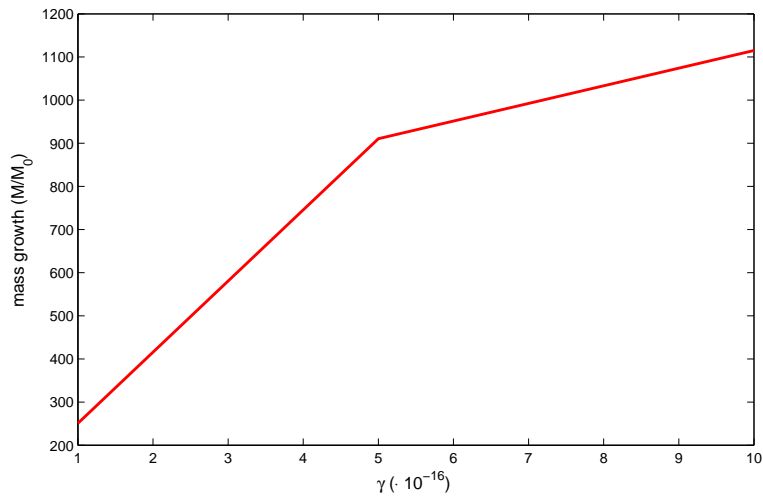

Figure 6.6: Mass growth: M/M_0 as function of γ, with $\gamma = 10^{-16}$ (cm^2/sec^2), $\gamma = 5 \cdot 10^{-16}(cm^2/sec^2)$ and $\gamma = 10 \cdot 10^{-16}$ (cm^2/sec^2) with their corresponding mass growth.

front in Figure 6.7. Using a linear fit on the curves of Figure 6.7, we can find the velocity of the front movement and we plot it as a function of $\sqrt{\gamma}$ in Figure 6.8. This approximation can be compared with experimental data in order to estimate the parameter γ, once the values of other parameters are known.
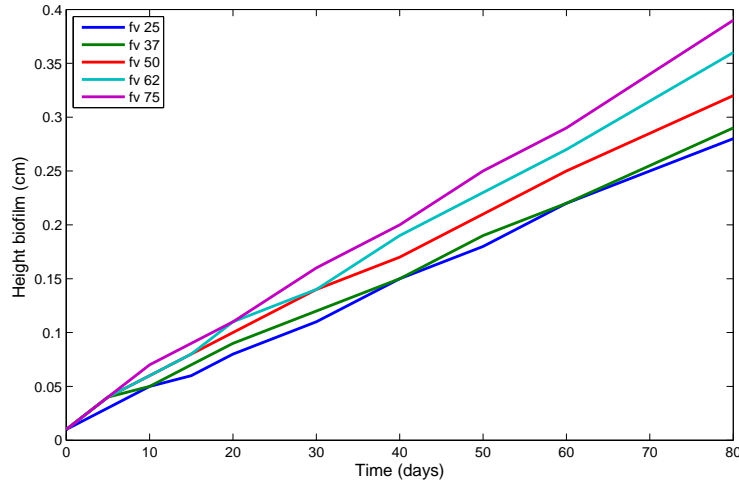

Figure 6.7: Front movement for different γ values: $\gamma = 2.5 \cdot 10^{-16}$ (cm^2/sec^2), $\gamma = 3.7 \cdot 10^{-16}$ (cm^2/sec^2), $\gamma = 5 \cdot 10^{-16}$ (cm^2/sec^2), $\gamma = 6.2 \cdot 10^{-16}(cm^2/sec^2)$ and $\gamma = 7.5 \cdot 10^{-16}(cm^2/sec^2)$.
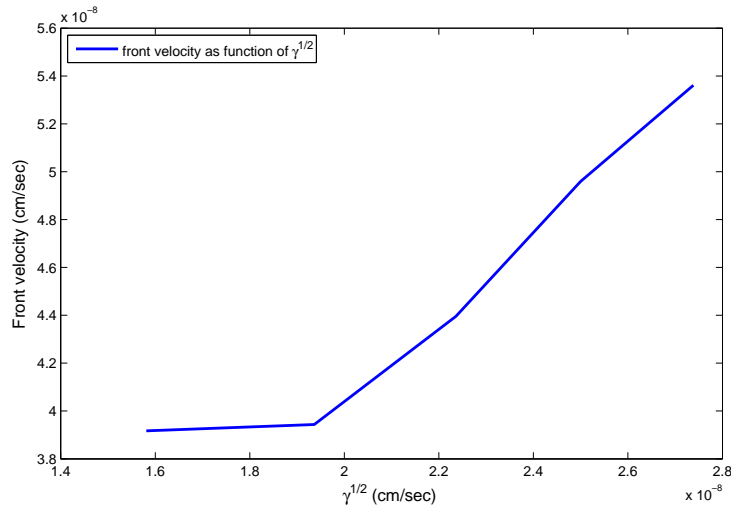

Figure 6.8: Front velocity, obtained by a linear fit of the front growth for different $\sqrt{\gamma}$ values.

The three-dimensional case

In this last subsection, we present in Figure 6.9 a simulation in a three dimensional case with optimal constant rates ($k_B = k_{B0}$). We use the numerical scheme proposed in the previous section in the 3D case solving the system on a domain $\Omega = [0,1] \times [0,1] \times [0,0.5]$ (cm^3). In our simulations

the initial condition for the cyanobacteria volume fraction B is a sum of Heaviside functions whose amplitude is assumed to be of the order of the cell dimensions $h_x = h_y = h_z = 0.02$ (cm).

Here, we see the dependence of the process velocity on the parameter γ. Using two different values for γ, we can observe the influence of this parameter on the process diffusion. As a matter of fact, as observed in the previous cases a larger value for γ leads to a faster evolution. We can notice that, with the choice $\gamma = 10^{-15}(cm^2/sec^2)$, we get an homogeneous layer of the solid components by a quick aggregation.

Moreover some simulations with variable rates are displayed at Figure 6.10 and compared with constant rates. We can notice that variable light intensity and temperature clearly influence the growth of the biofilm. Infact in the case of optimal rates, the biofilm growth is larger than in the case of variable rates.

Moreover we can observe in particular in Figure 6.11 a simulation of the light intensity. Let us notice that, following equation (6.11) the light intensity $I(x, y, z, t)$ is attenuated by the biofilm. Then a lower value of the light intesity is obtained due to the presence of layer of solid components.

It has to be noticed that on these three last figures, namely Figures 6.9, 6.10 and 6.11, the scale for the volume of cyanobacteria changes since the variation in the volume of biofilms is important, whereas the scale for intensity is fixed in order to see better the variations.
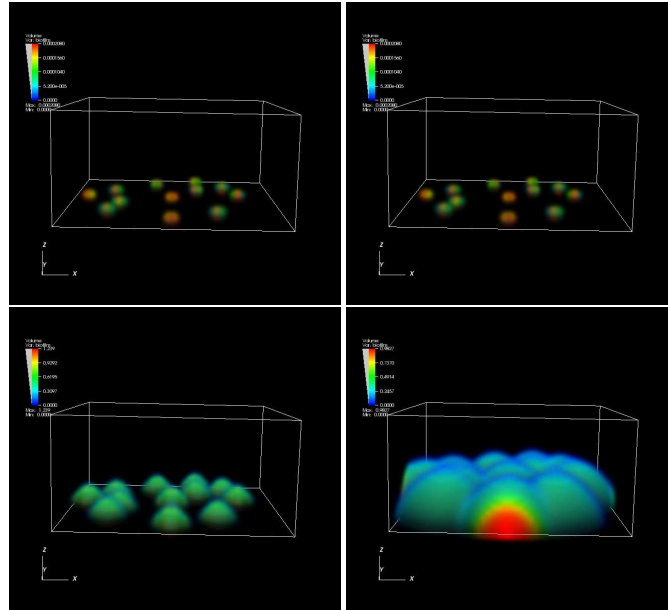

Figure 6.9: Numerical simulation of the biofilm after 45 days with optimal constant rates and two different values of the parameter γ. On the left, we use $\gamma = 10^{-16}$ (cm^2/sec^2) and on the right $\gamma = 10^{-15}(cm^2/sec^2)$. Our numerical domain is $\Omega = [0, 1] \times [0, 1] \times [0, 0.5](cm^3)$ and the spatial steps h_x, h_y, h_z are all equal to 0.02 (cm). We consider as initial datum a sum of Heaviside functions randomly distributed for cyanobacteria while the other variables are equal to zero.
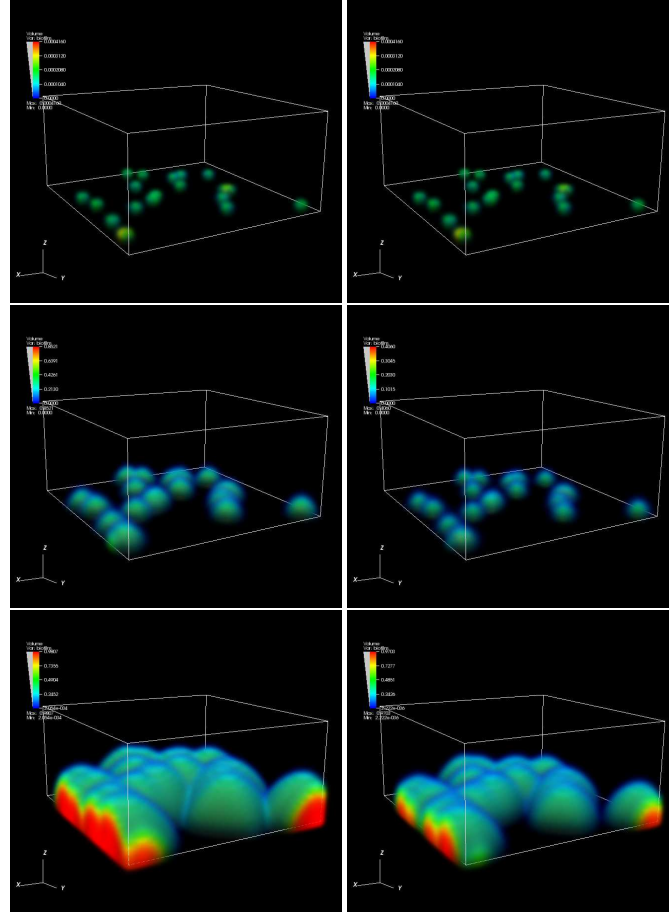
Figure 6.10: Numerical simulation of the biofilm at different times ($T = 0, 15, 30$ days) with optimal constant rate (on the left) and variable constant rate (on the right) with $\gamma = 10^{-15}(cm^2/sec^2)$. Our numerical domain is $\Omega = [0,1] \times [0,1] \times [0,0.5](cm^3)$ and the spatial steps h_x, h_y, h_z are all equal to 0.02 (cm). We consider as initial datum for B a sum of Heaviside functions randomly distributed, $E_0 = B_0/25$ and $D_0 = 0$.
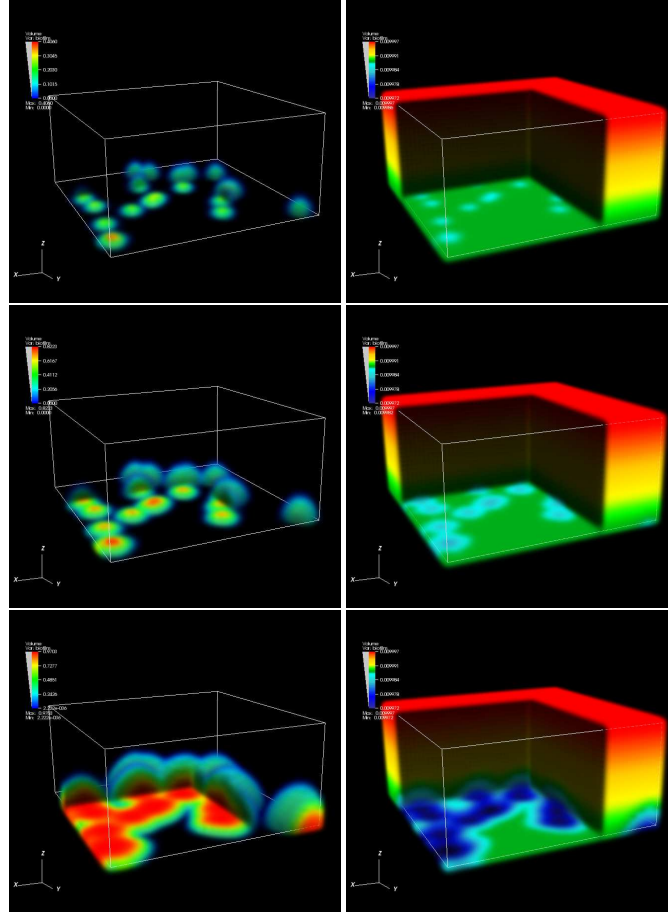
Figure 6.11: Numerical simulation of the biofilm at different times ($T = 15, 22, 30$ days) with variable constant rate with $\gamma = 10^{-15}(cm^2/sec^2)$. On the left, we show the evolution of fraction volume of cyanobacteria B and on the right, we present the light intensity variation. Our numerical domain is $\Omega = [0,1] \times [0,1] \times [0,0.5](cm^3)$ and the spatial steps h_x, h_y, h_z are all equal to 0.02 (cm). We consider as initial datum for B a sum of Heaviside functions randomly distributed, $E_0 = B_0/25$ and $D_0 = 0$.

Bibliography

[1] J. Adler. Chemotaxis in bacteria. *Science*, (153):708–716, 1966.

[2] R. H. Adrian and M. W. Marshall. Action potentials reconstructed in normal and myotonic muscle fibres. *J Physiol*, 258:125–143, 1976.

[3] S. E. Akopov, N. A. Simonian, and G. S. Grigorian. Dynamics of polymorphonuclear leukocyte accumulation in acute cerebral infarction and their correlation with brain tissue damage. *Stroke*, 27:1739–1743, 1996.

[4] E. Alpkvist and I. Klapper. A multidimensional multispecies continuum model for heterogeneous biofilm development. *Bull. Math. Biol.*, 69:765–789, 2007.

[5] W. Alt. Biased random walk models for chemotaxis and related diffusion approximations. *J. Math. Biol.*, 9(2):147–177, 1980.

[6] W. Alt and D. A. Lauffenburger. Transient behavior of a chemotaxis system modelling certain types of tissue inflammation. *J. Math. Biol.*, 24(6):691–722, 1987.

[7] D. Ambrosi, F. Bussolino, and L. Preziosi. A review of vasculogenesis models. *J. Theor. Med.*, 6(1):1–19, 2005.

[8] D. Ambrosi and L. Preziosi. On the closure of mass balance models for tumor growth. *Math. Models Methods Appl. Sci.*, 12(5):737–754, 2002.

[9] K. Anguige, J. R. King, and J. P. Ward. A multi-phase mathematical model of quorum sensing in a maturing *pseudomonas aeruginosa* biofilm. *Math. Biosci.*, 203(2):240–276, 2006.

[10] M. Ankarcrona, J. M. Dypbukt, E. Bonfoco, B. Zhivotovsky, S. Orrenius, S. A. Lipton, and P. Nicotera. Glutamate-induced neuronal death: a succession of necrosis or apoptosis depending on mitochondrial function. *Neuron*, 15:961–973, 1995.

[11] D. Aregba-Driollet, M. Briani, and R. Natalini. Asymptotic high-order schemes for 2×2 dissipative hyperbolic systems. *SIAM J. Numer. Anal.*, 46(2):869–894, 2008.

[12] D. Aregba-Driollet and R. Natalini. Convergence of relaxation schemes for conservation laws. *Appl. Anal.*, 61(1-2):163–193, 1996.

[13] D. Aregba-Driollet and R. Natalini. Discrete kinetic schemes for multidimensional systems of conservation laws. *SIAM J. Numer. Anal.*, 37(6):1973–2004 (electronic), 2000.

[14] S. Astanin and L. Preziosi. Multiphase models of tumour growth. In *Selected topics in cancer modeling*, Model. Simul. Sci. Eng. Technol., pages 223–253. Birkhäuser Boston, Boston, MA, 2008.

[15] M.D. Baker, P.M. Wolanin, and J.B. Stock. Signal transduction in bacterial chemotaxis. *Bioessays*, 28(1):9–22, 2006.

[16] H.C. Berg and Brown D.A. Chemotaxis in escheria coli. Analysis by three-dimensional traking. *Nature*, (239):500–504, 1972.

[17] S. Bianchini, B. Hanouzet, and R. Natalini. Asymptotic behavior of smooth solutions for partially dissipative hyperbolic systems with a convex entropy. *Communications Pure Appl. Math.*, 60:1559–1622, 2007.

[18] P. Biler. Global solutions to some parabolic-elliptic systems of chemotaxis. *Adv. Math. Sci. Appl.*, 9(1):347–359, 1999.

[19] M. L. Block and J. S. Hong. Microglia and inflammation-mediated neurodegeneration: multiple triggers with a common mechanism. *Prog. Neurobiol.*, 76:77–98, 2005.

[20] T. Boehm, J Folkman, T. Browder, and M.S. O' Reilly. Antiangiogenic therapy of experimental cancer does not induce acquired drug resistance. *Nature*, 390:404–407, 1997.

[21] F. Bouchut. Construction of BGK models with a family of kinetic entropies for a given system of conservation laws. *J. Statist. Phys.*, 95(1-2):113–170, 1999.

[22] F. Bouchut. Entropy satisfying flux vector splittings and kinetic BGK models. *Numer. Math.*, 94(4):623–672, 2003.

[23] I. Brazzoli, S.P. Corgnati, M. Filippi, and S. Viazzo. On a kinetic theory approach to modelling degradation phenomena in conservation sciences. *Mathematical and Computer Modelling*, 45(9-10):1201–1213, 2007.

[24] M. Briani and R. Natalini. Asymptotic high-order schemes for integro-differential problems arising in markets with jumps. *Commun. Math. Sci.*, 4(1):81–96, 2006.

[25] H. M. Byrne and M. R. Owen. A new interpretation of the Keller-Segel model based on multiphase modelling. *J. Math. Biol.*, 49(6):604–626, 2004.

[26] V. Calvez and L. Corrias. The parabolic-parabolic Keller-Segel model in $\mathbb{R}^2$. *Commun. Math. Sci.*, 6(2):417–447, 2008.

[27] C. Capone, S. Frigerio, S. Fumagalli, M. Gelati, M.-C. Principato, C. Storini, M. Montinaro, R. Kraftsik, M. De Curtis, E. Parati, and M.-G. De De Simoni. Neurosphere-derived cells exert a neuroprotective action by changing the ischemic microenvironment. *PLoS ONE*, 2(4):e373, 2007.

[28] C. Cattaneo. Sulla conduzione del calore. *Atti Sem. Mat. Fis. Univ. Modena*, 3:83–101, 1949.

[29] C. Cercignani. *The Boltzmann equation and its applications*, volume 67 of *Applied Mathematical Sciences*. Springer-Verlag, New York, 1988.

[30] C. Cercignani, R. Illner, and M Pulvirenti. *The mathematical theory of dilute gases*, volume 106 of *Applied Mathematical Sciences*. Springer-Verlag, New York, 1994.

[31] F. A. C. C. Chalub, P. A. Markowich, B. Perthame, and C. Schmeiser. Kinetic models for chemotaxis and their drift-diffusion limits. *Monatsh. Math.*, 142(1-2):123–141, 2004.

[32] M.A. Chaplain. Mathematical modelling of angiogenesis. *J. Neurooncol.*, 50(1-2):37–51, 2000.

[33] G. Chapuisat, T. Lelekov-Boissard, M.A. Dronne, and J.P. Boissel. A detailed model of neuronal inflammation during ischemic stroke. (For a Philosophical Transaction of The Royal Society: Proceedings B), 2008.

[34] M.A.S. Chaudhry and Beg S.A. A review on the mathematical modeling of biofilm processes: advances in fundamentals of biofilm modeling. *Chem. Eng. Technol.*, 9:701–710, 1998.

[35] S. Childress and J. K. Percus. Nonlinear aspects of chemotaxis. *Math. Biosci.*, 56(3-4):217–237, 1981.

[36] A. J. Chorin. Numerical solution of the Navier-Stokes equations. *Math. Comp.*, 22:745–762, 1968.

[37] A. J. Chorin and J. E. Marsden. *A Mathematical Introduction to Fluid Mechanics*, volume 4 of *Applied Mathematical Sciences*. Springer-Verlag, New York, 1993.

[38] F. Clarelli, C. Di Russo, R. Natalini, and M. Ribot. A fluid-dynamic model for the growth of phototrophic biofilms. *In preparation.*

[39] F. Clarelli, C. Di Russo, R. Natalini, and M. Ribot. Mathematical models for biofilms on the surface of monuments. *APPLIED AND INDUSTRIAL MATHEMATICS IN ITALY III, proceedings of SIMAI Conference 2008.*

[40] O. Cleaver and P. Krieg. Vegf mediates angioblast migration during development of the dorsal aorta in xenopus. *Development*, 125:3905–3914, 1998.

[41] J. Condeelis, R.H. Singer, and J.E. Segall. The great escape: when cancer cells hijack the genes for chemotaxis and motility. *Annu. Rev. Cell Dev. Biol.*, 21:695–718, 2005.

[42] A. Coniglio, A. de Candia, S. Di Talia, and A. Gamba. Percolation and Burgers's dynamics in a model of capillary formation. *Phys. Rev. E*, 69:051910, 2004.

[43] C.A. Crispim and C.C. Gaylarde. Cyanobacteria and biodeterioration of cultural heritage: A review. *Microb. Ecol.*, 49:1–9, 2005.

[44] R. Dautray and J.-L. Lions. *Mathematical analysis and numerical methods for science and technology. Vol. 6.* Springer-Verlag, Berlin, 1993. Evolution problems. II.

[45] G. del Zoppo, I. Ginis, J. M. Hallenbeck, C. Iadecola, X. Wang, and G. Z. Feuerstein. Inflammation and stroke: putative role for cytokines, adhesion molecules and inos in brain response to ischemia. *Brain Pathol.*, 10:95–112, 2000.

[46] C. Di Russo. Global existence of smooth solutions and time asymptotic behavior for the Cattaneo-Hillen model of chemotaxis. *In preparation.*

[47] C. Di Russo, J-B. Lagaert, G. Chapuisat, and M-A. Dronne. A mathematical model of inflammation during ischemic stroke. *ESAIM: Proceedings, CEMRACS 2009: Mathematical Modelling in Medicine*, 30, 2010.

[48] C. Di Russo, R. Natalini, and M. Ribot. Global existence of smooth solutions to a two-dimensional hyperbolic model of chemotaxis. *Communications in Applied and Industrial Mathematics*, 1, 2010.

[49] C. Di Russo and A. Sepe. Global existence and time asymptotic behavior for some quasilinear hyperbolic models of chemotaxis. *In preparation.*

[50] I. Dogsa, M. Kriechbaum, D. Stopar, and P. Laggnerz. Structure of bacterial extracellular polymeric substances at different ph values as determined by saxs. *Biophysical Journal*, 89:2711–2720, 2005.

[51] Y. Dolak and T. Hillen. Cattaneo models for chemosensitive movement: numerical solution and pattern formation. *J. Math. Biol.*, 46(2):153–170, 2003.

[52] D. Dormann and C.J. Weijer. Chemotactic cell movement during dictyostelium development and gastrulation. *Curr. Opin. Genet. Dev.*, 16(4):367–373, 2006.

[53] H. Eberl, E. Morgenroth, D. Noguera, C. Picioreanu, B. Rittmann, M. van Loosdrecht, and O. Wanner. *Mathematical modeling of biofilms.* 2006.

[54] L. Edelstein-keshet and A. Spiros. Exploring the formation of Alzheimer's disease senile plaques in silico. *J Theor Biol*, 216:301–326, 2002.

[55] P.H.C. Eilers and J.C.H. Peeters. A model for the relationship between light-intensity and the rate of photosynthesis in phytoplankton. *Ecol Model*, 42(3–4):199–215, 1988.

[56] Lawrence C. Evans. *Partial differential equations*, volume 19 of *Graduate Studies in Mathematics*. American Mathematical Society, Providence, RI, 1998.

[57] R. Eymard, T. Gallouet, and R. Herbin. Finite volume methods. *Handbook of numerical analysis*, 7:713–1018, 2000.

[58] A. Farina and L. Preziosi. On Darcy's law for growing porous media. *J. Math. Biol.*, 37:485–491, 2001.

[59] F. Filbet, P. Laurençot, and B. Perthame. Derivation of hyperbolic models for chemosensitive movement. *J. Math. Biol.*, 50(2):189–207, 2005.

[60] R. Firtel. Dictyiostelium cinema. *http://www-biology.ucsd.edu/firtel/movies.html*, 2001.

[61] J. Folkman. The vascularization of tumors. *Sci. Amer.*, 234:58–73, 1976.

[62] J. Folkman and C. Haudenschild. Angiogenesis in vitro. *Nature*, 288:551–556, 1980.

[63] Centre for Biofilm Engineering. http://www.biofilm.montana.edu/. *Montana State University*.

[64] Lauffenburger D.A. Ford, R.M and. Measurement of bacterial random motility and chemotaxis coefficients: II application of single cell based mathematical model. *Biotechnol. Bioeng.*, 37:661–672, 1991.

[65] J. Fort and V. Mendez. Wavefronts in time-delayed reaction-diffusion systems. Theory and comparison to experiment. *Rep. Prog. Phys.*, 65:895–954, 2002.

[66] A. Gamba, D. Ambrosi, A. Coniglio, A de Candia, S. Di Talia, E. Giraudo, G. Serini, L. Preziosi, and F. Bussolino. Percolation, morphogenesis, and Burgers dynamics in blood vessels formation. *Phys. Rev. Lett.*, 90, 2003.

[67] J. H. Garcia, K. F. Liu, Y. Yoshida, J. Lian, S. Chen, and G. J. del Zoppo. Influx of leukocytes and platelets in an evolving brain infarct (wistar rat). *Am J Pathol*, 144(1):188–199, Jan 1994.

[68] E. Godlewski and P.-A Raviart. *Hyperbolic systems of conservation laws*, volume 3/4 of *Mathématiques & Applications (Paris) [Mathematics and Applications]*. Ellipses, Paris, 1991.

[69] S. M. Gray and R. Brookmeyer. Estimating a treatment effect from multidimensional longitudinal data. *Biometrics*, 54:976–988, 1998.

[70] F. R. Guarguaglini, C. Mascia, R. Natalini, and M. Ribot. Stability of constant states of qualitative behavior of solutions to a one dimensional hyperbolic model of chemotaxis. *Discrete Contin. Dyn. Syst. Ser. B*, 12(1):39–76, 2009.

[71] L. Hall-Stoodley, J.W. Costerton, and P. Stoodley. Bacterial biofilms: from the natural environment to infectious diseases. *Nat. Rev. Microbiol.*, 2:95–108, 2004.

[72] J. M. Hallenbeck and A. J. Dutka. Background review and current concepts of reperfusion injury. *Arch. Neurol.*, 47:1245–1254, 1990.

[73] B. Hanouzet and R. Natalini. Global existence of smooth solutions for partially dissipative hyperbolic systems with a convex entropy. *Arch. Ration. Mech. Anal.*, 169(2):89–117, 2003.

[74] T. Hillen. Transport equations and chemosensitive movement. *University of Tubingen, Habilitation thesis*, 2001.

[75] T. Hillen. On the L^2-moment closure of transport equations: the Cattaneo approximation. *Discrete Contin. Dyn. Syst. Ser. B*, 4(4):961–982, 2004.

[76] T. Hillen and H. G. Othmer. The diffusion limit of transport equations derived from velocity-jump processes. *SIAM J. Appl. Math.*, 61(3):751–775 (electronic), 2000.

[77] T. Hillen and K. Painter. Global existence for a parabolic chemotaxis model with prevention of overcrowding. *Adv. in Appl. Math.*, 26(4):280–301, 2001.

[78] T. Hillen, K. Painter, and C. Schmeiser. Global existence for chemotaxis with finite sampling radius. *Discrete Contin. Dyn. Syst. Ser. B*, 7(1):125–144 (electronic), 2007.

[79] T. Hillen and K. J. Painter. A user's guide to PDE models for chemotaxis. *J. Math. Biol.*, 58(1-2):183–217, 2009.

[80] T. Hillen and A. Stevens. Hyperbolic models for chemotaxis in 1-D. *Nonlinear Anal. Real World Appl.*, 1(3):409–433, 2000.

[81] D. Horstmann. Lyapunov functions and L^p-estimates for a class of reaction-diffusion systems. *Colloq. Math.*, 87(1):113–127, 2001.

[82] D. Horstmann. From 1970 until present: the Keller-Segel model in chemotaxis and its consequences. II. *Jahresber. Deutsch. Math.-Verein.*, 106(2):51–69, 2004.

[83] C. Iadecola and M. Alexander. Cerebral ischemia and inflammation. *Curr. Opin. Neurol.*, 14:89–94, 2001.

[84] A. I. Ibragimov, C. J. McNeal, L. R. Ritter, and J. R. Walton. A mathematical model of atherogenesis as an inflammatory response. *Math Med Biol*, 22:305–333, 2005.

[85] S. Jin and Z. P. Xin. The relaxation schemes for systems of conservation laws in arbitrary space dimensions. *Comm. Pure Appl. Math.*, 48(3):235–276, 1995.

[86] S. Kawashima. *Systems of a hyperbolic-parabolic composite type, with applications to the equations of magnetohydrodynamics.* PhD thesis, Kyoto. University, 1983.

[87] S. Kawashima and Y. Shizuta. On the normal form of the symmetric hyperbolic-parabolic systems associated with the conservation laws. *Tohoku Math. J. (2)*, 40(3):449–464, 1988.

[88] E.F. Keller and L.A. Segel. Initiation of slime mold aggregation viewed as an instability. *J. Theor. Biol.*, 26:399–415, 1970.

[89] E.F. Keller and L.A. Segel. Model for chemotaxis. *J. Theor. Biol.*, 30:225–234, 1971.

[90] E.F. Keller and L.A. Segel. Traveling band of chemotactic bacteria: A theoretical analysis. *J. Theor. Biol.*, 30:235–248, 1971.

[91] I. Klapper and J. Dockery. Mathematical description of microbial biofilms. *to appear SIAM Review*, 2009.

[92] R. Kowalczyk. Preventing blow-up in a chemotaxis model. *J. Math. Anal. Appl.*, 305(2):566–588, 2005.

[93] R. Kowalczyk, A. Gamba, and L. Preziosi. On the stability of homogeneous solutions to some aggregation models. *Discrete Contin. Dyn. Syst. Ser. B*, 4(1):203–220, 2004. Mathematical models in cancer (Nashville, TN, 2002).

[94] H. Kozono and Y. Sugiyama. Global strong solution to the semi-linear Keller-Segel system of parabolic-parabolic type with small data in scale invariant spaces. *J. Differential Equations*, 247(1):1–32, 2009.

[95] R. Kumar, G. Clermont, Y. Vodovotz, and C. C. Chow. The dynamics of acute inflammation. *J Theor Biol*, 230:145–155, 2004.

[96] R. Ladeby, M. Wirenfeldt, D. Garcia-Ovejero, L. Fenger, Dissing-Olesen, I. Dalmau, and B. Finsen. Microglial cell population dynamics in the injured adult central nervous system. *Brain Res Rev*, 48:196–206, 2005.

[97] A. Y. Lai and K. G. Todd. Microglia in cerebral ischemia: molecular actions and interactions. *Can J Physiol Pharmacol*, 84:49–59, 2006.

[98] A. Y. Lai and K. G. Todd. Differential regulation of trophic and pro-inflammatory microglial effectors is dependent on severity of neuronal injury. *Glia*, 56:259–270, 2008.

[99] K. A. Landman, G. J. Pettet, and D. F. Newgreen. Chemotactic cellular migration: smooth and discontinuous travelling wave solutions. *SIAM J. Appl. Math.*, 63(5):1666–1681 (electronic), 2003.

[100] I.R. Lapidus and R. Schiller. Model for the chemotactic response of a bacterial population. *Biophys. J.*, 16(7):779–789, 1976.

[101] B. Larrivee and A. Karsan. Signaling pathways induced by vascular endothelial growth factor (review). *Int. J. Mol. Med.*, 5(5):447–456, 2000.

[102] D. A. Lauffenburger and C. R. Kennedy. Analysis of a lumped model for tissue inflammation dynamics. *Mathematical Biosciences*, 53:189–221, 1981.

[103] D.A. Lauffenburger and K.H. Keller. Effects of leukocyte random motility and chemotaxis in tissue inflammatory response. *J. theor. Biol.*, 81:475–503, 1979.

[104] H. A. Levine and B. D. Sleeman. A system of reaction diffusion equations arising in the theory of reinforced random walks. *SIAM J. Appl. Math.*, 57(3):683–730, 1997.

[105] Y. Liu, C. Hong Yang, and Li J. Influence of extracellular polymeric substances on pseudomonas aeruginosa transport and deposition profiles in porous media. *Environ. Sci. Technol.*, 41:198–205, 2007.

[106] M. Luca, A. Chavez-Ross, L. Edelstein-Keshet, and A. Mogilner. Chemotactic signaling, microglia, and alzheimer's disease senile plaques: is there a connection? *Bull. Math.Biol.*, 65(4):693–730, 2003.

[107] A. Majda. *Compressible fluid flow and systems of conservation laws in several space variables*, volume 53 of *Applied Mathematical Sciences*. Springer-Verlag, New York, 1984.

[108] N. V. Mantzaris, Steve Webb, and H. G. Othmer. Mathematical modeling of tumor-induced angiogenesis. *J. Math. Biol.*, 49(2):111–187, 2004.

[109] M. J. Mentis, A. R. McIntosh, K. Perrine, V. Dhawan, B. Berlin, A. Feigin, C. Edwards, P. Mattis, and D. Eidelberg. Relationships among the metabolic patterns that correlate with mnemonic, visuospatial, and mood symptoms in Parkinson's disease. *Am J Psychiatry*, 159:746–754, 2002.

[110] E. Morgenroth, H.J. Eberl, M.C.M. van Loosdrecht, D.R. Noguera, G.E. Pizarro, C. Picioreanu, B.E. Rittmann, A.O. Schwarz, and O. Wanner. Comparing biofilm models for a single species biofilm system. *Wat. Sci. Tech.*, 49:145–154, 2004.

[111] I. Müller and T. Ruggeri. *Rational extended thermodynamics*, volume 37 of *Springer Tracts in Natural Philosophy*. Springer-Verlag, New York, second edition, 1998. With supplementary chapters by H. Struchtrup and Wolf Weiss.

[112] C. J.L Murray and A. D. Lopez. Mortality by cause for eight regions of the world: Global burden of disease study. *The Lancet*, 349(9061):1269–1276, May 1997.

[113] C. J.L Murray and A.D. Lopez. Global mortality, disability, and the contribution of risk factors: Global burden of disease study. *The Lancet*, 349(9063):1436–1442, May 1997.

[114] J. D. Murray. *Mathematical biology. I*, volume 17 of *Interdisciplinary Applied Mathematics*. Springer-Verlag, New York, third edition, 2002. An introduction.

[115] J. D. Murray. *Mathematical biology. II*, volume 18 of *Interdisciplinary Applied Mathematics*. Springer-Verlag, New York, third edition, 2003. Spatial models and biomedical applications.

[116] J.D. Murray and M.R. Myerscough. Pigmentation pattern formation on snakes. *J. Theor. Biol.*, 149(3):339–360, 1991.

[117] M.R. Myerscough, P.K. Maini, and K.J. Painter. Pattern formation in a generalized chemotactic model. *Bull. Math. Biol.*, 60(1):1–26, 1998.

[118] R. Natalini. Convergence to equilibrium for the relaxation approximations of conservation laws. *Comm. Pure Appl. Math.*, 49(8):795–823, 1996.

[119] R. Natalini. A discrete kinetic approximation of entropy solutions to multidimensional scalar conservation laws. *J. Differential Equations*, 148(2):292–317, 1998.

[120] R. Natalini and M. Ribot. Mass preserving schemes for inhomogeneous systems of dissipative hyperbolic equations. *IAC preprint 2010, Submitted.*

[121] B.J. Ni, R.J. Zeng, F. Fang, J. Xu, G.-P. Sheng, and H.-Q. Yu. A novel approach to evaluate the production kinetics of extracellular polymeric substances (eps) by activated sludge using weighted nonlinear least-squares analysis. *Environ. Sci. Technol*, 2009.

[122] K. Osaki and A. Yagi. Finite dimensional attractor for one-dimensional Keller-Segel equations. *Funkcial. Ekvac.*, 44(3):441–469, 2001.

[123] H. G. Othmer, S. R. Dunbar, and W. Alt. Models of dispersal in biological systems. *J. Math. Biol.*, 26(3):263–298, 1988.

[124] H. G. Othmer, S. R. Dunbar, and W. Alt. Models of dispersal in biological systems. *J. Math. Biol.*, 26(3):263–298, 1988.

[125] H. G. Othmer and T. Hillen. The diffusion limit of transport equations. II. Chemotaxis equations. *SIAM J. Appl. Math.*, 62(4):1222–1250 (electronic), 2002.

[126] H. G. Othmer and A. Stevens. Aggregation, blowup, and collapse: the ABCs of taxis in reinforced random walks. *SIAM J. Appl. Math.*, 57(4):1044–1081, 1997.

[127] M.R. Owen and J.A. Sherratt. Pattern formation and spatiotemporal irregularity in a model for macrophage- tumour interactions. *J. Theor. Biol.*, 189(1):63–80, 1997.

[128] K. J. Painter and T. Hillen. Volume-filling and quorum-sensing in models for chemosensitive movement. *Can. Appl. Math. Q.*, 10(4):501–543, 2002.

[129] K. J. Painter, P. K. Maini, and H. G. Othmer. Development and applications of a model for cellular response to multiple chemotactic cues. *J. Math. Biol.*, 41(4):285–314, 2000.

[130] F. Palla. Rivista semestrale del centro regionale progettazione e restauro. 2006.

[131] O. Palluy and M. Rigaud. Nitric oxide induces cultured cortical neuron apoptosis. *Neurosci. Lett.,* 208:1–4, 1996.

[132] H.T. Park and Y. Wu, J.and Rao. Molecular control of neuronalmigration. *Bioessays,* 24(9):821–827, 2002.

[133] Clifford S. Patlak. Random walk with persistence and external bias. *Bull. Math. Biophys.*, 15:311–338, 1953.

[134] K. Pearson. The problem of the random walk. *Nature*, (72), 1905.

[135] B. Perthame. *Transport equations in biology*. Frontiers in Mathematics. Birkhäuser Verlag, Basel, 2007.

[136] A.J. Perumpanani, J.A. Sherratt, J. Norbury, and H.M. Byrne. Biological inferences from a mathematical model for malignant invasion. *Invas. Metastas.*, 16(4-5):209–221, 1996.

[137] L. Preziosi and A. Tosin. Multiphase modelling of tumour growth and extracellular matrix interaction: mathematical tools and applications. *J. Math. Biol.*, 58(4-5):625–656, 2009.

[138] K. R. Rajagopal and L. Tao. *Mechanics of mixtures*, volume 35 of *Series on Advances in Mathematics for Applied Sciences*. World Scientific Publishing Co. Inc., River Edge, NJ, 1995.

[139] A. Reynolds, J. Rubin, G. Clermont, J. Day, Y. Vodovotz, and G. Bard Ermentrout. A reduced mathematical model of the acute inflammatory response: I. derivation of model and analysis of anti-inflammation. *J Theor Biol*, 242:220–236, 2006.

[140] P. G. Ridall, A. N. Pettitt, R. D. Henderson, and P. A. McCombe. Motor unit number estimation–a bayesian approach. *Biometrics*, 62:1235–1250, 2006.

[141] L.R. Ritter. A short course in modelling of chemotaxis.

[142] M.A. Rivero, R.T. Tranquillo, H.M. Buettner, and D.A. Lauffenburger. Transport models for chemotactic cell populations based on individual cell behavior. *Chem. Eng. Sci.*, 4:1–17, 1989.

[143] P. L. Roe. Upwind differencing schemes for hyperbolic conservation laws with source terms. In *Nonlinear hyperbolic problems (St. Etienne, 1986)*, volume 1270 of *Lecture Notes in Math.*, pages 41–51. Springer, Berlin, 1987.

[144] G. Roeselers, van Loosdrecht, M., and G. Muyzer. Heterotrophic pioneers facilitate phototrophic biofilm development. *Microbial Ecology*, 54(2):578–585, 2007.

[145] K. Rupalla, P. R. Allegrini, D. Sauer, and C. Wiessner. Superoxide dismutase delays neuronal apoptosis: a role for reactive oxygen species in programmed neuronal death. *Neuron*, 14:303–315, 1995.

[146] K. Rupalla, P. R. Allegrini, D. Sauer, and C. Wiessner. Time course of microglia activation and apoptosis in various brain regions after permanent focal cerebral ischemia in mice. *Acta Neuropathol.(Berl.)*, 96:172–178, 1998.

[147] M. Schilling, M. Besselmann, M. Muller, J. K. Strecker, E. B. Ringelstein, and R. Kiefer. Predominant phagocytic activity of resident microglia over hematogenous macrophages following transient focal cerebral ischemia: an investigation using green fluorescent protein transgenic bone marrow chimeric mice. *Exp. Neurol.*, 196:290–297, 2005.

[148] L. A. Segel. Incorporation of receptor kinetics into a model for bacterial chemotaxis. *J. Theor. Biol.*, 57(1):23–42, 1976.

[149] L. A. Segel. A theoretical study of receptor mechanisms in bacterial chemotaxis. *SIAM J. Appl. Math.*, 32:653–665, 1977.

[150] G. Serini, D. Ambrosi, E. Giraudo, A. Gamba, L. Preziosi, and F. Bussolino. Modeling the early stages of vascular network assembly. *The EMBO Journal*, 22:1771–1779, 2003.

[151] J. A. Sherratt. Chemotaxis and chemokinesis in eukaryotic cells: the Keller-Segel equations as an approximation to a detailed model. *Bull. Math. Biol.*, 56(1):129–146, 1994.

[152] J.A. Sherratt, E.H. Sage, and J.D Murray. Chemical control of eukaryotic cell movement: a newmodel. *J. Theor. Biol.*, 162(1):23–40, 1993.

[153] Y. Shizuta and S. Kawashima. Systems of equations of hyperbolic-parabolic type with applications to the discrete Boltzmann equation. *Hokkaido Math. J.*, 14(2):249–275, 1985.

[154] Thomas C. Sideris, Becca Thomases, and Dehua Wang. Long time behavior of solutions to the 3D compressible Euler equations with damping. *Comm. Partial Differential Equations*, 28(3-4):795–816, 2003.

[155] A. Stevens. The derivation of chemotaxis equations as limit dynamics of moderately interacting stochastic many-particle systems. *SIAM J. Appl. Math.*, 61(1):183–212 (electronic), 2000.

[156] C. Storini, E. Rossi, V. Marrella, M. Distaso, R. Veerhuis, C. Vergani, L. Bergamaschini, and M. G. De Simoni. C1-inhibitor protects against brain ischemia-reperfusion injury via inhibition of cell recruitment and inflammation. *Neurobiol. Dis.*, 19:10–17, 2005.

[157] John C. Strikwerda. *Finite difference schemes and partial differential equations.* Society for Industrial and Applied Mathematics (SIAM), Philadelphia, PA, second edition, 2004.

[158] D. W. Stroock. Some stochastic processes which arise from a model of the motion of a bacterium. *Z. Wahrscheinlichkeitstheorie und Verw. Gebiete*, 28:303–315, 1973/74.

[159] T Suzuki. *Free energy and self-interacting particles.* Progress in Nonlinear Differential Equations and their Applications, 62. Birkhäuser Boston Inc., Boston, MA, 2005.

[160] M. E. Taylor. *Partial differential equations. III*, volume 117 of *Applied Mathematical Sciences*. Springer-Verlag, New York, 1997. Nonlinear equations, Corrected reprint of the 1996 original.

[161] R. Temam. Une méthode d'approximation de la solution des équations de Navier-Stokes. *Bull. Soc. Math. France*, 96:115–152, 1968.

[162] J.M. Thebault and S. Rabouille. Comparison between two mathematical formulations of the phytoplankton specific growth rate as a function of light and temperature, in two simulation models (aster & yoyo). *Ecol. Model.*, 163:145–151, 2003.

[163] P. Tiano. http://www.arcchip.cz/w09/w09tiano.pdf. 2009.

[164] A. Tosin, D. Ambrosi, and L. Preziosi. Mechanics and chemotaxis in the morphogenesis of vascular networks. *Bull. Math. Biol.*, 68(7):1819–1836, 2006.

[165] R.T. Tranquillo and D. A. Lauffenburger. Analysis of leukocyte chemosensory movement. *Cell Biophys.*, 66:29–38, 1988.

[166] R.T. Tranquillo and Douglas A. Lauffenburger. Consequences of chemosensory phenomena for leukocyte chemotactic orientation. *Cell Biophys.*, 8:1–46, 1986.

[167] R. Tyson, S. R. Lubkin, and J. D. Murray. A minimal mechanism for bacterial pattern formation. *Proc. R. Soc. Lond. B*, 266:299–304, 1999.

[168] J. J. L. Velázquez. Point dynamics in a singular limit of the Keller-Segel model. I. Motion of the concentration regions. *SIAM J. Appl. Math.*, 64(4):1198–1223 (electronic), 2004.

[169] F. Vilhardt. Microglia: phagocyte and glia cell. *Int. J. Biochem. Cell Biol.*, 37:17–21, 2005.

[170] X. Wang and G. Z. Feuerstein. Induced expression of adhesion molecules following focal brain ischemia. *J Neurotrauma*, 12(5):825–832, Oct 1995.

[171] X. Wang, T. L. Yue, P. R. Young, F. C. Barone, and G. Z. Feuerstein. Expression of interleukin-6, c-fos, and zif268 mrnas in rat ischemic cortex. *J Cereb Blood Flow Metab*, 15(1):166–171, Jan 1995.

[172] O. Wanner, H.J. Eberl, E. Morgenroth, D. Noguera, B.E. Picioreanu, C. Rittmann, and M.C.M. Van Loosdrecht. *Mathematical Modeling of Biofilms, IWA Scientific and Technical Report No.18*. IWA Publishing, 2006.

[173] O. Wanner and W. Gujer. Competition in biofilms. *Wat. Sci. Tech.*, 17:27–44, 1984.

[174] O. Wanner and W. Gujer. A multispecies biofilm model. *Biotechnol. Bioeng.*, 28:314–328,, 1986.

[175] M. Winkler. Absence of collapse in a parabolic chemotaxis system with signal-dependent sensitivity.

[176] D. Wrzosek. Global attractor for a chemotaxis model with prevention of overcrowding. *Nonlinear Anal.*, 59(8):1293–1310, 2004.

[177] D. Wrzosek. Long-time behaviour of solutions to a chemotaxis model with volume-filling effect. *Proc. Roy. Soc. Edinburgh Sect. A*, 136(2):431–444, 2006.

[178] D. Wu. Signaling mechanisms for regulation of chemotaxis. *Cell Res.*, 15(1):52–56, 2005.

[179] T. Zhang, N. Cogan, and Q. Wang. Phase-field models for biofilms II. 2-d numerical simulations of biofilm-flow interaction. *Commun. Comput. Phys.*, 4(2):72–101, 2008.